R-7450-2

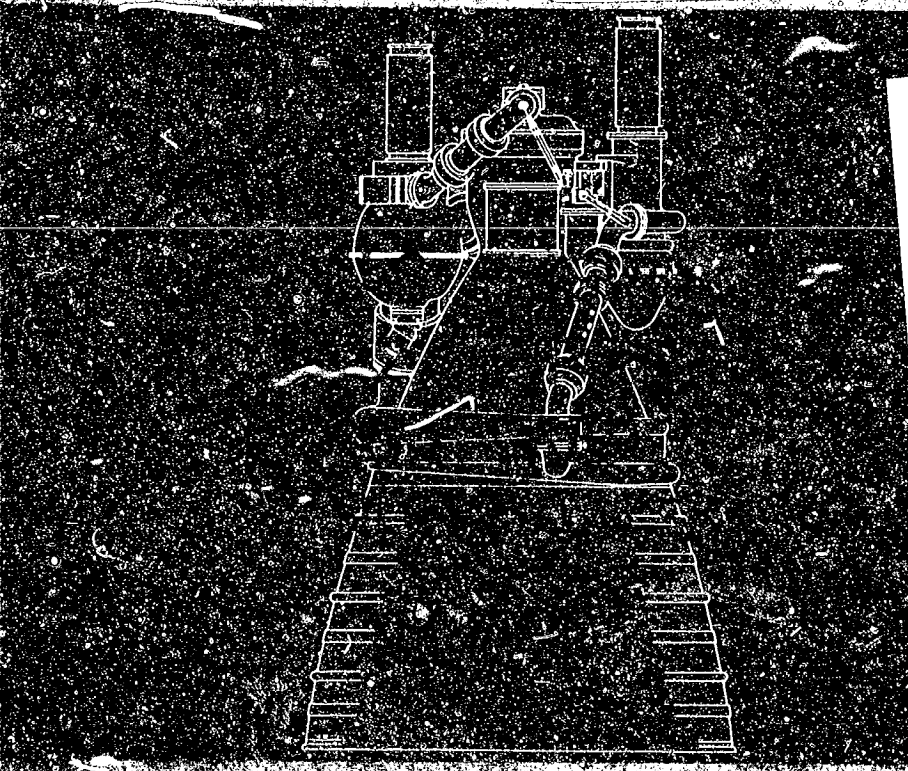

VOLUME 2: S-II STAGE FAILURE ANALYSIS

ROCKETDYNE

A DIVISION OF NORTH AMERICAN ROCKWELL CORPORATION

6633 CANOGA AVENUE, CANOGA PARK, CALIFORNIA 91304

ROCKETDYNE
A DIVISION OF NORTH AMERICAN ROCKWELL CORPORATION
6633 CANOGA AVENUE, CANOGA PARK, CALIFORNIA 91304

R-7450-2

9

J-2 ENGINE AS-502 (APOLLO 6)
FLIGHT REPORT
S-II AND S-IVB STAGES

VOLUME 2: S-II STAGE FAILURE ANALYSIS

Contract NAS8-19
Exhibit A
Para. A.3.a

PREPARED BY

Rocketdyne Engineering
Canoga Park, California

APPROVED BY

P. D. Castenholz
J-2 Program Manager

NO. OF PAGES 284 & xiv

REVISIONS

DATE 17 June 1968

DATE	REV. BY	PAGES AFFECTED	REMARKS

FORM R18-G REV. 9-67

FOREWORD

This report was prepared by Rocketdyne, a division of North American Rockwell Corporation, under Contract NAS8-19.

ABSTRACT

This is Volume 2 of a five-volume report on the operation of the J-2 engines during the flight of Apollo/Saturn AS-502. This volume presents the analysis of the premature shutdown of J-2 engines J2044 and J2058.

The volumes of this report are:

- Volume 1: Flight Performance Analysis
- Volume 2: S-II Stage Failure Analysis
- Volume 3: S-IVB Stage Failure Analysis
- Volume 4: Flight Failure Verification Testing
- Volume 5: Post-Flight Design Modifications

CONTENTS

ILLUSTRATIONS

TABLES

INTRODUCTION

This report presents results of analysis and investigation of S-II stage J-2 engine and related system operation during flight of the AS-502 vehicle. Information as contained herein supplements the J-2 Engine Performance Analysis Report for Flight AS-502, S-II and S-IVB stages, and relates primarily to flight anomalies associated with early shutdown of S-II engine 202 (J2044). Included are: a summary of S-II events from AS-502 vehicle liftoff through S-II staging and final cutoff, including anomalies noted; a description of the primary failure mode; conclusions with regard to flight failure related anomalies; discussion of flight failure related anomalies, including hypotheses or conclusions, analyses, calculations, and corroborative data; discussion of anomalies not related to the flight failure; testing accomplished in support of the AS-502 flight; and alternate hypotheses considered.

SUMMARY

DESCRIPTION OF EVENTS

Operation of S-II stage J-2 engines was normal until approximately 220 seconds range time, at which point a series of events commenced which culminated in failure and shutdown of engine 202 (J2044) and subsequent shutdown of engine 203 (J2058). The general hypothesis stated in the following paragraphs was developed from analysis of flight data and engine test data conducted in support of flight failure analysis.

220 to 260 Seconds Range Time

Observed Occurrences. Gradual decrease of S-II engine compartment temperatures.

Causes. Partial failure of engine 202 ASI fuel line downstream bellows, resulting in approximately 1 lb/sec fuel leakage into the engine compartment, with attendant cryogenic chilldown of compartment area. Reduction in ASI fuel flow resulted in ASI mixture ratio increase to above 2.5, raising ASI combustion temperature, and initiating erosion of the ASI nozzle (main injector).

260 to 319 Seconds Range Time

Observed Occurrences. Continued chilling of engine compartment area; engine 202 components indicate chilling. Engine 202 gradual performance decay becomes apparent. At 282 seconds range time, the engine 202 yaw hydraulic actuator ΔP indicates an increase and engine 202 EAS (engine actuation system) hydraulic temperatures indicate chilling.

Causes. Gradual increase in ASI fuel line leakage to approximately 2 lb/sec, resulting in engine gradual performance decay of approximately 6 psi. Progressive ASI fuel leakage resulted in increased ASI mixture

ratio to above 8, with attendant increased ASI combustion temperature and accelerated erosion of the ASI nozzle (main injector). Cryogenic chilldown of the engine 202 yaw hydraulic actuator ΔP transducer resulted in an erroneous ΔP indication. Engine 202 EAS hydraulic temperature decreases resulted from increased ASI fuel line leakage.

319 Seconds Range Time

Observed Occurrences. Engine 202 rapid performance decay (22.9-psia chamber pressure decrease). Engine 202 yaw and pitch hydraulic actuators indicate compressive forces (7800 and 7150 pounds, respectively). General chilling of engine compartment and engine components continues.

Causes. Erosion of ASI nozzle progressed beyond penetration of the main injector fuel manifold, resulting in structural degradation of the injector face (Rigimesh) and oxidizer feed posts. A fragment of the central portion of the injector face, fuel sleeves, or ASI nozzle broke away from the injector, and was accelerated through the thrust chamber throat, striking the interior wall of the thrust chamber near the exit prior to ejection from the chamber; rupture of several thrust chamber tubes with attendant fuel leakage to the interior of the thrust chamber bell occurred. Engine performance degraded as a result of the thrust chamber fuel leakage (approximately 9 lb/sec). Fuel leakage to the interior of the thrust chamber bell caused displacement of the engine thrust vector in such a manner as to result in compressive loading of the yaw and pitch hydraulic actuators to the values measured. Engine 202 rebalance occurred, stabilizing both ASI fuel line leakage and engine performance; performance continued to be relatively stable until 412.3 seconds range time. Main injector internal erosion continued, including violation of oxidizer injector manifold passages.

412.3 to 412.921 Seconds Range Time

Observed Occurrences. Engine 202 slight performance decay followed by rapid performance decay, characterized by increase in oxidizer and fuel

flows and decrease in main chamber pressure. Engine compartment forward temperatures and pressures increased rapidly with associated aft parameters lagging behind. Operation of engine 202 terminates at 412.921 seconds range time.

Causes. Continued erosion of the ASI nozzle finally resulted in failure of the ASI-to-main injector seal, providing a low resistance path for the oxidizer, fuel, and hot gases pouring into the nozzle area. This oxidizer-rich flow of hot gases past the ASI injector into the engine compartment area quickly eroded into the oxidizer dome proper, resulting in a slight initial performance decay followed by overboard flow of oxidizer, rapid dropoff of performance, and dropout of mainstage OK (oxidizer injection) pressure switches, and cutoff of the engine.

414.2 Seconds Range Time

Observed Occurrences. S-II engine 203 (J2058) operation was prematurely terminated.

Causes. Cutoff of engine 203 was typical of a normal oxidizer depletion cutoff, and was initiated by dropout of the engine mainstage OK pressure switches. Engine 203 cutoff resulted from an oxidizer prevalve closing signal originating in the engine 202 prevalve control circuit, i.e., crossed oxidizer prevalve control commands between engines 202 and 203.

AS-502 S-II EVENTS

The AS-502 vehicle was launched on schedule from launch complex 39-A at Kennedy Space Center on 4 April 1968. Events prior to liftoff were normal, and the final 8 hours of countdown proceeded without interruption.

Flight events recorded during the S-IC stage and S-II stage boost portions of the AS-502 flight are listed in Table 1.

Operation of J-2 engine J2044, S-II engine 202 (Fig. 1), is described in general in the following paragraphs.

Fuel Feed System

Engine 202 fuel feed system operation (upstream of the main fuel valve) was satisfactory through cutoff. Rapid decay of fuel inlet pressure at cutoff has been attributed to a ruptured instrument sensing line and not a major leak in the fuel feed system. Investigation of other system parameters indicates that the fuel feed system upstream of the main fuel valve was basically intact following cutoff. Flight data indicate that ASI fuel feed system leakage existed as early as 220 seconds range time and that fuel feed system leakage downstream of the main fuel valve resulted from damage to the thrust chamber at 319 seconds range time.

Oxidizer Feed System

Oxidizer feed system operation was satisfactory until cutoff, at which time system integrity appears to have been lost.

Gas Generator and Exhaust System

Several anomalies occur in this system during flight and following engine 202 cutoff; however, system operation was generally satisfactory. During the range time period from 220 seconds to 413 seconds, the gas generator valve position trace indicates valve closure of approximately 5 percent. Engine performance, however, does not reflect this change, and subsequent laboratory tests revealed that cryogenic chilldown of a gas generator valve potentiometer resulted in indication of the closing characteristic observed in the flight data. At approximately 416 seconds range

TABLE 1

FLIGHT AS-502 S-IC/S-II STAGE BOOST FLIGHT EVENTS

	Range Time, seconds	Events
S-IC Boost	0 (Ref.)	AS-502 liftoff
	100 to 140	Vehicle vibration loading as recorded in the upper stages was approximately three times greater than experienced during AS-501 flight.
	134	A vibration shock was recorded throughout the vehicle.
	144	S-IC inboard engine cutoff
	148.2	S-IC outboard engine cutoff
	149	S-IC staging
S-II Boost	149.8	S-II engine start; all J-2 engines experienced satisfactory starts.
	179.1	S-II second plane separation (normal)
	187.5	S-II aft camera jettison
	220 to 319	Engine compartment temperature gradual decrease; also reflected by No. 2 engine ECA, primary instrumentation package, and auxiliary instrumentation package temperature measurements.
	260 to 319	No. 2 engine gradual performance decay (approximately 1 psia/10 seconds).
	282	No. 2 engine yaw hydraulic actuator ΔP increase; No. 2 engine hydraulic system temperatures begin to decrease.
	310	Engine compartment temperatures begin to decrease at a greater rate.
	319	No. 2 engine performance suddenly decreases; chamber pressure decreases 22.9 psia; No. 2 engine yaw and pitch actuators indicators indicate compressive forces, respectively, of 7800 and 7150 pounds; general chilling of engine compartment and engine components increases.

TABLE 1
(Concluded)

	Range Time, seconds	Events
S-II Boost	412.3	No. 2 engine performance decay, characterized by slight increase in oxidizer flows and attendant decrease in chamber pressure (10 to 15 psia).
	412.7	No. 2 engine rapid performance dropoff
	412.921	No. 2 engine performance decayed to a point where dropout of the mainstage OK pressure switches (sensing oxidizer injection pressure) resulted in signalling of engine cutoff to the vehicle instrumentation unit.
	413.368	The vehicle instrumentation unit commanded No. 2 engine prevalves closed; No. 2 engine fuel prevalve and No. 3 engine oxidizer prevalve responded to the command and closed.
	413.4	No. 2 engine start tank pressure starts to decay.
	414.277	No. 3 engine cutoff initiated by dropout of the mainstage OK pressure switches because of erroneous signal to close No. 3 engine oxidizer prevalve.
	414.710	Vehicle instrumentation unit commands No. 3 engine prevalves closed; No. 2 engine oxidizer prevalve and No. 3 engine fuel prevalve responded to the command and closed.
	576.6	Operation of S-II engines No. 1, 4, and 5 terminated normally after extended duration associated with premature shutdown of No. 2 and 3 engines (oxidizer low level cutoff).
	577.08	S-II staging (normal).

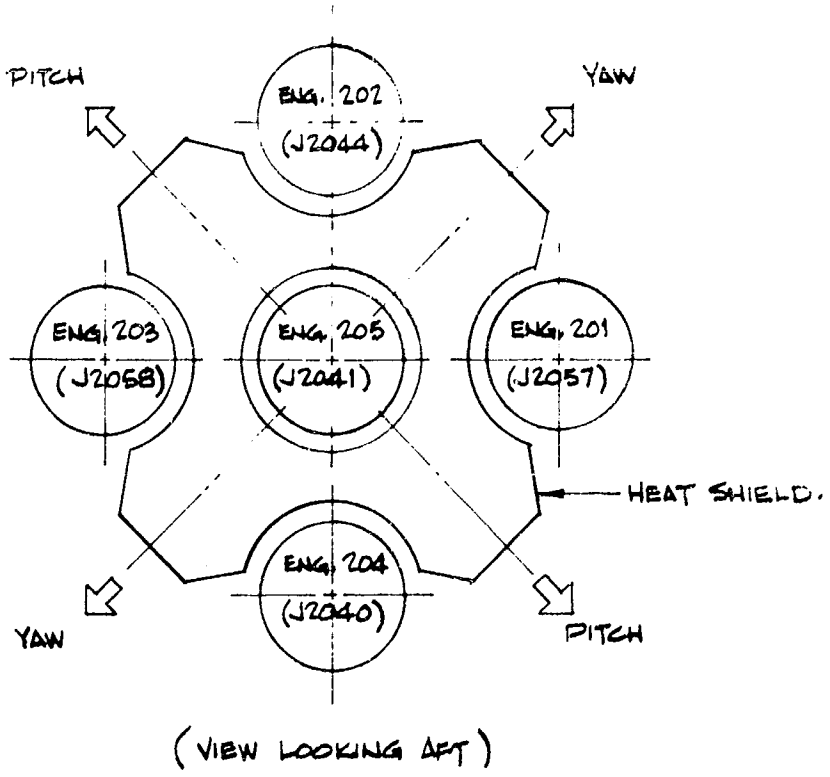

Figure 1. AS-502 S-II Engine Cluster Positions and Serial Numbers

time (following cutoff of engine 202), the gas generator valve actually reopened, as indicated by flight data. During the engine 202 cutoff transient, gas generator chamber pressure spiked to 450 psia; this occurrence is a result of the type of shutdown experienced by engine 202. Following cutoff, the engine 202 oxidizer turbine bypass valve did not open fully.

Gaseous Hydrogen Start System

Start system performance was satisfactory during engine 202 operation, but system integrity was lost following cutoff, as evidenced by rapid dropoff of start tank pressure.

Pneumatic System

Engine 202 pneumatic system operation was satisfactory until the cutoff transient, at which time the oxidizer turbine bypass valve opening control line appears to have been damaged. This damage resulted in slow opening of the OTBV and reopening of the gas generator valve following cutoff. The gas generator oxidizer injection purge appears to have been obstructed at cutoff.

Instrumentation Systems

Operation of engine 202 primary and auxiliary flight instrumentation systems was satisfactory, and valid data were given throughout the flight.

Fuel Pressurization System

Overall operation of the engine 202 fuel pressurization system was satisfactory throughout operation of the engine, with tank ullage pressure maintained within the required limits.

Oxidizer Pressurization System

Operation of the engine 202 oxidizer tank pressurization system was satisfactory until engine cutoff. Flight data indicate failure of the engine 202 heat exchanger outlet flex line downstream of the heat exchanger outlet temperature transducer and upstream of the stage oxidizer pressurization manifold check valve.

Related Systems and Conditions

Stage Hydraulic System. Operation of the stage hydraulic system associated with engine 202 was satisfactory until 282 seconds range time, when abnormal drift was indicated by the yaw actuator ΔP transducer.

S-II Engine Environment. The S-II engine compartment temperature environment during the AS-502 flight was lower than experienced during AS-501 operation. Environmental parameters exhibited normal trends until 220 seconds, at which time cryogenic chilling of the engine compartment was noted. The chilling effect continued through the remainder of engine 202 operation.

CONCLUSIONS

Operation of AS-502 S-II J-2 engines was normal until approximately 220 seconds range time.

A leakage failure of the engine 202 ASI fuel line occurred at approximately 220 seconds range time, precipitating the following events and eventually resulting in premature termination of engine 202 operation:

1. Cryogenic chilldown of the engine compartment area, engine components, and stage components (chilldown continued until engine 202 cutoff)

2. Reduction in ASI fuel flow, with attendant high ASI operating mixture ratios and erosion of the ASI nozzle (main injector). The erosion process continued, structurally weakening the central portion of the injector until, at approximately 319 seconds range time, a fragment of the injector broke away, was ejected through the thrust chamber throat, and struck the interior of the thrust chamber nozzle near the exit, resulting in damage to thrust chamber tubes, leakage of fuel to the interior of the thrust chamber, a shift in engine performance, and loading of the gimbal actuators.

3. Degradation of ASI-to-injector sealing capability occurred at approximately 412.3 seconds range time because of continued erosion internal to the main injector, producing a leakage path for oxidizer, fuel, and combustion products to atmosphere.

4. These oxidizer-rich hot gases escaping through the degraded ASI sealing surface rapidly eroded and penetrated the oxidizer dome. Engine performance decayed rapidly at approximately 412.7 seconds range time and oxidizer injection pressure was lowered to the point where dropout of the engine mainstage OK pressure switches occurred, signalling engine cutoff at approximately 412.921 seconds.

5. Hot-gas leakage to the interior of the engine compartment, combined with oxidizer and fuel leakage external to engine 202, produced a fire within the engine compartment, as evidenced by rapid rise in compartment temperatures and pressures. The fire at cutoff of engine 202 produced other anomalies.

Engine 202 hydraulic actuator Δ P anomalies occurring from approximately 260 to 319 seconds range time were erroneous, and resulted from malfunction of actuator Δ P transducers when chilled to cryogenic temperatures.

Engine 202 hydraulic actuator Δ P indications noted at 319 seconds range time resulted from creation of a loading moment about the gimbal bearing created by leakage of fuel to the interior of the thrust chamber nozzle.

Engine 202 hydraulic actuator Δ P indications following cutoff of the engine are attributed to loading because of pressurization of the fuel inlet duct.

Premature termination of engine 203 operation resulted from crossed prevalve control signals between S-II cluster positions 2 and 3, i.e., shutdown of engine 202 resulted in closing of the engine 202 fuel prevalve and the engine 203 oxidizer prevalve, thus precipitating on oxidizer depletion-type cutoff of engine 203.

Performance shifts noted for S-II engines remaining in operation following cutoff of engines 202 and 203 were erroneous, and resulted from a shift in telemetry signal strength.

AS-502 S-II ANOMALIES

Anomalies discussed in this section are directly associated with cutoff of engines 202 and 203, either as contribution factors or as resulting from contribution factors.

S-II THERMAL ENVIRONMENT

Temperature Decay: Range Time 220 Seconds

Description of Event. Engine component and stage temperature parameters indicate that portions of the S-II boattail region experienced a cooling trend beginning at approximately 220 seconds range time. Temperature plots (Fig. 2 through 28) illustrate boattail thermal characteristics as a function of time. The engine compartment cooling region generally related to the area occupied by engines 201, 202, and 205, and extended from the heat shield forward to the base of the oxidizer tank. Comparative data from flight AS-501 are included in Fig. 1 through 24 to illustrate that the cooling trend was not encountered during that flight. The chilling trend continued through S-II flight until cutoff of engines 202 and 203 (range times 412.925 and 414.277 seconds, respectively).

Hypothesis. Cryogenic leakage into the engine compartment resulted in the area temperature decay. The source of cryogenic leakage was primarily the engine 202 ASI fuel line at or near the downstream flex section. The cryogenic leakage increased with time until it reached approximately 2 seconds at 290 seconds range time. At 319 seconds range time, a fragment of the eroding main injector struck several thrust chamber nozzle tubes, resulting in an engine performance shift. Cryogenic leakage continued after this abrupt performance shift until engine 202 cutoff was initiated, maintaining the compartment chilling trend. Data also indicate the possibility of a small cryogenic leak of similar nature in the engine 205 ASI fuel line. This possible leak has no effect on stage operation other than local chilling.

Corroboration of Hypothesis. Definite indications of engine 202 performance decay commenced at approximately 260 seconds range time.

Additional Comments. The overall pattern of engine compartment chilling is difficult to attribute to a single leak source located at the downstream end of the engine 202 ASI fuel system. In particular, thrust cone stringer temperature 897, thrust cone forward ambient temperature, instrumentation container aft surface temperature 514, and engine 205 main oxidizer valve and closing control line temperatures C032 and C033 are relatively remote from the hypothesized engine 202 ASI fuel line leakage location; these parameters suggest the existance of several cryogenic leak sources, not necessarily related to shutdown of engine 202. In particular, data indicate a small leak from the engine 205, possibly a failure of the ASI fuel line.

Heat Flux Increase: Range Time 319 Seconds

Description of Event. The three heat flux measurements C665, C722 and C858 around engine 202 indicate a step increase of approximately 10 percent at 319 seconds range time (Fig. 2).

Hypothesis. A calculated fuel loss of approximately 7.9 lb/sec occurring at 319 seconds would result in a thrust chamber mixture ratio change of +0.4 to +0.5 mixture ratio units This increase in mixture ratio would, in turn, cause the heat flux from the thrust chamber exhaust plume to increase approximately 10 percent, thus accounting for the indicated flux increase.

Corroboration of Hypothesis. Calculations indicating the 10-percent heat flux increase are based on MSFC-supplied thermal environment data which yield an increase in Q of 25 percent when changing the mixture ratio from 4.7 to 5.5. The indicated change in thrust chamber mixture ratio of +0.4 mixture ratio units was extrapolated from the MSFC data, yielding the approximate increase in heat flux that was noted during flight. The outboard location of the ruptured nozzle tubes is such that minimum effect of the fuel discharging into the exhaust plume is seen by the calorimeters. Thus, the calorimeters can sense the change in injector end combustion accurately.

Foldout Frame 1

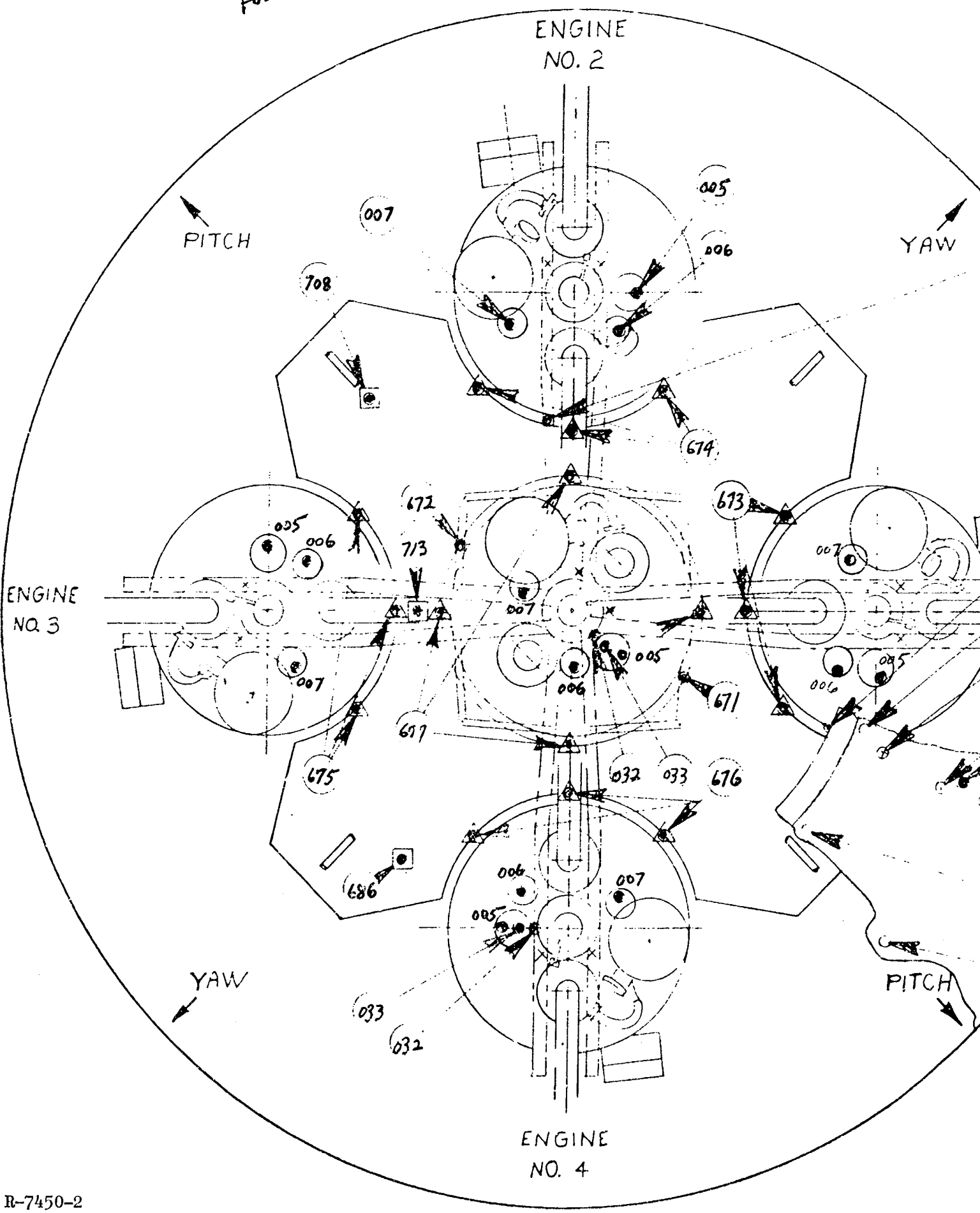

Foldout FRAME 2

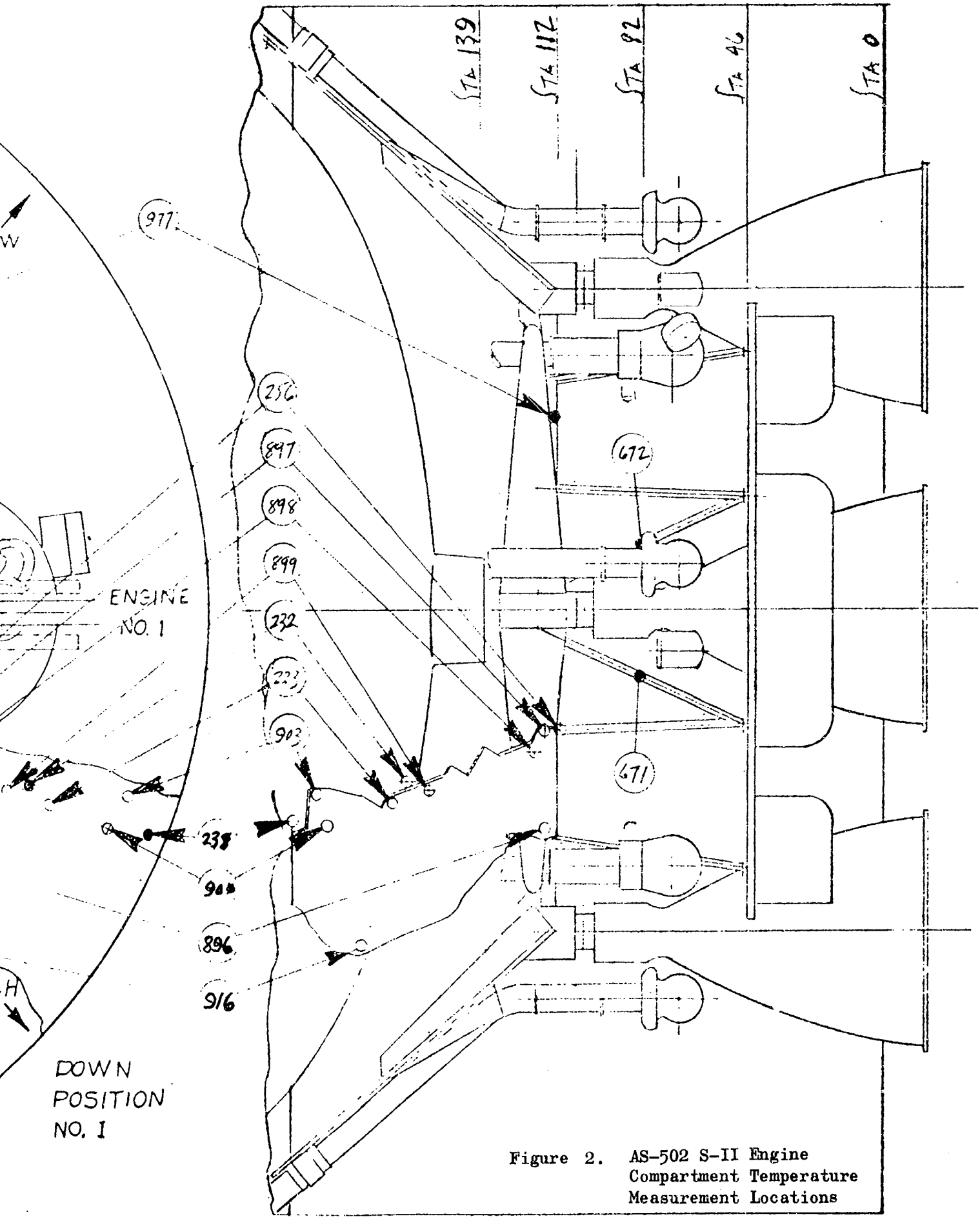

Figure 2. AS-502 S-II Engine Compartment Temperature Measurement Locations

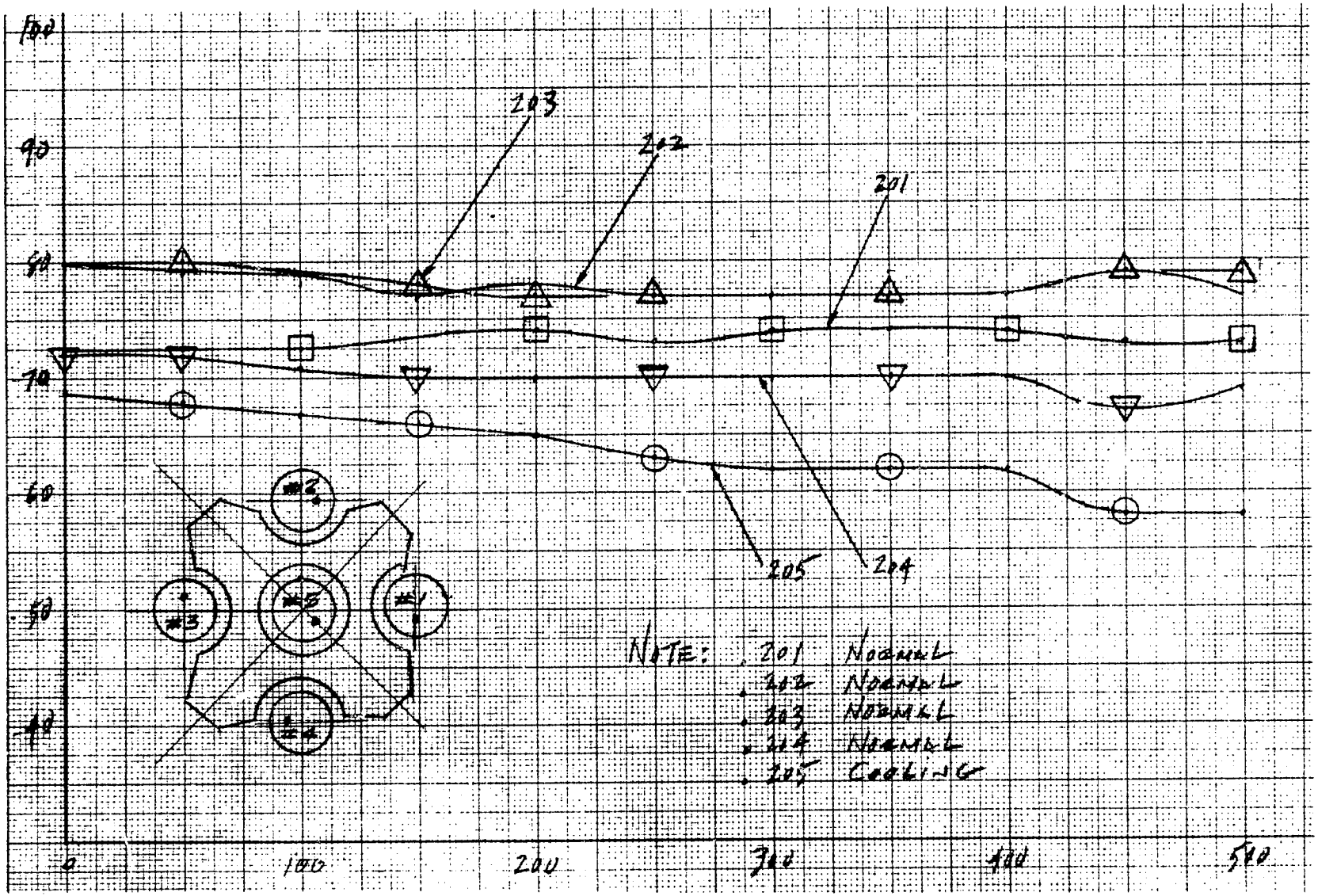

Figure 3. Electrical Control Package Temperatures (C0005)

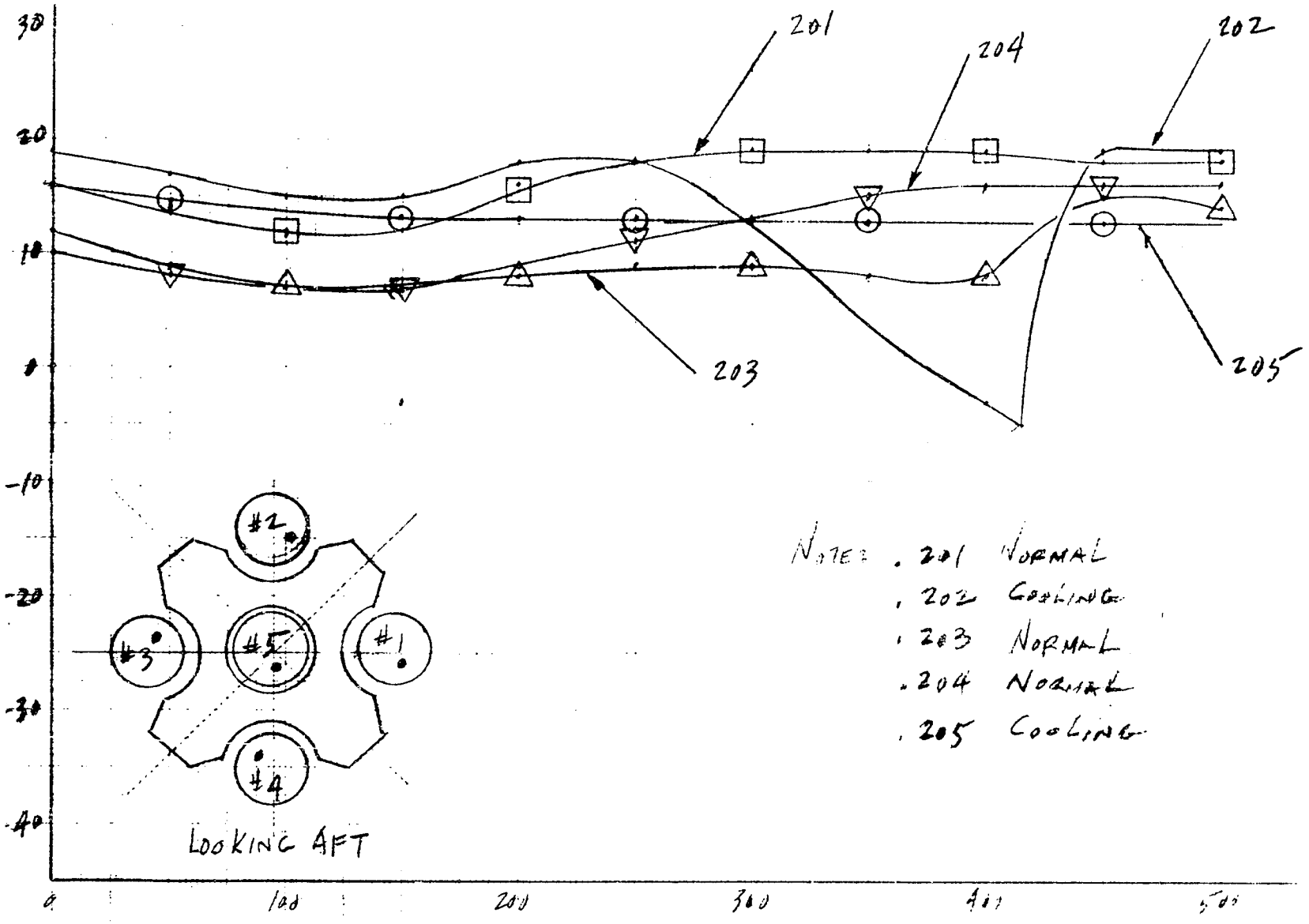

Figure 4. Primary Instrumentation Package Temperatures (C0006)

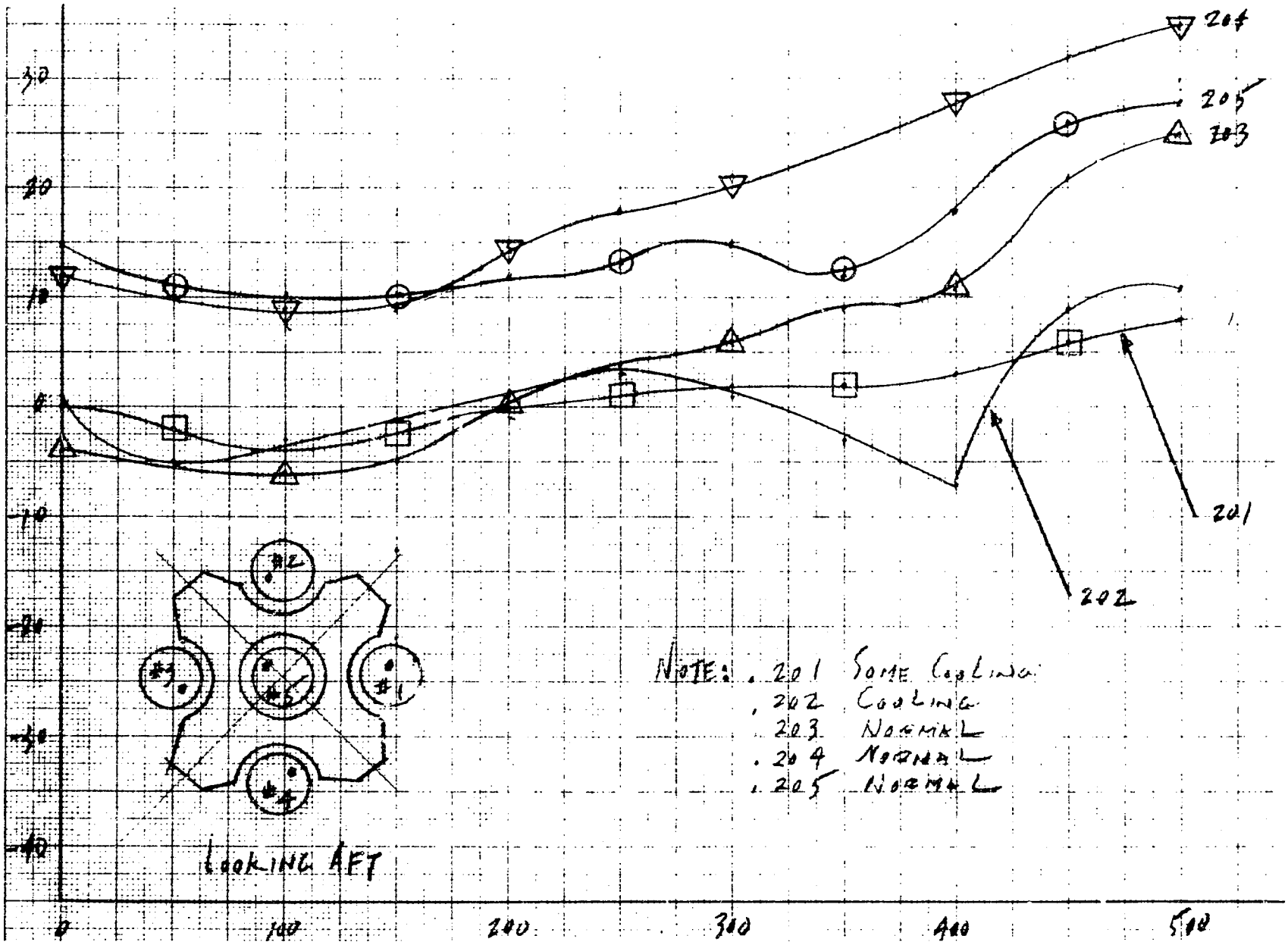

Figure 5. Auxiliary Instrumentation Package Temperatures (C0007)

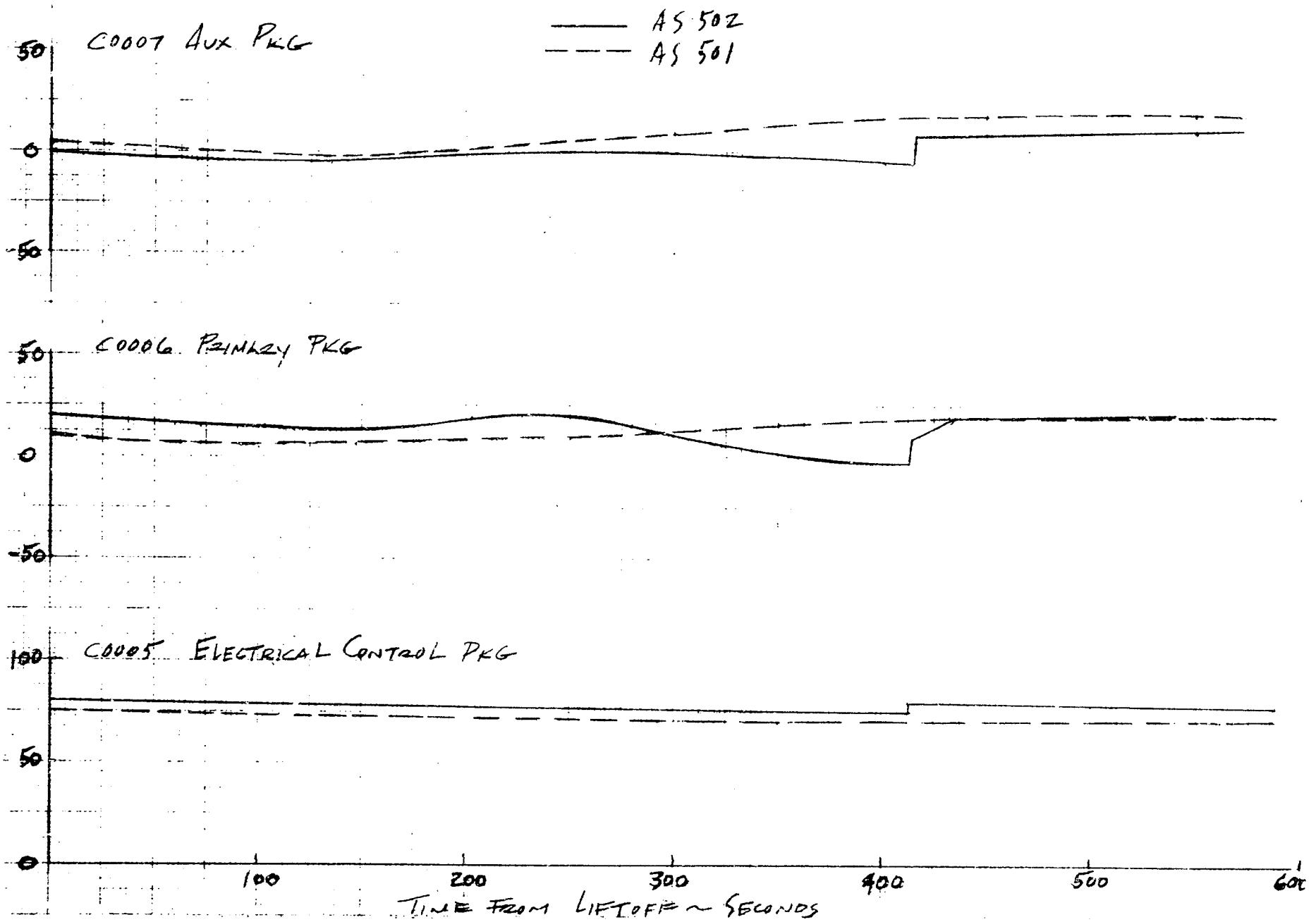

Figure 6. No. 2 Engine Package Temperatures, AS-501 and AS-502

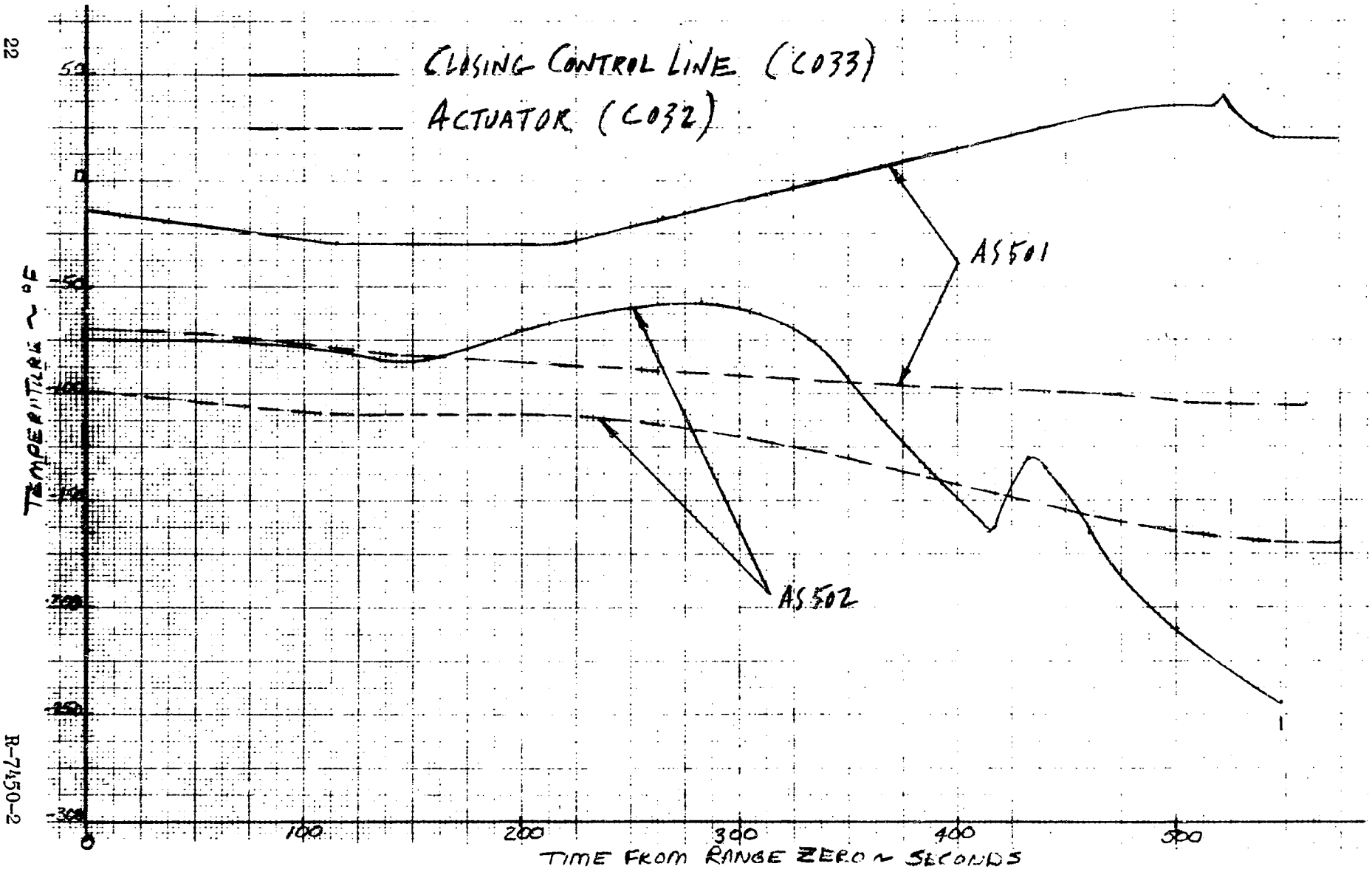

Figure 7. Main Oxidizer Valve Temperatures, Engine 205

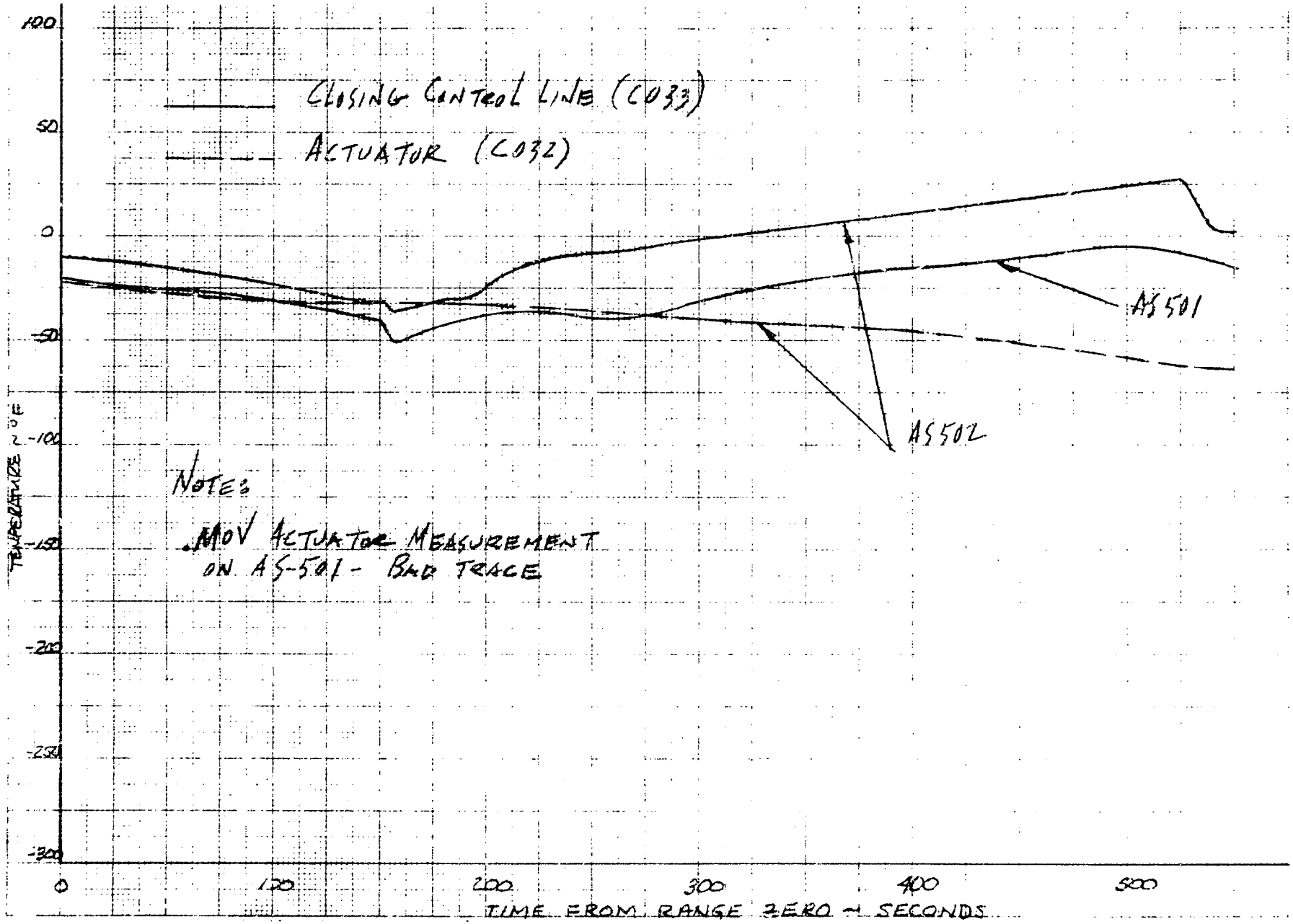

Figure 8. Main Oxidizer Valve Temperatures, Engine 204

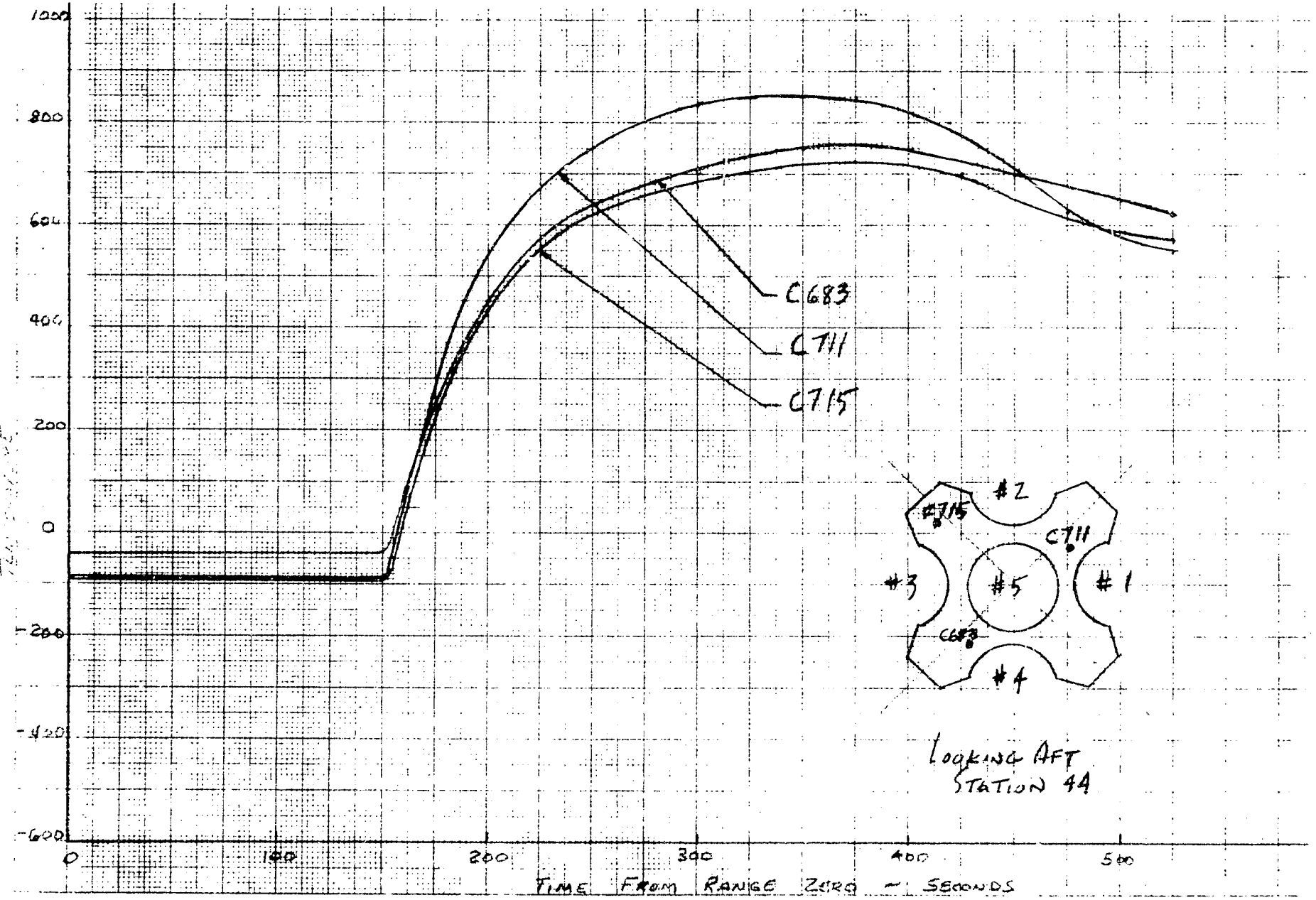

Figure 9. Heat Shield Aft Surface Temperatures, Station 44

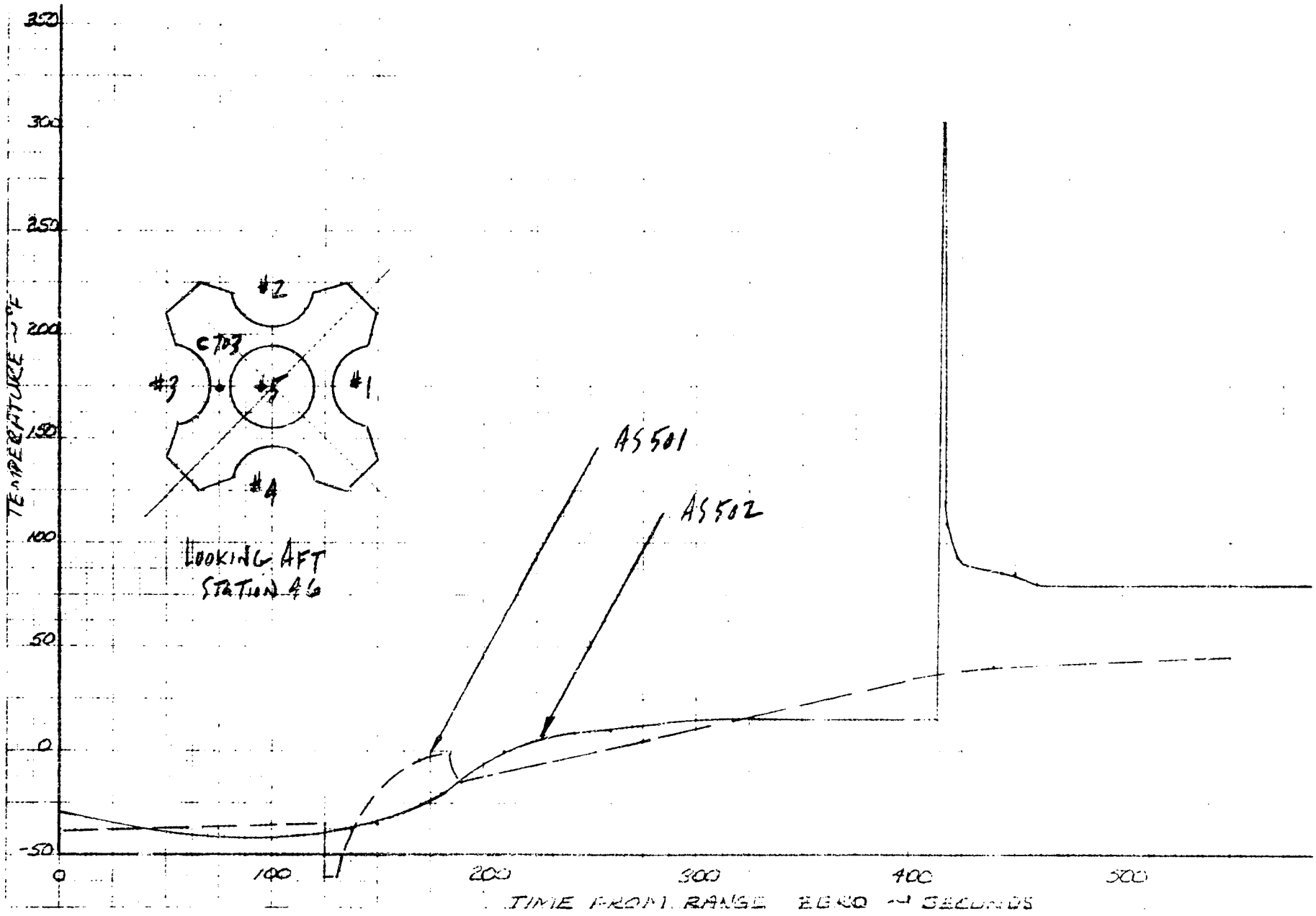

Figure 10. Heat Shield Forward Surface Temperature (C703), Station 46

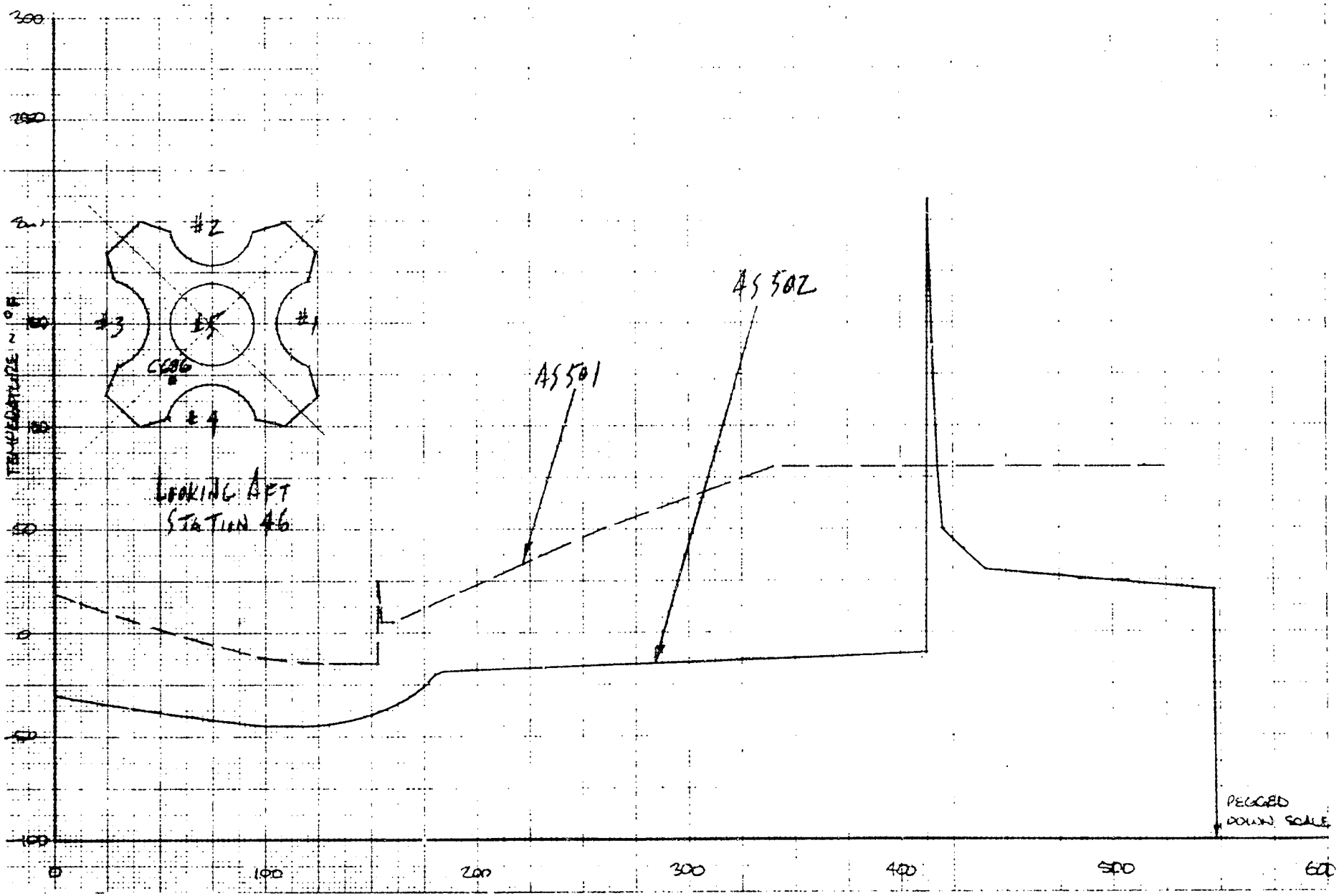

Figure 11. Heat Shield Forward Surface Temperature (C686), Station 46

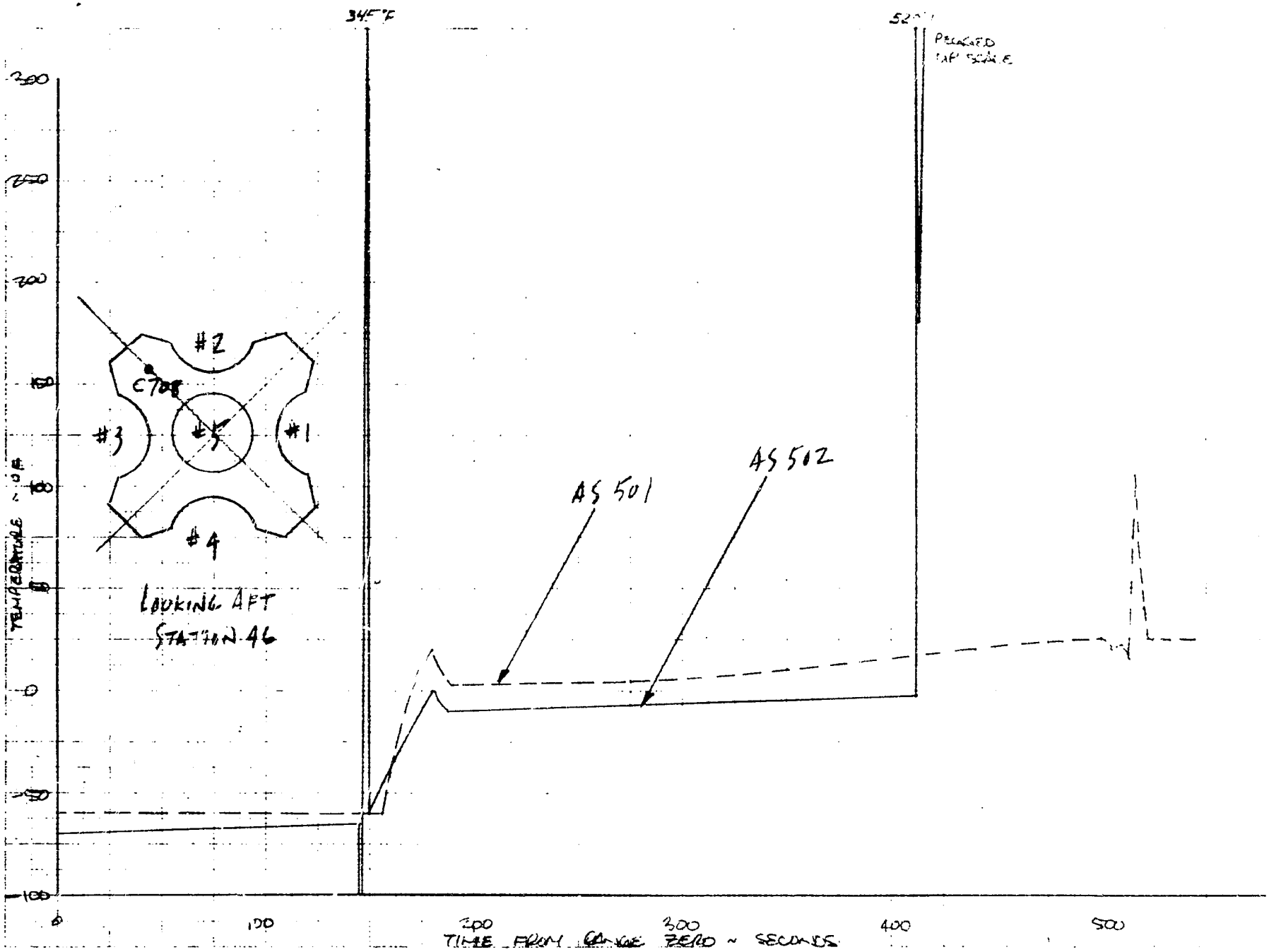

Figure 12. Heat Shield Forward Surface Temperature (C708), Station 46

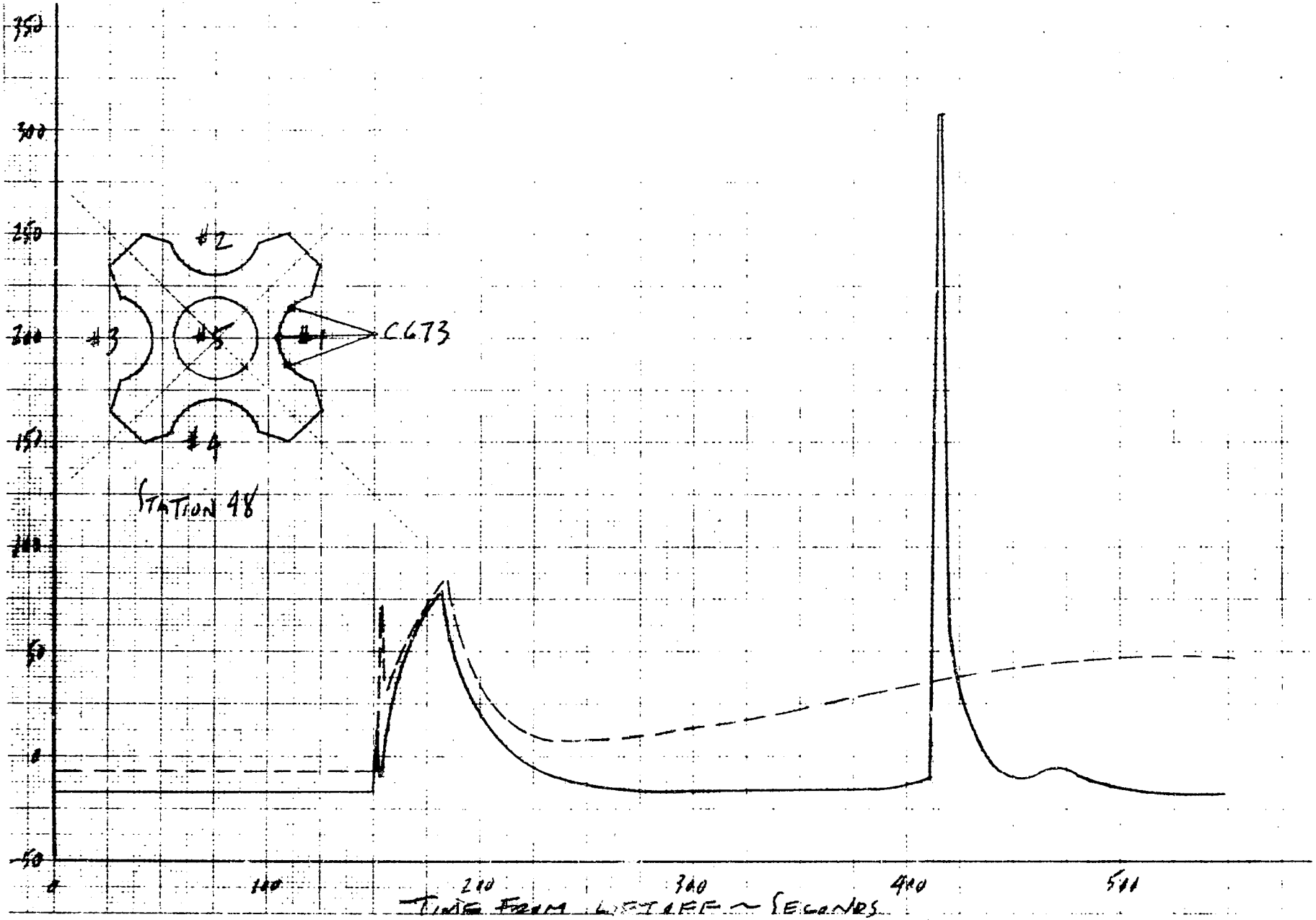

Figure 13. Heat Shield Curtain Gas Temperature (C673), Station 48

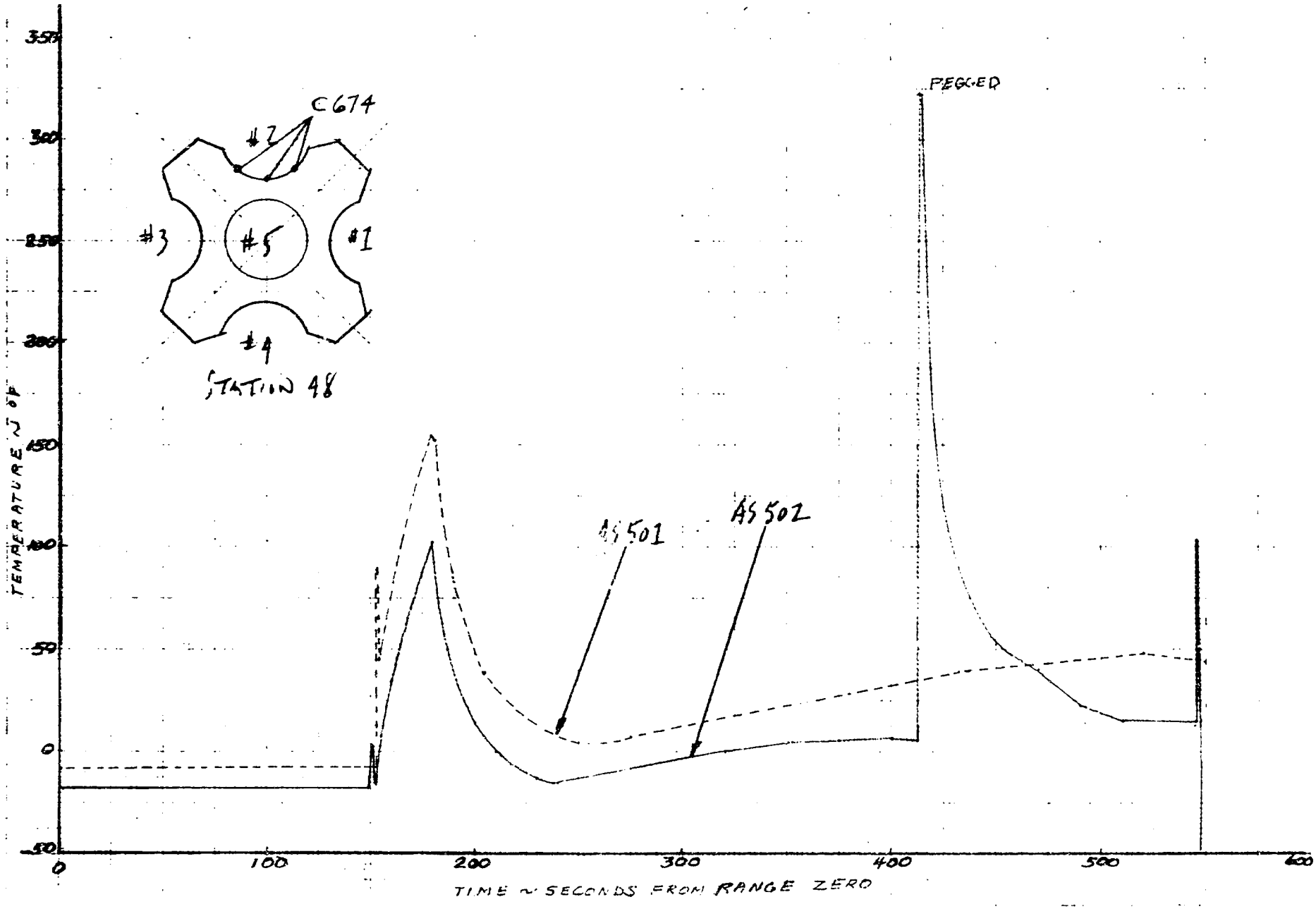

Figure 14. Heat Shield Curtain Gas Temperature (C674), Station 48

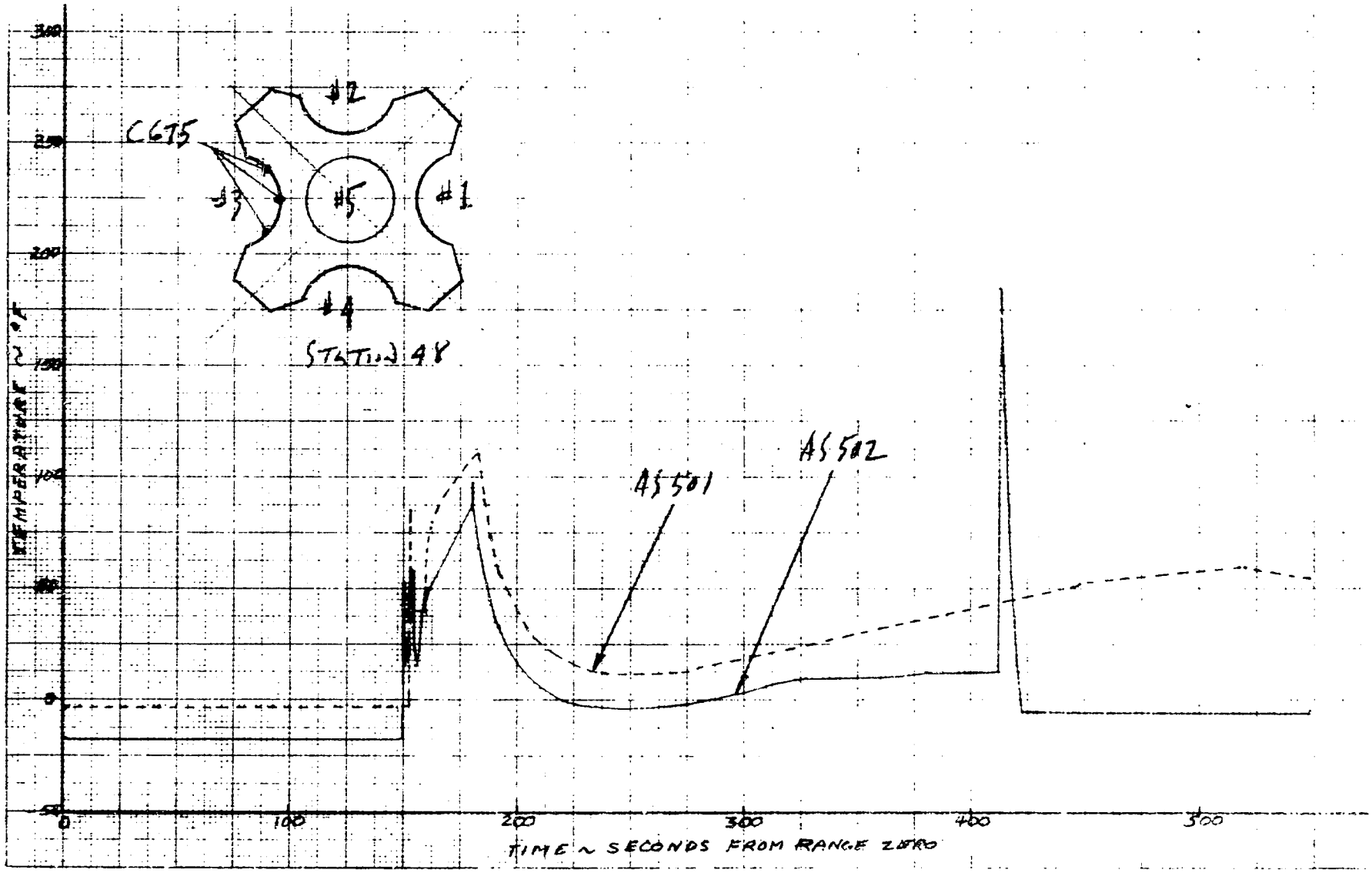

Figure 15. Heat Shield Curtain Gas Temperature (C675), Station 48

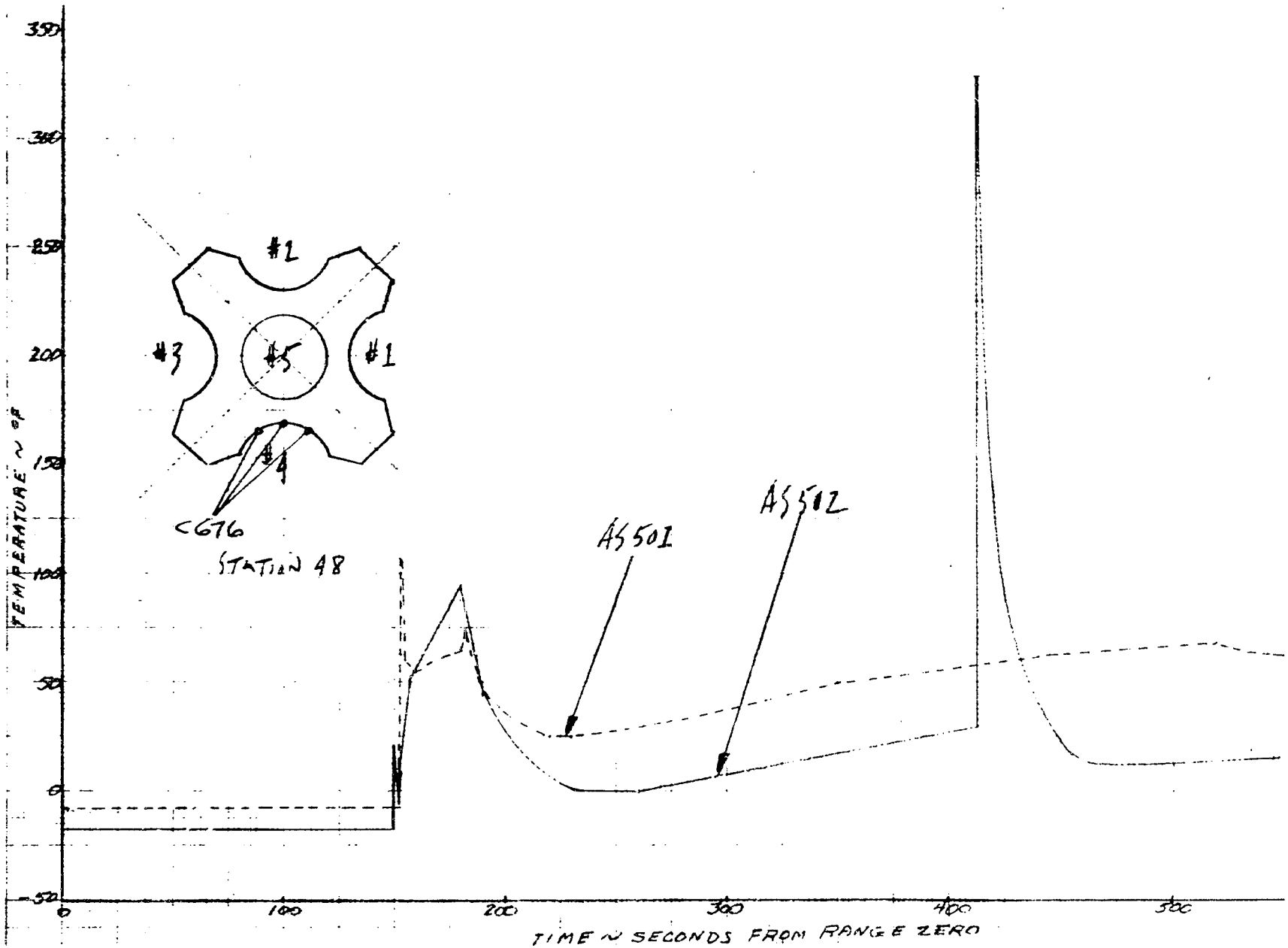

Figure 16 Heat Shield Curtain Gas Temperature (C676), Station 48

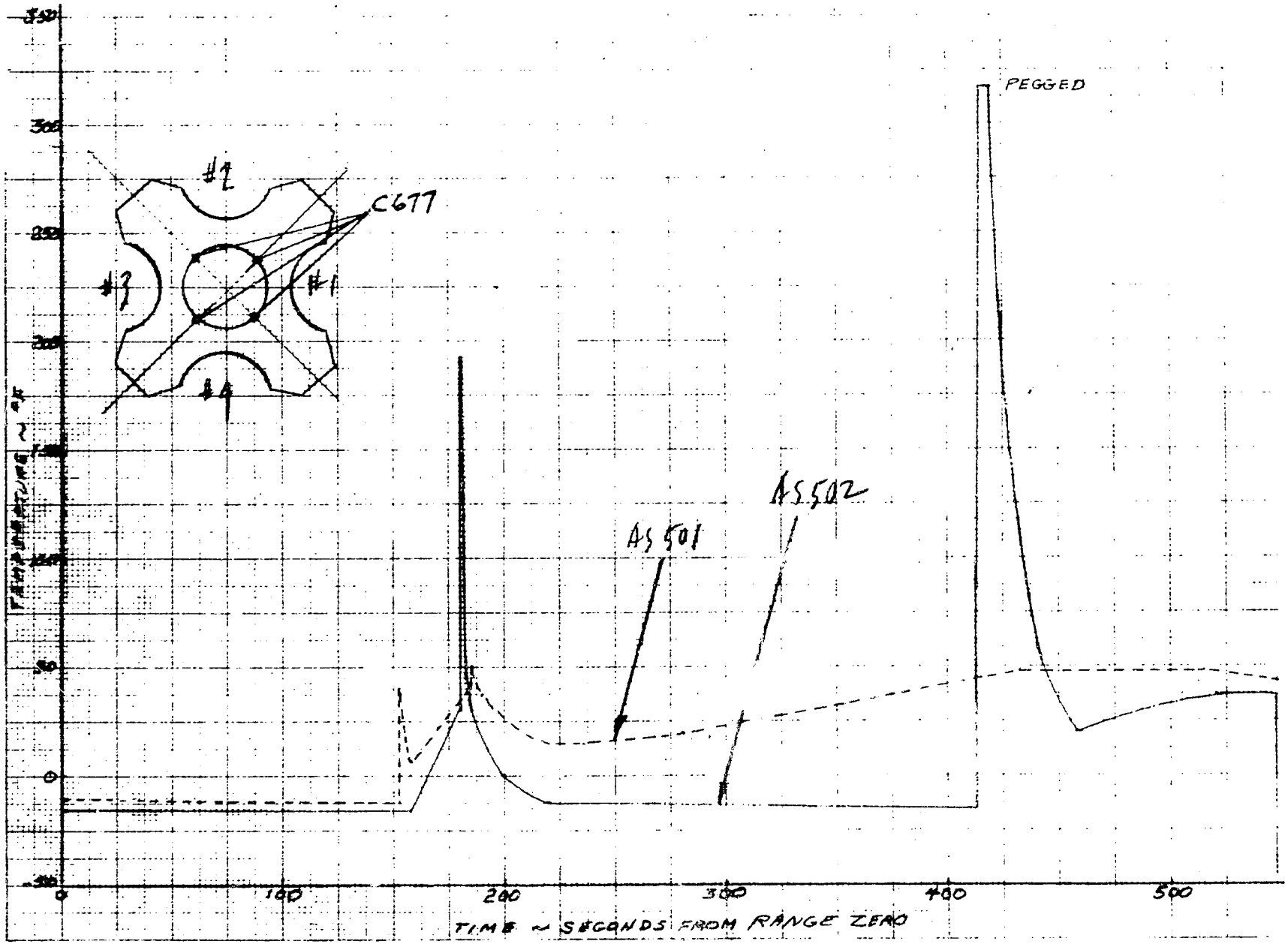

Figure 17. Heat Shield Curtain Gas Temperature (C677), Station 48

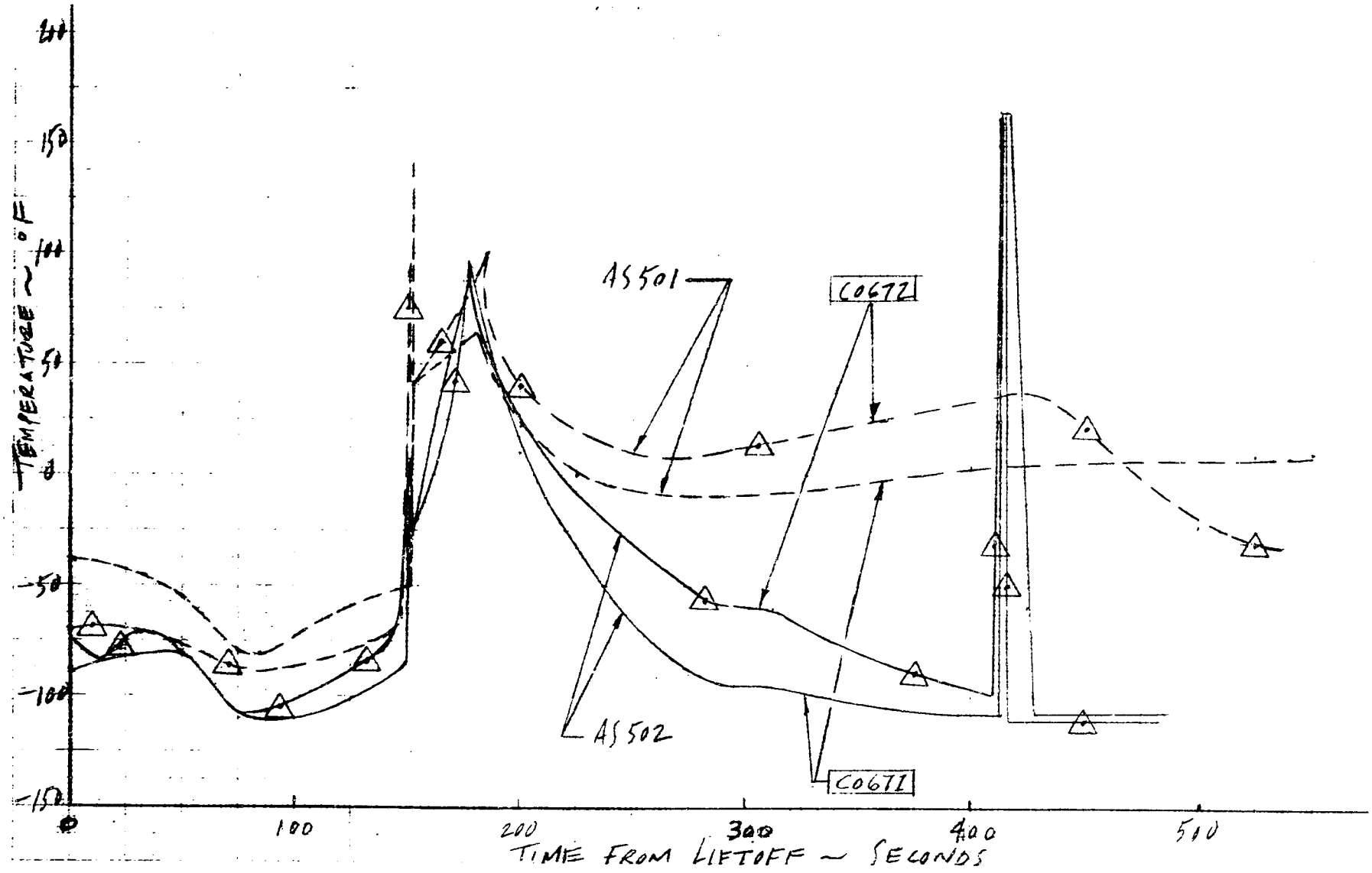

Figure 18. Engine Compartment Gas Temperat re, Station 82

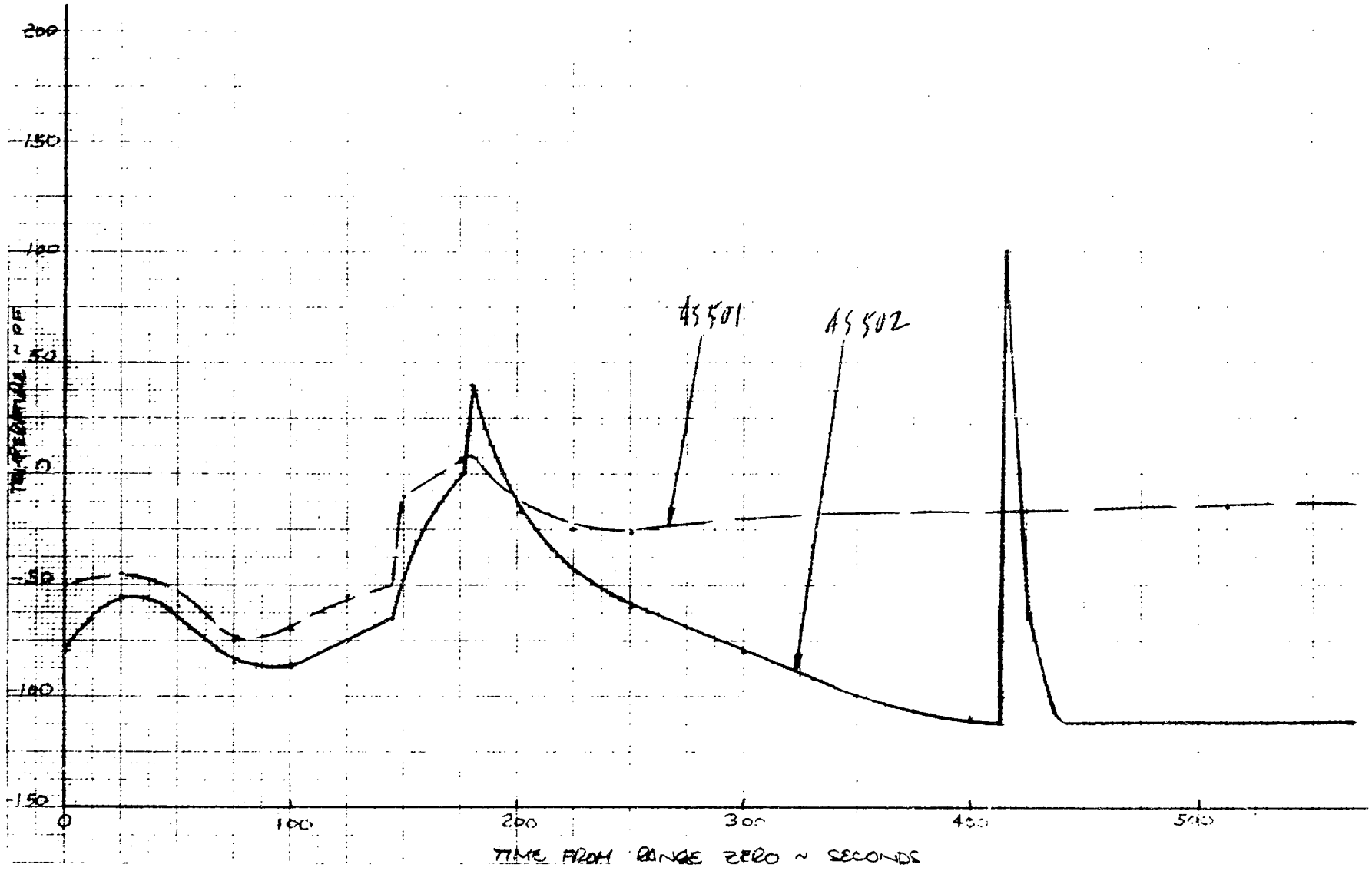

Figure 19. Thrust Cone Forward Ambient Temperature (C256), Station 112

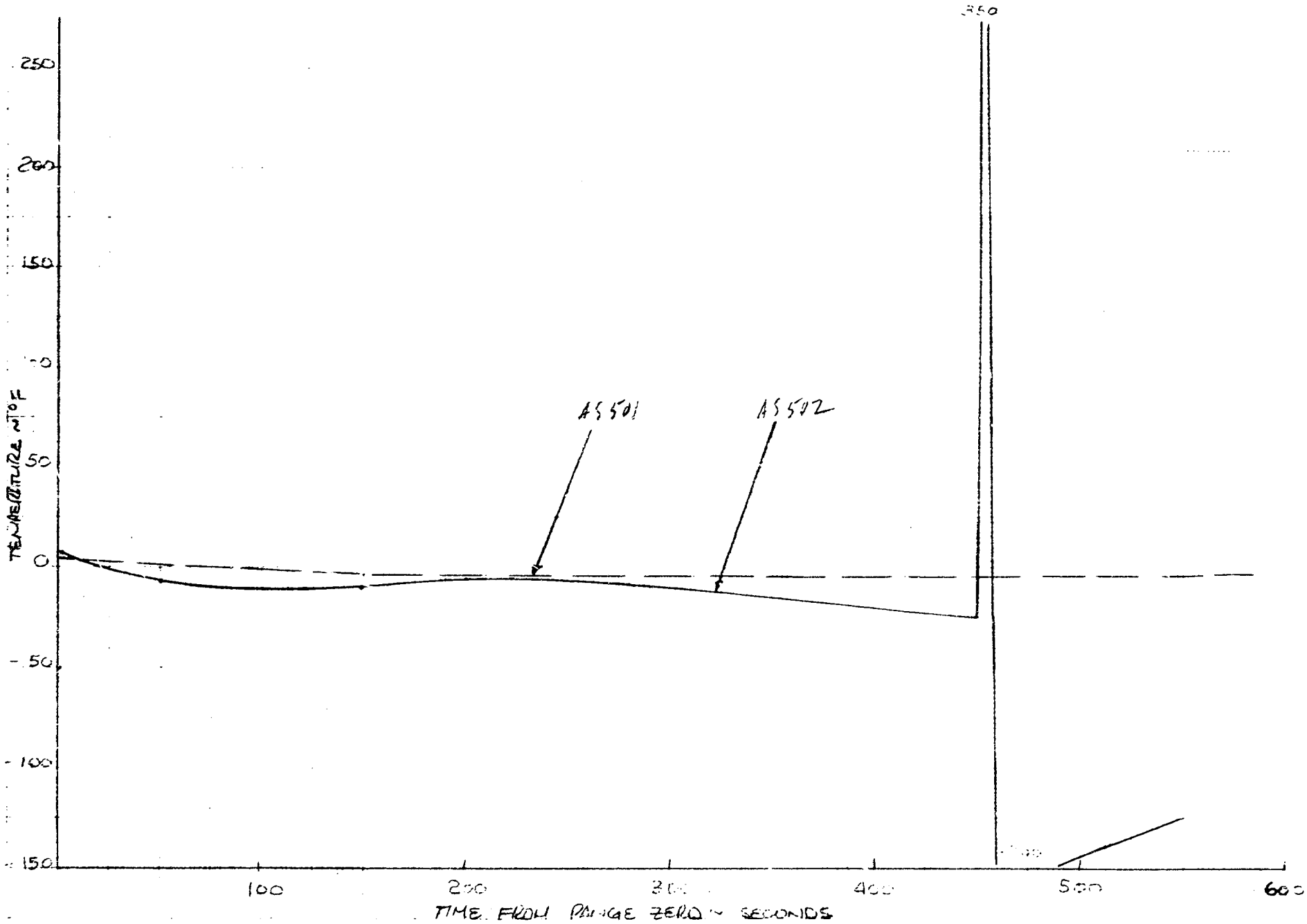

Figure 20. Center Engine Beam Surface Temperature (C977), Station 112

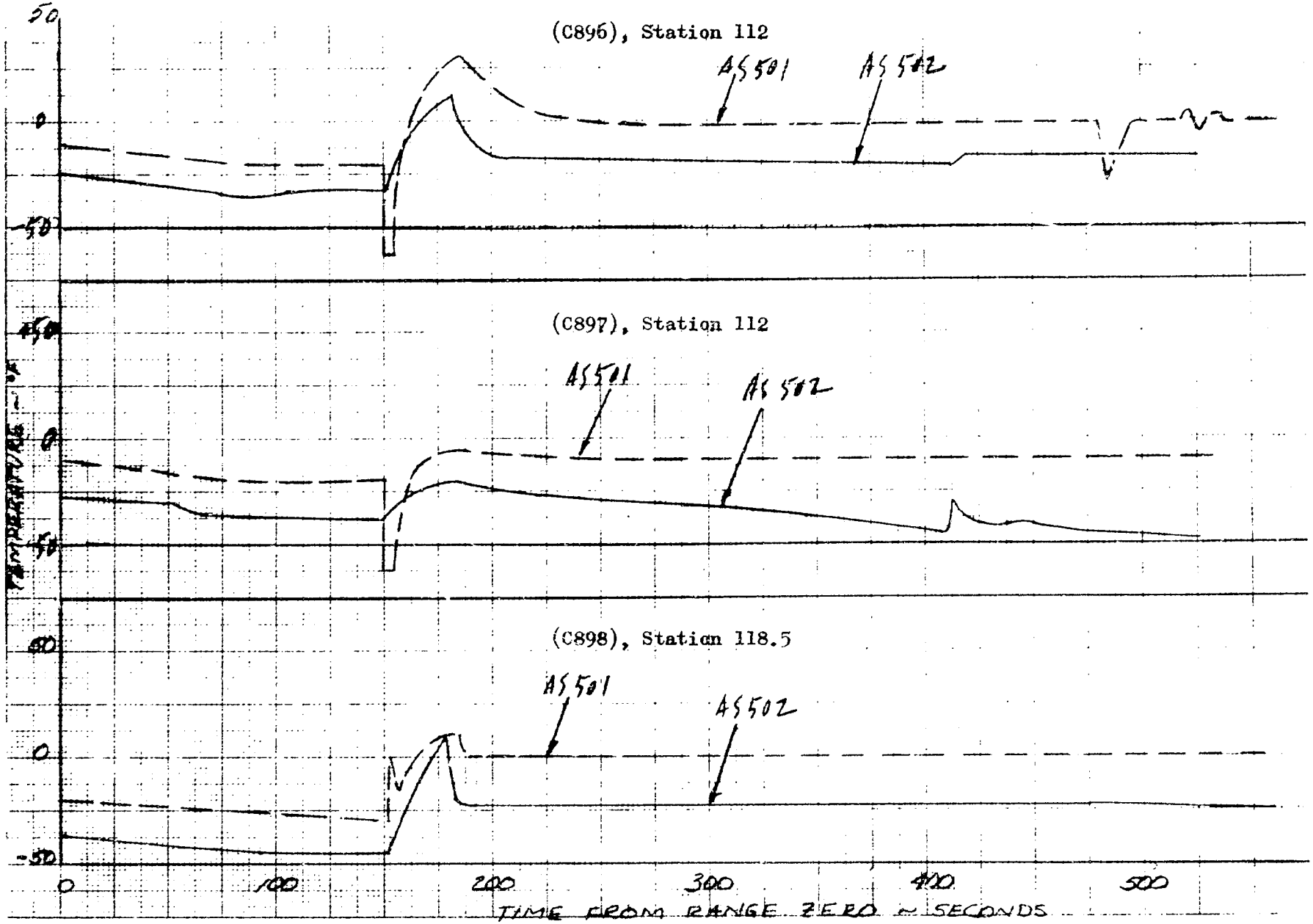

Figure 21 Thrust Cone Stringer Surface Temperatures

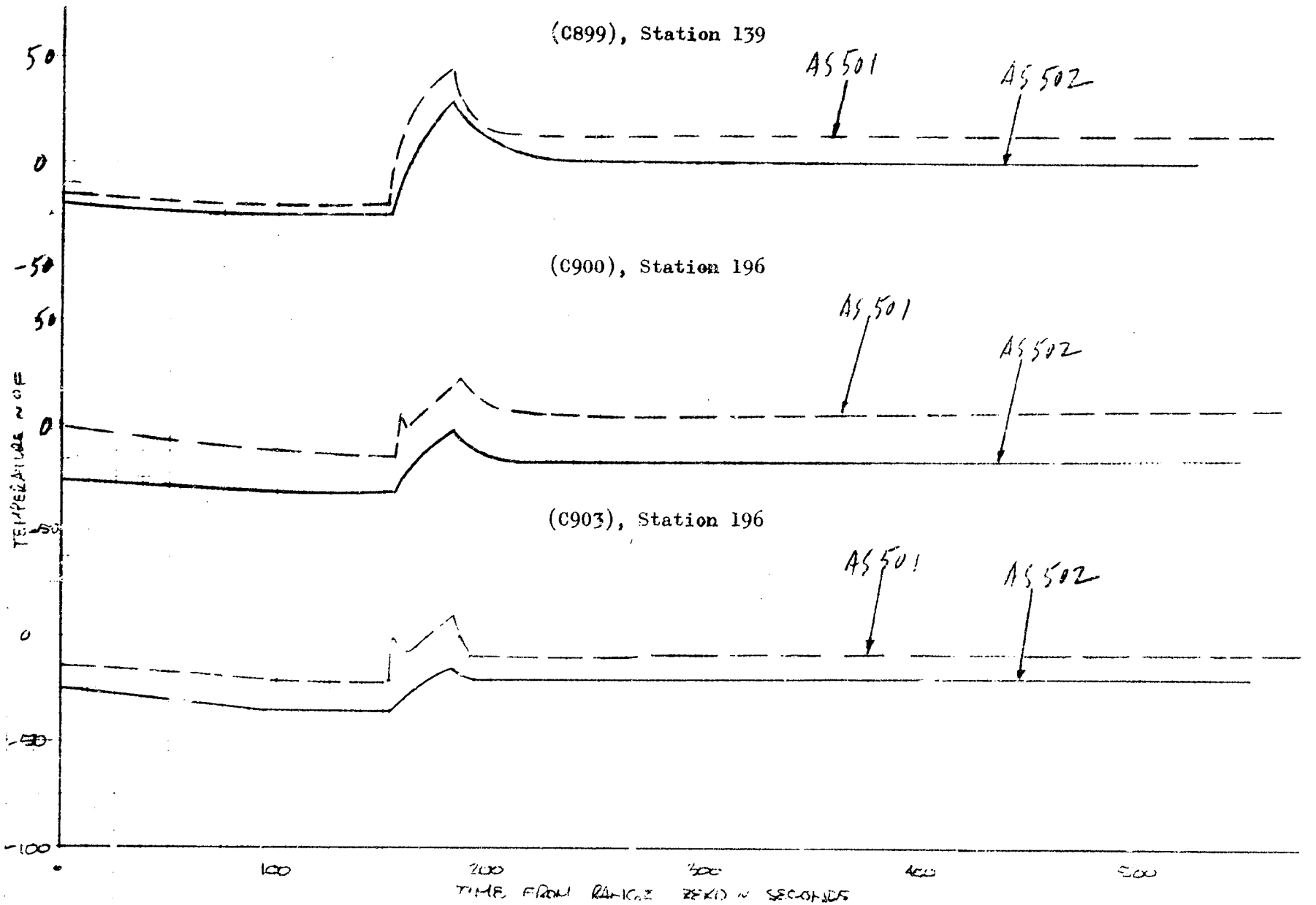

Figure 22. Thrust Cone Stringer Surface Temperatures

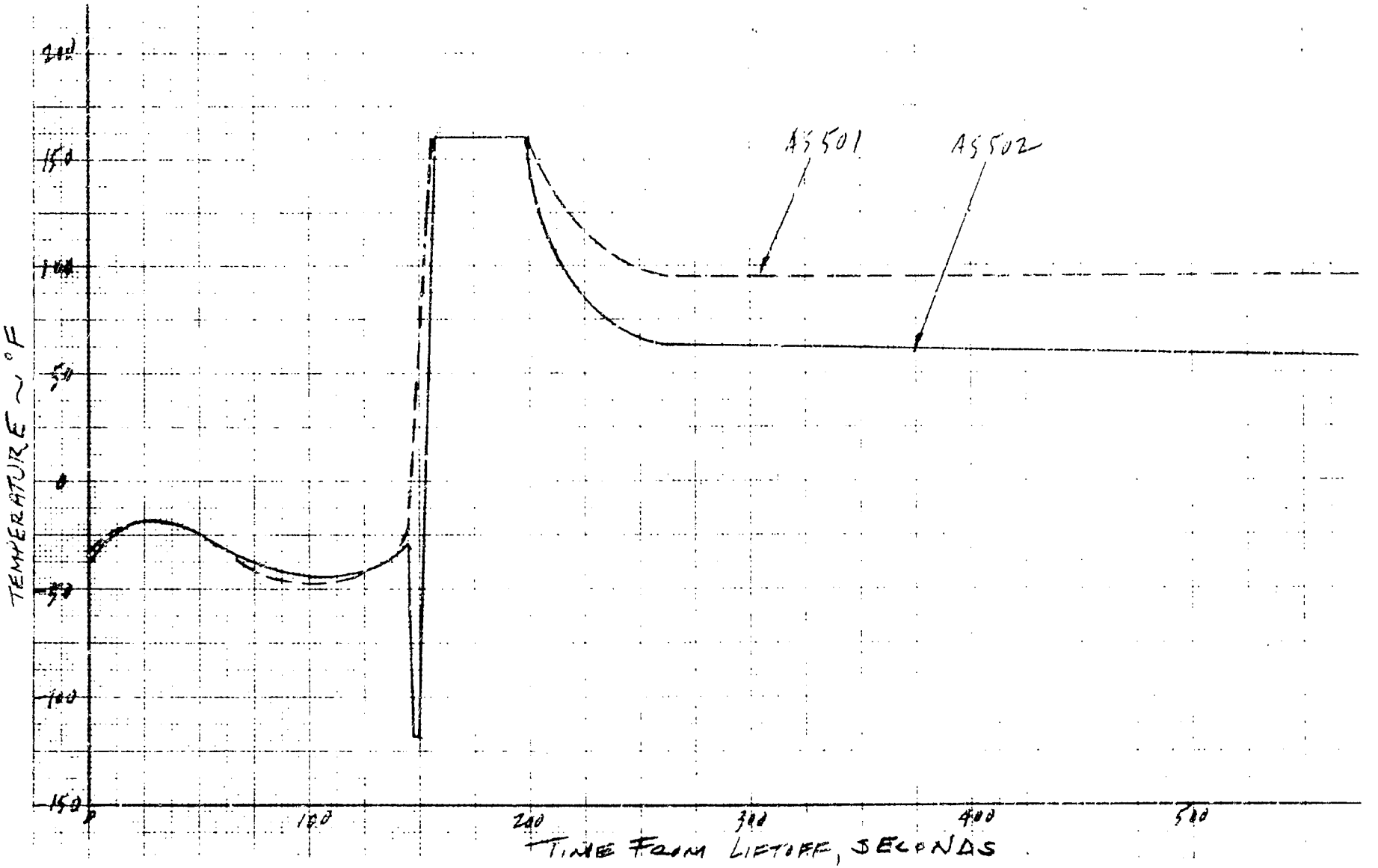

Figure 23. Thrust Cone After Ambient Temperature (C223), Station 133

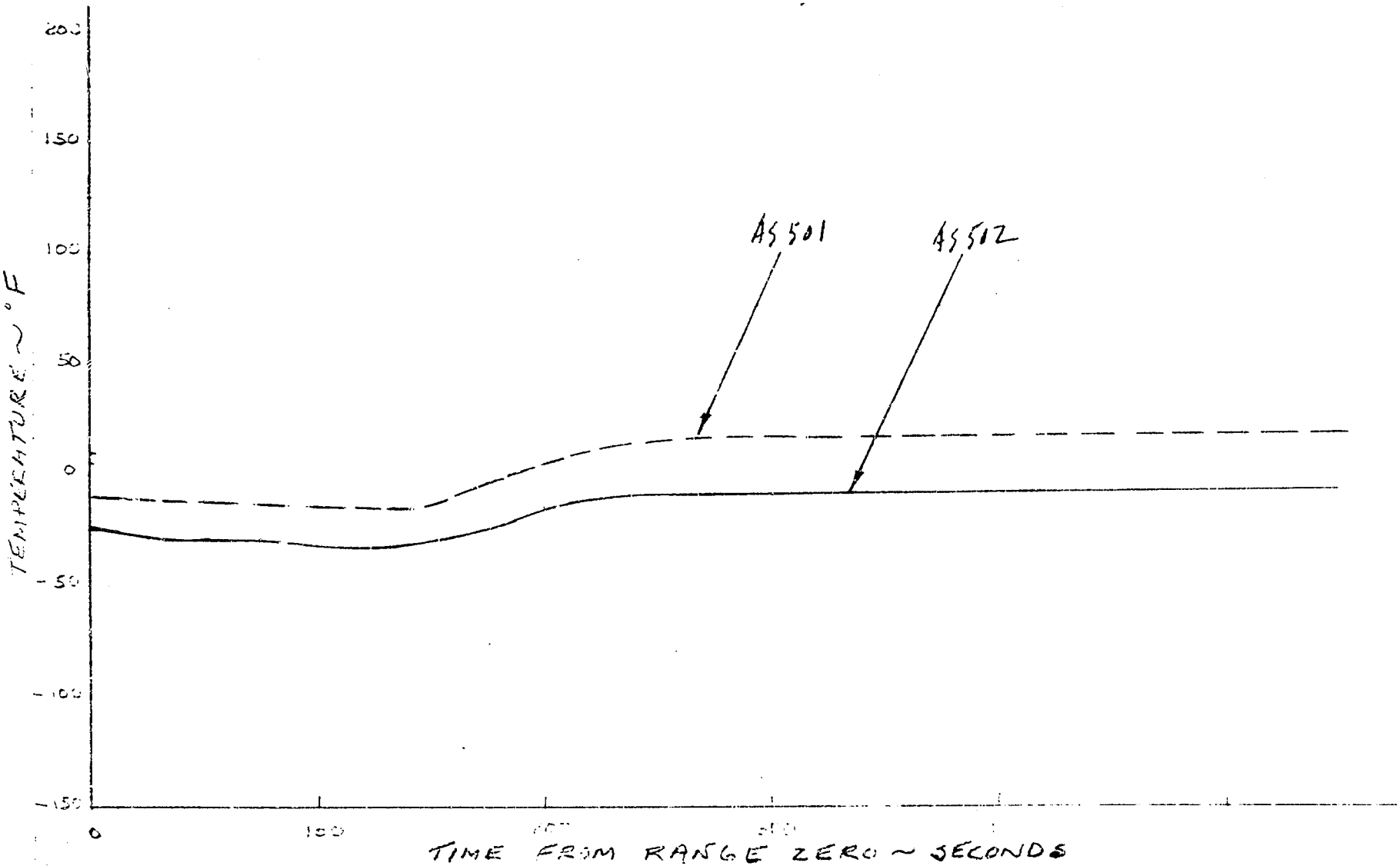

Figure 24. Thrust Cone Forward Surface Temperature (C232), Station 153

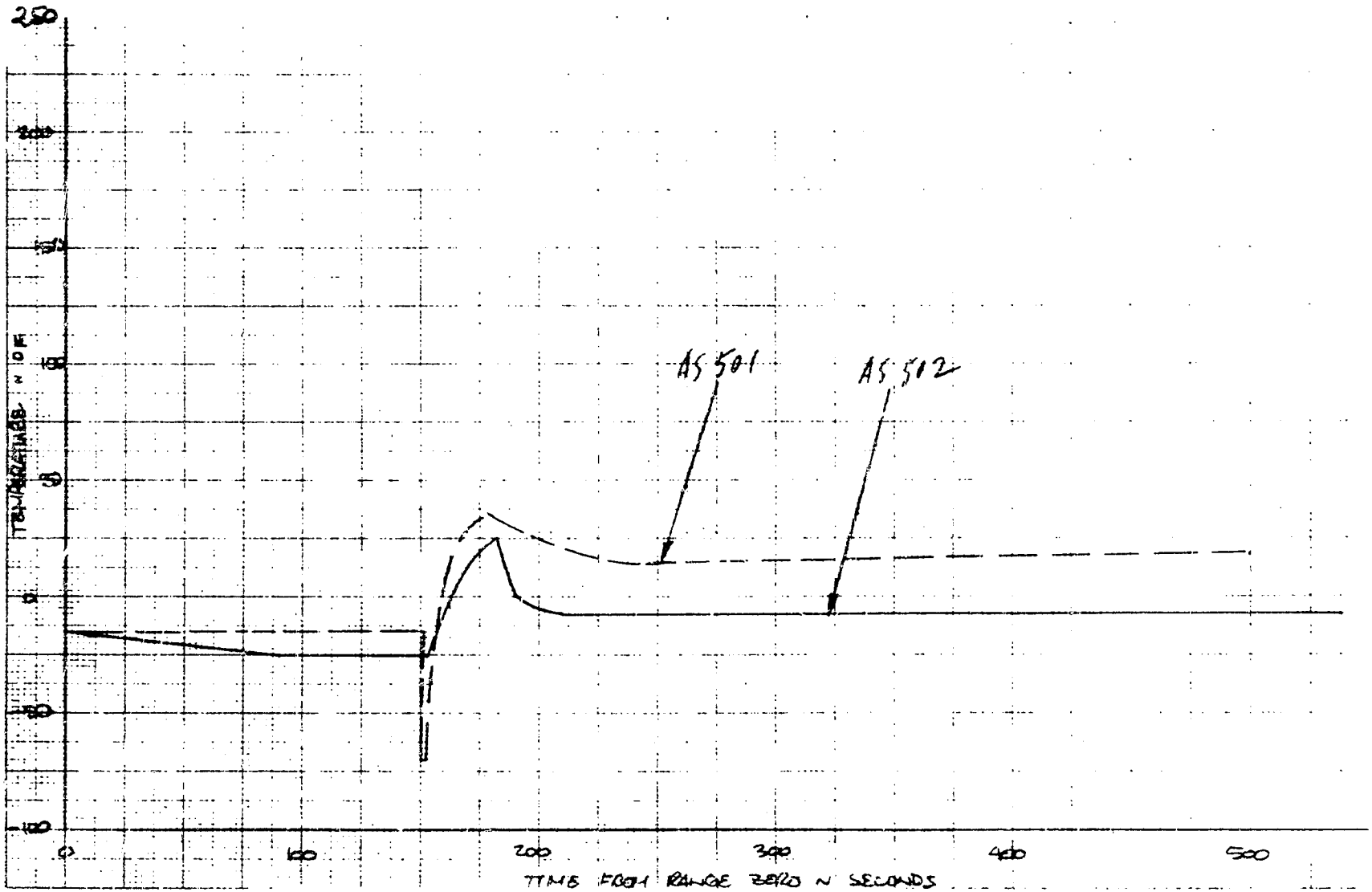

Figure 25. Engine Compartment Thrust Cone Surface Temperature (C916), Station 167

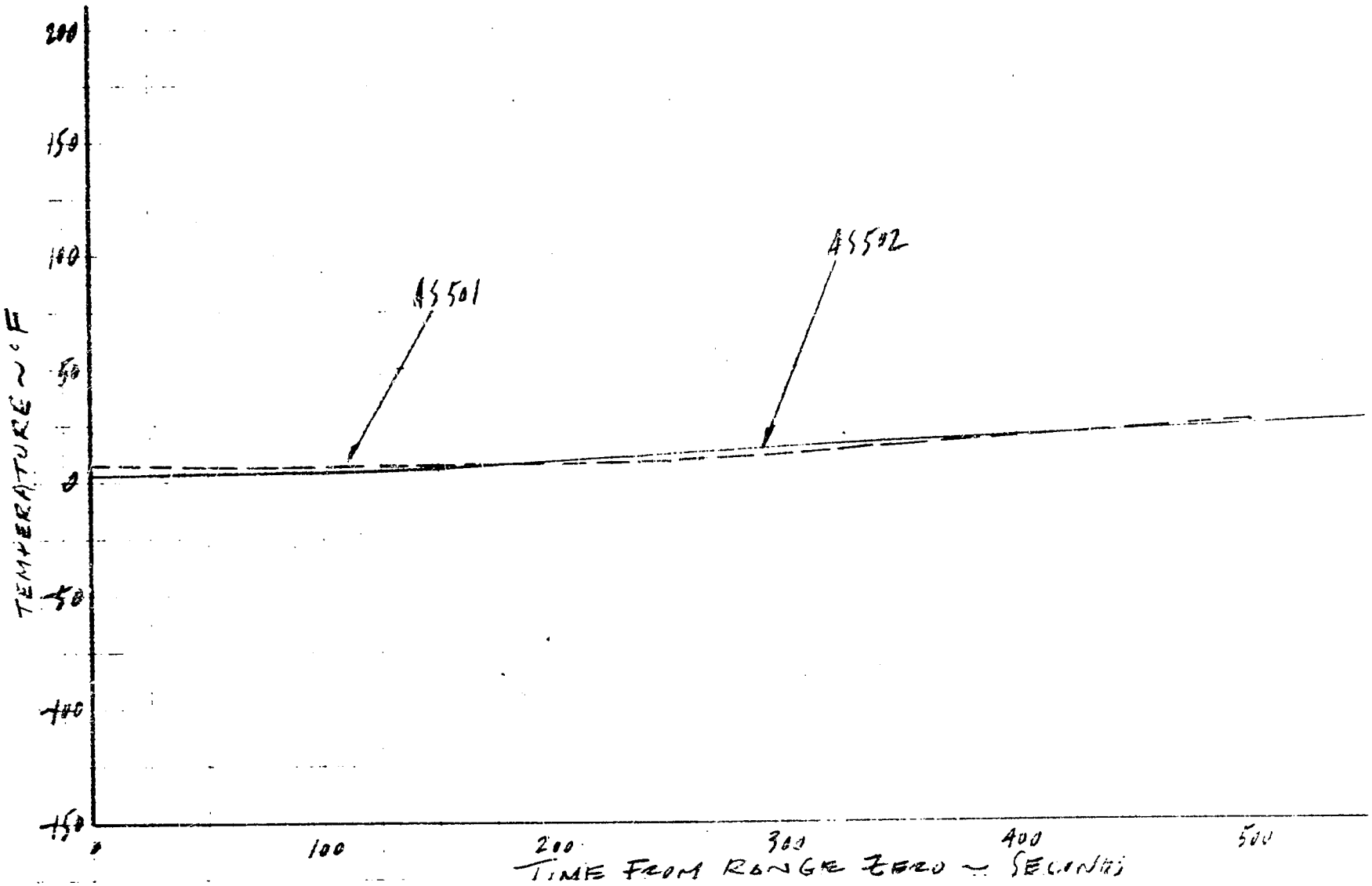

Figure 26. Thrust Cone Forward Surface Temperature (C238), Station 223

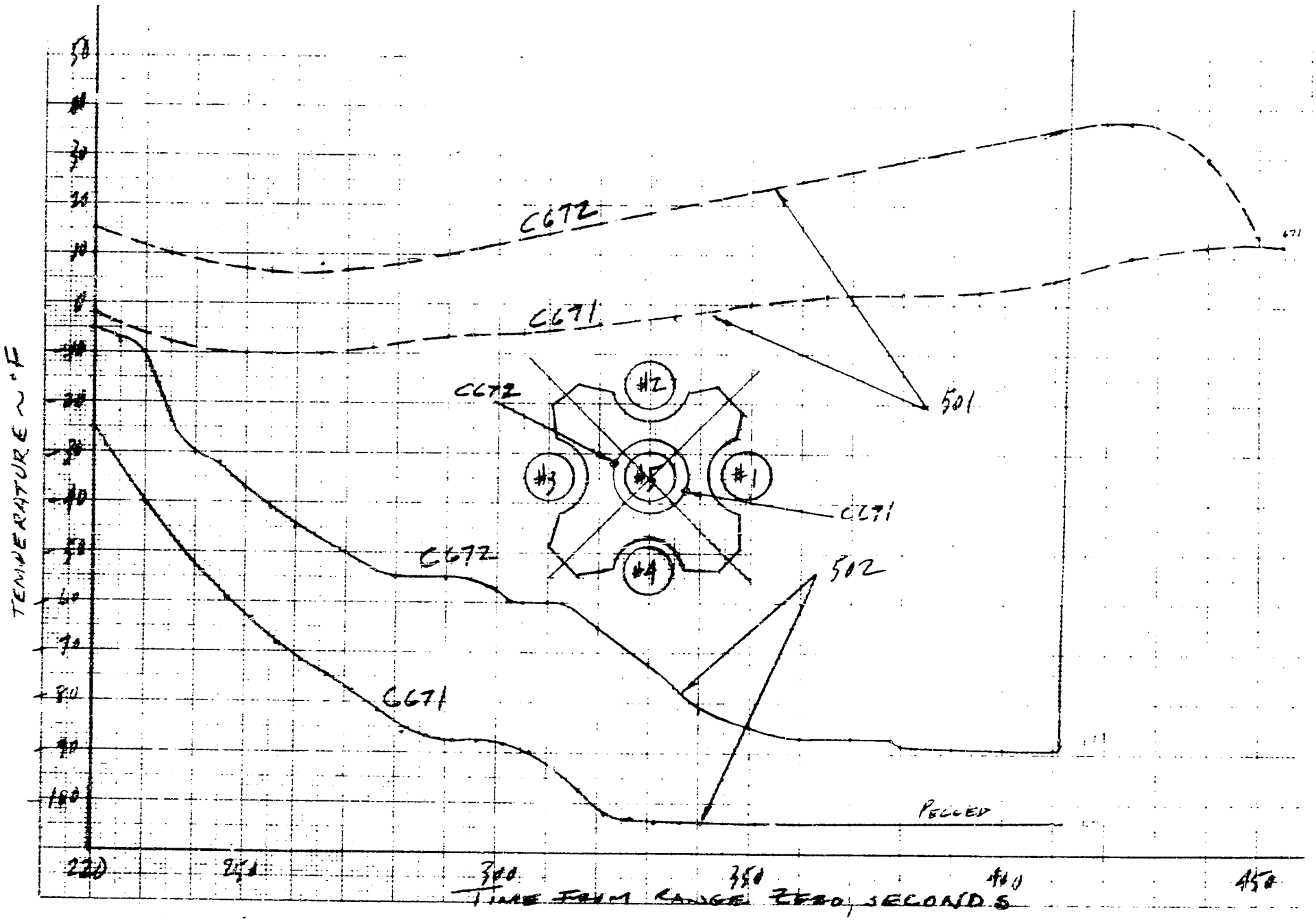

Figure 27. Engine Compartment Gas Temperature, Station 82

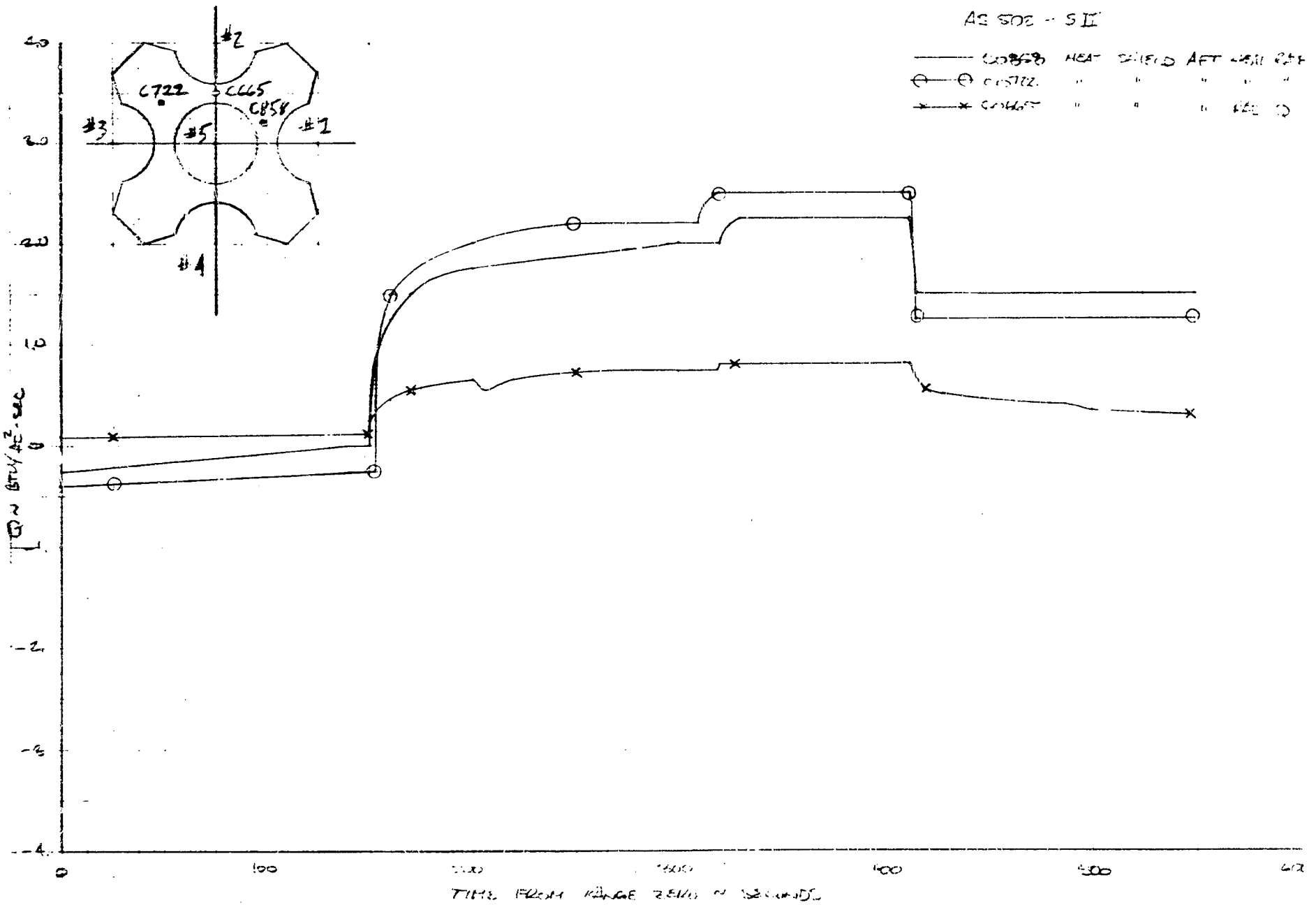

Figure 28. AS-502 S-II Heat Shield Rate and Flux

PERFORMANCE

Engine 202 Performance Decay: Range Time 260 to 319 Seconds

Description of Event. A number of engine parameters indicated a gradual decay in engine 202 performance beginning approximately at the 260-second range time period and continuing to the 319-second point, at which time an abrupt downshift in engine performance was experienced. A list of engine parameters over this time interval is presented in Table 2. Graphic plots of main chamber pressure and gas generator chamber pressure are presented in Fig. 29 and 30, illustrating the gradual decay in these parameters.

Hypothesis. Cryogenic leakage, which had begun to chill down the engine compartment at approximately 220 seconds range time, was progressive in nature, increasing with time. After 260 seconds range time, it was of sufficient magnitude to be noted in measured performance parameters. The source of leakage was the ASI fuel feed system, in or near the downstream 1/2-inch bellows section. Based on the fuel pump flow coefficient relationship Q/N, leakage from the ASI fuel line increased to a maximum level of approximately 2 lb/sec at 290 seconds. At 319 seconds range time, an abrupt performance loss occurred. The 319-second performance shift is explained in the next section.

Corroboration of Hypothesis. Fuel pump speeds and flows for all five engines were compared over the 250 to 318 seconds interval (Table 3). The ratio of Δpump speed/Δpump flow was the lowest for the No. 2 engine fuel pump, suggesting a decrease in downstream resistance (fuel pump outlet and main chamber pressure). Stage acceptance data for this pump were then compared over the same portion of the acceptance test (Table 3). A higher ratio of Δpump speed/Δpump flow was noted during the acceptance test than on the flight indicating that a change in engine 202 pump speed/flow characteristics had occurred during the flight.

TABLE 2

ENGINE 202 PERFORMANCE CHANGES, 250 to 318 SECONDS RANGE TIME

(Engine J2044 In-Run Flight Performance Shifts)

Parameter Number	Parameter	Measured Flight Shift (250 to 318 seconds)
		Temperature, F
C001-202	Fuel Pump Discharge	+0.03
C002-202	Oxidizer Pump Discharge	-0.02
C003-202	Fuel Turbine Inlet	-0.7
C004-202	Oxidizer Turbine Inlet	-3.4
C008-202	Gas Generator Fuel Valve Inlet	-0.52
C009-202	Gas Generator Oxidizer Valve Inlet	+0.04
C014-202	Main Fuel Injection	+1.3
C326-202	Oxidizer Turbine Outlet	-4.0
C329-202	Thrust Chamber Jacket	-1.0
C585-202	Heat Exchanger Outlet	-65.7
C663-202	Engine Inlet Oxidizer	-0.02
C664-202	Engine Inlet Fuel	+0.03
		Pressure, psi
D001-202	Main Fuel Injection	+4.0
D002-202	Gas Generator Fuel Injection	+4.0
D004-202	Fuel Pump Balance Piston Cavity	-2.1
D005-202	Fuel Pump Discharge	-1.3
D006-202	Main Oxidizer Injection	-2.5
D007-202	Gas Generator Oxidizer Injection	+3.2
D008-202	Oxidizer Turbine Inlet	+0.6
D010-202	Oxidizer Turbine Outlet	-0.1
D011-202	Oxidizer Pump Discharge	-7.7
D013-202	Thrust Chamber	-6.4
D014-202	Gas Generator Chamber	-7.9
D091-202	Engine Inlet Oxidizer	+0.18
D092-202	Engine Inlet Fuel	-0.49
D166-202	Yaw Actuator	+1270.4
D167-202	Pitch Actuator	+26.1
D191-202	PC Valve Outlet	-0.1
D192-202	Oxidizer Pump Primary Seal	+0.5
D231-202	Fuel Tank Pressure Regulator Inlet	-4.6
		Flowrate gpm
F001-202	Main Fuel	+86.9
F002-202	Main Oxidizer	-2.2
		Speed, rpm
T001-202	Fuel Pump	+105.8
T002-202	Oxidizer Pump	-22.2

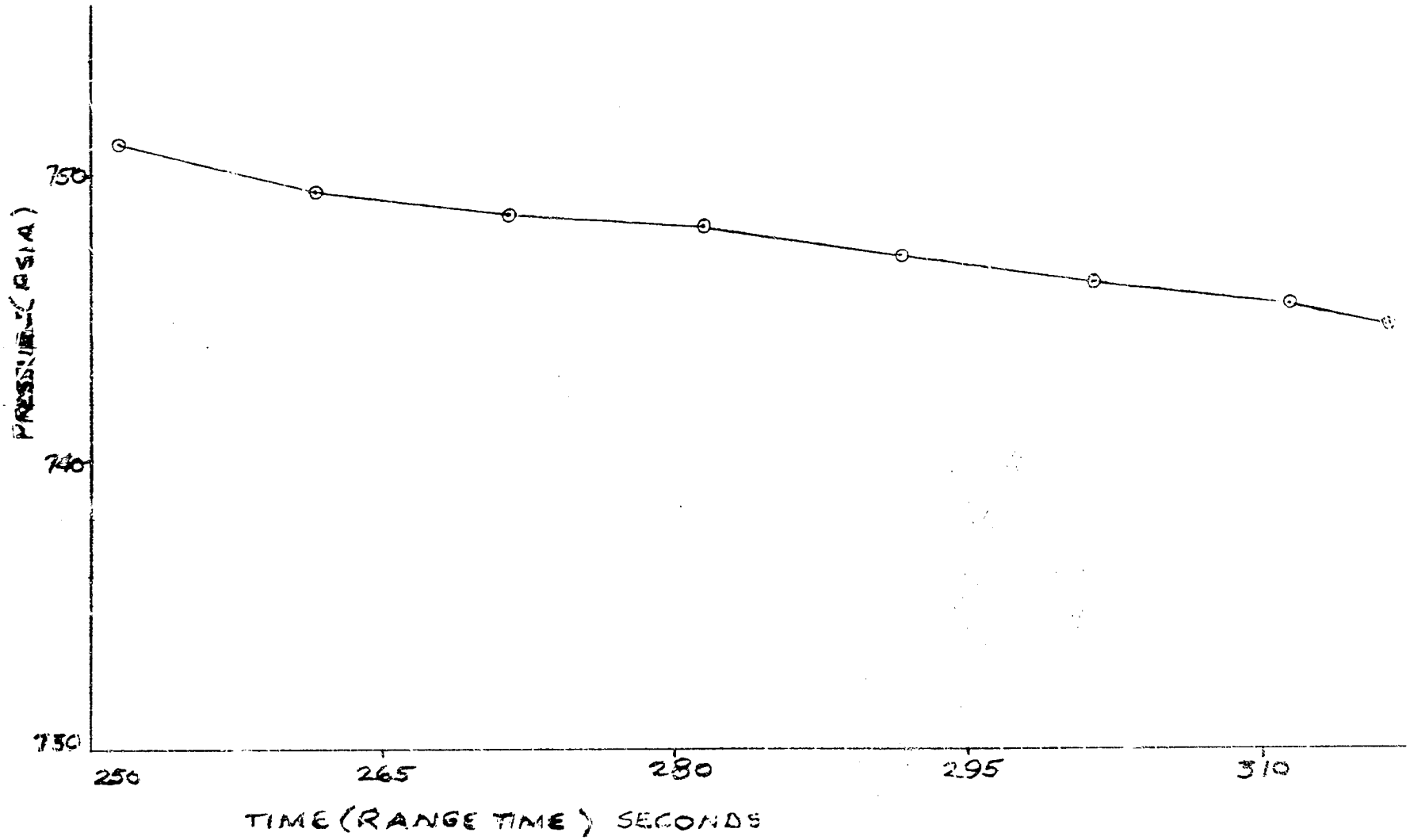

Figure 29. AS-502 S-II Main Chamber Pressure Performance Decay, 250 to 318 Seconds Range Time (Engine J2044)

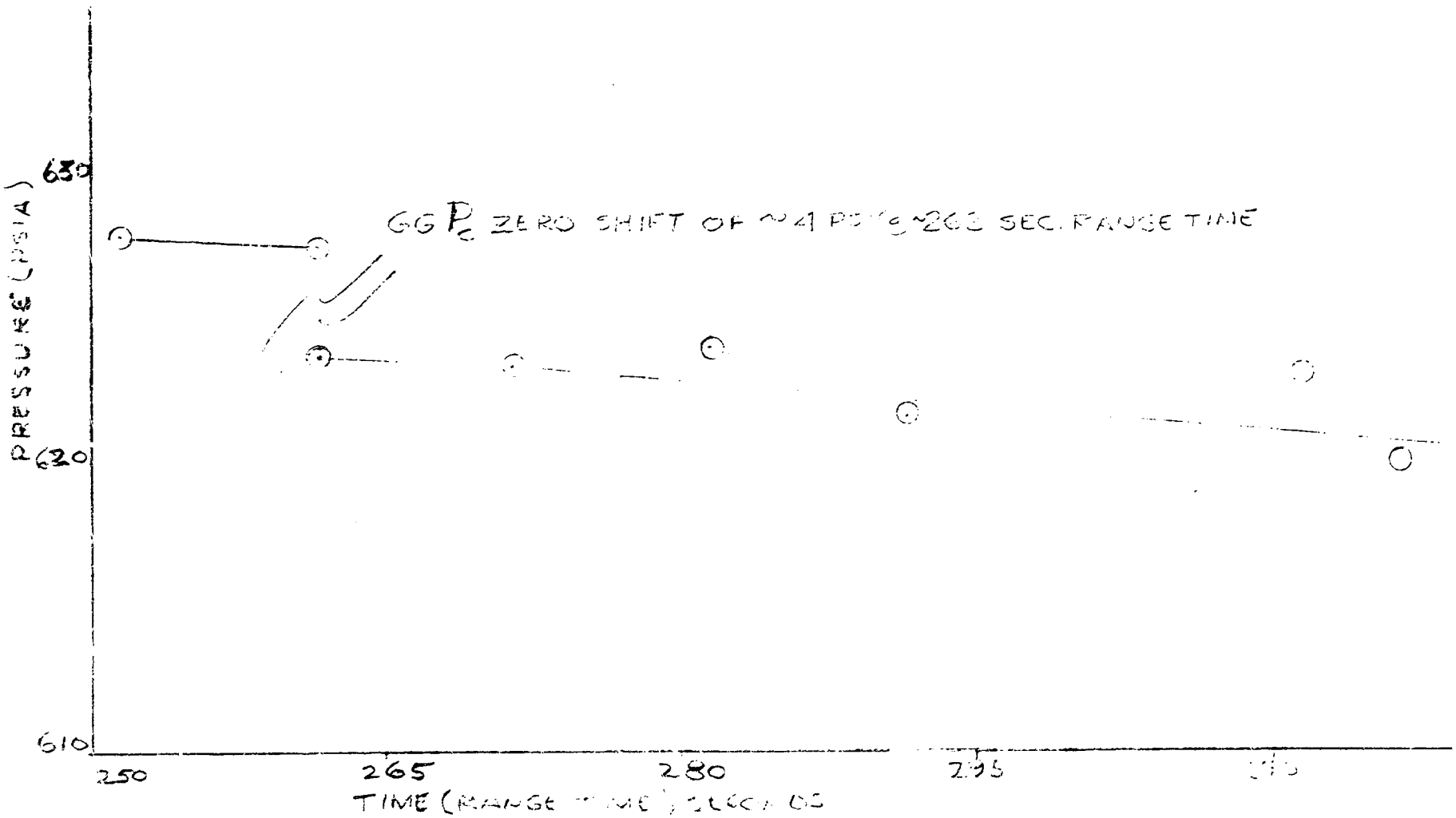

Figure 30. AS-502 S-II Gas Generator Chamber Pressure Performance Decay, 250 to 318 Seconds Range Time (Engine J2044)

TABLE 3

COMPARATIVE PERFORMANCE OF S-II ENGINES

	Range Time, seconds	Engine Number				
		201	202	203	204	205
Flight Data AS-502						
Fuel rpm	250	27,217	26,499	27,048	26,890	27,320
Fuel rpm	318	27,313	26,597	27,178	26,988	27,390
△ rpm	250 to 318	+96	+98	+130	+98	+70
Fuel gpm	250	7,901	7,803	7,836	7,995	8,119
Fuel gpm	318	7,923	7,850	7,875	8,017	8,130
△ gpm	250 to 318	+22	+27	+39	+22	+11
Ratio △rpm/△gpm		4.36	2.08	3.33	4.45	6.36
Oxidizer rpm	250	8,569	8,547	8,611	8,620	8,603
Oxidizer rpm	318	8,563	8,526	8,602	8,617	8,601
△ rpm	250 to 318	-6	-21	-9	-3	-2
Oxidizer gpm	250	2,846	2,820	2,854	2,841	2,837
Oxidizer gpm	318	2,846	2,813	2,848	2,836	2,835
△ gpm	250 to 318	0	-7	-6	-5	-2
Stage Acceptance Data						
Fuel rpm	250	-	26,625	-	-	-
Fuel rpm	318	-	26,773	-	-	-
△ rpm	250 to 318	-	+148	-	-	-
Fuel gpm	250	-	7,845	-	-	-
Fuel gpm	318	-	7,893	-	-	-
△ gpm	250 to 318	-	+48	-	-	-
Ratio △rpm/△gpm		-	3.08	-	-	-
Oxidizer rpm	250	-	8,651	-	-	-
Oxidizer rpm	318	-	8,653	-	-	-
△ rpm	250 to 318	-	+2	-	-	-
Oxidizer gpm	250	-	2,854	-	-	-
Oxidizer gpm	318	-	2,856	-	-	-
△ gpm	250 to 318	-	+2	-	-	-

Oxidizer pump speed and flow relationships for all five engines were also compared (Table 5). Over the 250- to 318-second time interval, characteristically the oxidizer flows and speed are normally quite stable. The only noteworthy observation was that engine 202 oxidizer pump speed decreased more than twice the rpm of any other engine (although the range was small). Stage acceptance data were then compared over the same portion of the acceptance test. Flight and acceptance flowrates agreed well in character, but the acceptance pump speed did not show the fall-off in rpm that was observed during the flight. The implication is that the decrease in downstream resistance (namely, oxidizer pump outlet pressure and main chamber pressure) is a real phenomenon, since it was confirmed by both fuel and oxidizer pump characteristics.

Of eight critical pressure parameters related to gas generator and thrust chamber operation, five indicated gradual decreases: gas generator chamber, main chamber, oxidizer injection, and fuel and oxilizer pump discharge pressures.

A 1.3 F increase in fuel injection temperature was noted during the 250- to 318-second time interval, despite the slight increase in total engine fuel flow in that same period, suggesting that less fuel was passing through the thrust chamber. The difference between less thrust chamber fuel flow and more engine total fuel flow can be considered as cryogenic leakage chilling the engine area.

Oxidizer system resistance data during this performance downtrend remained unaffected, even holding firm after the 319-second performance shift. Hence, the oxidizer system integrity for engine 202 during the time period in question is not suspect.

Data Not in Agreement

In general, engine data over a 68-second interval are influenced by many separate trend characteristics, so that a clear confirmation or refutation

of a gradual small performance degradation is difficult. Some of the contradictory data are:

1. Three critical pressure parameters increased during this time interval: main fuel injection, gas generator fuel injection, and gas generator oxidizer injection pressures. These contradict the performance decay trend indicated by the other five previously noted pressure measurements.

2. The possibility was investigated that the chilldown in instrumentation package temperatures was responsible for transducer drift and, therefore, misleading measurements. Although such drift can occur, the gas generator and main chamber pressure downtrends halted after 319 seconds range time, despite continued chilling of the instrument packages. Therefore, the temperature effect, if any, on these transducers is not a factor in the observed performance trend.

Engine 202 Gas Generator Performance Shift: Range Time 262 Seconds

Description of Event. The 100-sample/second trace of gas generator chamber pressure indicated an abrupt shift at 262 seconds range time. Data samples taken before (261.5 seconds) and after (266.5 seconds) indicate the gas generator chamber pressure dropped 4 psi (Fig. 30).

Conclusions. An instrument zero shift occurred at this point, giving a false reading from this point on through the remainder of duration.

Corroboration of Hypothesis. Engine data reduction immediately before and after the indicated chamber pressure shift revealed an increase in both gas generator system resistances postshift. The system resistances then remained essentially at their increased value for the remainder of the test (Table 4).

TABLE 4

ENGINE DATA AT 262 SECONDS

Parameter	Range Time, seconds				
	211.5 (60-second performance slice)	261.5 (Pre-gas generator shift)	266.5 (Post-gas generator shift)	317.0 (Pre-engine shift)	327.0 (Post-engine shift)
Gas Generator Chamber Pressure, psia	634.6	634.1	630.1	626.6	614.8
Gas Generator Oxidizer System Resistance, pounds	173.3	173.7	182.3	182.4	179.2
Gas Generator Fuel System Resistance, pounds	343.1	343.8	357.0	361.6	360.4
Fuel Turbine Pressure Ratio*	7.12	7.11	7.06	6.98	6.99

*Fuel turbine pressure ratio is normally a constant and a function of fuel turbine inlet pressure (GG P_c) and fuel turbine outlet pressure. The decline in the ratio indicates an error in the upstream pressure (GG P_c).

Engine 202 Performance Shift: Range Time 319 Seconds

Description of Event. At 319 seconds range time, engine 202 experienced a rapid performance shift. Changes in significant parameters are recorded in Table 5 and shown in Fig. 31 through 47. At the same time as the performance shift, engine environment chilldown rates became greater, indicating cryogenic leakage of increased severity; further, hydraulic ΔP transducers on both of the engine gimbal actuators indicated a compressive loading of approximately 600 psi each.

Hypothesis. The engine 202 performance shift noted at 319 seconds range time resulted from partial failure of the main injector, a portion of which struck the interior of the thrust chamber bell near the exit plane, rupturing several fuel tubes. Gradual performance decay of engine 202, commencing at 220 seconds, was caused by gradual failure of the ASI fuel line, which resulted in progressive erosion of the central portion of the injector. At 319 seconds, the erosion had progressed to the point that a section of the main injector broke away and struck the chamber. The ruptured thrust chamber tubes leaked a total of 7 to 10 lb/sec of fuel, resulting in the sudden performance shift and displacement of the thrust vector with attendant loads of approximately 7800 pounds in each actuator.

Corroboration of Hypothesis. Initial analysis of flight data indicated a decrease in all pressures, an increase in gas generator temperatures, and an increase in main fuel injection temperature for engine 202 at 319 seconds range time. An initial postulation of external fuel leakage was made, based upon flight data coupled with the decrease in environmental temperatures. Using engine model data and engine performance calculations (Table 6), an oxidizer leak was rejected as a possibility.

Observed specific impulse shift of -15.0 seconds is equivalent to a 10.6 lb/sec fuel flow leakage upstream of the thrust chamber. The following

TABLE 5

AS-502 S-II IN-RUN FLIGHT PERFORMANCE SHIFTS

(Engine J2044)

Parameter Number	Parameter	Measured Flight Shift (319 seconds)
		Temperature, F
C001-202	Fuel Pump Discharge	-0.31
C002-202	Oxidizer Pump Discharge	-0.09
C003-202	Fuel Turbine Inlet	+11.9
C004-202	Oxidizer Turbine Inlet	+10.0
C008-202	Gas Generator Fuel Valve Inlet	-0.26
C009-202	Gas Generator Oxidizer Valve Inlet	-0.17
C014-202	Main Fuel Injection	+13.8
C326-202	Oxidizer Turbine Outlet	+7.9
C329-202	Thrust Chamber Jacket	-2.5
C585-202	Heat Exchanger Outlet	+16.7
C663-202	Engine Inlet Oxidizer	+0.04
C664-202	Engine Inlet Fuel	+0.03
		Pressure, psi
D001-202	Main Fuel Injection	-31.4
D002-202	Gas Generator Fuel Injection	-13.9
D004-202	Fuel Pump Balance Piston Cavity	-24.4
D005-202	Fuel Pump Discharge	-41.9
D006-202	Main Oxidizer Injection	-22.7
D007-202	Gas Generator Oxidizer Injection	-14.5
D008-202	Oxidizer Turbine Inlet	-1.6
D010-202	Oxidizer Turbine Outlet	-0.6
D011-202	Oxidizer Pump Discharge	-28.2
D013-202	Thrust Chamber	-22.9
D014-202	Gas Generator Chamber	-11.8
D091-202	Engine Inlet Oxidizer	-0.16
D092-202	Engine Inlet Fuel	-0.28
D166-202	Yaw Actuator ΔP	+657.5
D167-202	Pitch Actuator ΔP	+499.9
D191-202	PU Valve Outlet	-5.0
D192-202	Oxidizer Pump Primary Seal	+0.3
D231-202	Fuel Tank Pressure Regulator Inlet	-3.9
		Flowrate, gpm
F001-202	Main Fuel	+117.5
F002-202	Main Oxidizer	-7.4
		Speed, rpm
T001-202	Fuel Pump	-83.0
T002-202	Oxidizer Pump	-53.5

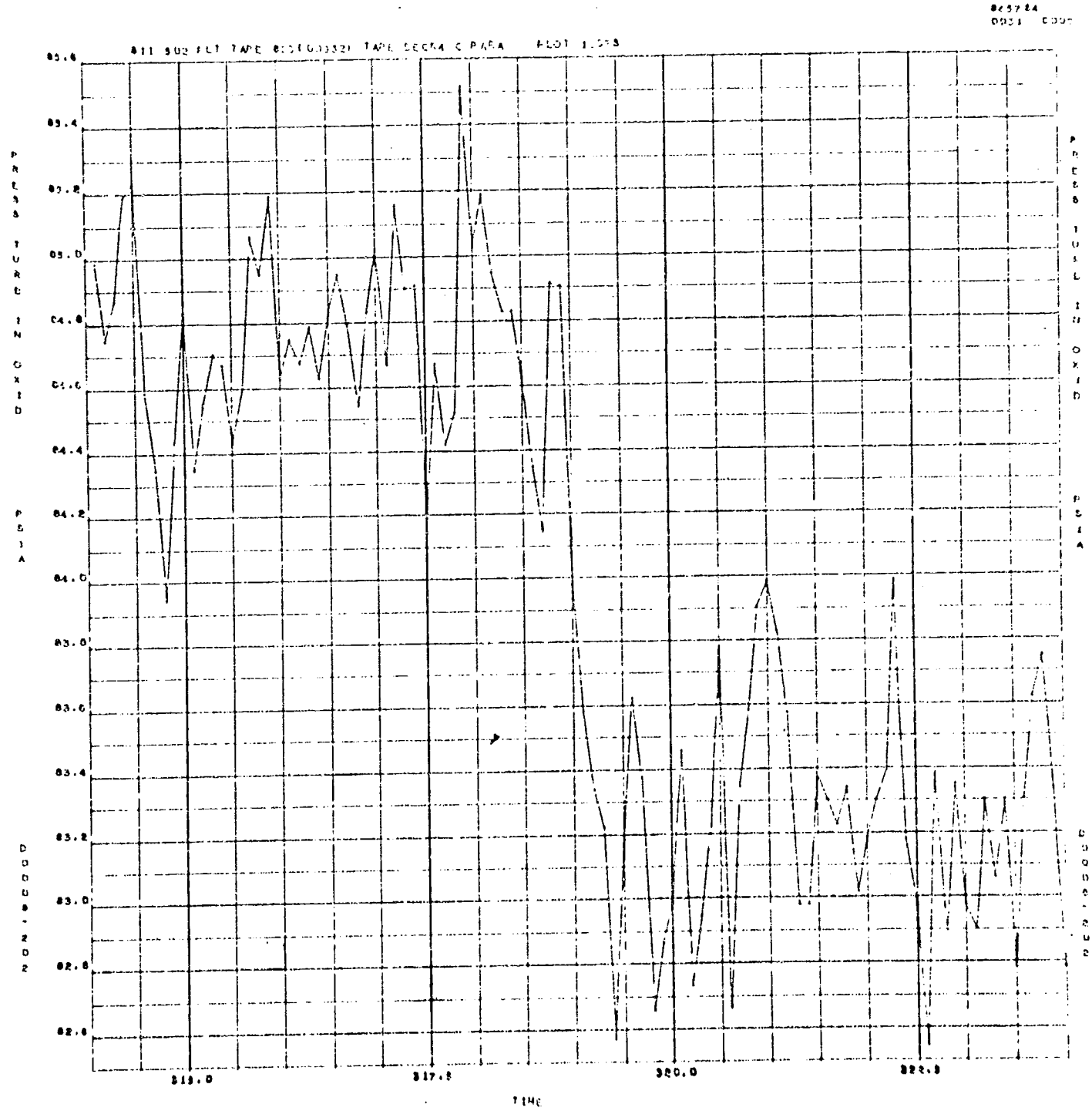

Figure 31. Turbine Inlet Oxidizer Pressure

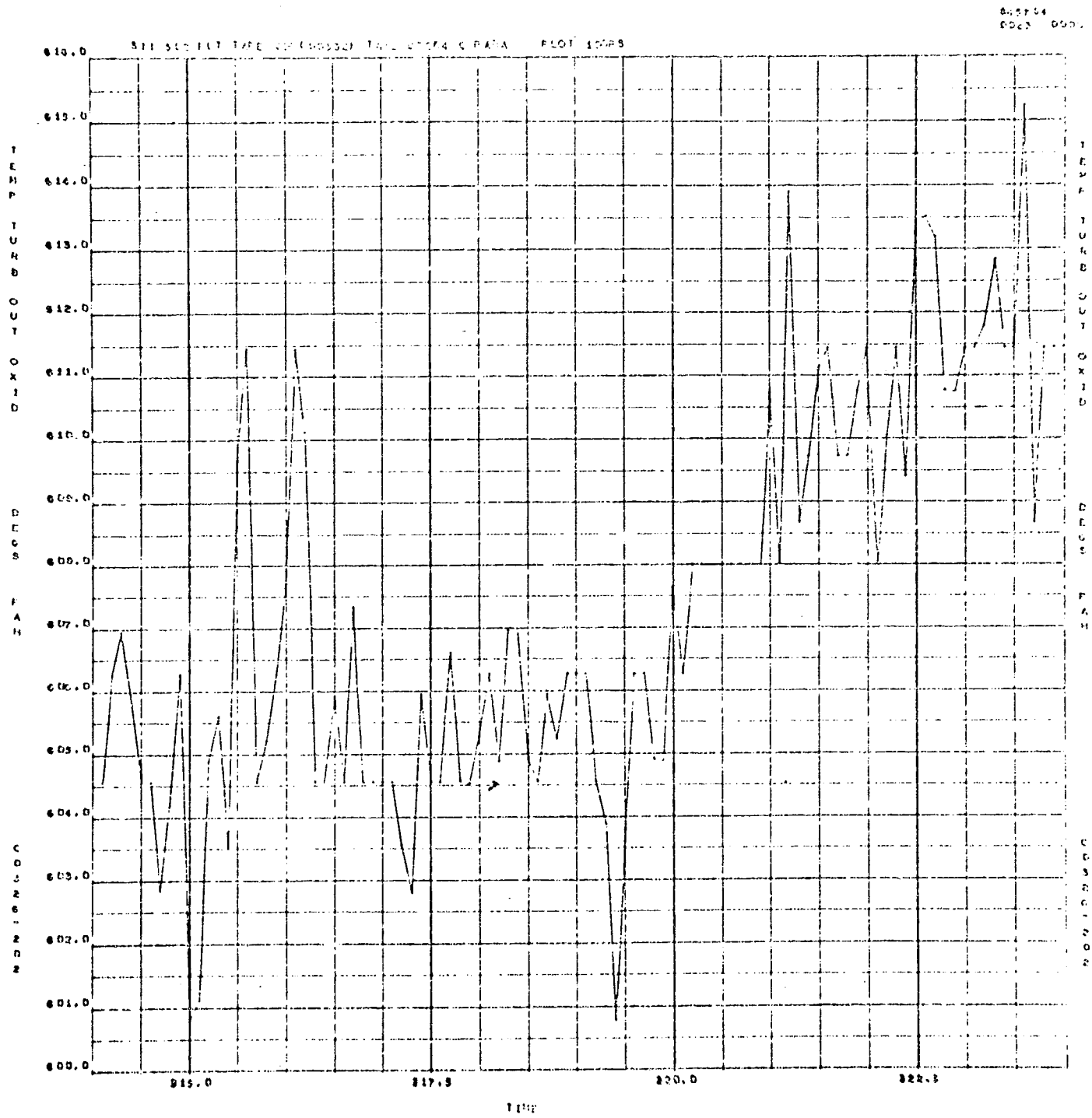

Figure 32. Turbine Outlet Oxidizer Temperature

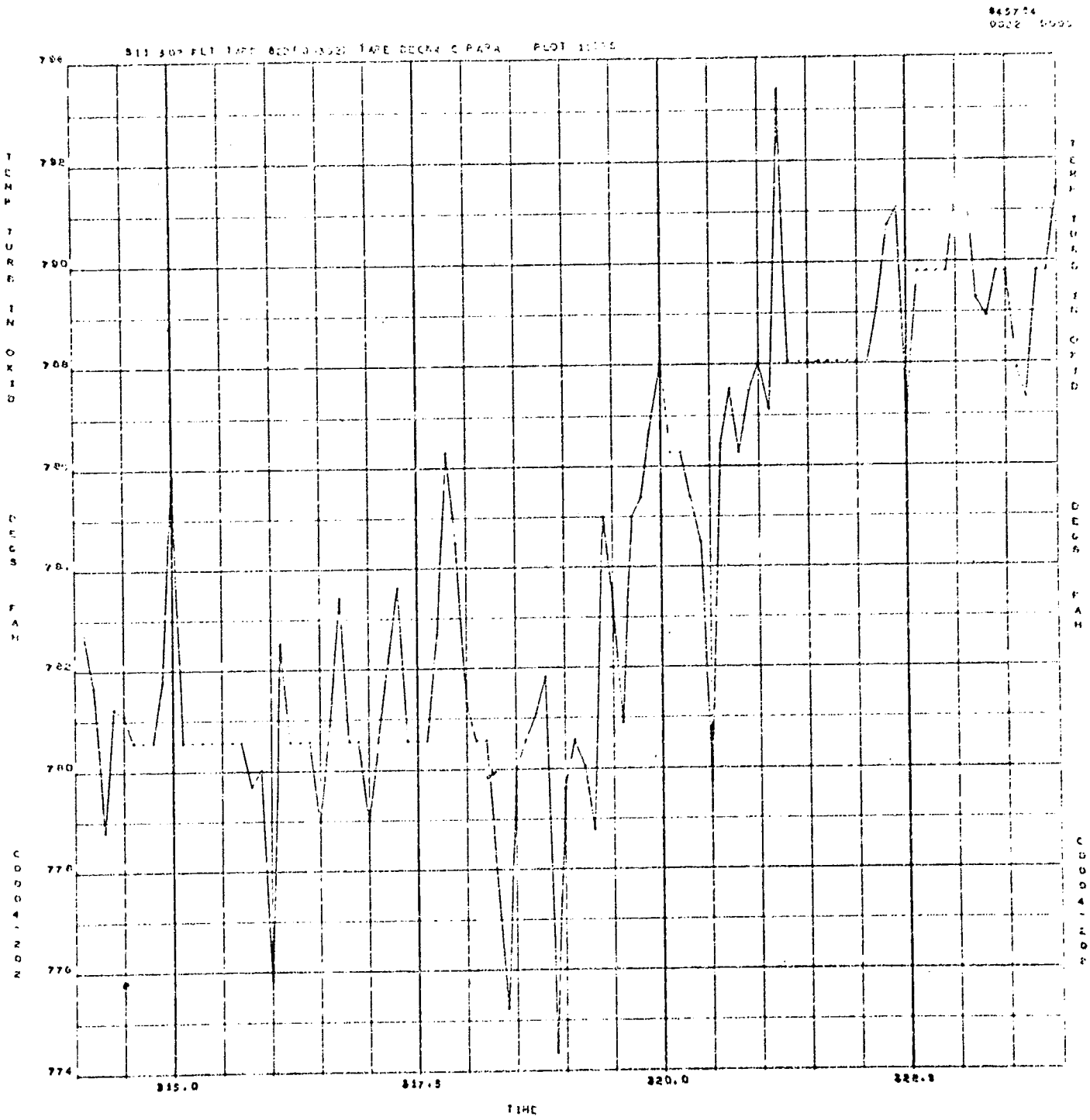

Figure 33. Turbine Inlet Oxidizer Temperature

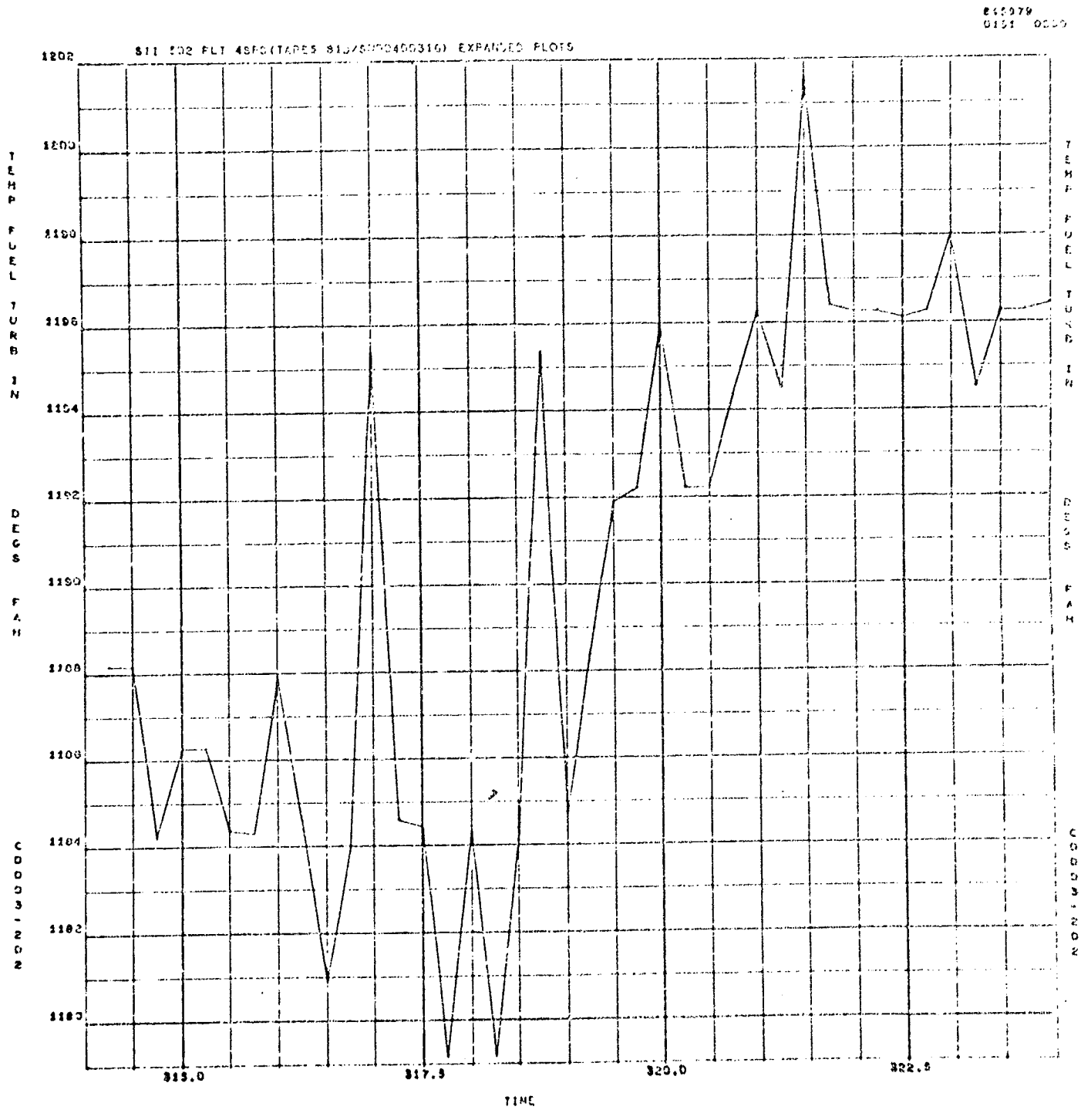

Figure 34. Fuel Turbine Inlet Temperature

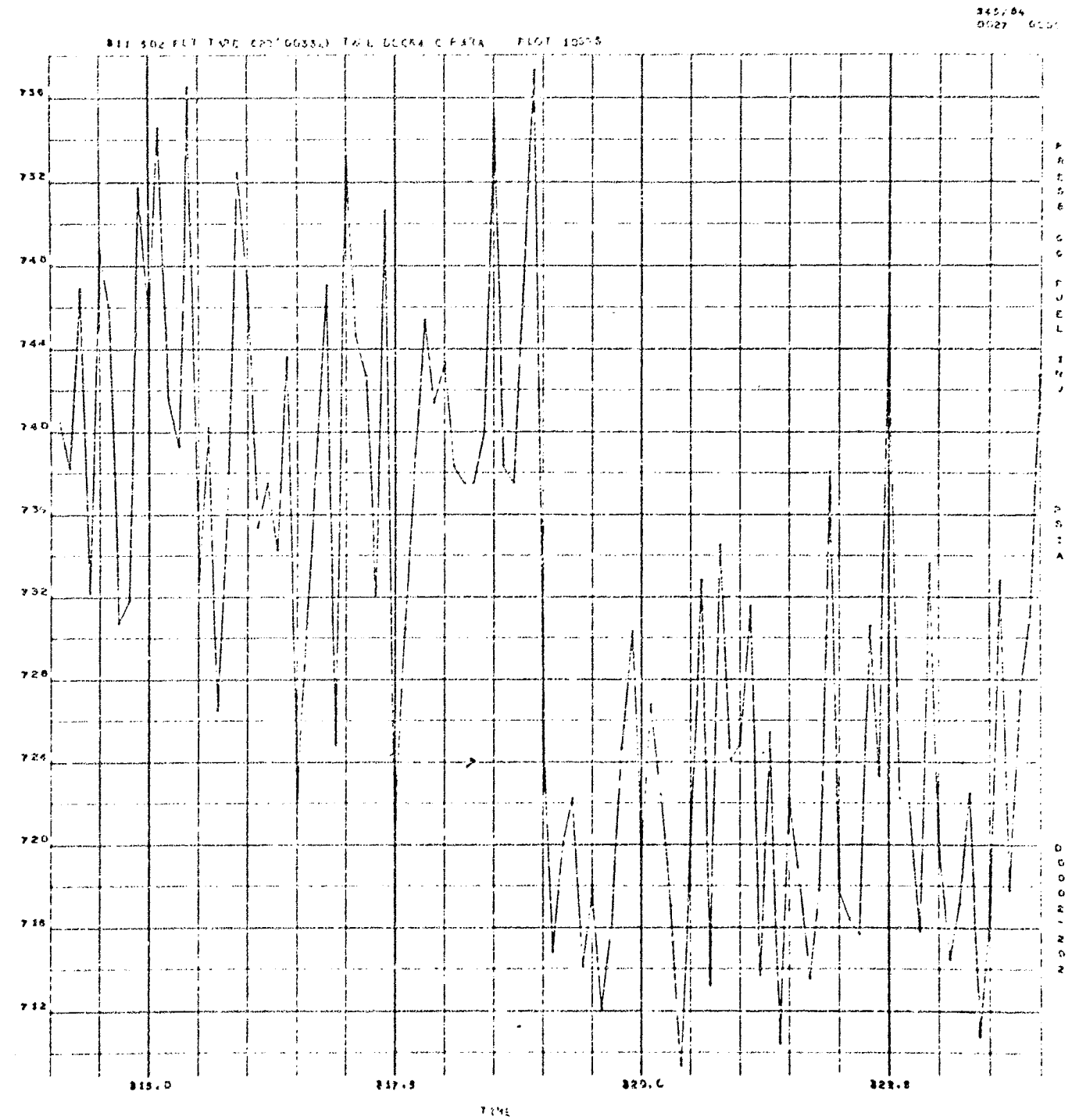

Figure 35. Gas Generator Fuel Injector Pressure

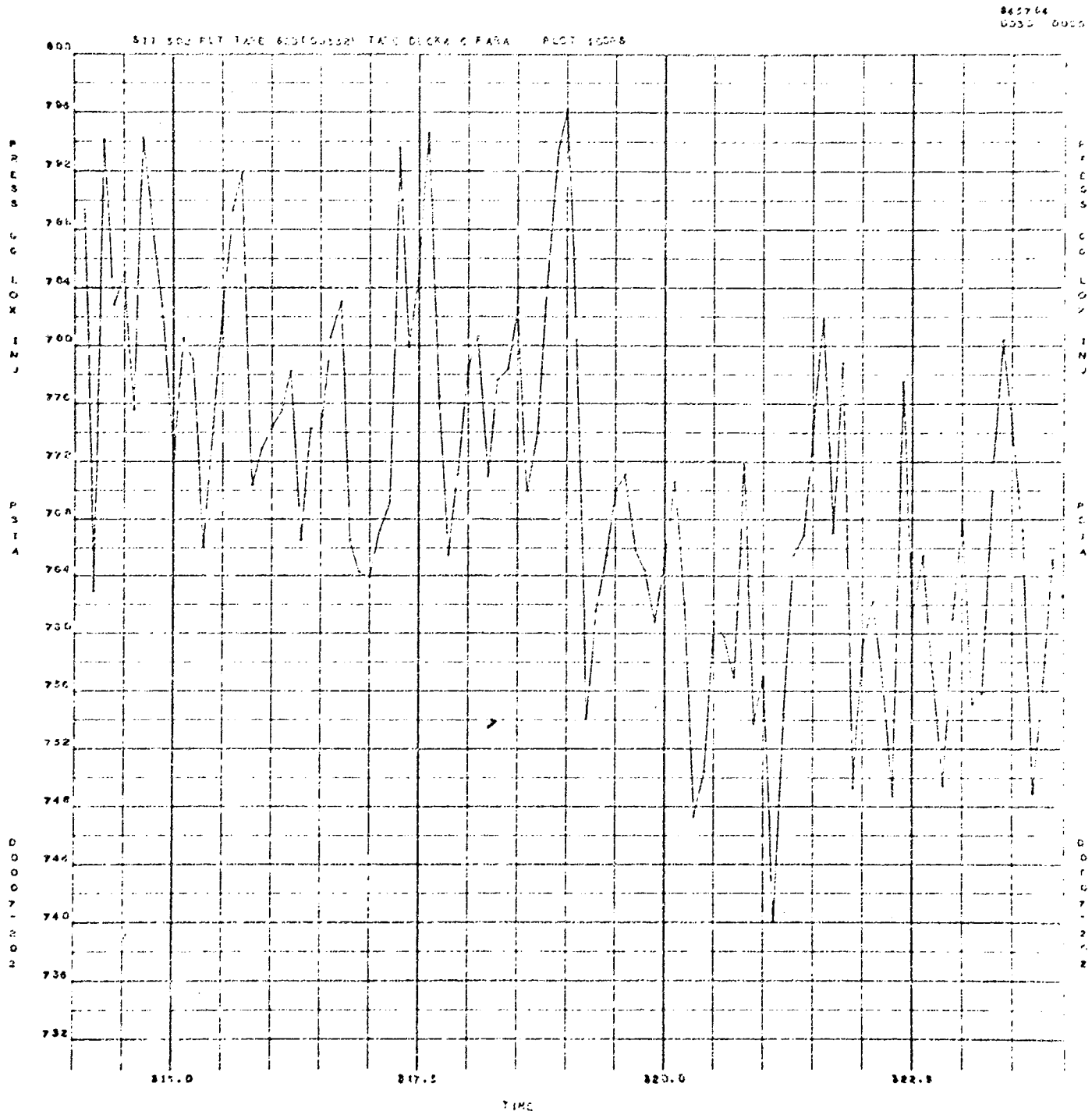

Figure 36. Gas Generator Oxidizer Injector Pressure

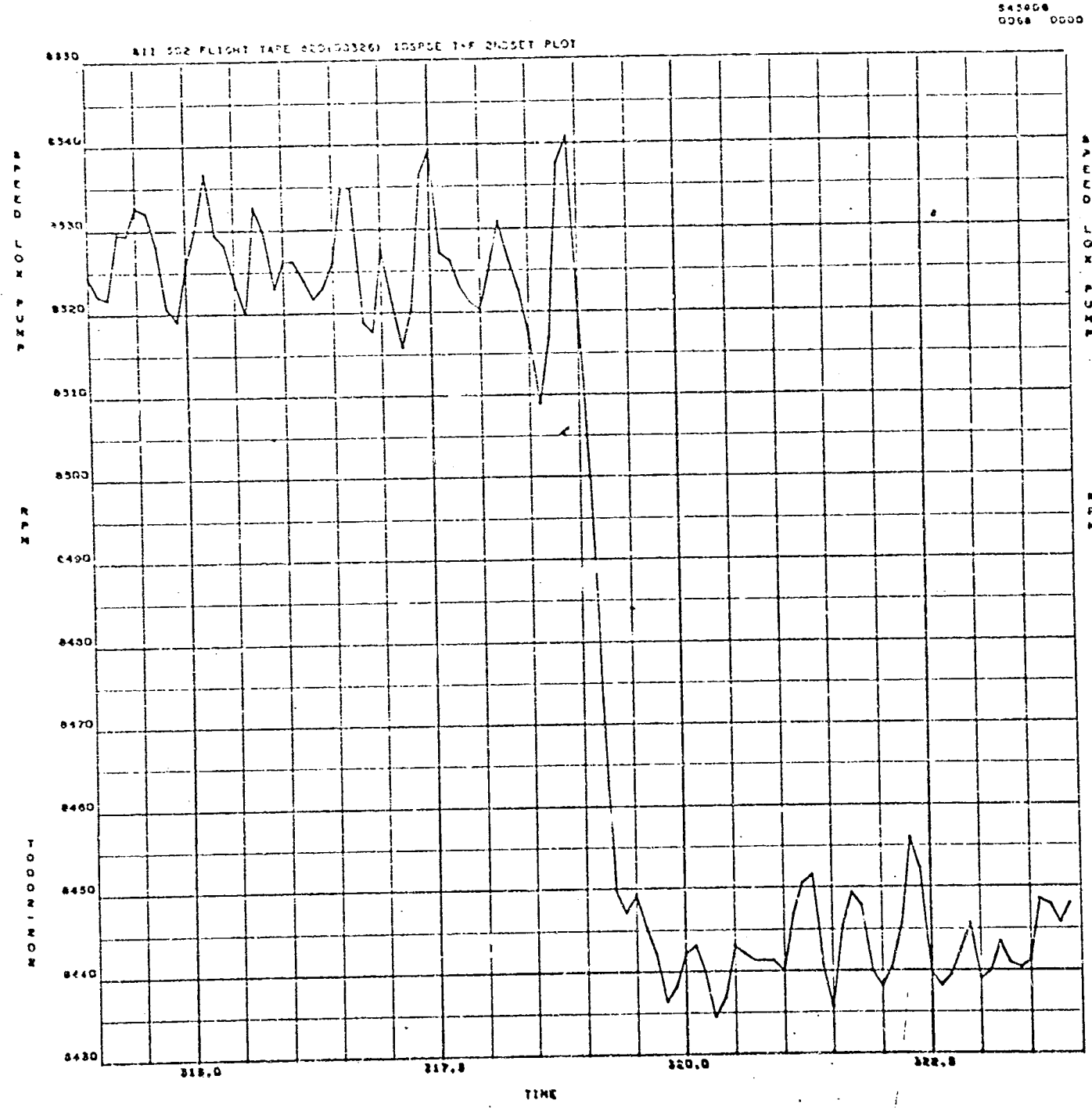

Figure 37. Oxidizer Pump Speed

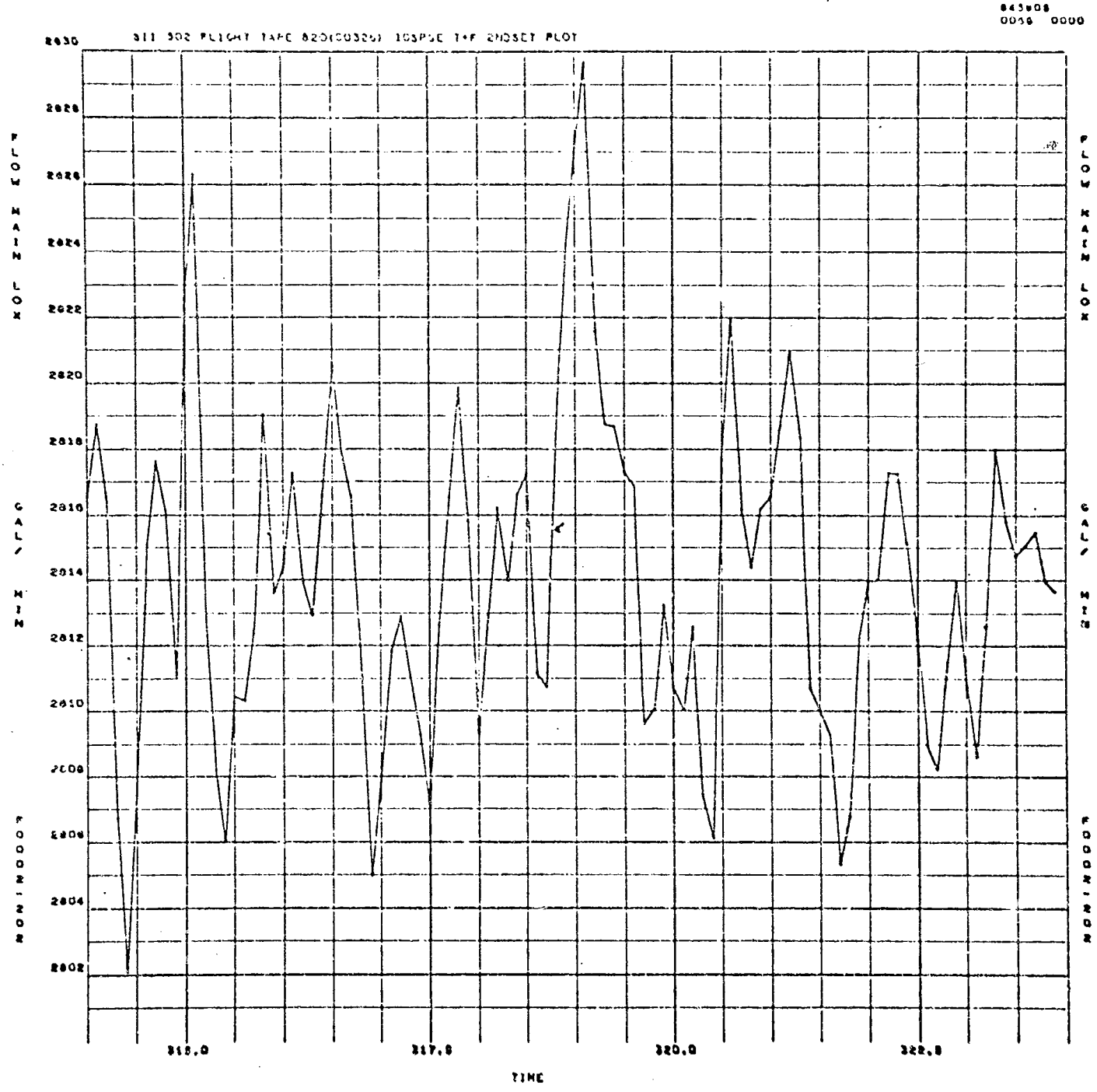

Figure 38. Mainstage Oxidizer Flow

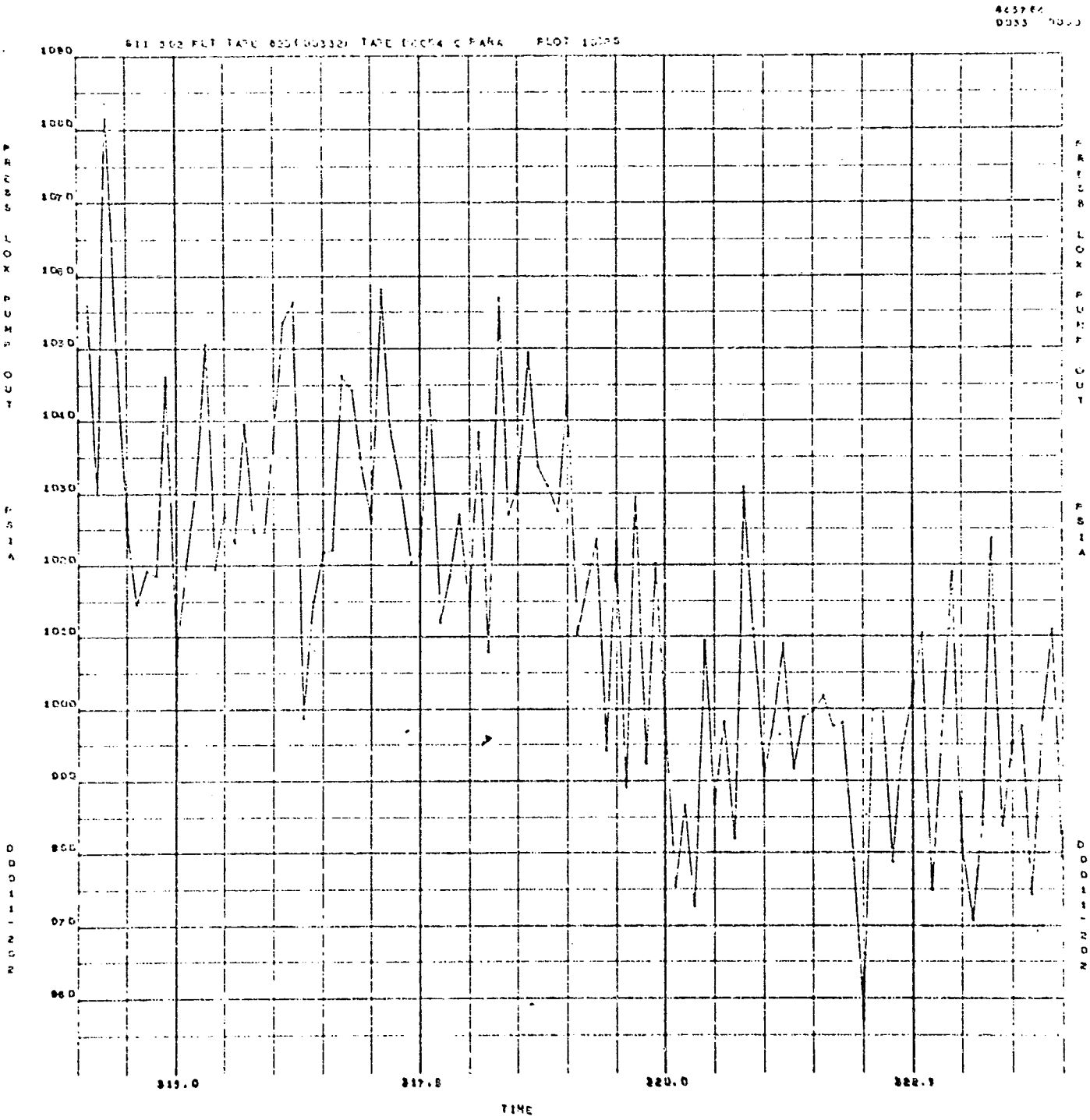

Figure 39. Oxidizer Pump Outlet Pressure

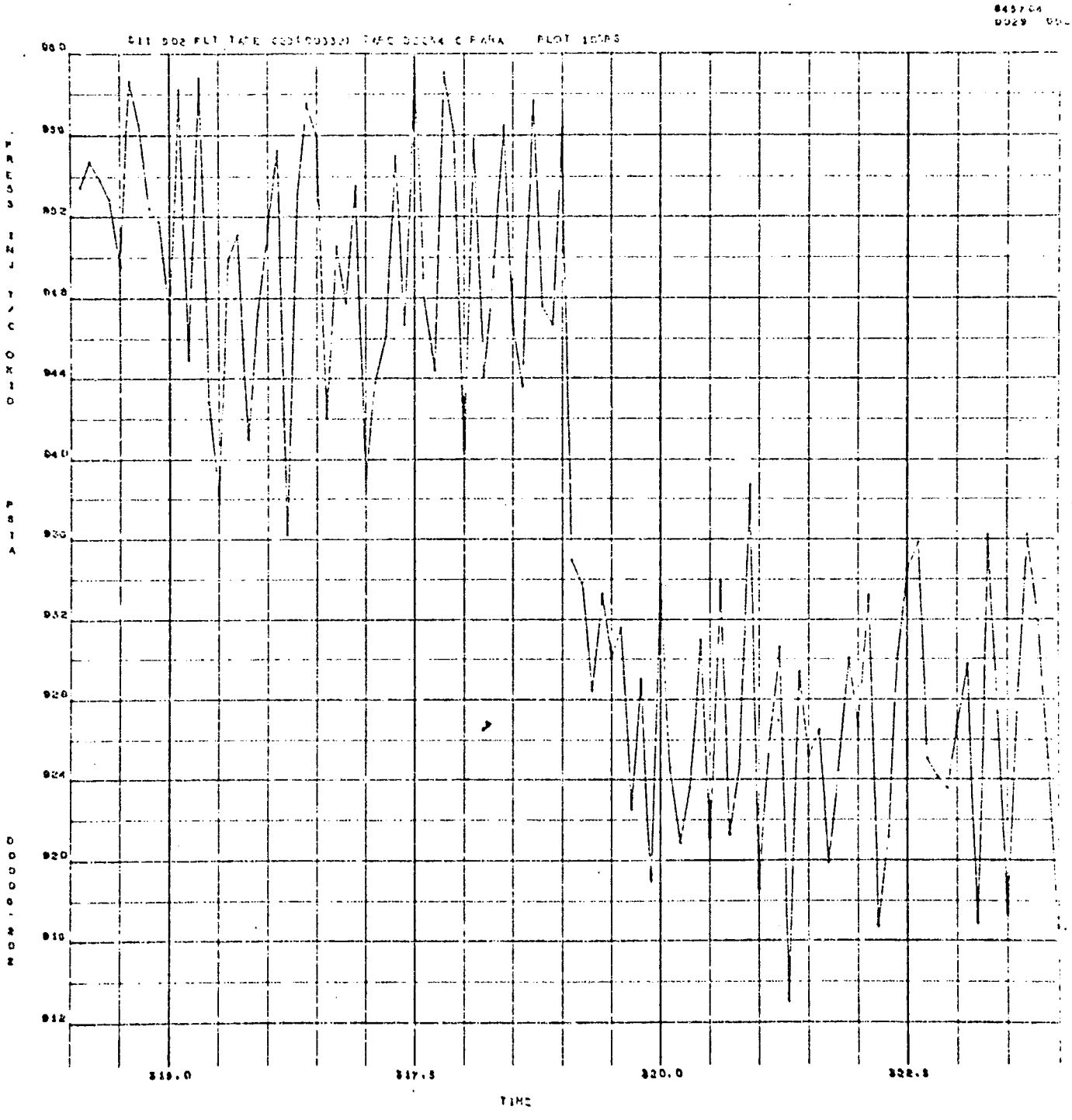

Figure 40. Injector Thrust Chamber Oxidizer Pressure

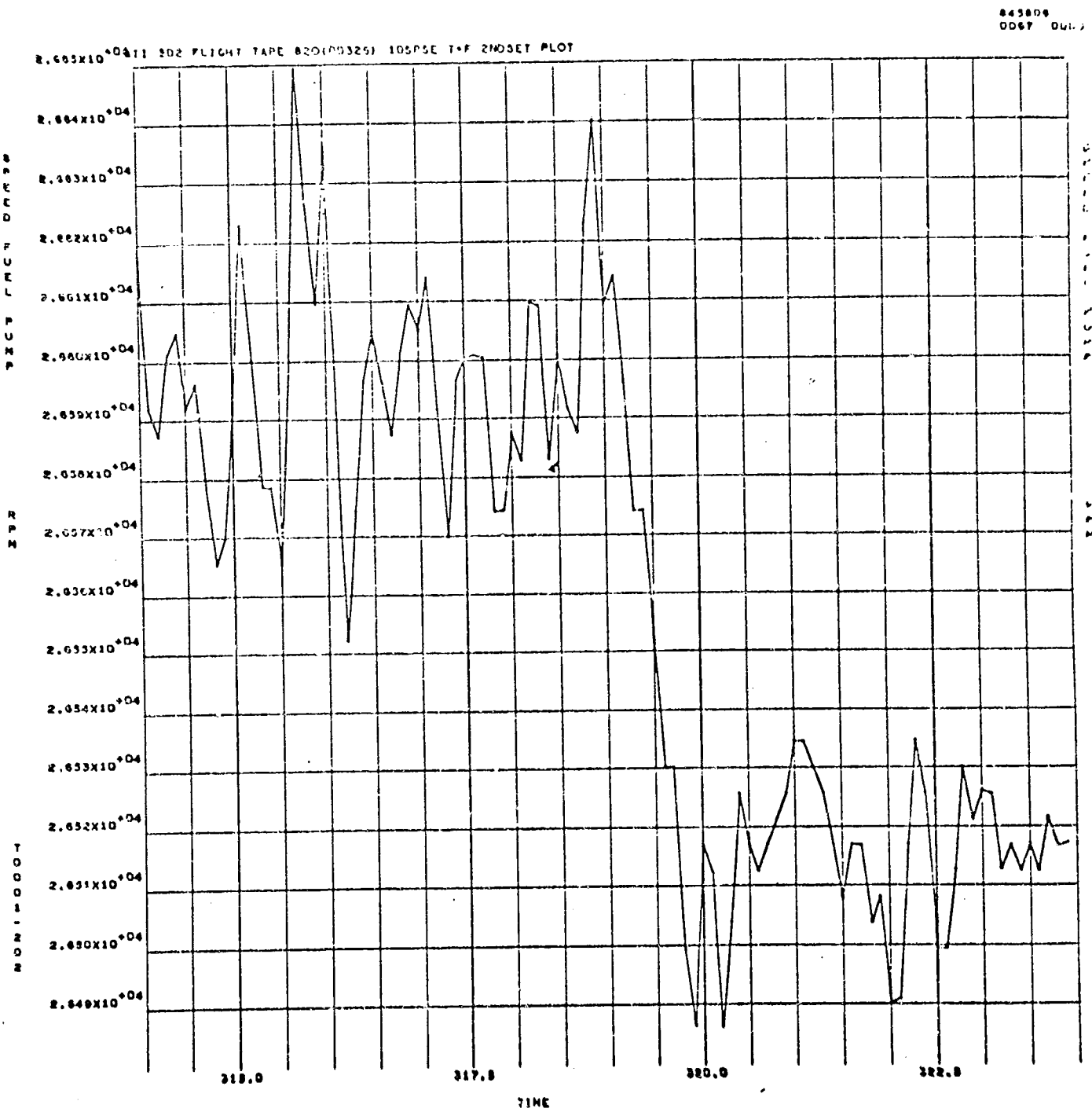

Figure 41. Fuel Pump Speed

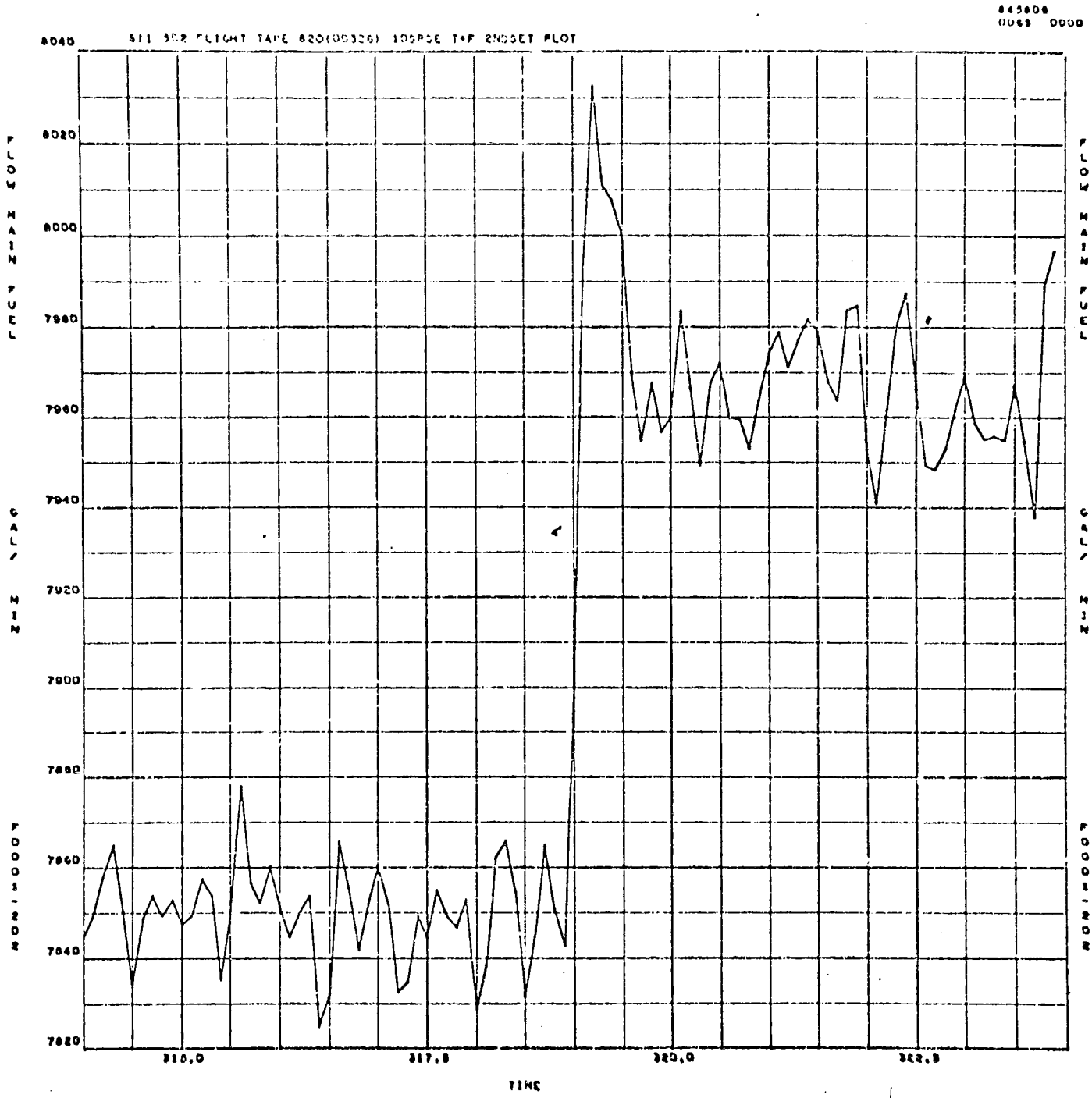

Figure 41. Mainstage Fuel Flow

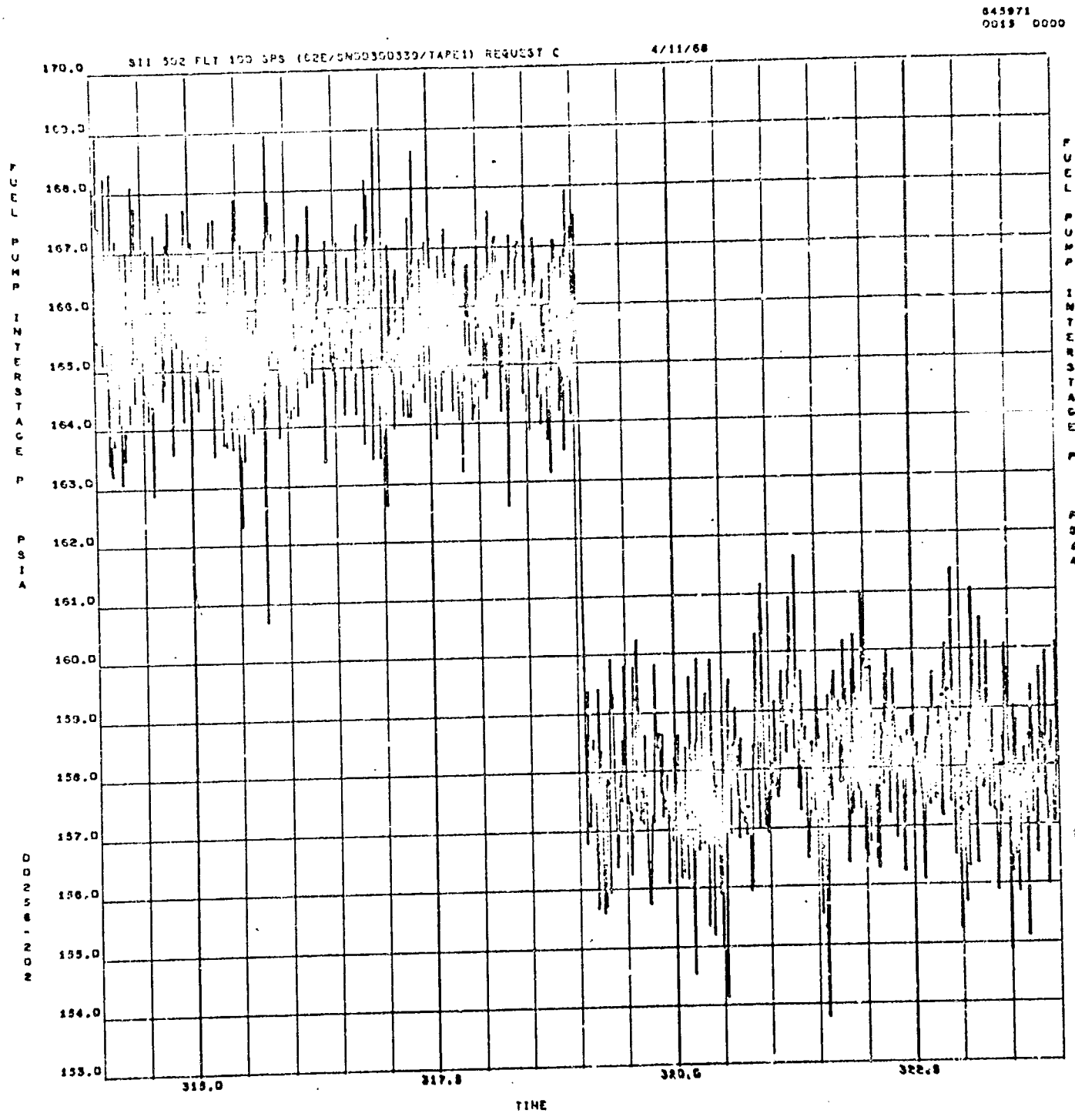

Figure 43. Pump Interstage Fuel Pressure

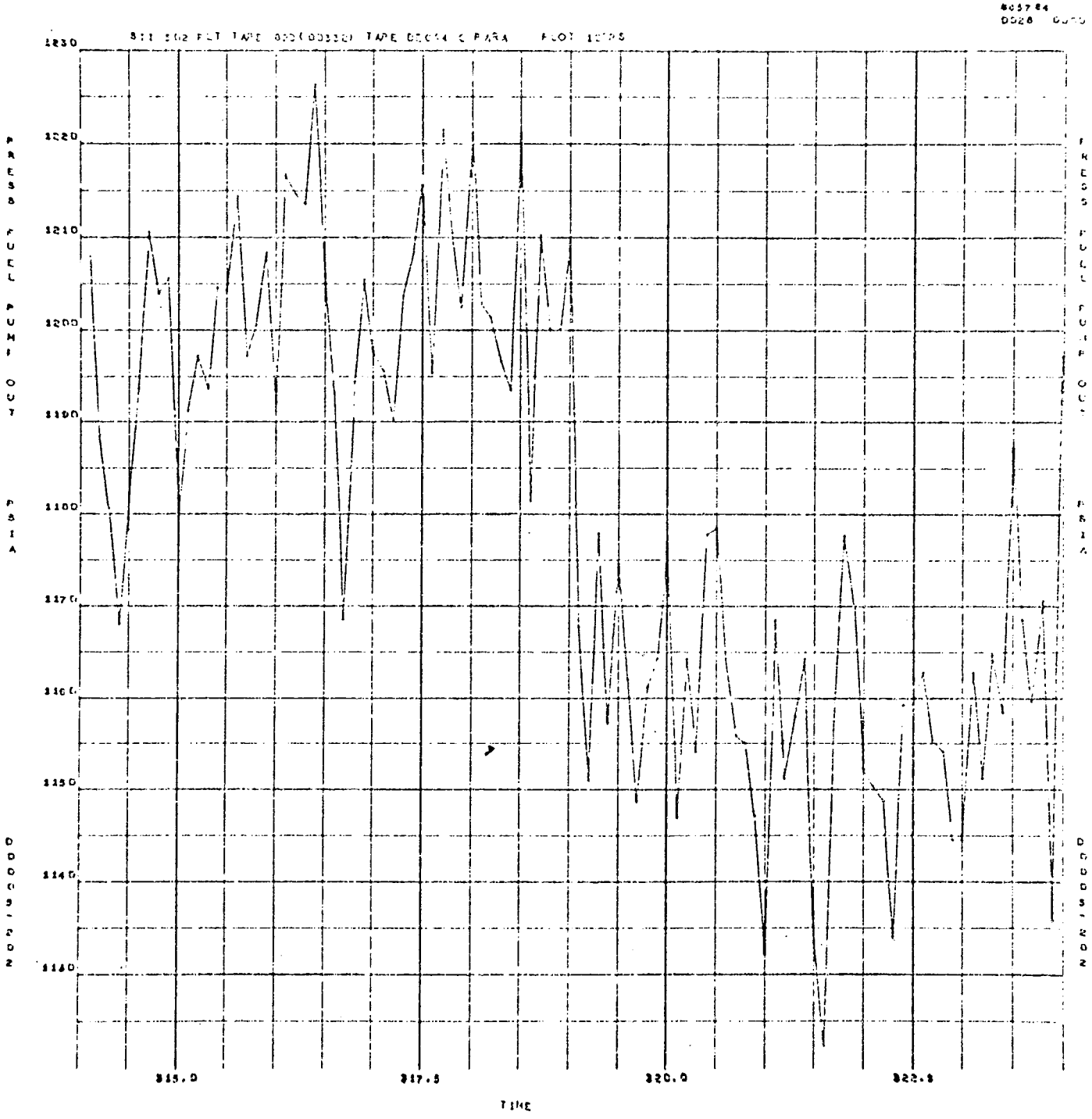

Figure 44. Fuel Pump Outlet Pressure

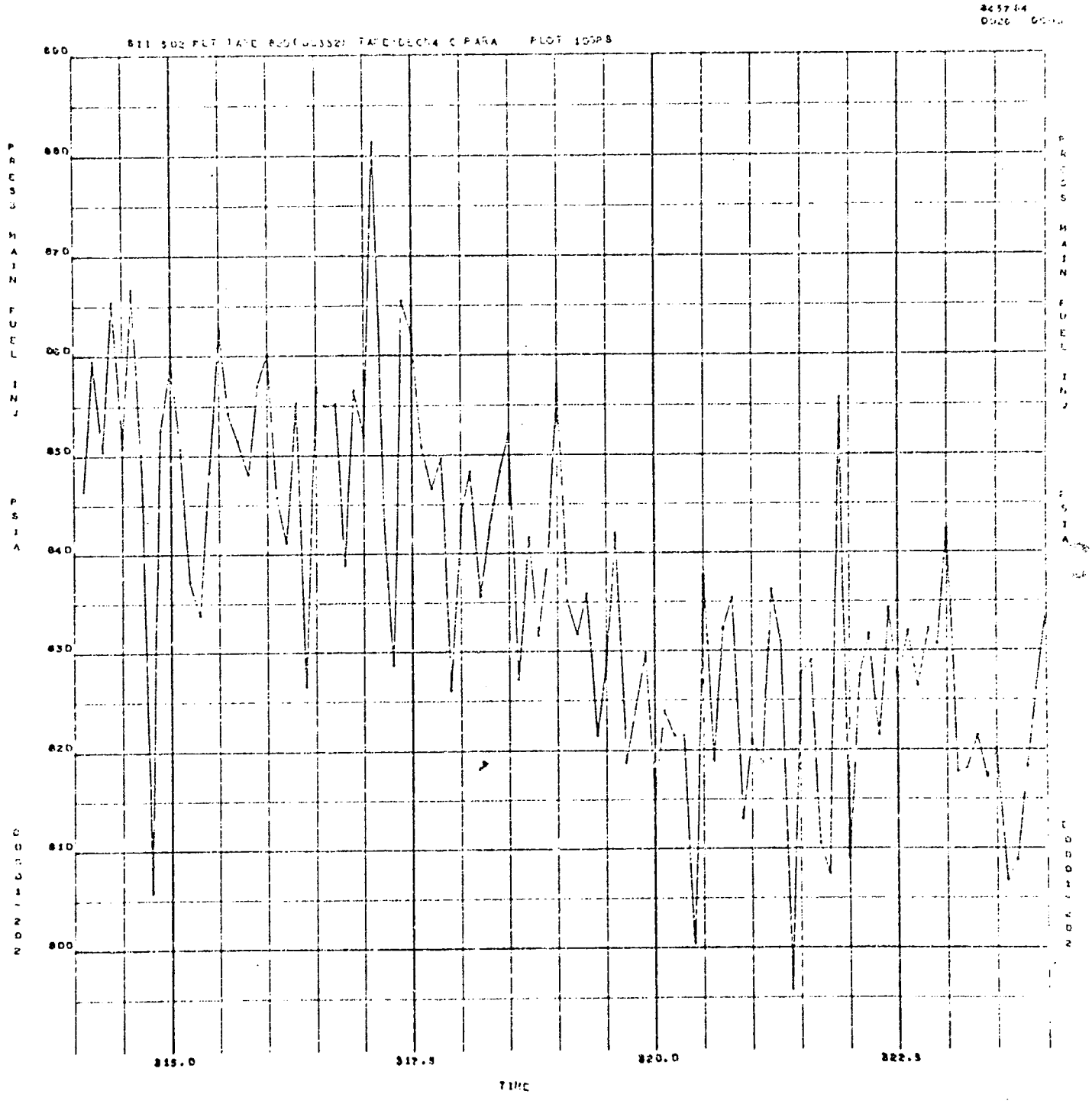

Figure 45. Mainstage Fuel Injector Pressure

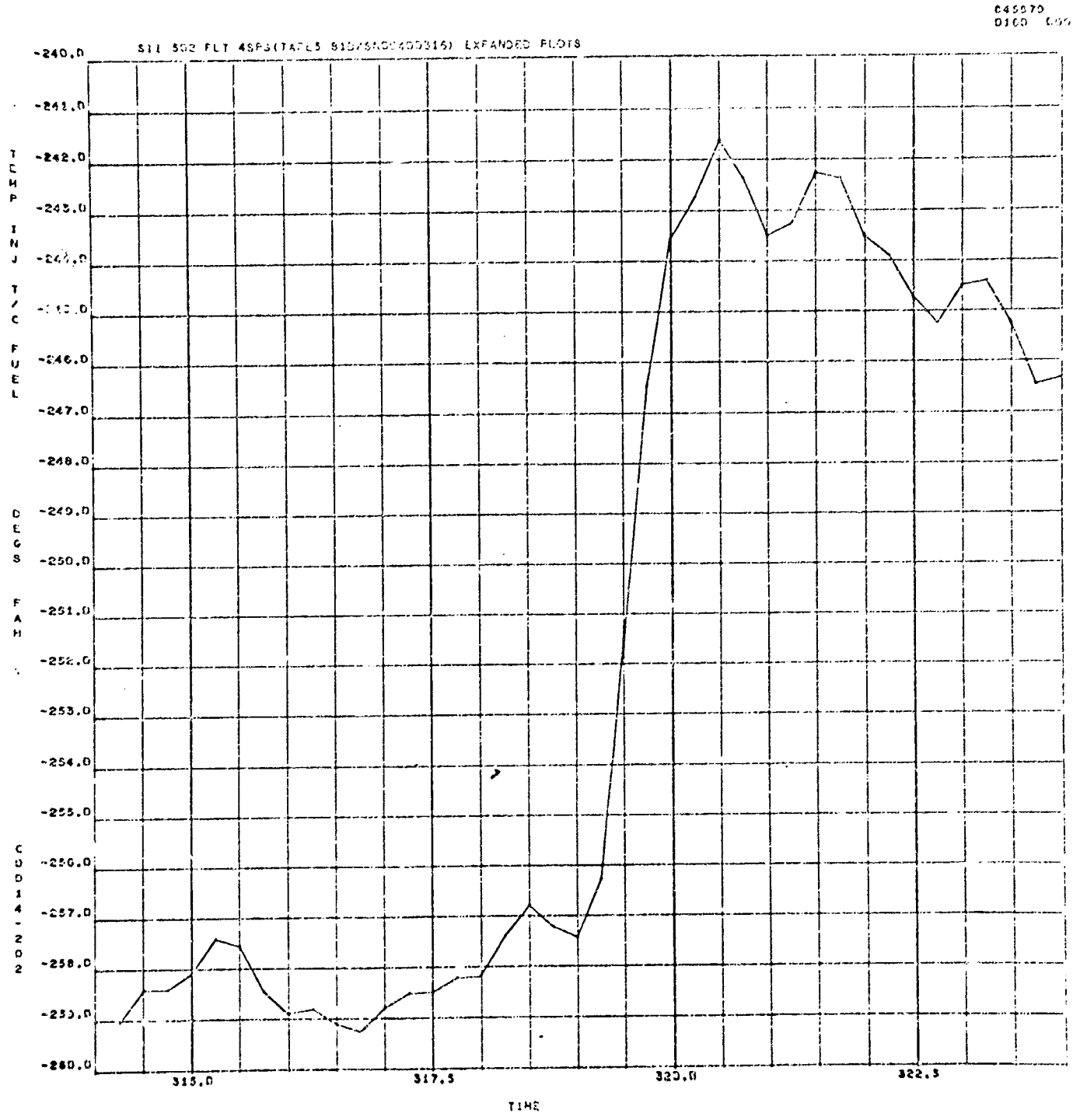

Figure 46. Injector Thrust Chamber Fuel Temperature

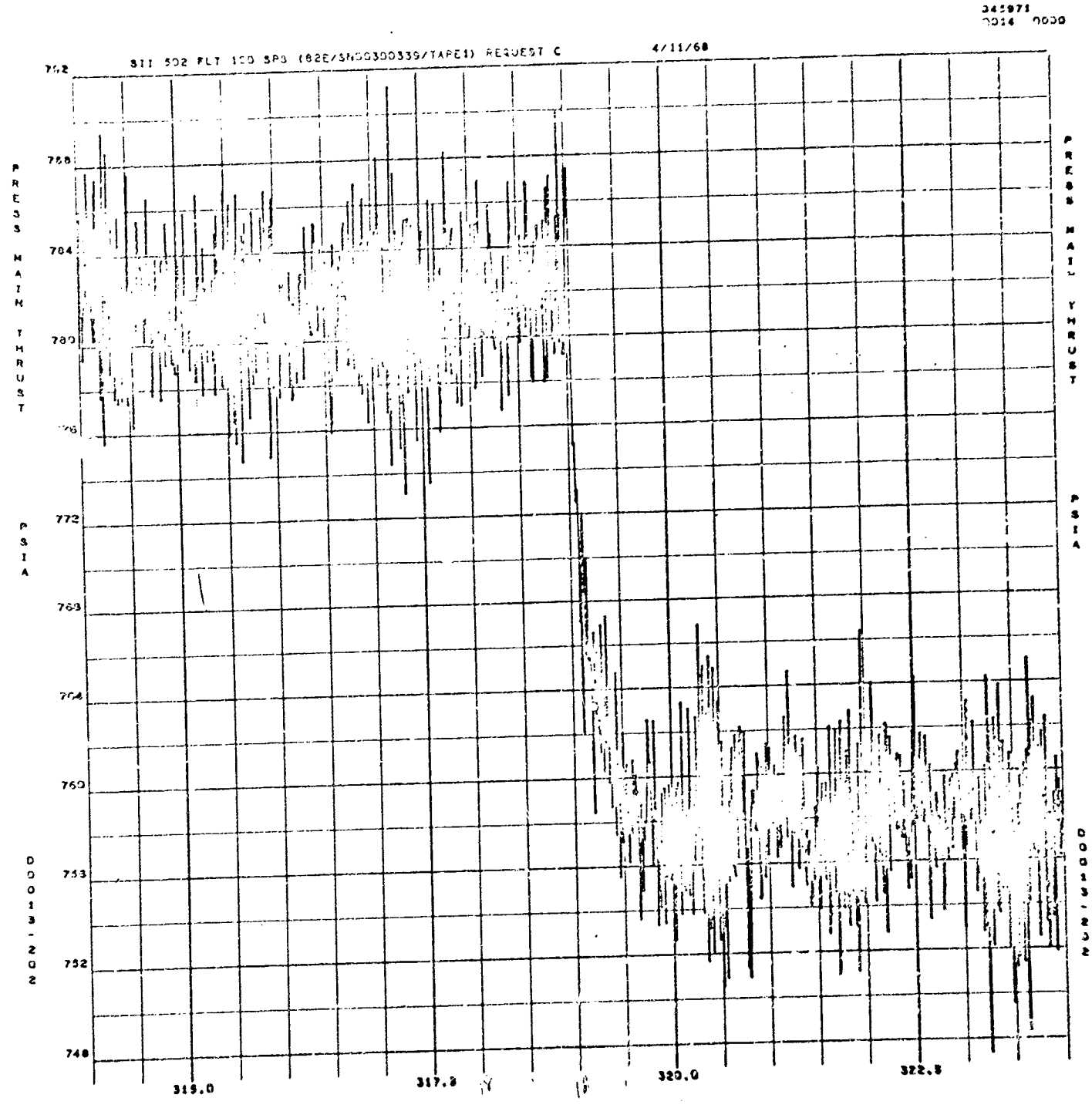

Figure 47. Mainstage Thrust Pressure

TABLE 6

LEAKAGE CALCULATIONS

Parameter	Slice Time (Range Time) 165.5 sec	175.5 sec	Calculations	Indicated Leakage
Thrust Chamber Jacket				
Main Fuel Injection Temperature, R	201.5	215.3		
Thrust Chamber Inlet Manifold Pressure, psi	1160.2	1118.3		
Main Fuel Injection Pressure, psi	860.7	829.3		80.01
Thrust Chamber ΔP	299.5	289.0		-73.90
Thrust Chamber Fuel Flow, gpm	79.77	80.01	73.90	6.11
Fuel Density at Injector	0.786	0.700	0.700	
$\varphi \Delta P$	235.4	202.3	202.3	
$\dot{w}_{T/C}^2$	6363.3		5469.0	
$R_{T/C} = \varphi \Delta P / \dot{w}^2$	0.03699	→	0.03699	
Injector				
Main Fuel Injection Pressure, psi	860.7	829.3		
Thrust Chamber Pressure, psi	753.9	731.0		79.82
Main Fuel Injector ΔP	106.8	98.3		-71.80
Fuel Injection Flow, gpm	79.14	79.82	71.80	8.02
Fuel Density at Injector	0.786	0.700	0.700	
$\varphi \Delta P$	83.9	68.8	68.8	
$\dot{w}_{inj}^2$	6263.1		5138.2	
$R_{inj} = \varphi \Delta P / \dot{w}^2$	0.01339	→	0.01339	

calculation is based on a gain factor obtained from an input error evaluation of the altitude reduction program: -1 lb/sec input error in fuel flow = 1.41 seconds error in specific impulse; therefore, for the observed specific impulse shift of -15.0 seconds, -15.0 -1.41 = 10.6 lb/sec (error or indicated fuel flow leakage).

Effect of ASI Fuel Leak on ASI Operation

Comparative analysis of Q/N plots for all five S-II engines during the flight (Fig. 48) indicates that, at 220 seconds range time, a loss in resistance began to appear on the fuel side of engine 202 (J2044). As flight time progressed, the Q/N plot departed further from the Q/N plots of the other four engines until the abrupt engine performance shift of 519 seconds. At that time, an extreme Q/N shift occurred. The Q/N shifts were then related to fuel leakage flow as shown in Fig. 49. From this figure it may be seen that ASI fuel leakage, which began after 220 seconds range time, increased to approximately 2 lb/sec at 290 seconds range time. These data are consistent with compartment chilling data from a time standpoint. S-II stage compartment and engine temperature data do not indicate any source of "heating" until engine 202 cutoff; therefore, it is assumed that no reverse flow of warm ASI gases into the engine compartment took place, such as is indicated for the S-IVB stage.

Based on the no-reverse-flow premise, it is hypothesized that a partial failure of the ASI fuel line occurred, sufficient "head" being maintained to continue supplying the ASI with minimal fuel from 290 seconds range time through the remainder of engine operation.

From 270 seconds on, the ASI chamber was subjected to high mixture ratio operation, which resulted in erosion damage to the main injector assembly. There were no ASI flight flow measurements to determine what the ASI mixture ratio was that caused this damage. Mixture ratio was first estimated at 8.0, based on passing 0.1 lb/sec fuel to the ASI injector.

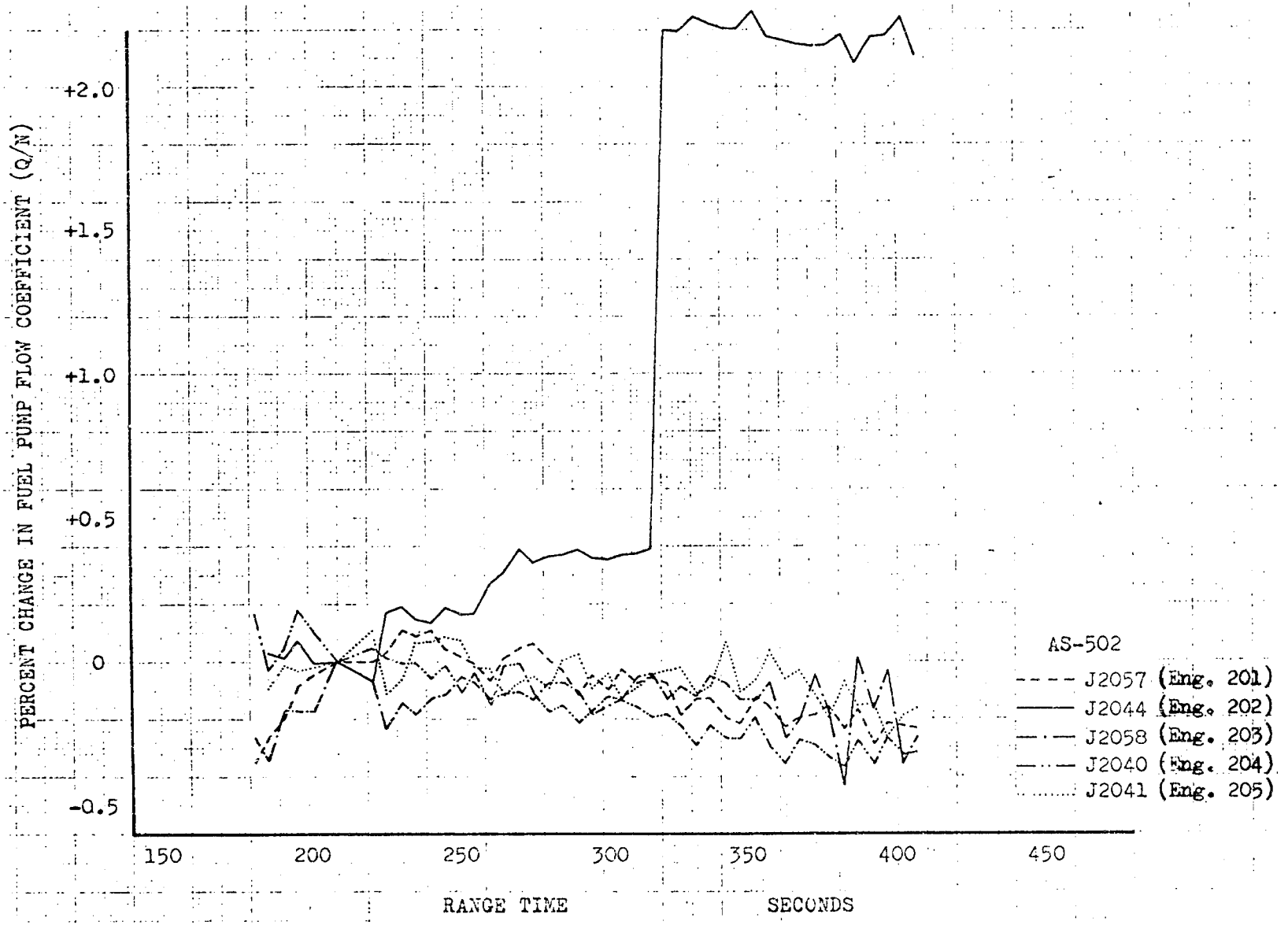

Figure 48. Fuel Flow Coefficient Plot

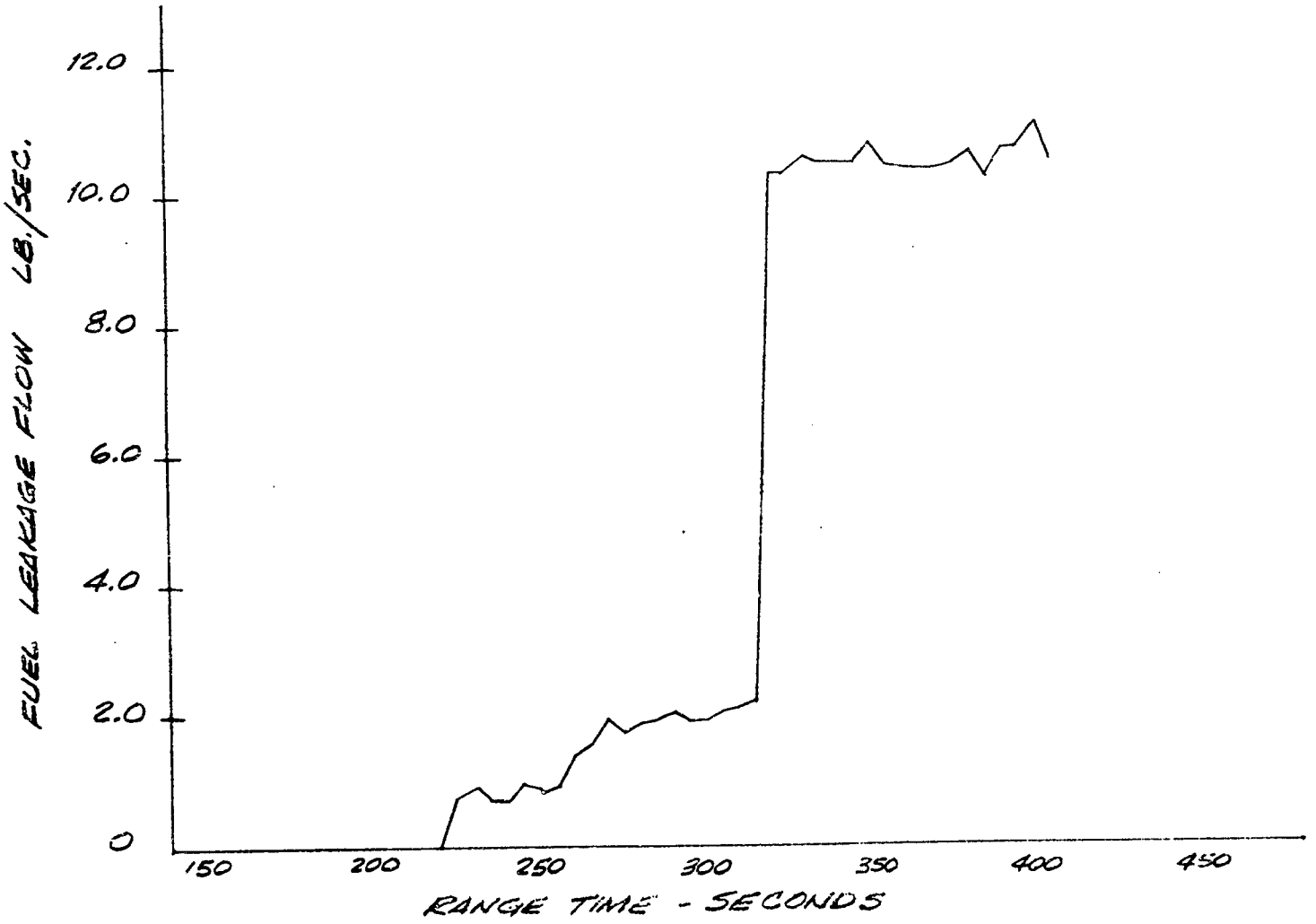

Figure 49. AS-502 Engine 202 (J2044) Fuel Leakage vs Time

Tests were then conducted at both SSFL and MSFC, in which ASI fuel flow was restricted to obtain ASI mixture ratios as high as 10:1 to establish damage potential to the main injector assembly. Erosion capability was demonstrated when the ASI was operated at mixture ratios of 2.4 and above. Rapid severe erosion was noted during MSFC test 217-4, in which the ASI mixture ratio was raised to between 9 and 10:1. During that test an eroded injector fragment was expelled within 10 seconds of high-mixture-ratio ASI operation. During flight, therefore, the ASI mixture ratio passed through the 2.4 mixture ratio erosion threshold and stabilized at a value sufficient to deteriorate the main injector in 40 seconds to the point (319 seconds range time) where similar injector damage occurred. Based on the data from the supporting erosion tests, an ASI mixture ratio between 5 and 9 probably existed on engine 202 from approximately 270 seconds range time until the end of engine operation. An ASI mixture ratio of 6 was assumed at the 290-second range time point, yielding a fuel flow to the ASI of 0.13 lb/sec. The ASI fuel system was then analyzed to determine what location could support an external leak of approximately 2 lb/sec and still deliver the minimal amount of fuel to the ASI.

The ASI system is schematically represented in Fig. 50. The range of oxidizer-side resistance and fuel-side resistance from the block to ASI chamber pressure was determined from engine J2044 ASI acceptance data. The range of resistance from the block upstream to the thrust chamber inlet manifold was that which could be expected from hardware variation. Using these data, a 2-lb/sec leak would have to be located between the middle flex section and the downstream 0.5-inch-diameter flex section to permit the 0.13-lb/sec fuel flow to continue to the ASI injector. The most probable location is in the downstream 0.5-inch-diameter flex section. With a 2-pound leak rate at 290 seconds range time, and a leak location within the downstream flex section as the basic assumption, the ASI operation (weight flows and mixture ratio) was reconstructed from 220 seconds range time (normal operation) through to 326 seconds, i.e., after the abrupt performance shift (Fig. 51 and 52). No significant change in ASI operation is visualized from that time on to engine cutoff.

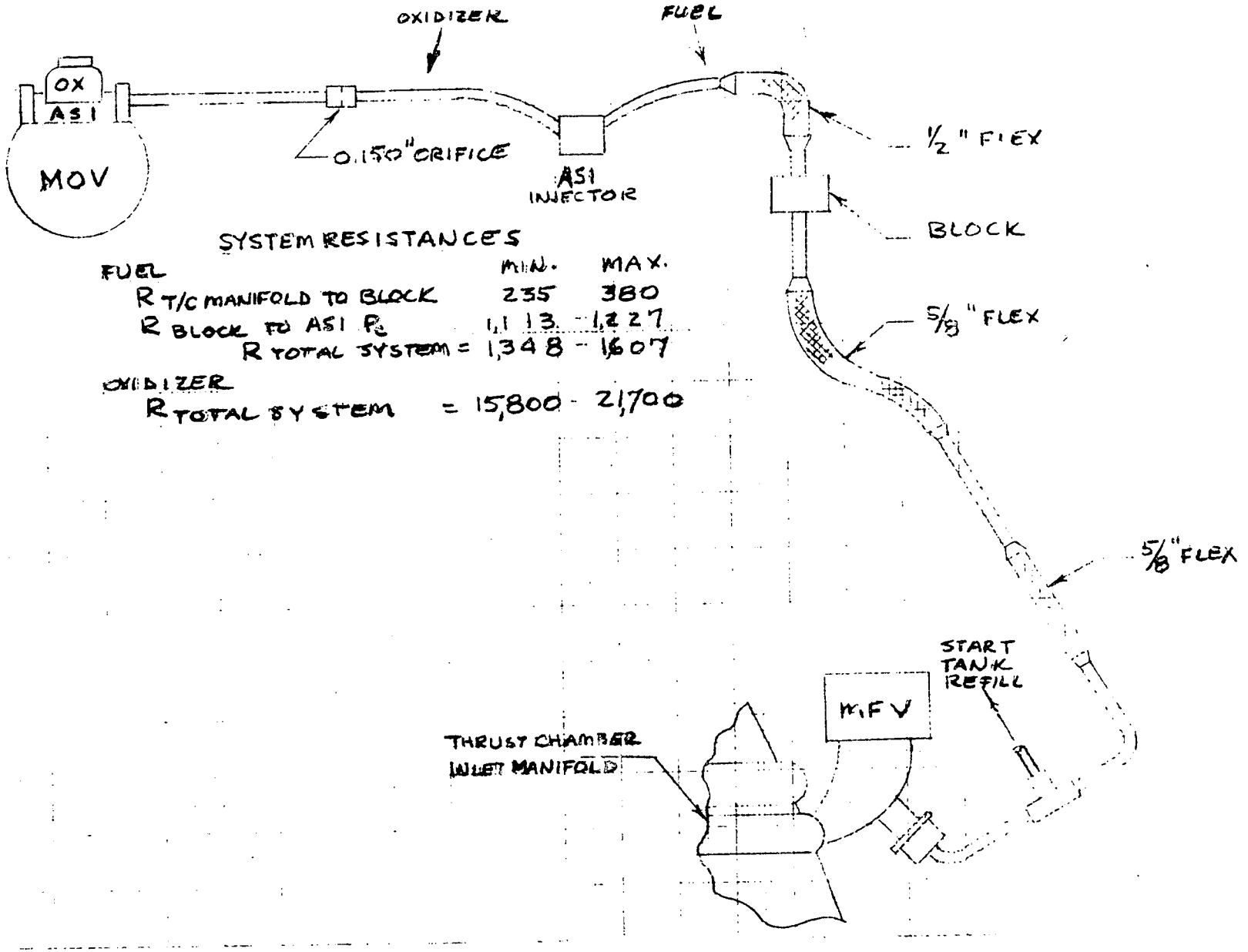

Figure 50. AS-502 S-II ASI System Schematic Diagram

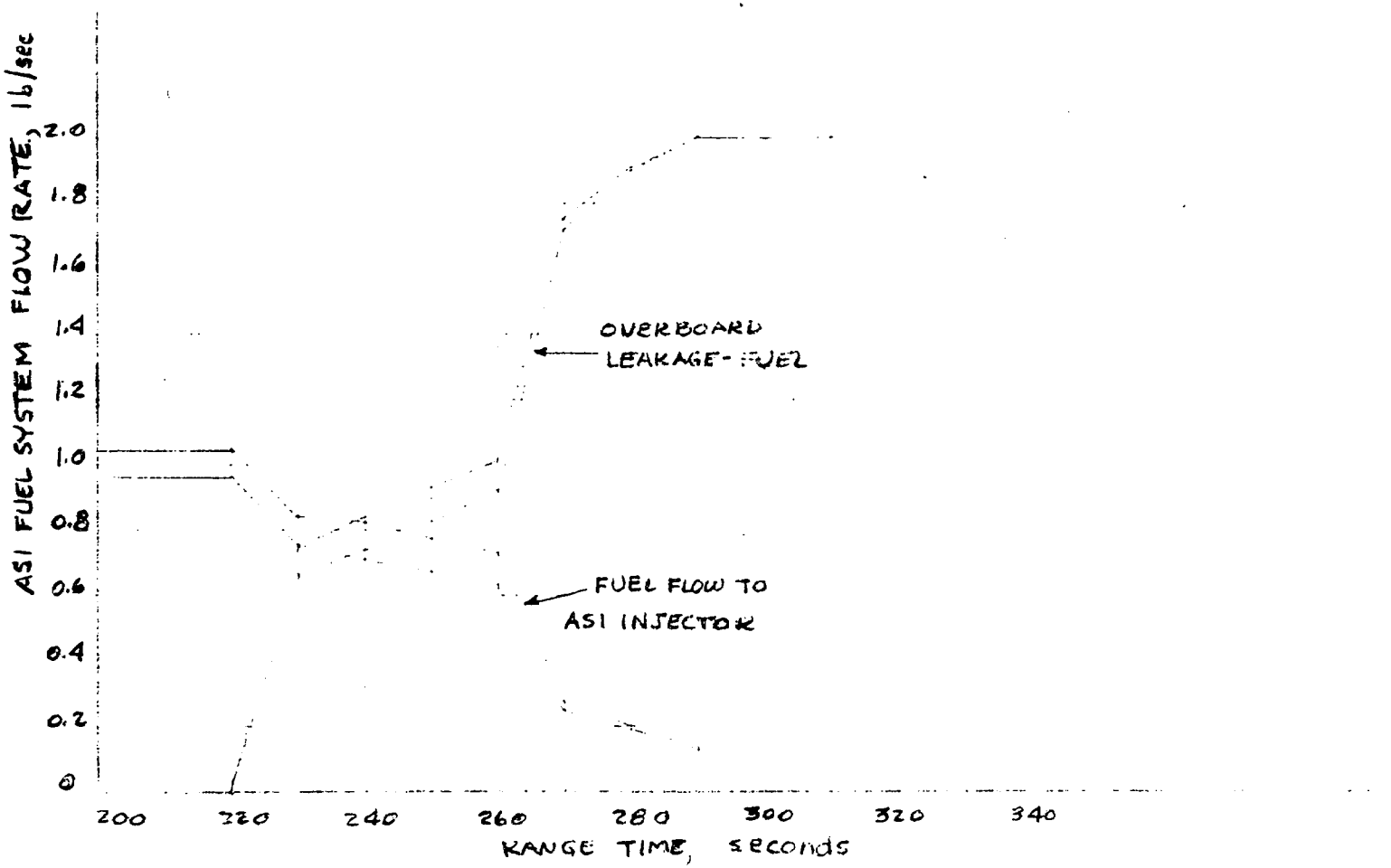

Figure 51. AS-502 S-II ASI Fuel Flow and Overboard Leakage vs Range Time (Engine J2044)

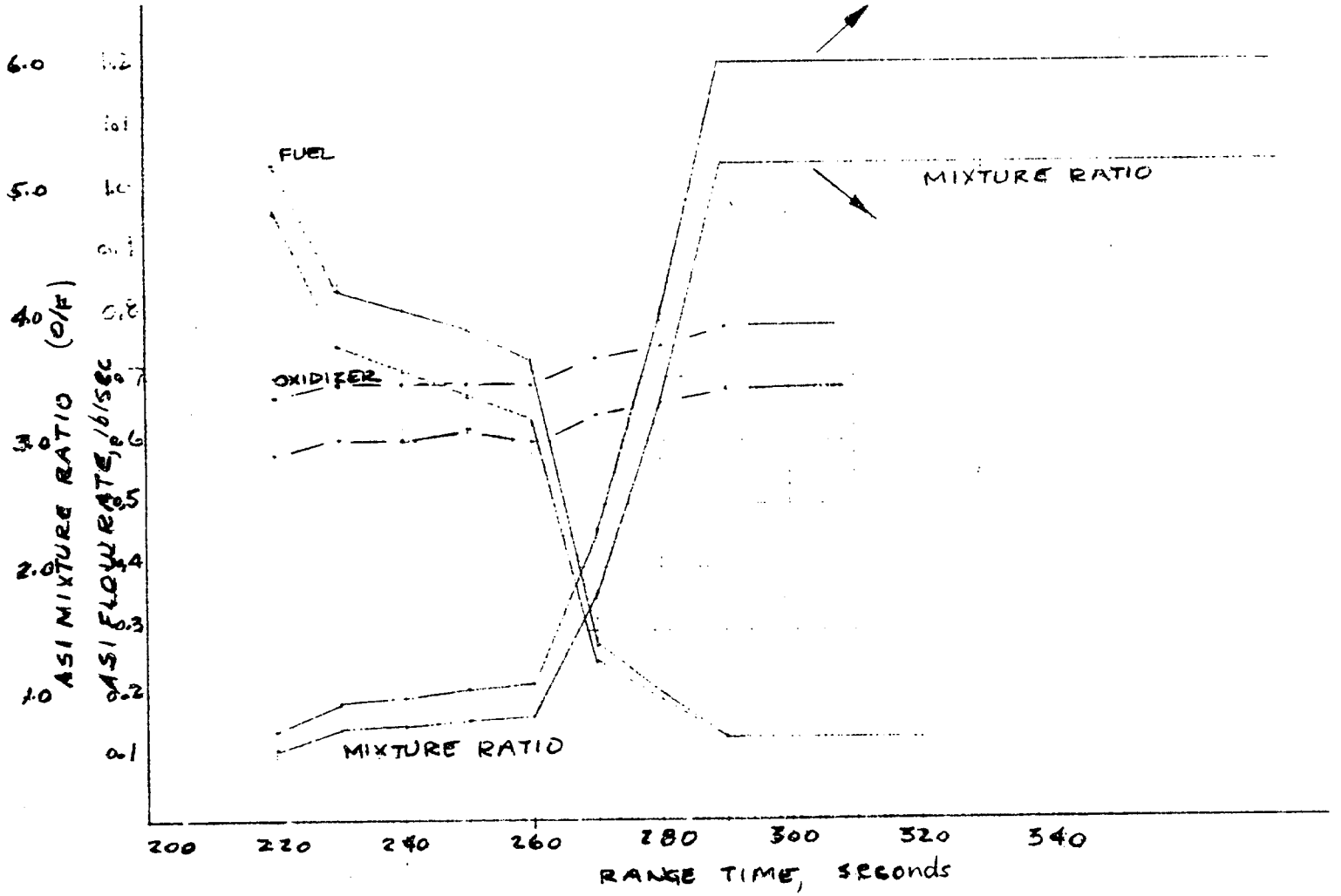

Figure 52. AS-502 S-II ASI Propellant Flowrates and Mixture Ratio vs Range Time (Engine J2044)

When the ASI reaches high mixture ratio conditions, it should be noted that the system ΔP downstream of the leak location is low (approximately 4 psi). A minor upward fluctuation in ASI chamber pressure would therefore have a large effect upon the fuel flow into the ASI. Fuel flow variations, in turn, would have a magnified effect on ASI chamber pressure. The ASI operation after 270 seconds range time is thus characterized by highly oscillatory pressure and flow functions. Burning of parent metal (main injector and ASI) is intermittent, as the ASI mixture ratio tends to swing from infinity (fuel flow stoppage) to 2:1 (as ASI chamber pressure approaches main chamber pressure.

Other S-II-mounted engine temperatures suggest the possibility that cryogenic leakage emanated from engine 205 (J2041). Chilling of the engine 205 main oxidizer valve actuator and closing control line, which began at 250 seconds range time, are best explained by a cryogenic leak of local origin. The data further suggest that the leak direction is from the downstream 0.5-inch-diameter flex section of the ASI fuel line. Analysis of the chilling rates of these two measurements indicates the amount of leak to be approximately 0.1 lb/sec. A leak of this small amount is beyond the flight measurement ability to discriminate, so there is no flight data to confirm the analytically determined leakage rate. The Q/N plot of engine 205 remains within the four-engine data envelope throughout the engine operation (engine 202 is excluded because of known leakage).

HYDRAULIC SYSTEM ANOMALIES

Engine 202 Yaw Actuator Δ P Indication:
282 Seconds Range Time

Description of Event. At approximately 282 seconds range time, the engine 202 engine actuation system (EAS) yaw actuator Δ P measurement indicated a Δ P rise rate of 35 psid/sec; this indication continued for approximately 37 seconds. At 319 seconds range time, an additional step of +600 psid was indicated; this step also was reflected in the pitch actuator Δ P measurement. Yaw actuator Δ P indicated a further rise to +2200 psid following the 319-second shift. At 340 seconds range time, the yaw actuator Δ P measurement indicated a decay rate of 25 psid/sec which persisted until engine 202 cutoff at 412.9 seconds; the indicated Δ P at cutoff was +250 psid. Following engine 202 cutoff, yaw actuator Δ P exhibited a step rise to +1700 psid at 442 seconds range time and then a decay to -500 psid at 530 seconds range time (Fig. 53); the pitch actuator Δ P indication also was -500 psid at 530 seconds range time.

Related Engine and Supporting System Anomalies. During the period 250 to 318 seconds range time, there was a gradual decay of engine 202 performance.

Beginning at 220 seconds, there was general chilling of the engine compartment area forward of the heat shield.

At approximately 250 seconds range time, engine 202 EAS hydraulic fluid reservoir temperature started to decrease (Fig. 54); comparison of this measurement to EAS fluid reservoir temperatures for engines 201, 203, and 204 indicates a decay of 16 F by 319 seconds range time. A stage equipment container located just forward of the engine 202 hydraulic fluid reservoir indicated a cooling trend at 319 seconds range time; this container was insulated and equipped with an internally mounted temperature transducer.

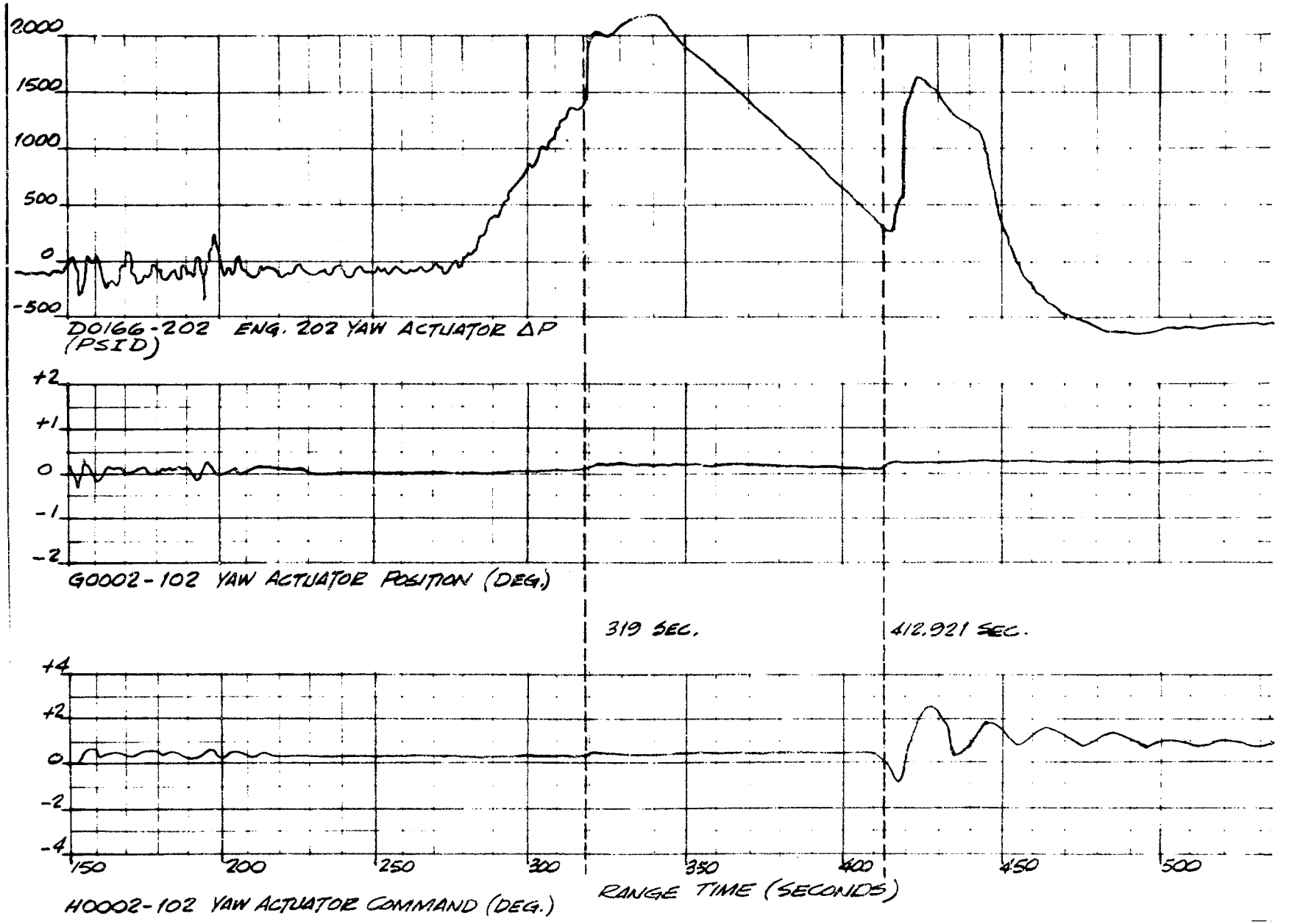

Figure 53. Engine 202 Yaw Hydraulic Actuator Data

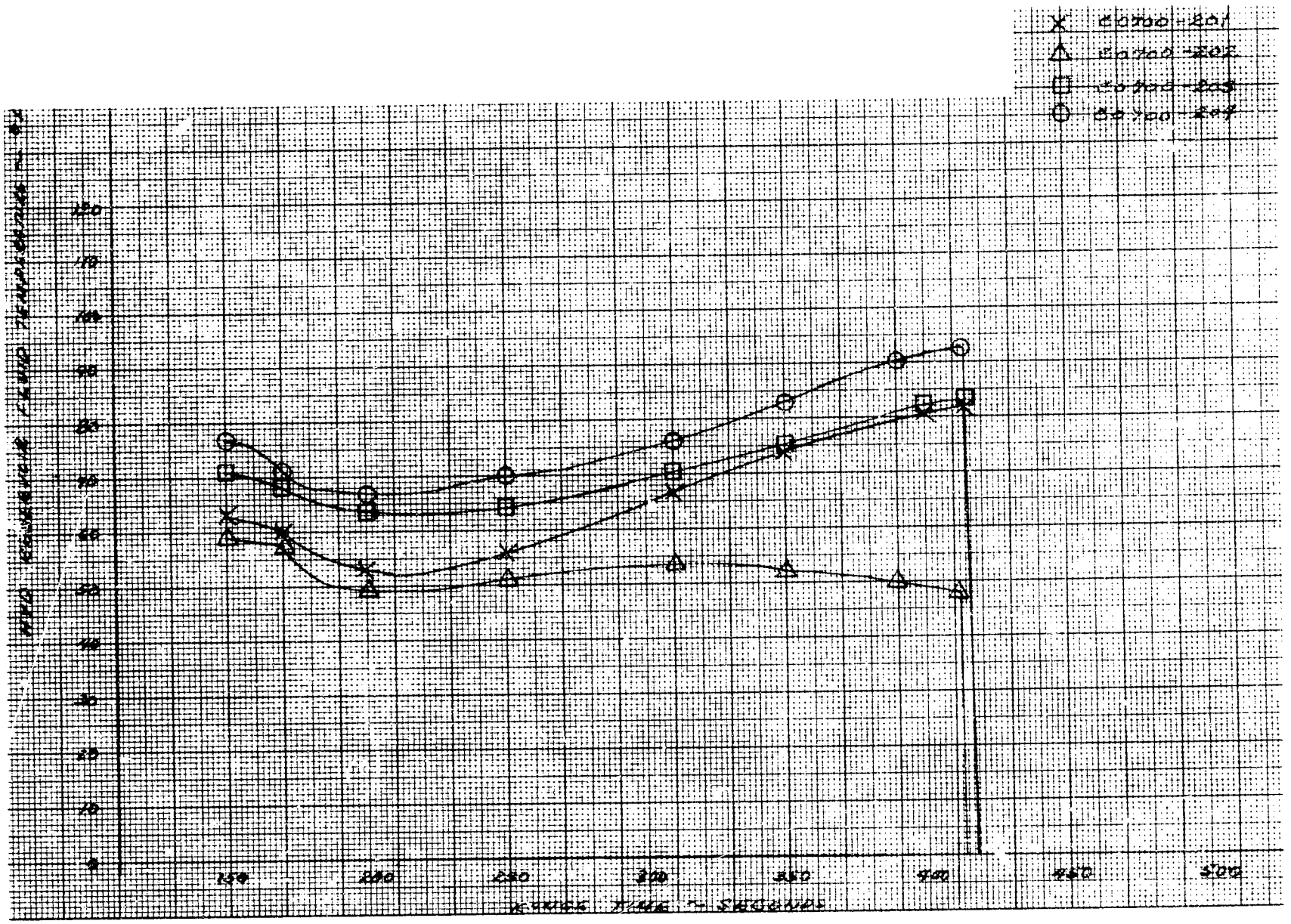

Figure 54. Hydraulic Reservoir Fluid Temperature vs Time

Engine 202 primary and auxiliary flight instrumentation package transducers indicated progressive chilling starting at approximately 260 seconds range time and continuing until engine 202 cutoff. The primary flight instrumentation package exhibited the greater temperature drop.

Hypothesis. Engine 202 yaw actuator Δ P indications were erroneous.

Corroboration of Hypothesis. During the range time interval 292 to 319 seconds, where the engine 202 yaw actuator Δ P indication was observed to rise, there were no significant changes in command or position signal, as shown by Fig. 53. This would indicate that the actuator Δ P transducer was affected by some influence external to the engine actuation system.

Chilldown testing of the hydraulic actuator performed at Space Division of North American Rockwell Corporation, Seal Beach, California, indicates that the actuator Δ P transducer is adversely affected by low temperature. The transducer is of the double bourdon tube type, and is located on the outboard side of the actuator (as installed on the engine); a resistance potentiometer modulates a signal in direct proportion to the differential pressure across the actuator low- and high-pressure sides. Test testing consisted of monitoring the output of the Δ P transducer while chilling the transducer with a liquid nitrogen spray. As the transducer was chilled, the Δ P output signal ramped upward at the rate of 20 psid/sec to a peak value of 800 psid. As the chilling continued, the Δ P ramped downward to 0 psid at about the same rate as the upward ramp. Chilldown with the LN_2 spray was discontinued and, shortly afterward, the Δ P output rose rapidly to 2570 psid and then decayed to zero (Fig. 55). The test data are in good agreement in the pattern indicated by flight data, i.e., a Δ P rise with initial chilling, Δ P decay with continued chilling, and Δ P surge upon termination of chilling (removal of leakage sources).

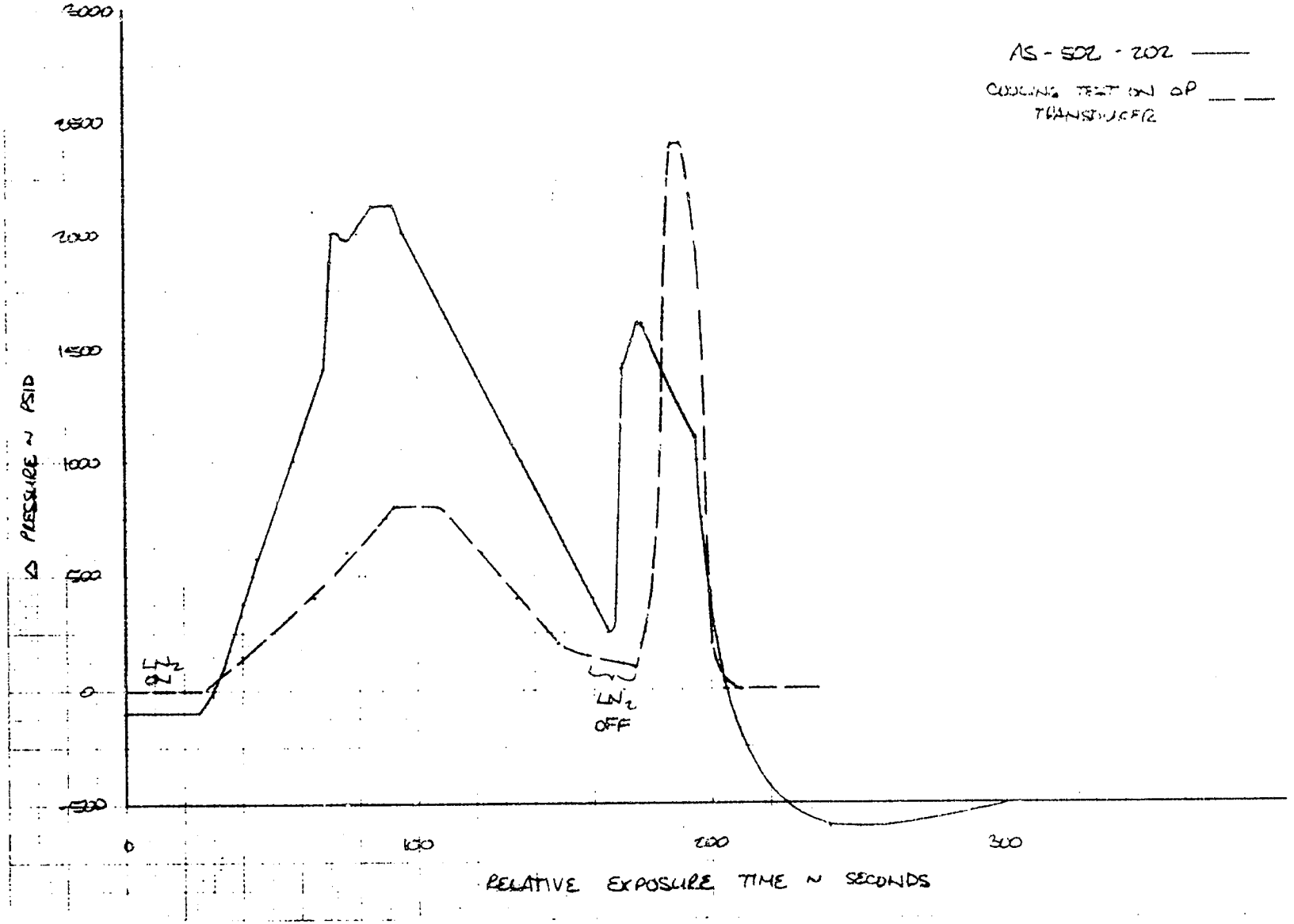

Figure 55. Yaw Actuator Differential Pressure

Engine 202 Yaw and Pitch Actuator Δ P Shift:
319 Seconds Range Time

Description of Event. At 319 seconds range time, engine 202 yaw and pitch actuator Δ P measurements indicated a shift of -600 psid. The step in pitch actuator Δ P persisted until cutoff of engine 202, at which time the indication changed from -600 to -400 psid. The yaw actuator Δ P measurement, while indicating the -600 psid shift at 319 seconds, failed to respond properly because of cryogenic chilling (Fig. 53 and 56).

Hypothesis. The engine 202 yaw and pitch actuator Δ P shift which occurred at 319 seconds range time was caused by a force external to the engine actuation system.

The force resulted from a portion of the main injector being ejected from the thrust chamber, and striking and splitting several tubes near the thrust chamber exit in the process.

Fuel leakage (8 to 9 lb/sec) resulting from rupture of the thrust chamber tubes produced a localized high-pressure area internal to the chamber near the exit, and created a predominantly lateral internal load on the chamber in the direction of the leak. This load was reflected by yaw and pitch actuator Δ P measurements.

Corroboration of Hypothesis. To ascertain whether or not engine 202 actuator Δ P shifts at 319 seconds were results of a force external to the engine actuation system, an analysis was made of stage guidance commands relative to actuator position changes:

1. The engine 202 performance shift (thrust decrease) at 319 seconds would cause the vehicle to experience + pitch and - yaw.

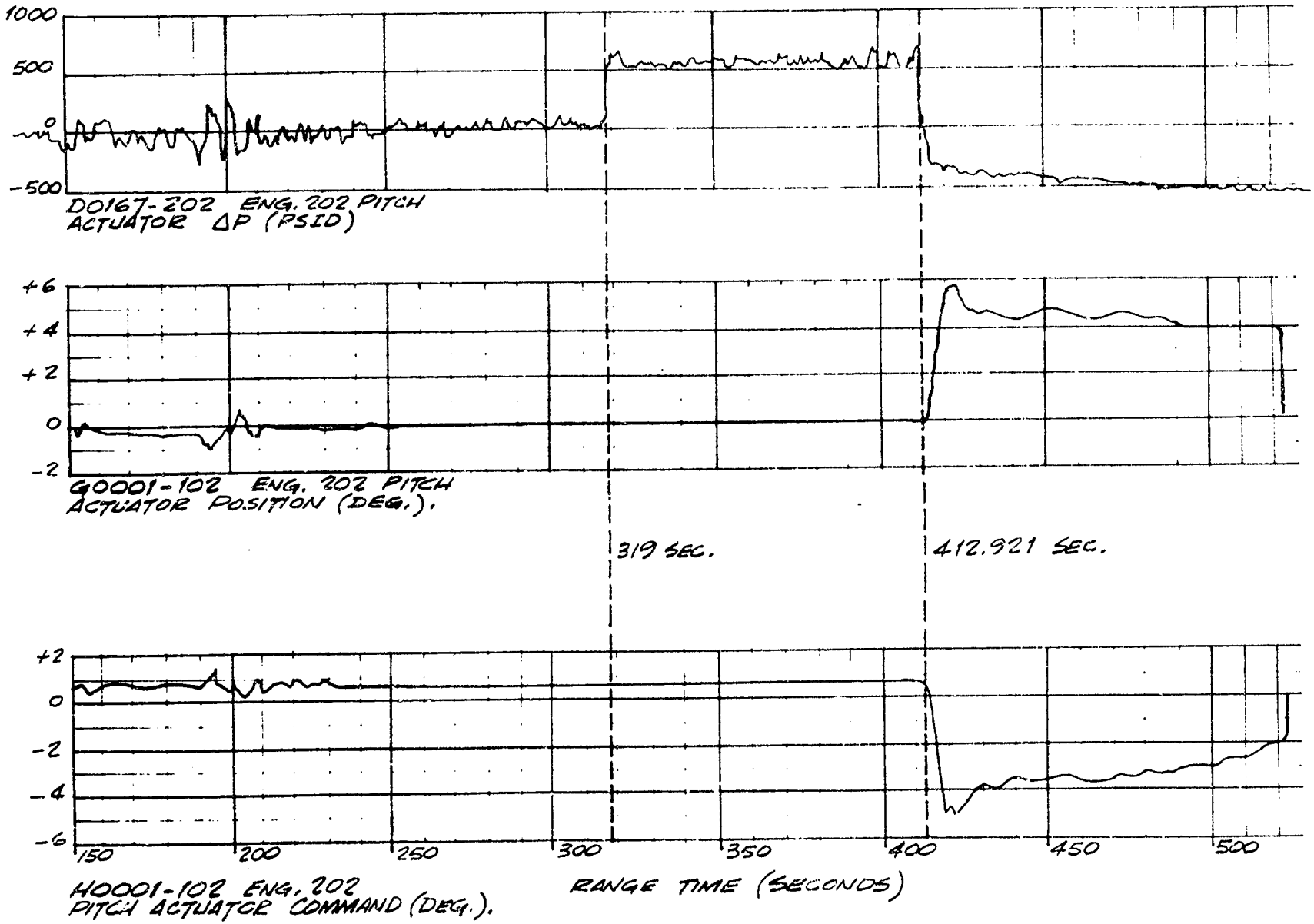

Figure 56. Engine 202 Pitch Hydraulic Actuator Data

2. The required corrections determined by analysis are:

   a. All engines must move -0.04 degree pitch

      Engine 202: extend
      Engine 201: retract
      Engine 203: extend
      Engine 204: retract

   b. All engines must move -0.04 degree yaw

      Engine 202: extend
      Engine 201: extend
      Engine 205: retract
      Engine 204: retract

   c. Considering the possible thrust misalignment of all engines, plus the compliance (springback) to the stage structure, a roll correction of unknown magnitude also would be required.

3. In accordance with the vehicle instrumentation unit system, commands given to the engines at approximately 319 seconds were to correct for a + pitch and counterclockwise roll error of approximately 1/7 degree.

4. Rocketdyne tests conducted on a hot-fired engine with the gimbal bearing chilled to -99 F indicate that a gimbal actuator load change of 12,000 pounds (resulting in an apparent thrust vector rotation of 0.37 degree, as determined by actuator deflection) occurs before gimbal friction is overcome. This test was conducted at 170K sea level thrust with the engine installed in a battleship stand. At a 225K thrust level, the actuator force would be 15,900 pounds and the apparent rotation would be 0.49 degree. Because the spring rate of the vehicle may be expected to be less than that of the battleship stand, it is possible that thrust vector changes in excess of 0.5 degree may occur without overcoming gimbal bearing friction.

5. Engine compartment temperature data indicate occurrence of cryogenic leak (fuel) in the vicinity of the engine 202 fuel injection manifold, beginning at approximately 220 seconds range time. The elapsed time of approximately 99 seconds between first indication of the fuel leak and occurrence of the performance shift at 319 seconds could result in chilldown of the gimbal bearing.

6. Command altitude corrections at 319 seconds were small enough in magnitude not to overcome cold gimbal bearing friction for engine 202; therefore, the altitude corrections could be accomplished by elastic deflection of the engine and mount structure (i.e., the required actuator forces would be applied and maintained to resist springback until another altitude correction command was applied).

7. Actuator pressure traces for all AS-502 S-II stage engines exhibit small, fairly steady differential pressures with short-duration pressure perturbations occurring whenever a command signal from the instrumentation unit is given to change engine attitude. This indicates that thrust alignment of each engine is fairly good, requiring small actuator forces to keep engine freebody in equilibrium. The sudden compressive force in the engine 202 pitch and yaw actuators at 319 seconds indicates the presence of a new force on the engine freebody that was reacted against by the actuators to keep the freebody in equilibrium.

8. Analysis of actuator tapes revealed that the engine 202 pitch actuator was in a 0.13-degree retract position at 319 seconds when the loss in engine thrust occurred. The pitch actuator then moved to a 0.20-degree retract position (0.07-degree retract motion) at 319.1 seconds; no command signal was given to cause this motion. The pitch actuator started a corrective extend motion when, at 319.9 seconds, an extend command was ordered by the vehicle instrumentation system. The system actuator stabilized at 322 seconds in the 0.08-degree retract position (extended 0.05 degree from the pre-performance shift position) with a locked-in

indicated ΔP of 600 psi. Because no command signal was given at 319.1 seconds, the actuator compression must have been caused by an external load on engine 202.

9. Analytical and test results not in agreement with (1) through (6) above are as follows:

   a. Rocketdyne tests on a hot-fired engine with the gimbal bearing at ambient temperature indicates that a gimbal actuator load change of 4500 pounds (resulting in an apparent thrust vector rotation of 0.1 degree, as determined by actuator deflection) occurs before gimbal friction is overcome. These sea level data extrapolated at 225K altitude thrust result in a 6000-pound force and an apparent rotation of 0.13 degree before gimbal friction is overcome. No such forces occurred for pitch and yaw actuators of engines 201, 203, and 204 at 319 seconds range time.

   b. The mass of the gimbal bearing and the presence of the protective boot surrounding the gimbal bearing would result in relatively slow chilldown of the bearing. In laboratory testing conducted at Rocketdyne to study gimbal bearing friction, a substantial period of time was required to cool the gimbal bearing, even when the boot was removed and the complete gimbal and the complete gimbal joint was submerged in liquid nitrogen.

In addition to ascertaining the source of engine 202 actuator loads, an analysis was made to determine the effects of gimbal bearing friction on these loads in terms of moments about the gimbal bearing. Gimbal bearing friction envelopes or hysteresis loops were generated by cross plotting telemetered actuator position and pressure data at discrete points in time. Results of this analysis are as follows:

1. Both the pitch and yaw actuator loads are compressive, i.e., an external force attempted to rotate engine 202 in the direction of the two actuators.

2. Accounting for the gimbal bearing friction, the moment about the engine pitch axis is -65,200 in.-lb, and the moment about the engine yaw axis is +77,075 in.-lb. The resultant moment is 100,000 in.-lb, the force of which acted in a plane located 5 degrees clockwise from a plane bisecting the fuel and oxidizer turbopumps (looking aft).

3. Calculations: The calculations are presented below.

Engine No. 2 Thrust Misalignment:

$\Delta X = -0.010$

$\Delta Z = +0.178$

TH = 225K | Engine 2044 Acceptance Data Test No. 624077

$$F_p = \frac{TH}{16.78} (-) (\Delta Z - \Delta X) = -2520 \text{ pounds compression}$$

$$F_y = \frac{TH}{16.78} (-) (\Delta Z + \Delta X) = -2270 \text{ pounds compression}$$

where

F_p = pitch actuator force

F_y = yaw actuator force

Engine No. 2 Inlet Separating Load:

Fuel Inlet = 28.5 psia Area = 62 $in.^2$

Oxidizer Inlet = 42.0 psia Area = 62 $in.^2$

$P_f = 28.5 (62) = 1700$ pounds

$P_o = 42.0 (62) = 2600$ pounds

$M_x = -21.0 (2600 - 1700) = -18,900$ lb-in.

$$F_p = F_y = \frac{-18,900}{2(0.707)11.875} = -1120 \text{ pounds compression}$$

Actuator Loads With No Gimbal Friction:

$F_p = -(2520 - 1120)$ = -3640 pounds compression

$F_y = -(2270 - 1120)$ = -3390 pounds compression

$M_p = -3640\ (11.875)$ = -43,100 in.-lb

$M_y = (-)\ -3390\ (11.875)$ = -40,200 in.-lb

Actuator loads were essentially zero prior to 319-second failure, indicating misalignment and inlet moment were carried by gimbal friction or were less than expected.

Example: At 196 seconds, the pitch actuator indicated zero load and the yaw actuator -1000 pounds

Because the No. 2 engine actuator loads were normally low on the AS-502 flight, it appeared that the gimbal friction might be carrying the moment resulting from thrust misalignment and inlet differential pressure.

Actuator force and position data were then compared for the yaw actuators of engines No. 1 and 2, as shown in Fig. 57. (Note the thrust alignment bias of -3000 pounds on engine No. 1.) Calculations on engine No. 1 thrust alignment and inlet loads indicate the yaw actuator should have had a load of 2800 pounds compression for static equilibrium. Data indicate good agreement with calculations. The No. 2 engine yaw actuator indicates a force bias of -1000 pounds and calculations indicate it should have had a -3400-pound bias. This indicates the effective thrust misalignment of No. 2 engine was much less than expected. This is probably the result of changing the gimbal bearing on this engine in the field.

The plots in Fig. 57 also show that a change in force occurs with approximately a 0.2-degree gimbal motion. This indicates the point at which gimbal friction is overcome. (Note for the point shown there is reasonable agreement on the magnitude of the friction force for engines No. 1 and 2.)

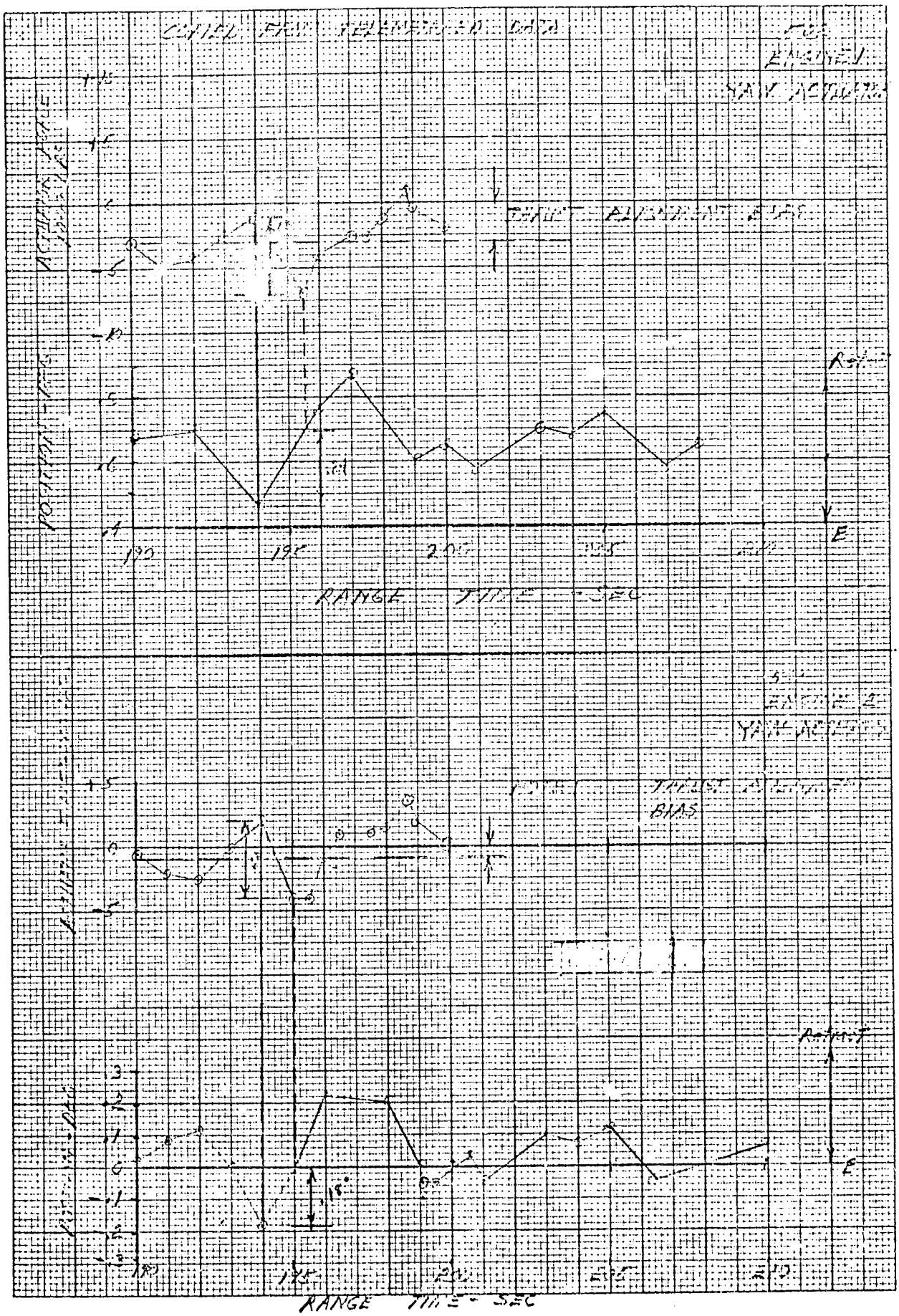

Figure 57. Engines No. 1 and 2 Yaw Actuator Comparison

Cross plots of the AS-502 engine No. 2 pitch and yaw actuator force and position data were then prepared to determine the magnitude of the friction moment, as shown in Fig. 58 through 60.

Because the thrust alignment of the No. 2 engine is different than expected, it will be treated as an unknown.

Resolution of Actuator Forces at 319 Seconds (Prior to Failure):

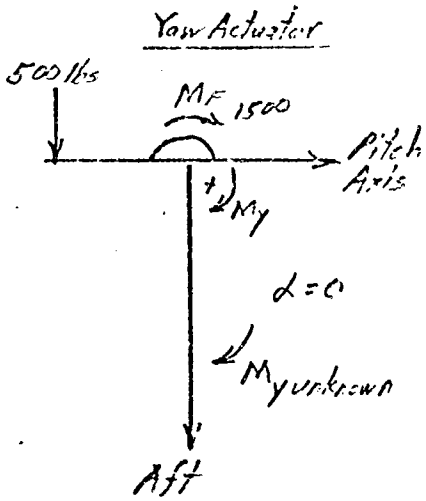

Gimbal friction is resisting actuator extension and is +1500 pounds

$$\Sigma M_y = 0$$

$$0 = -11.875\ (500) + 1500\ (11.875) + M_{yu}$$

$$M_{yu} = -11.875 \text{ in.-lb}$$

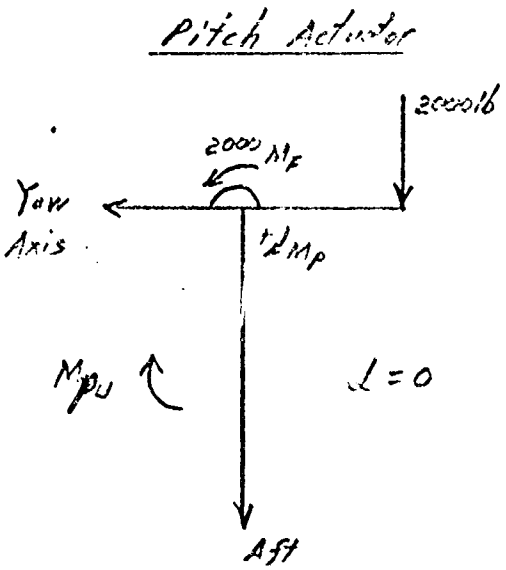

Gimbal friction is resisting actuator extension and is -2000 pounds

$$\Sigma M_p = 0$$

$$0 = +2000\ (11.875) - 2000\ (11.875) + M_{pu}$$

$$M_{pu} = 0$$

Resolution of Actuator Anomalies on No. 2 Engine at 318 to 321 Seconds:

Geometry

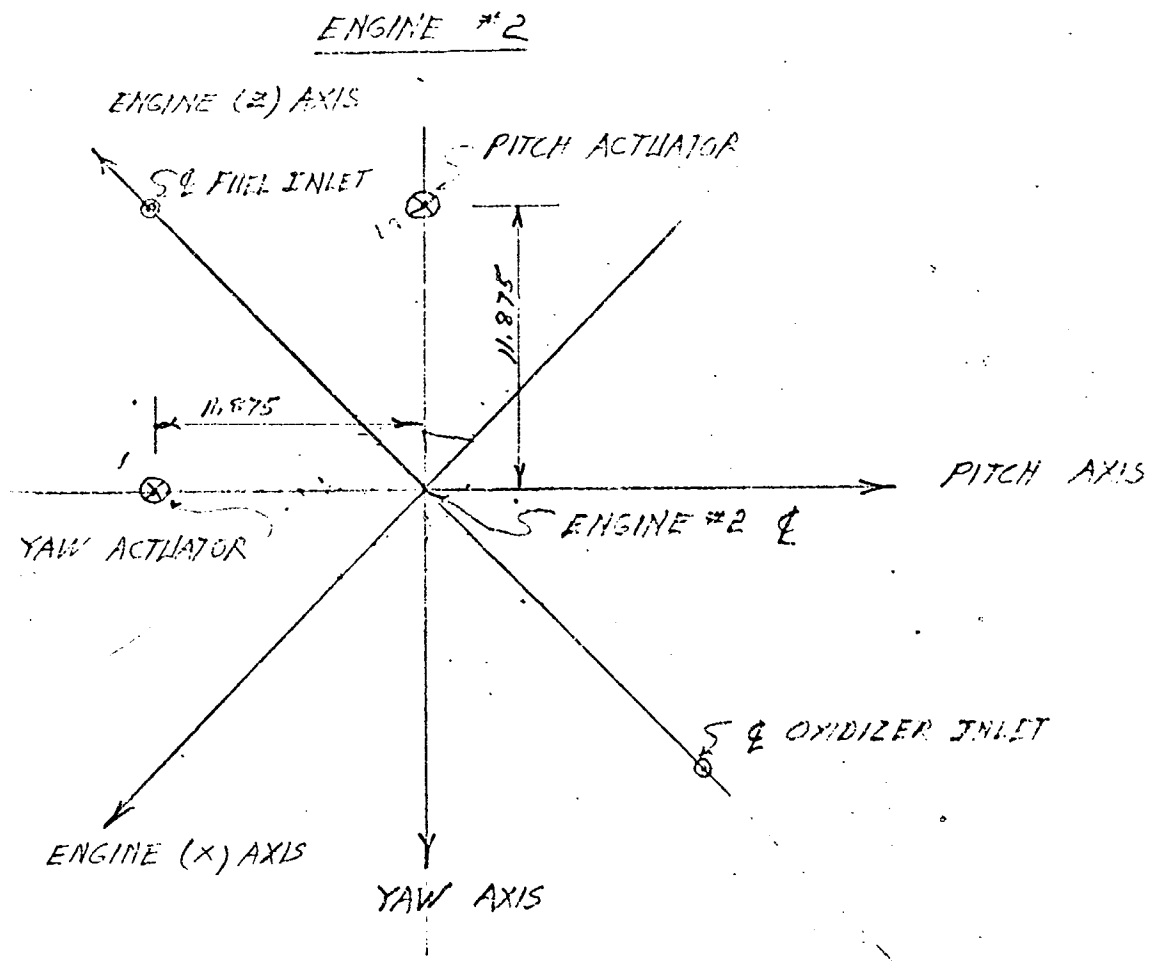

Looking Forward

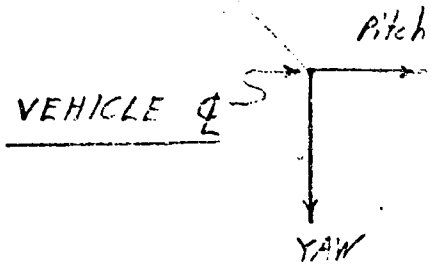

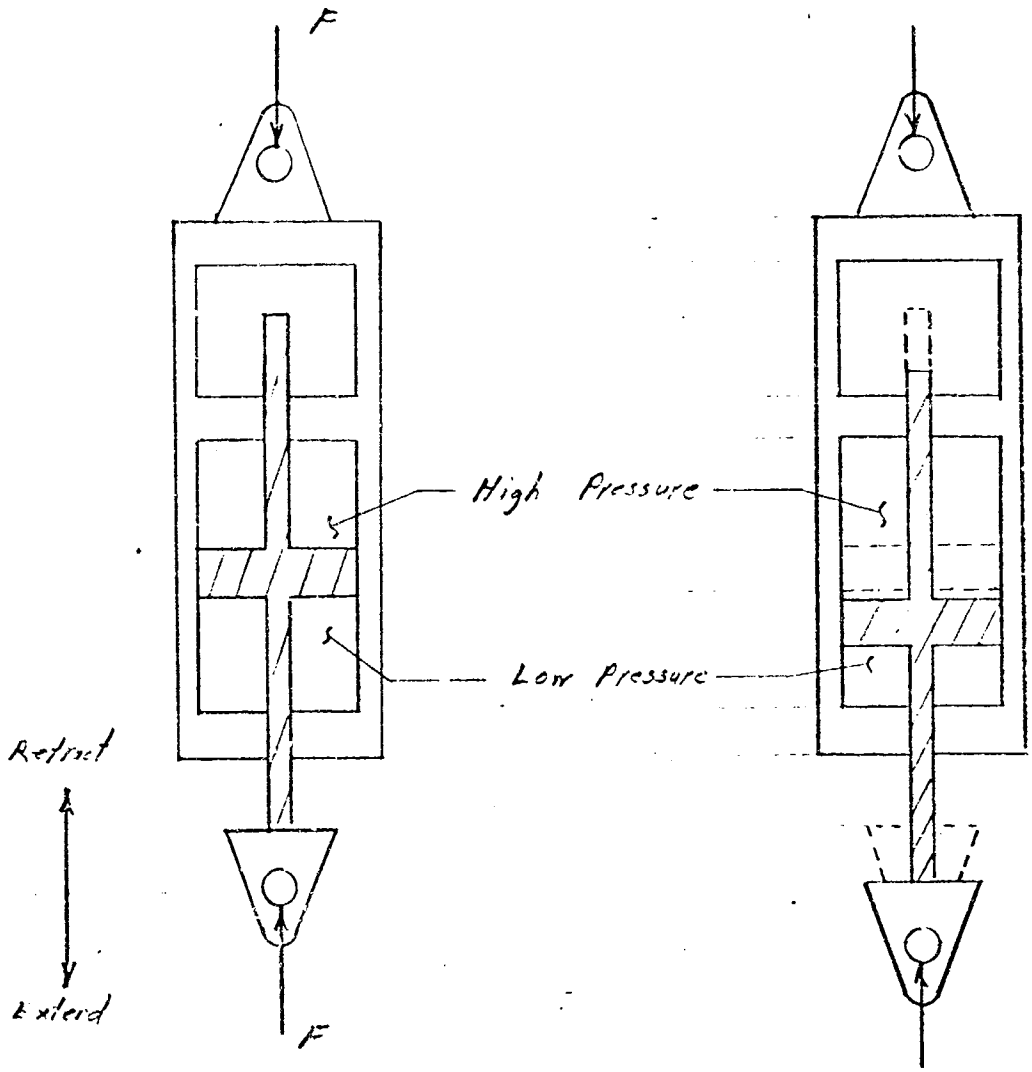

An external applied compressive force on the actuator results in the same sign pressure differential as an actuator commanded extension.

Figure 58. Actuator Sign Convention

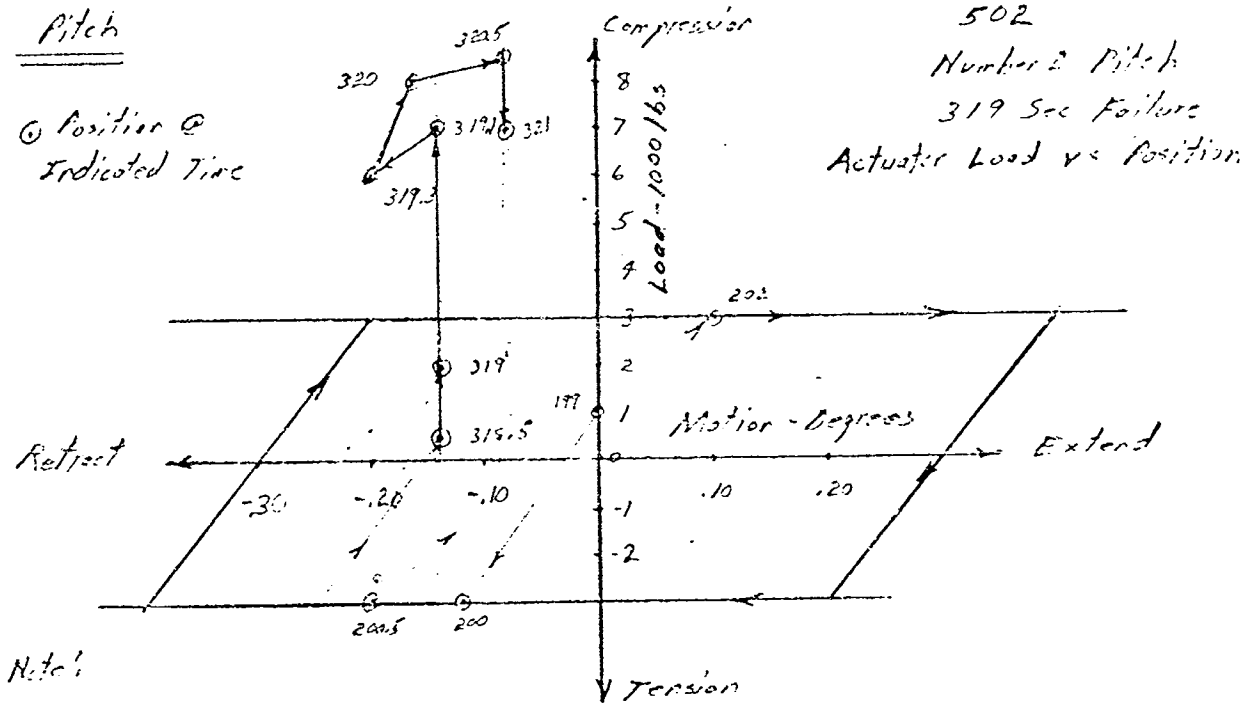

Figure 59. No. 2 Engine Gimbal Friction (Pitch)

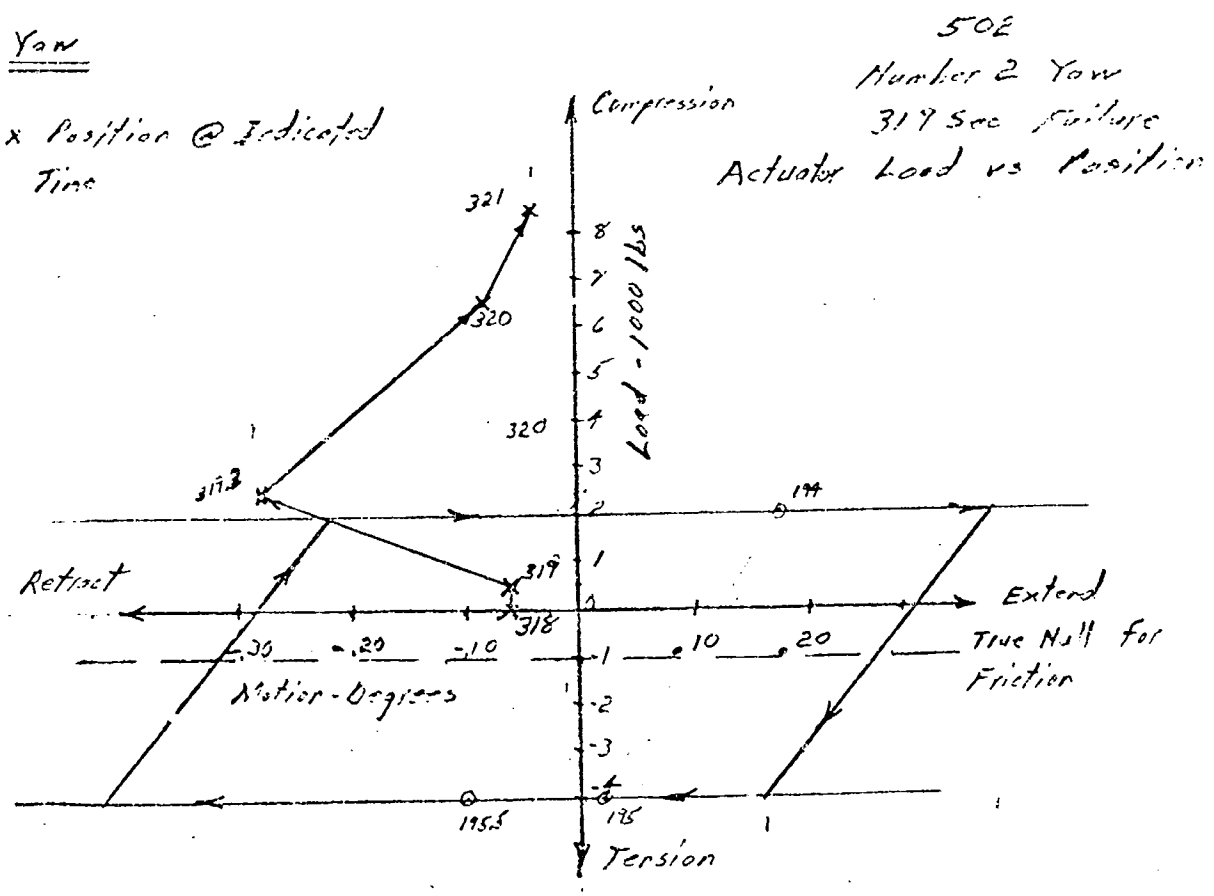

Figure 60. No. 2 Engine Gimbal Friction (Yaw)

Resolution of Actuator Forces at 321 Seconds (After Failure):

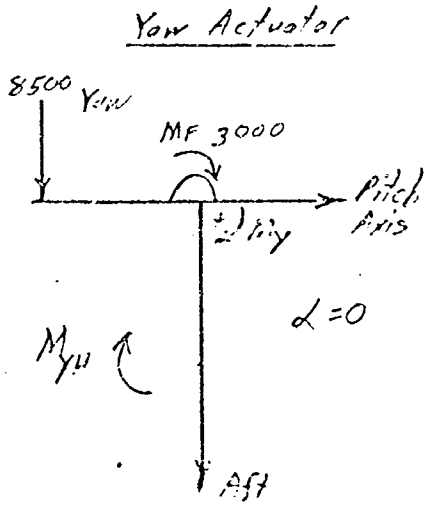

Between 319.3 and 321 seconds, an extended motion of the actuator took place (0.24 degree) sufficient to lock in a maximum + friction moment

$$\Sigma M_y = 0$$

$$0 = -8500\ (11.875) + 3000\ (11.875) + M_{yu}$$

$$M_{yu} = +65{,}200 \text{ in.-lb}$$

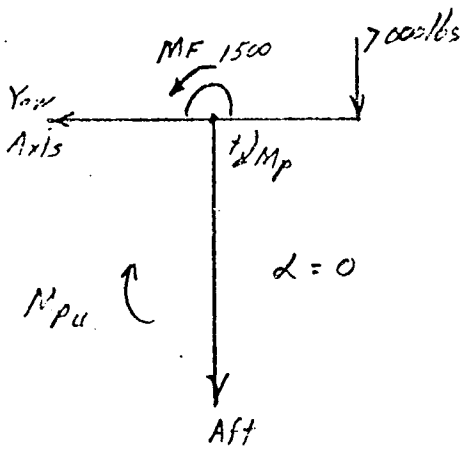

Between 319.3 and 320.5 seconds, an extend motion of the actuator took place (0.12 degree) sufficient to lock in a maximum - moment, but load then dropped 1500 pounds. Assume residual $(-M_f) = -1500$

$$\Sigma M_p = 0$$

$$0 = 7000\ (11.875) - 1500\ (11.875) + M_{pu}$$

$$M_{pu} = -65{,}200 \text{ in.-lb}$$

The applied unknown moment is the difference between the pre-failure and the post-failure moments.

$$M_y = 65{,}200 - (-11{,}875) = +77{,}075 \text{ in.-lb}$$

$$M_p = -65{,}200 - 0 = -65{,}200 \text{ in.-lb}$$

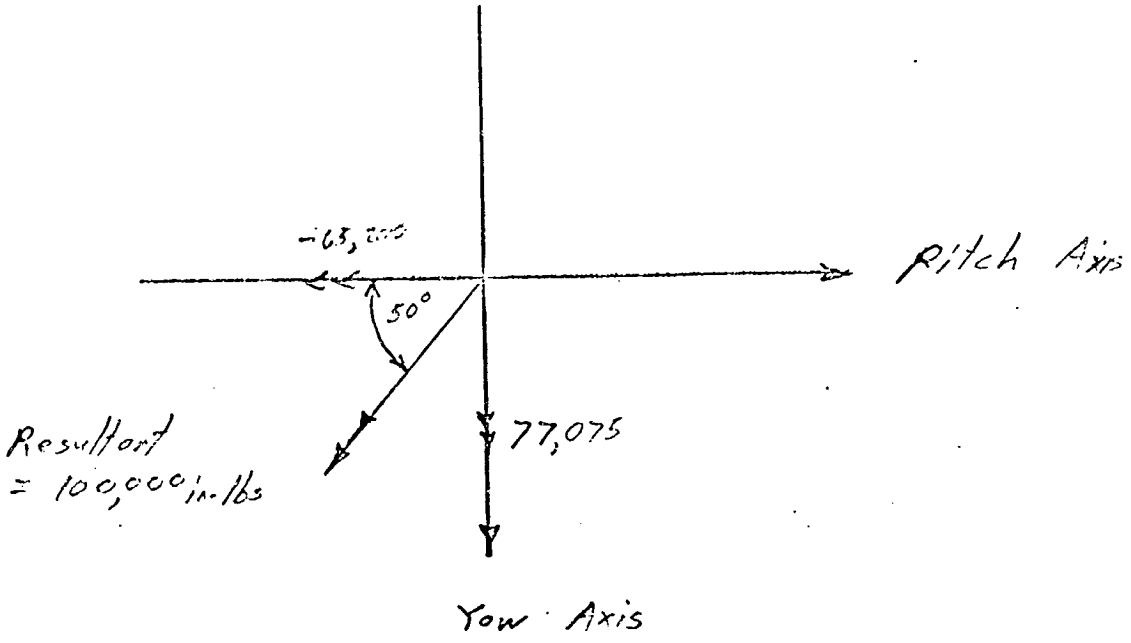

No. 2 Engine (Looking Forward)

An effort was made to resolve the force, i.e., to find the location, direction, and magnitude of a single force that would cause the engine 202 movements noted and vehicle movements as reported by NASA. Results are as follows:

1. Analysis revealed that the movements were inconsistent. The resulting equations could not be solved without simplifying assumptions. The inconsistency is probably caused by the loss of thrust in engine 202; this thrust loss would introduce a roll moment of indeterminate magnitude on the vehicle because of initial thrust misalignment and springback of the vehicle thrust structure.

2. If the observed vehicle and engine moments are assumed to have resulted from a lateral force, this force would have a magnitude of 800 to 840 pounds, and would be located at the extreme aft end of the thrust chamber. This force must act radially outboard

at an angle of 13 to 40 degrees from the + pitch axis toward the + yaw axis. This would aid in corroboration of that portion of the hypothesis wherein the actuator ΔP shift resulted from a thrust chamber leak at the interior of the chamber near the exit.

3. Calculations: The calculations are presented below.

Force Resolution: NASA reports the unknown force produced the following moments about the vehicle centerline:

Pitch	-023 degrees	M_{mp} = -10,900 ft-lb
Yaw	+0.103 degrees	M_{my} = +48,600 ft-lb
Roll	-0.085 degrees	M_{mr} = -2080 ft-lb

Rocketdyne gimbal actuator analysis indicates the unknown force produced the following moments about the engine gimbal centerline:

Pitch	M_{ep}	= -5430 ft-lb
Yaw	M_{ey}	= +6430 ft-lb

Problem: Determine the magnitude and direction of the force necessary to cause these moments.

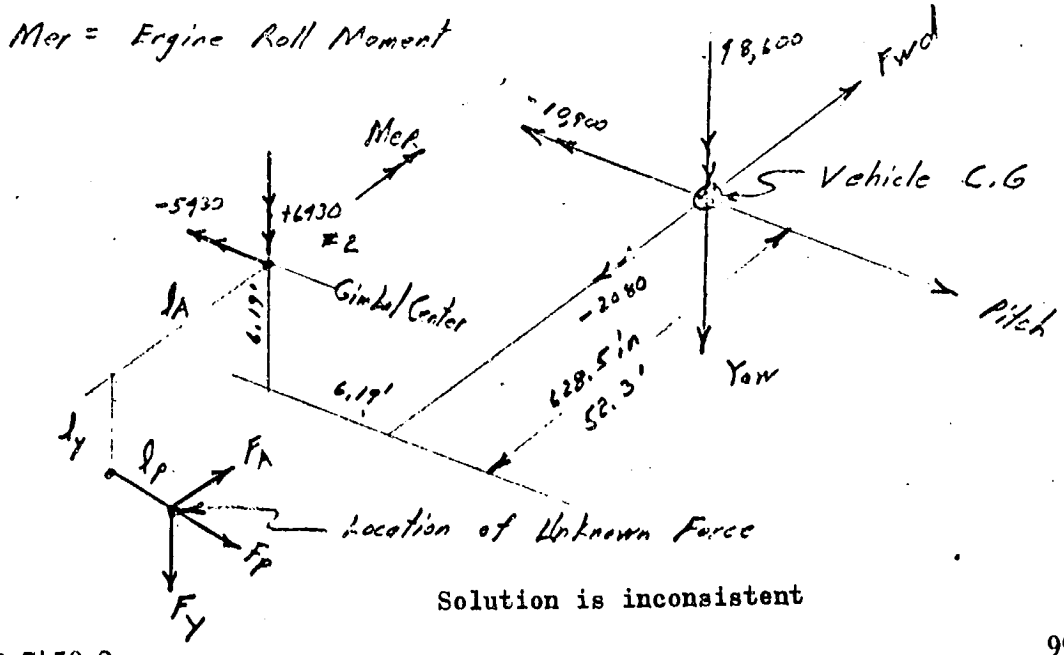

$$M_{er} = F_p \ell_y + F_y \ell_p \quad (1)$$

$$M_{ey} = F_p \ell_a - F_a \ell_p \quad (2)$$

$$M_{ep} = F_a \ell_y - F_y \ell_a \quad (3)$$

$$M_{mr} = -F_y (6.19 - \ell_p) + F_p (6.19 - \ell_y) \quad (4)$$

$$M_{my} = -F_p (52.3 + \ell_a) + F_a (6.19 - \ell_p) \quad (5)$$

$$M_{mp} = -F_a (6.19 - \ell_y) + F_y (52.3 + \ell_a) \quad (6)$$

Assume $M_{er} = 0$

$$0 = -F_p \ell_y + F_y \ell_p \quad (7)$$

$$6430 = -F_p \ell_a - F_a \ell_p \quad (8)$$

$$-5430 = +F_y \ell_a + F_a \ell_y \quad (9)$$

$$-2080 = F_p (6.19 \ell_y) - F_y (6.19 - \ell_p) \quad (10)$$

$$48{,}600 = -F_p (52.3 + \ell_a) + F_a (6.19 - \ell_p) \quad (11)$$

$$-10{,}900 = +F_y (52.3 \ell_a) - F_a (6.19 - \ell_y) \quad (12)$$

From Eq. 1 :

$$F_p = \frac{F_y \ell_p}{\ell_y} \quad (13)$$

From Eq. 3 :

$$\ell_a = \frac{-5430 - F_a \ell_y}{F_y} \quad (14)$$

Substituting in Eq. 2 :

$$6430 = -\frac{F_y \ell_p}{\ell_y} \left(\frac{-5430 - F_a \ell_y}{F_y} \right) - F_a \ell_p$$

$$6430 = + 5430 \frac{\ell_p}{\ell_y} + F_a \ell_p - F_a \ell_p \qquad (15)$$

$$\ell_p = 1.18 \ell_y$$

Substituting in Eq. 4 :

$$-2080 = F_y \frac{1.18 \ell_y}{\ell_y} (6.19 - \ell_y) - F_y (6.19 - 1.18 \ell_y)$$

$$-2080 = 6.19 (1.18) F_y - 1.18 F_y \ell_y - 6.19 F_y + 1.18 F_y \ell_y$$

$$-2080 = 1.113 F_y$$

$$Fy = 1865 \text{ lbs}$$

From Eq. 7 :

$$F_p = - 1865 \left(\frac{1.18 \ell_y}{\ell_y} \right)$$

$$F_p = - 2200 \text{ lbs}$$

Substituting in Eq. 5 :

$$48,600 = - (-2200)(52.3 + \ell_a) + F_a (6.19 - \ell_p)$$

$$48,600 = 115,000 + 2200 \ell_a + 6.19 F_a - F_a \ell_p$$

$$-66,400 = 2200 \ell_a + 6.19 F_a - F_a \ell_p \qquad (16)$$

From Eq. 2 :

$$6430 = - F_p \ell_a - F_a \ell_p$$

$$-F_a \ell_p = 6430 - 2200 \ell_a \qquad (17)$$

Substituting Eq. 11 in Eq. 10:

$$-66,400 = 2200\,\ell_a = 6.19\,F_a + 6430 - 2200\,\ell_a$$

$$F_a = -\frac{72,830}{6.19}$$

$$F_a = -11,750 \text{ pounds}$$

From Eq. 11:

$$0 = 6430 - 2200\,\ell_a - 11,75_p$$

$$\ell_a = 2.92 - 5.34\,\ell_p \qquad (18)$$

From Eq. 6 :

$$-10,900 = -1865\,(52.3 + \ell_a) + 11,750\,(6.19 - \ell_y)$$

$$-10,900 = -97,500 - 1865\,\ell_a + 72,600 - 11,750\,\ell_y$$

$$0 = -14,000 - 1865\,\ell_a - 11,750\,\ell_y$$

$$0 = -7.5 - \ell_a - 6.3\,\ell_y \qquad (19)$$

Substituting Eq. 9 and 12 in Eq. 13 :

$$0 = -7.5 - (2.92 - 5.34\,(1.18\,\ell_y)) - 6.3\,\ell_y$$

$$0 = -7.5 - 2.92 + 6.3\,\ell_y - 6.3\,\ell_y$$

$$0 \neq -4.58$$

Solution is in error; equations are not consistent.

Including the loss in thrust, NASA reports the following total moments induced on the vehicle:

$$\text{Pitch } M_{mp} = +26{,}100 \text{ ft-lb}$$

$$\text{Yaw } M_{my} = +11{,}800 \text{ ft-lb}$$

$$\text{Roll } M_{my} = -2080 \text{ ft-lb}$$

Modify the equations to incorporate a -6000-pound thrust at gimbal center and the above moments

$$0 = -F_p \ell_y + F_y \ell_p \tag{20}$$

$$6430 = -F_p \ell_a - F_a \ell_p \tag{21}$$

$$-5430 = +F_y \ell_a + F_a \ell_y \tag{22}$$

$$-2080 = F_p (6.19 - \ell_y) - F_y (6.19 - \ell_p) \tag{23}$$

$$11{,}800 = -F_p (523 + \ell_a) - 6000 (6.19) + F_a (6.19 - \ell_p) \tag{24}$$

$$26{,}100 = +6000 (6.19) + F_y (52.3 + \ell_a) - F_a (6.19 - \ell_y) \tag{25}$$

From Eq. 20:

$$F_p = F_y \frac{\ell_p}{\ell_y} \tag{26}$$

From Eq. 22:

$$\ell_a = \frac{-5430 - F_a \ell_y}{F_y} \tag{27}$$

From Eq. 21:

$$\ell_p = 1.18 \ell_y \tag{28}$$

Substituting in Eq. 23 :

$$-2080 = F_y \frac{1.18\ \ell_y}{\ell_y} (6.19 - \ell_y) - F_y (6.19 - 1.18\ \ell_y)$$

$$-2080 = 6.19\ (1.18)\ F_y - 1.18\ F_y - 6.19\ F_y + 1.18\ F_y \ell_y$$

$$-2080 = 1.113\ F_y$$

$$F_y = 1865 \text{ lbs}$$

From Eq. 26 :

$$F_p = -2200 \text{ pounds}$$

Substituting in Eq. 24 :

$$0 = -48{,}800 + 2200\ (52.3 + \ell_a) + F_a\ (6.19 - \ell_p)$$

$$0 = -48{,}800 + 115{,}000 + 2200\ \ell_a + 6.19\ F_a - F_a \ell_p$$

$$0 = 66{,}200 + 2200\ \ell_a + 6.19\ F_a - F_a \ell_p \qquad (29)$$

From Eq. 21:

$$-F_a \ell_p = 6430 - 2200\ \ell_a \qquad (30)$$

Substituting Eq. 30 in Eq. 29:

$$0 = 66{,}200 + 2200\ \ell_a + 6.19\ F_a + 6430 - 2200\ \ell_a$$

$$F_a = \frac{-72{,}630}{6.19}$$

$$F_a = -11{,}750$$

From Eq. 30 :

$$\ell_a = 2.92 - 5.34\ \ell_p \qquad (31)$$

From Eq. 25:

$$26{,}100 = 37{,}000 - 1865\ (52.3 + \ell_a) + 11{,}750\ (6.19 - \ell_y)$$

$$0 = -14.0 + 19.85 - 52.3 - \ell_a + 39 - 6.3\ \ell_y$$

$$0 = -7.45 - \ell_a - 6.3\ \ell_y \qquad (32)$$

Substituting Eq. 28 and 31 in Eq. 32 :

$$0 = -7.45 - 2.92$$

$$0 \neq 4.33$$

Solution in error; equations are not consistent.

Assumed Lateral Force:

1. NASA Data

Ignoring roll moment, the vehicle moments caused by the unknown force can be resolved as follows:

$49{,}900 = F\ \ell$

Missile center of gravity to aft of engine

$\ell = 52.3 + \frac{119.56}{12}$

$\ell = 62.3$ feet

$F = \frac{49{,}900}{62.3}$

$F = 800$ pounds at aft end of thrust chamber

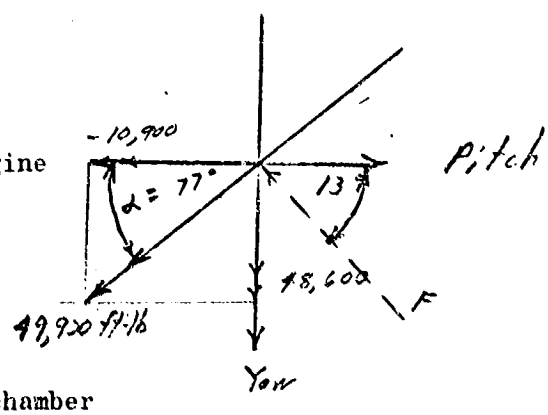

2. Rocketdyne Data

8400 F ℓ

ℓ $\frac{116.56}{12} = 9.6$

F $\frac{8400}{10}$

F 870 pounds at aft end of thrust chamber

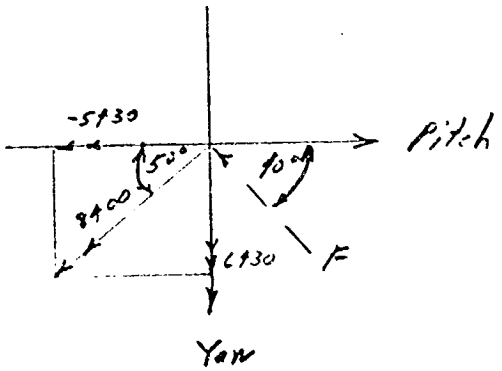

No. 9 Actuator Anomalies:

If the observed vehicle moments and engine moments are caused by a single side force, determine the magnitude and location of this force.

Solution: 800 to 870 pounds in exhaust plane of the engine.

① F $\frac{49,900}{62.3-x}$ ② F $\frac{8400}{9.6-x}$

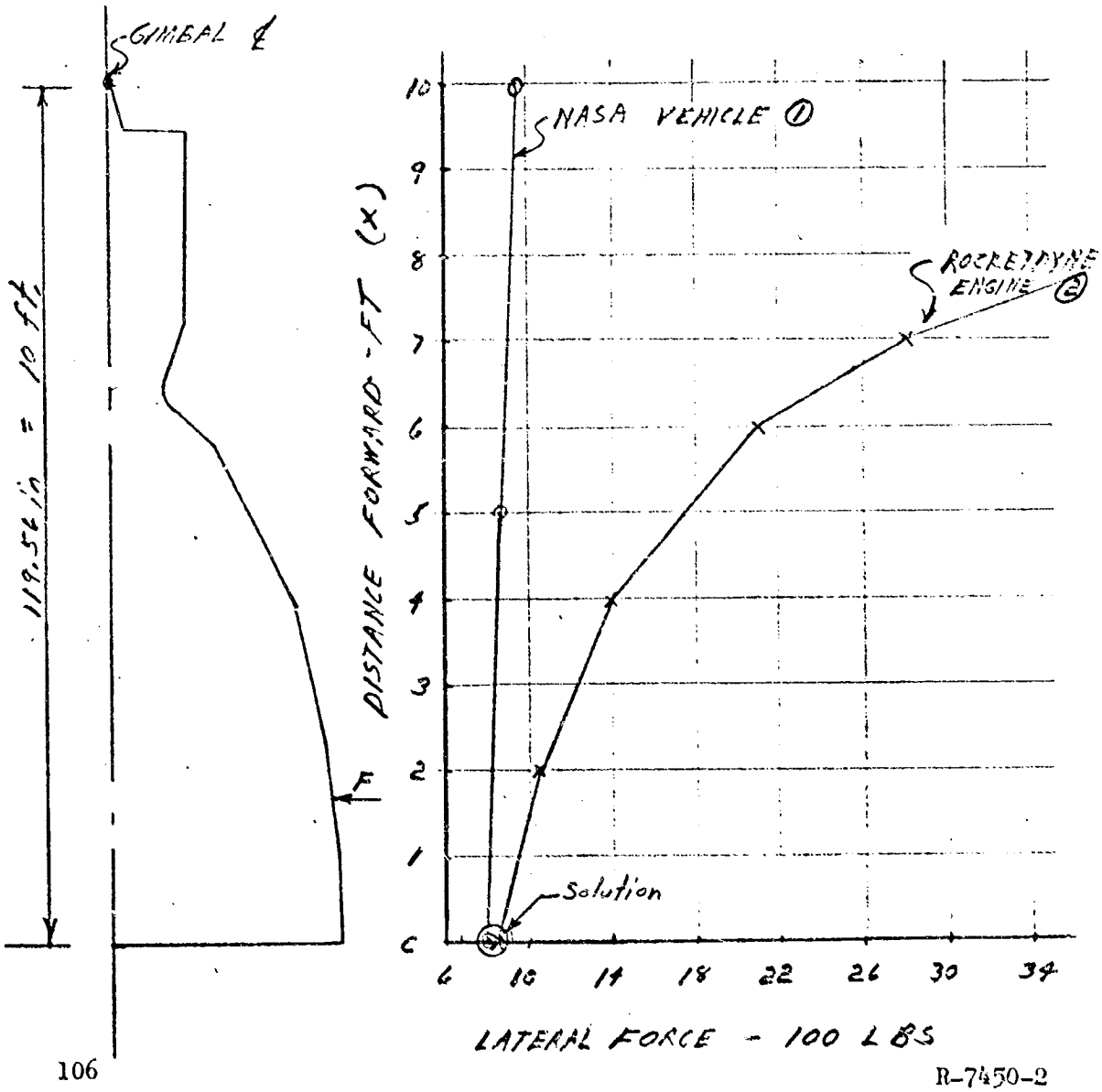

Further corroboration resulted from flight support testing conducted at the MSFC high-pressure thrust chamber component stand. During the second of two tests conducted with high ASI mixture ratios, and resultant erosion of the ASI and main injector, two adjacent thrust chamber up tubes sustained gate-type splits. The tube damage was located approximately 7 inches from the nozzle exit, at the interior (hot gas) side of the nozzle, and was apparently caused by ejected injector debris. Fuel flow from the tube splits, estimated at 7 to 8 lb sec, produced a 145,000 in.-lb moment load at the gimbal bearing. Analysis of the MSFC thrust chamber component testing included calculations of leakage resulting from the thrust chamber damage and calculations of resultant side loads. These calculations are presented below and on the following pages.

Leakage Calculations (MSFC), Flight 502 Simulation:

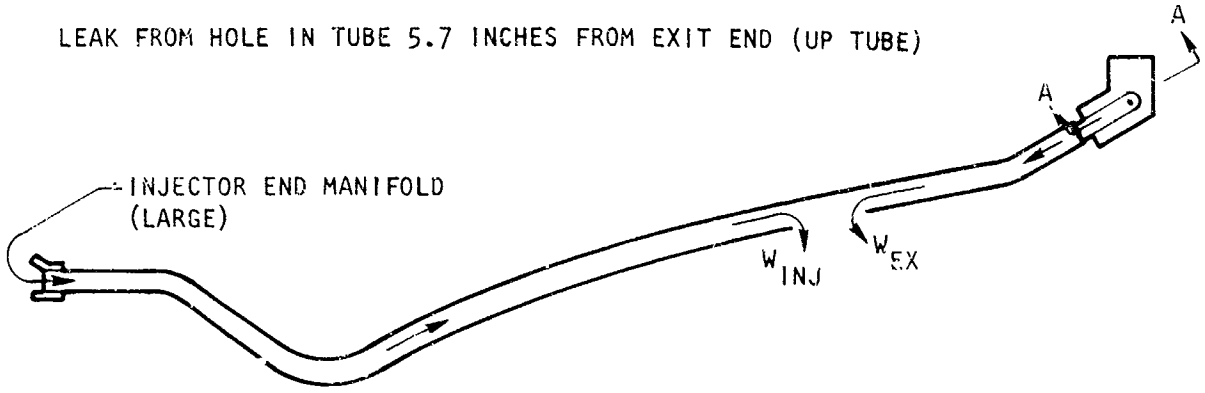

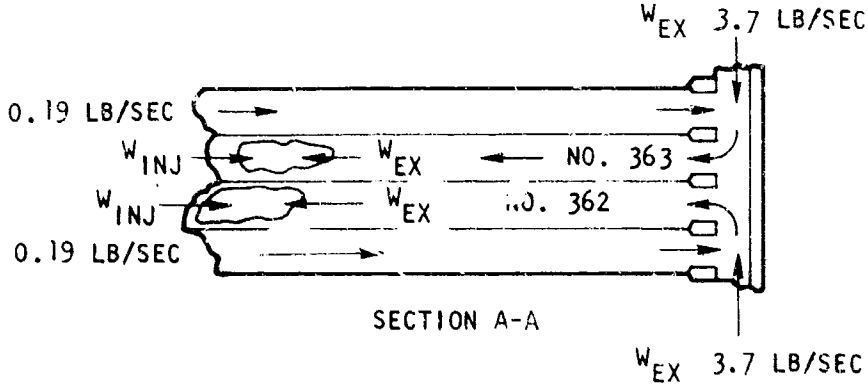

SIMULATION TEST 217-4

SPLIT TUBES { #362, 5 3/4" U/S OF EXIT 1 1/2" LG
#363, 5" U/S OF EXIT 1" LG

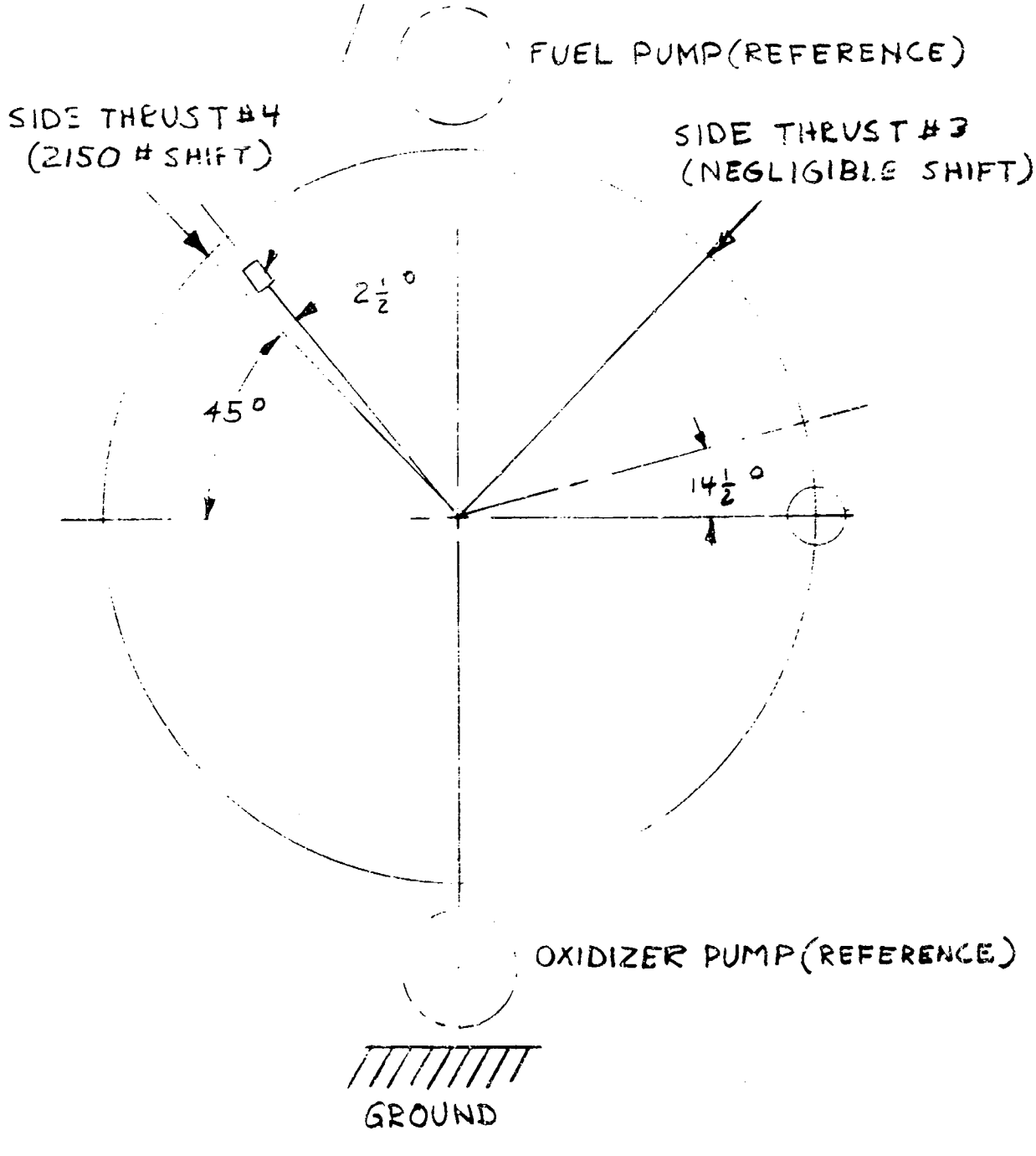

VIEW LOOKING AFT

Side Load Test Summary (MSFC), Flight 502 Simulation:

$X_{SL\#4} = 67.28$ (AXIAL DIST. FROM GIMBAL ℄)

$M = 67.28 \times 2150 = \boxed{145{,}000\text{"}\#}$ MOMENT ABOUT GIMBAL ℄ DUE TO LEAK

$X_{362} = 116 - 5.8 = 110.2"$ (AXIAL DIST. OF LEAK FOR TUBE 362 TO GIMBAL ℄)

SIMILARLY

$X_{363} = 116 - 5 = 111"$

$\bar{X}_{LEAK} = (X_{362} + X_{363})/2 = 110.6"$

THEREFORE:

F_S (EFFECTIVE SIDE LOAD IN PLANG OF LEAK)

$$= \frac{M}{\bar{X}_{LEAK}} = \frac{145{,}000}{110.6} = 1310\ \#$$

$$I_{SP} = \frac{F_S}{W} = \frac{1310}{7.78} = \boxed{168\ \text{SEC}}$$

EFFECTIVE SIDE LOAD I_{SP} FOR AN INTERNAL LEAK 5.4" FROM EXIT

PART I (LEAKAGE FROM RETURN MANIFOLD - W_{EX})

1) TUBE # 362

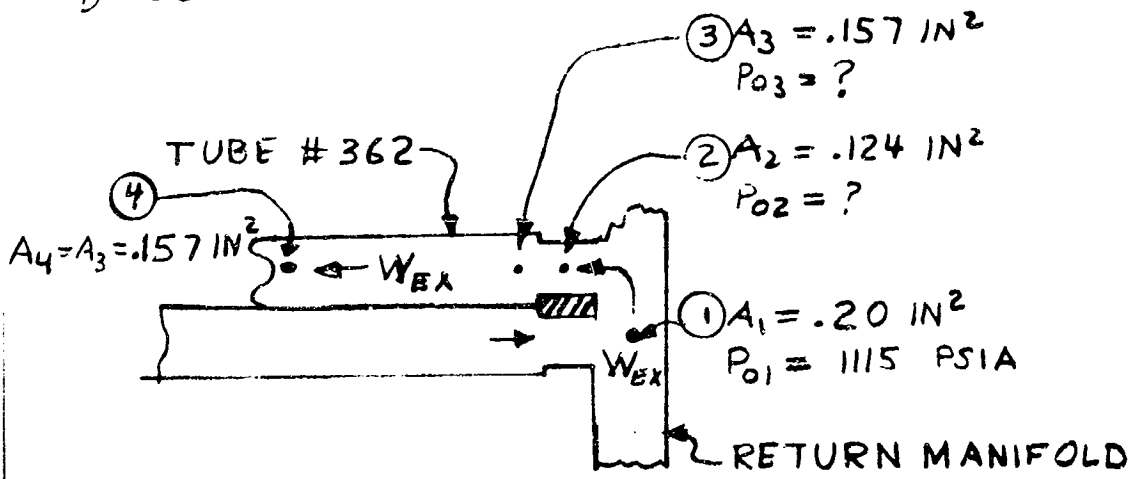

ASSUMPTIONS:

1. HOLE SIZE DOES NOT RESTRICT FLOW
2. TEMPERATURE = 60 R
3. STAGNATION PRESSURE IN RETURN M MANIFOLD (P_{01}) = 1100 PSIA
4. MAXIMUM FLOW LIMITED BY CAVITATION AT A_2 (P_2 = 150 PSIA); LESS FLOW IF THE RESISTANCES ARE SUFFICIENTLY HIGH.
5. STAGNATION PRESSURE LOSSES =
   - A. 1 VELOCITY HEAD AT A_1
   - B. $\frac{1}{2}$ VELOCITY HEAD ENTRANCE LOSS AT A_2
   - C. SUDDEN EXPANSION A_2 TO A_3 (FOR NON CAVITATING FLOW).
   - D. FRICTION DROP BETWEEN SECTION 3 AND 4 (FOR NON CAVITATING FLOW).

BY TRIAL AND ERROR W_{EX} = 3.70 #/SEC FOR CAVITATING FLOW. CHECK AS FOLLOWS:

ρ = DENSITY AT SECTION 1 = 4.06 #/FT³ (FOR PRESSURE = 1100 PSIA AND TEMPERATURE = 60 R)

V_1 = VELOCITY AT SECTION 1.

$$= \frac{W_{EX}}{\rho_1 A_1} = \frac{3.70 \times 144}{4.06 \times .20} = 655 \text{ FT/SEC}$$

ρ_2 = DENSITY AT SECTION 2 = 3.94 #/FT³

V_2 = VELOCITY A SECTION 2

$\cong \frac{3.70 \times 144}{3.94 \times .124} = 1092$ FT/SEC

ΔP_{01-02} = STAGNATION PRESSURE DROP FROM SECTION

$= \frac{1}{2g}\rho_1 V_1^2 + \frac{1}{2}\left(\frac{1}{2g}\rho_2 V_2^2\right)$

$= \frac{4.06(655)^2}{64.4 \times 144} + \frac{3.94(1092)^2}{2 \times 64.4 \times 144} = 187 + 255$

$= 442$ PSID

$P_{02} = P_{01} - \Delta P_{01-02} = 1100 - 442$

$= 658$ PSIA

$P_2 = P_{02} - \frac{1}{2g}\rho_2 V_2^2 = 658 - 510 = \underline{148 \text{ PSIA}}$

SINCE VAPOR PRESSURE = 150 PSIA $\cong P_2$, CHOKING CONDITION IS MET. ADDITIONAL CHECK IS REQUIRED TO DETERMINE IF FLOW IS RESTRICTED BY TUBE RESISTANCES AS FOLLOWS:

FOR SUDDEN EXPANSION FROM SECTION 2 TO SECTION 3:

$\frac{A_2}{A_3} = \frac{.124}{.157} = .79$, $K = .04$

$\Delta P_{02-03} = K \frac{1}{2g}\rho_2 V_2^2 = .04 \times \frac{3.95(1092)^2}{64.4 \times 144}$

$= \underline{20.4 \text{ PSID}}$

FOR FRICTION DROP FROM SECTION 3 TO SECTION 4:

L = LENGTH FROM SECT. 3 TO SECT 4 = 5.2"

f = FRICTION FACTOR = .014

D_H = HYDRAULIC TUBE DIAM. = .43"

$V_3 = \frac{3.70 \times 144}{3.94 \times .157} = 860$ FT/SEC

$$\Delta P_{03-04} = \frac{L}{D_H} \times f \times \frac{1}{2g} \rho_3 V_3^2 = \frac{5.2}{.43} \times .014 \times \frac{3.94(860)^2}{64.4 \times 144}$$

$$= \underline{53.4 \text{ PSID}}$$

$$\therefore P_4 = P_{02} - \Delta P_{02-03} - \Delta P_{03-04} - \frac{1}{2g} \rho_3 V_3^2$$

$$= 658 - 20.4 - 53.4 - 375$$

$$= \underline{209 \text{ PSIA}}$$

SINCE P_4 IS LESS THAN VAPOR PRESSURE OF 150 PSIA FLOW IS LIMITED BY CHOKING IN SECTION 2 AND

$\boxed{W_{EX} = 3.70 \text{ \#/SEC}}$ FOR FLOW FROM RETURN MANIFOLD IN TUBE #362

SINCE L FOR TUBE #363 IS LESS THAN FOR TUBE #362 THE FLOWS IN BOTH TUBES ARE THE SAME.

PART II (LEAKAGE FROM INJECTOR END - W_{INJ}):

BY TRIAL AND ERROR $W_{INJ} = .19$ #/SEC, CHECK AS FOLLOWS:

K_{INJ} = OVERALL RESISTANCE TO LEAKAGE POINT
= 4.1 IN^5/SEC (AS DETERMINED FROM COMPUTER PROGRAM WHERE:

$$K_{INJ} = \frac{\Delta P \bar{\rho}}{W_{INJ}^2}$$

$\dot{Q}$ = APPROX. HEAT TO TUBE = 110 $\frac{BTU}{SEC}$ (FROM COMPUTOR PROGRAM).

$$\Delta T = \frac{\dot{Q}}{\bar{C}_p W_{INJ}} = \frac{110}{3.7 \times .19} = 157 R$$

$$\bar{T} = 200 + \frac{157}{2} = 279 R$$

$\bar{P}$ = AVG PRESSURE OF HYDROGEN = (830+20)/2
= 425 PSIA

THEREFORE:

$\bar{\rho}$ = AVG. DENSITY = .0001606 #/IN^3

AND

$$W_{INJ} = \sqrt{\frac{(830-20)(.0001606)}{4.1}}$$

= .18 SUFFICIENTLY CLOSE TO .19 USE:

W_{INJ} = .19 #/SEC LEAKAGE IN TUBE FROM INJECTOR END.

THEREFORE:

3.70 + .19 = 3.89 #/SEC LEAKAGE FROM ONE TUBE

2 × 3.89 = 7.78 #/SEC LEAKAGE FROM TWO TUBES NOS 362 & 363

A review of R&D testing accomplished at SSFL yielded further corroborative evidence that thrust chamber tube splits internal to the chamber near the exit would produce the type of lateral loading exhibited by engine 202.

1. R&D engine J024-3 incurred thrust chamber damage during an injector combustion stability test (623-005) when a bomb fragment was ejected from the combustion zone and struck the interior of the thrust chamber wall near the exit. Two tube splits resulted (one 1/4 by 1-1/4 inch, located approximately 15 inches from the exit, and one 3/8 by 1/2 inch, located approximately 4 inches from the exit).

2. The following calculations of loads resulting from test 623-005 thrust chamber damage indicates that the lateral force caused by the fuel leak is located approximately 26 inches forward of the chamber exit, approximately 11 inches forward of the most forward damage point; it is believed that the center of pressure of the bow shock set up by the fuel leak is forward of the actual leak location (Fig. 61 and 62).

Engine 202 Yaw and Pitch Actuator Δ P Indications: 413-550 Seconds Range Time

Description of Event. At 413 to 550 seconds range time, i.e., during the period following engine 202 cutoff, the pitch actuator Δ P measurement indicated -500 psid, signifying loading in tension. The yaw actuator Δ P measurement, apparently slow in responding, indicated -500 psid at approximately 530 seconds range time (Fig. 53 and 56). There were no engine or supporting system anomalies during this time period that would contribute to the event in question; operation of engine 202 had been terminated, and the EAS hydraulic reservoir associated with engine 202 had gone "flat", i.e., had lost fluid.

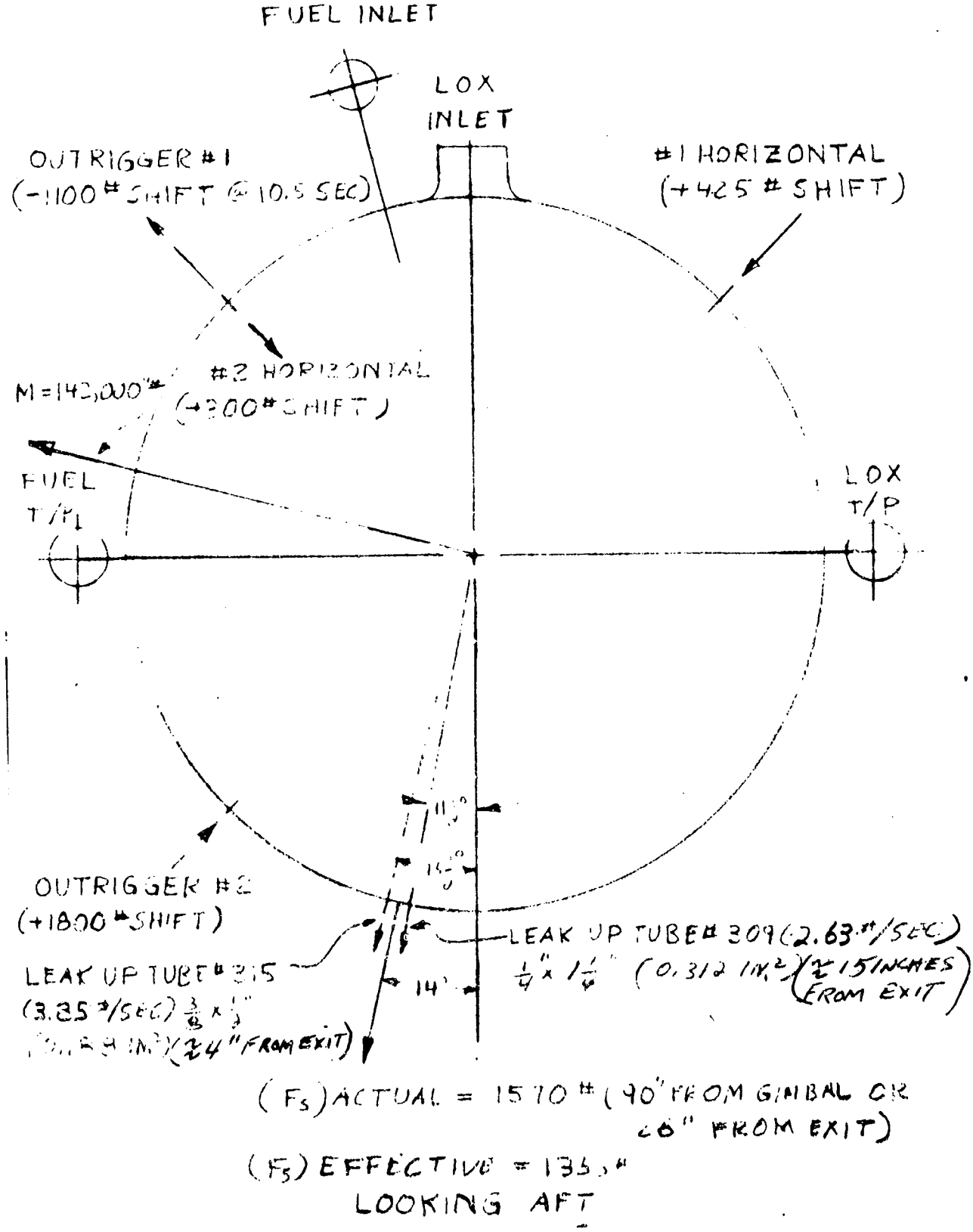

Figure 61. Engine J024-3 Test No. 623005 Load Analysis

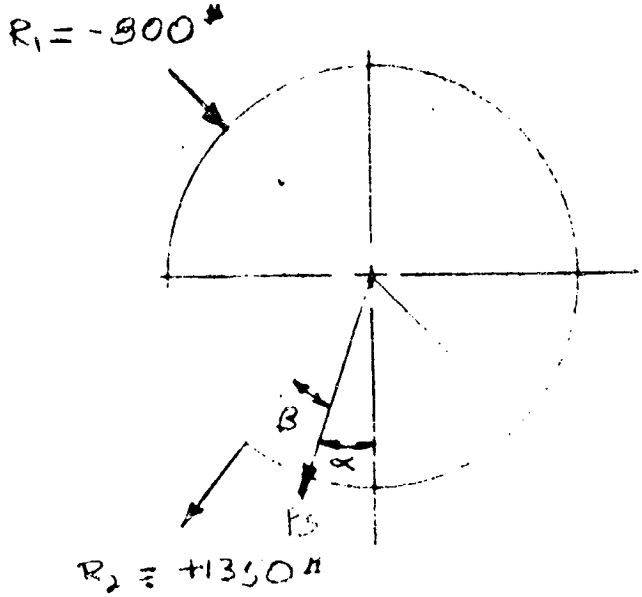

$R_1 = -1100 + 300 = -800^{\#}$

$R_2 = +1800 - 450 = +1350^{\#}$

$F_S = \sqrt{900^2 + 1350^2} = \sqrt{2460000} = \boxed{1570^{\#}}$ ACTUAL SIDE LOAD

$\beta = \tan^{-1}\frac{800}{1350} = \tan^{-1}.592 = 30.6°$

$\alpha = 45 - 30.6$, $\boxed{\alpha = 14°}$

R = RESULTANT FORCE AT OUTRIGGER

$= \sqrt{1100^2 + 1800^2} = \sqrt{445,0000} = \boxed{2110^{\#}}$

M = MOMENT ABOUT GIMBAL = $2110 \times 67.2 = \boxed{142,000^{\#"}}$

X_M = MOMENT ARM = $\frac{142\,000}{1570} = \boxed{90.3" \text{ FROM GIMBAL OR } 26" \text{ FROM EXIT}}$

NOTE: CENTER OF FORCE IS UPSTREAM OF LEAKS, IF TRUE A BOW SHOCK AHEAD OF LEAK MAY ACCOUNT FOR THIS.

Figure 61 (Continued)

CALCULATE (F_s) EFFECTIVE (S-SECONDARY INJECTION)

(F_s) EFFECTIVE FOR TUBE 309 = $(I_{sp})_{EFF} \times W_{309}$

= 168 x 85 = 612 POUNDS

$(I_{sp})_{EFF}$ OBTAINED FROM LINEAR EXTRAPOLATION OF MSFC TEST

(F_s) EFFECTIVE FOR TUBE 315

$$= \frac{142,000 - 612 \times 112}{101} = \frac{142,000 - 65,000}{101} = \frac{77,000}{101}$$

= 766 POUNDS

(F_s) EFFECT. = 612 + 766 = 1378 POUNDS

$$(I_{sp})_{EFF} \text{ TUBE 315} = \frac{766}{2.63} = 292 \text{ SEC}$$

$$(I_{sp})_{ACTUAL} = \frac{1570}{6.48} = 243 \text{ SEC}$$

$$K' \text{ (ACTUAL)} = \frac{243}{425} = 0.572$$

Figure 61 (Concluded)

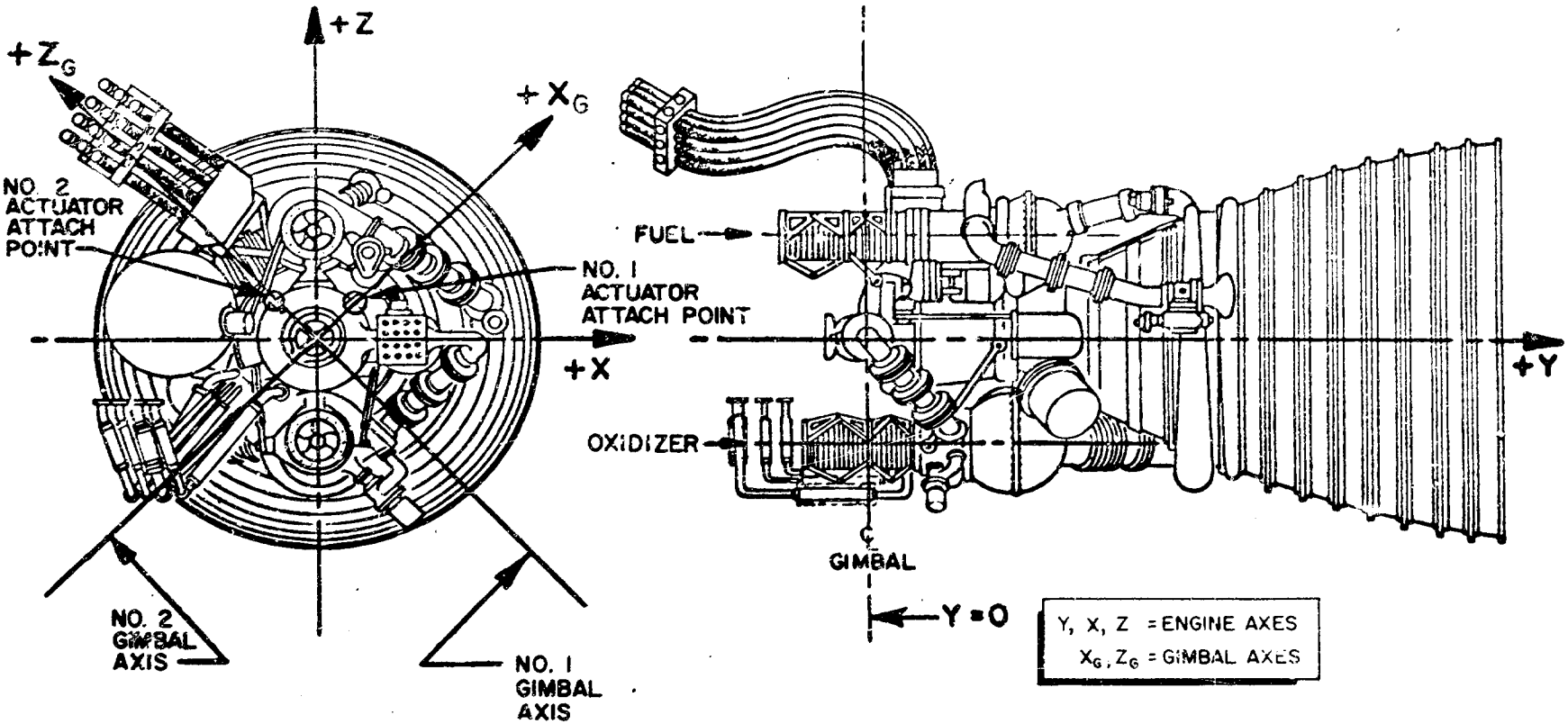

Figure 62. J-2 Engine Coordinate Axes Diagram

Hypothesis Engine 202 was externally loaded in such a manner as to result in tension loading of both the pitch and yaw actuators; the loading was being applied by the pressurized fuel inlet duct.

Corroboration of Hypothesis. Corroboration that tension loading of the engine 202 pitch and yaw actuators was caused by the pressurized fuel inlet duct was accomplished by balancing of pressure forces existing at range time 550 seconds.

It was determined that the engine 202 fuel inlet duct was pressurized to approximately 80 psia at 550 seconds. Although the fuel pump inlet pressure measurement was lost at cutoff of engine 202 (412.9 seconds), fuel pump discharge and fuel pump interstage pressure measurements both indicated approximately 80 psia. The 80-psia pressure level results from summation of the 35-psia fuel pump inlet pressure observed prior to engine cutoff and the 40 ±5 psid operating pressure of the stage fuel manifold vent valve. Oxidizer pump inlet pressure at 550 seconds was zero, indicating a loss of oxidizer feed system integrity.

The calculations on the following pages corroborate the hypothesis that pitch and yaw actuator tension loads observed at 550 seconds were caused by the pressurized fuel inlet duct; the calculations also include the case where the oxidizer inlet duct, rather than the fuel inlet duct, is pressurized, and show that in such a case the actuator loads would be in compression instead of tension and would be of greater magnitudes than observed from S-II flight data.

J-2044 ACTUATOR LOAD SHIFT FROM START TO POST-CUTOFF (550 SECONDS)

	Actuator (-is Tension Load)	
	Pitch, pounds	Yaw, pounds
Measured Load Shift:		
at 550 seconds	-7150	-6900
at start	-1300	-1300
Difference	-5850	-5600
Calculated Load Shift:		
w 80 psi in LH_2 duct		
0 psi in LOX duct		
Inlet Duct Loads		
Pressure	-7200	-7200
Gimbaling	+1800	+1800
Inertial Loads	+ 700	+ 220
Total	-5320	-5800
Error (Measured-Calculated)	- 530	+ 200
Calculated Load Shift (Reverse Δ P Pressure After Cutoff)		
w/80 psi in LOX duct		
0 psi in LH_2 duct		
Inlet Duct Loads		
Pressure	+5100	+5100
Gimbaling	+1180	+1180
Inertial Loads	+ 700	+ 220
Total	+6980	+6500
Error (Measured-Calculated)	-12830	-12100

ENGINE PARAMETERS USED IN ANALYSIS

Parameter	Start	After Cutoff at 550 Seconds
Oxidizer Inlet Pressure, psia	42	0
Fuel Inlet Pressure, psia	28.5	80
G-Load	0	1.0
Gimbal Angle		
Pitch	0	4.0 (ext.)
Yaw	0	0
Actuator Δ P		
Pitch, psi	- 100	- 550
Pitch, pounds	-1300	-7150
Yaw, psi	- 100	- 550
Yaw, pounds	-1300	-6900

Inlet Duct Spring Rates: LOX = 435 lb/in.
LH_2 = 480 lb/in.

Engine CG and Weight (Dry): Weight = 3376 pounds
Y = 31.34 inches
X_G = 0.760 inch
Z_G = -0.135 inch

ACTUATOR LOAD DIFFERENCE BETWEEN ENGINE START (148 SECONDS) AND AFTER SHUTDOWN (≈500 SECONDS)

Parameters	Start (150 seconds)	At Cutoff (≈550 seconds)
LOX Inlet Pressure, psia	42	0
LH_2 Inlet Pressure, psia	28.5	80-82
G-Load	0	1.0
Gimbal Angle, degrees		
Pitch	0.0	4.0 (ext.)
Yaw	0.0	≈0
Gimbal Actuator Δ P		
Pitch, psi	- 100	- 550
(-) tension, pounds	-1300	-7150
Yaw, psi	- 100	- 530
F = Δ PA = -13Δ P, pounds	-1300	-6900

Engine Weight and CG :

	Weight	Y	X_e	Z_e	X_G	Z_G
Dry	3376 pounds	31.34	0.639	0.436	0.760	-0.135
Wet	3510 pounds	30.73	0.730	0.117	0.610	-0.430

After cutoff, the engine is closer to the dry weight

CALCULATION OF ACTUATOR LOAD DIFFERENTIAL FROM -START TO 550 SECONDS

Inlet Line Loads:

The actuator loads from inlet line loads are approximately equal for gimbaling or from pressurization. The loads can be approximated from the following equation:

$$F_a = \frac{+M_x}{2\left(\frac{11.875}{1\sqrt{2}}\right)} = \frac{+21}{11.875\sqrt{2}}\left[A(P_L - P_F) - \Delta(K_L + K_F)\right]$$

where

A = Duct Area = 62 $in.^2$

Δ = Duct Deflection = 21 sin α_x = 0.366 α_x

α_x = Projection of Cant Angle on α_x Axis

K_L and K_F = Duct Spring Rates

K_L = 435 lb/in. Spec Value (maximum)

K_F = 480 lb/in. Spec Value (maximum)

P_L = Oxidizer Inlet Pressure

P_F = Fuel Inlet Pressure

$-F_A \longrightarrow$ Compression

For a 4-degree pitch (extension):

$$\alpha_x = \frac{4}{\sqrt{2}} = -2.80 \text{ degrees}$$

Combining terms, F_a becomes:

$$F_a = +1.25\left[62(P_L - P_f) - 0.366\,\alpha_x(435+480)\right]$$

$$F_a = +77.5(P_L - P_f) - 420\,\alpha_x$$

At Start:

F_a = +77.5 (42 - 28.5) + 420 (0)
= +1050 pounds (compression)

At +550 seconds:

$F_a = +77(0-80) - 420(-2.8)$

$F_a = -6150 + 1180$ pounds

$-F_a$ Start = -1050 + 0

F_a 550 = 6150 + 1180

ΔF_a = 7200 + 1180 = -6020 pounds (tension)

$\Delta F_a = F_a$ 550 $- F_a$ Start

Change in actuator loads from inlet lines

CG Shift Effects :

At start, G load $\approx$ 0

At 550 seconds, G load = 1G

CG POSITION (DRY WEIGHT)

	Y	X_G	Z_G
0 Gimbal Angle	31.34	0.764	-0.135
Shift from 4-degree Pitch (31.34 sin 4 degrees)	0	0	-2.18
Total	31.34	0.764	-2.30

Pitch $F_a = 3376 \frac{(2.30)}{11.875}$

$= +655$ pounds (compression)

Yaw $F_a = 3376 \frac{(+0.76)}{11.875}$

$= -215$ pounds (tension)

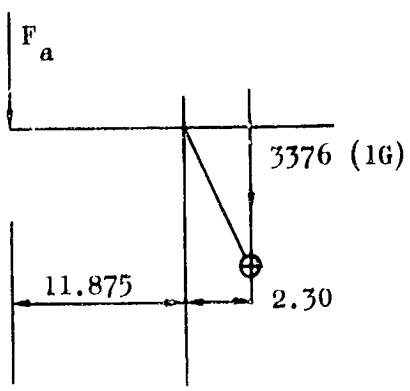

TOTAL SHIFT FROM START TO 550 SECONDS

Pitch	Yaw	
-6020	-6020	Inlet
655	215	G Load
-5365 pounds	-5805 pounds	(tension)

TOTAL MEASURED SHIFT

Pitch	Yaw	
-(-1300)	-(-1300)	
-7150	-6900	
-5850 pounds	-5600 pounds	(tension)
Difference : - 495 pounds	+ 205 pounds	

ENGINE 202 PERFORMANCE DECAY AND CUTOFF

Description of Events

Engine Performance Anomalies. Engine oxidizer flow began to increase at 412.3 seconds range time and continued to rise until 412.921 seconds, at which time engine cutoff was signaled by dropout of the mainstage OK pressure switches (Fig. 63).

Engine fuel flow increased, starting at 412.3 seconds (Fig. 63).

Main oxidizer injection pressure decayed very rapidly prior to main oxidizer valve closing; oxidizer pump discharge pressure decayed more slowly, and more closely approximated a normal shutdown (Fig. 64).

Thrust chamber pressure decreased 10 to 15 psi as oxidizer flow began to increase at 412.3 seconds.

Engine Compartment Anomalies. Engine compartment gas curtain and heat shield forward temperatures increased starting at 412.3 seconds (Fig. 65 and 66).

Engine compartment pressures increased starting at 412.5 seconds (Fig. 67).

Hypothesis

Engine 202 performance decay (beginning at 412.3 seconds range time) and subsequent cutoff resulted from failure of the oxidizer dome, precipitated by the following sequence of events:

1. Failure of the ASI fuel line at 220 seconds range time resulted in fuel leakage into the engine compartment and higher than normal ASI mixture ratios; the high ASI mixture ratio initiated erosion of the main injector/ASI nozzle, which continued until 319 seconds.

2. At 319 seconds range time, erosion of the main injector/ASI nozzle reached the peak of severity because of progressive worsening of the ASI fuel line leakage; erosion at this time had progressed into the inner row of oxidizer elements and some of the oxidizer passages (doghouses) supplying these elements. The higher flow-rate of oxidizer at this point resulted in a marked reduction in the erosion rate. The injector had been so structurally weakened by internal erosion that, at 319 seconds, a segment of the injector came free and struck the chamber wall near the exit, rupturing tubes; this resulted in a fuel leak of approximately 9 lb/sec to the interior of the thrust chamber, resulting in the observed performance shift and actuator loading.

3. Erosion of the injector at the upper portion of the ASI nozzle continued at a reduced rate until the ASI seal and sealing surface integrity was destroyed at 412.3 seconds; oxidizer and combustion products escaped into the engine compartment, causing further rapid erosion and performance decay.

4. Oxidizer injection pressure decayed until engine cutoff was signaled by dropout of the mainstage OK pressure switches.

Corroboration of Hypothesis

Inorease in oxidizer flow at 412.3 seconds precedes changes in all other engine parameters, indicating loss of oxidizer system integrity downstream of the oxidizer flowmeter.

Increase in fuel flow resulted from decrease in main chamber pressure.

Decreases in main fuel injection temperature, fuel turbine inlet temperature, resulted from a decrease in main chamber and gas generator mixture ratios during the performance decay. The shift of mixture ratios resulted from reduction of oxidizer flow to the thrust chamber and gas generator because of failure of the oxidizer system downstream of the flowmeter.

The oxidizer system failure occurred downstream of the main oxidizer valve; oxidizer feed system integrity upstream of the main oxidizer valve following cutoff is supported by data indicating that the system held approximately 20-psia pressure until the oxidizer bleed valve opened.

Rapid decay of main oxidizer injection pressure, as compared with oxidizer pump discharge pressure and increasing oxidizer flow, is indicative of oxidizer system failure downstream of the main oxidizer valve.

Model studies based on the assumption that oxidizer system failure occurred downstream of the main oxidizer valve closely approach the actual cutoff conditions (Fig. 63 through 76).

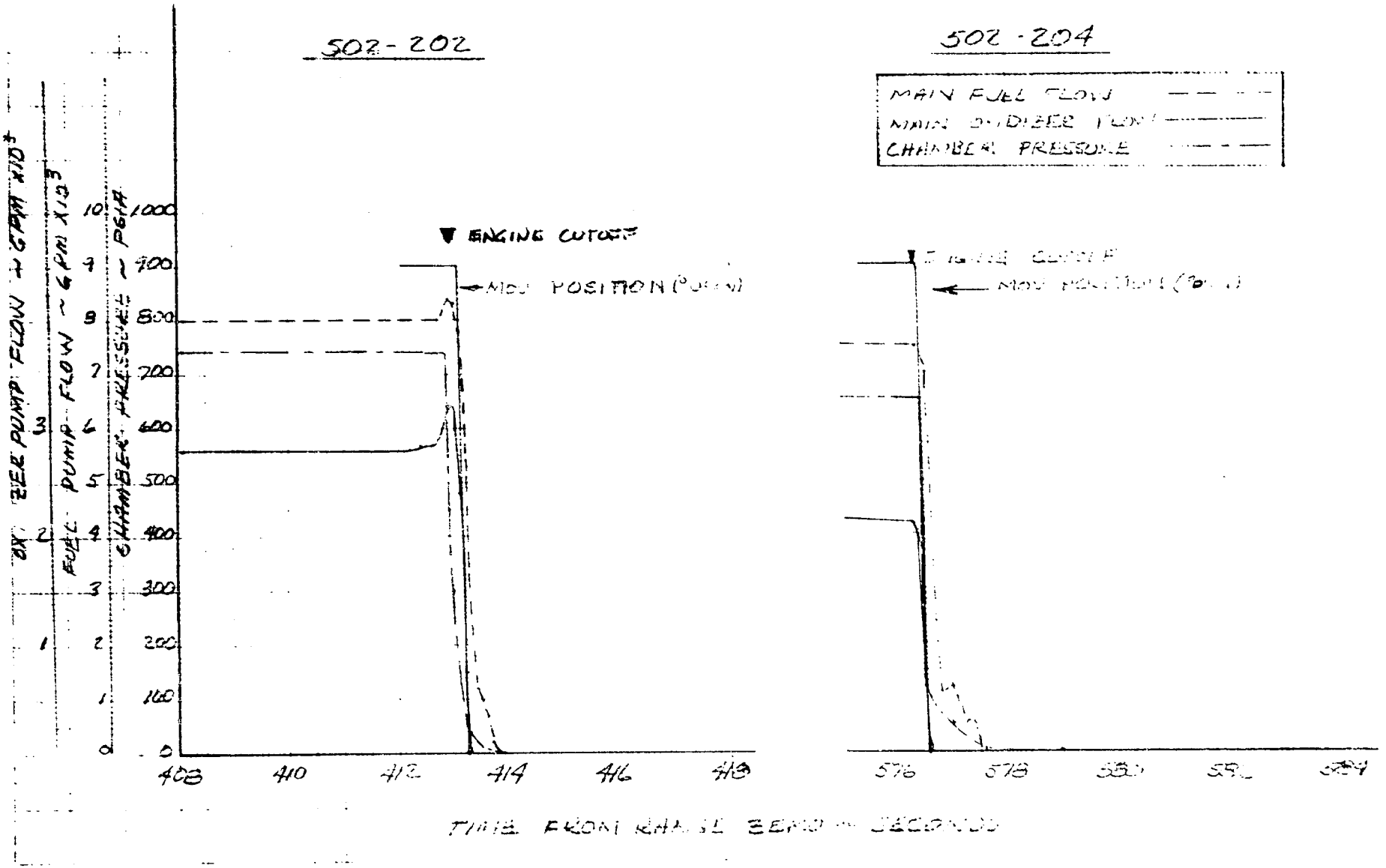

Figure 63. Pump Flows and Chamber Pressures vs Time

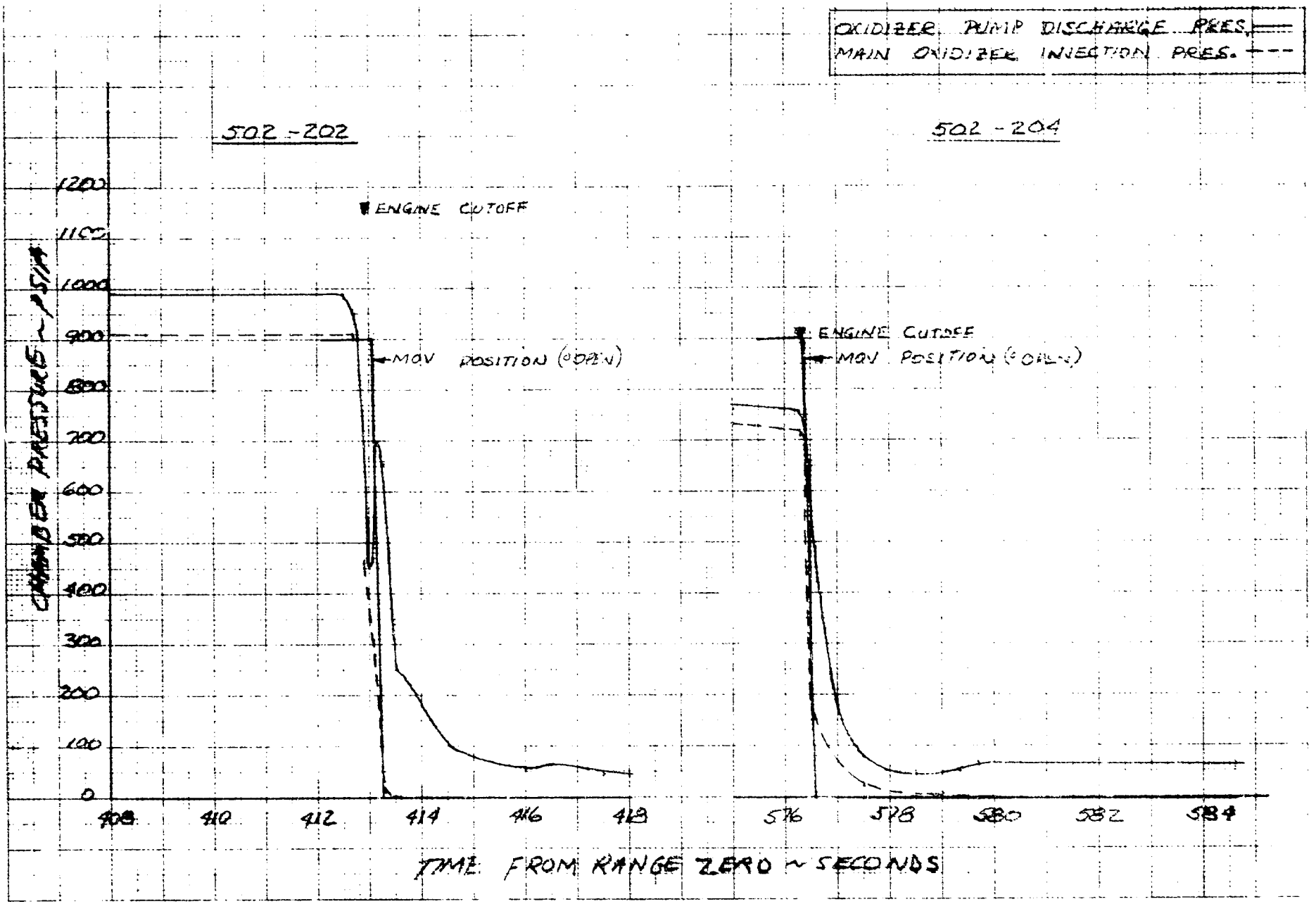

Figure 64. Chamber Pressure vs Time

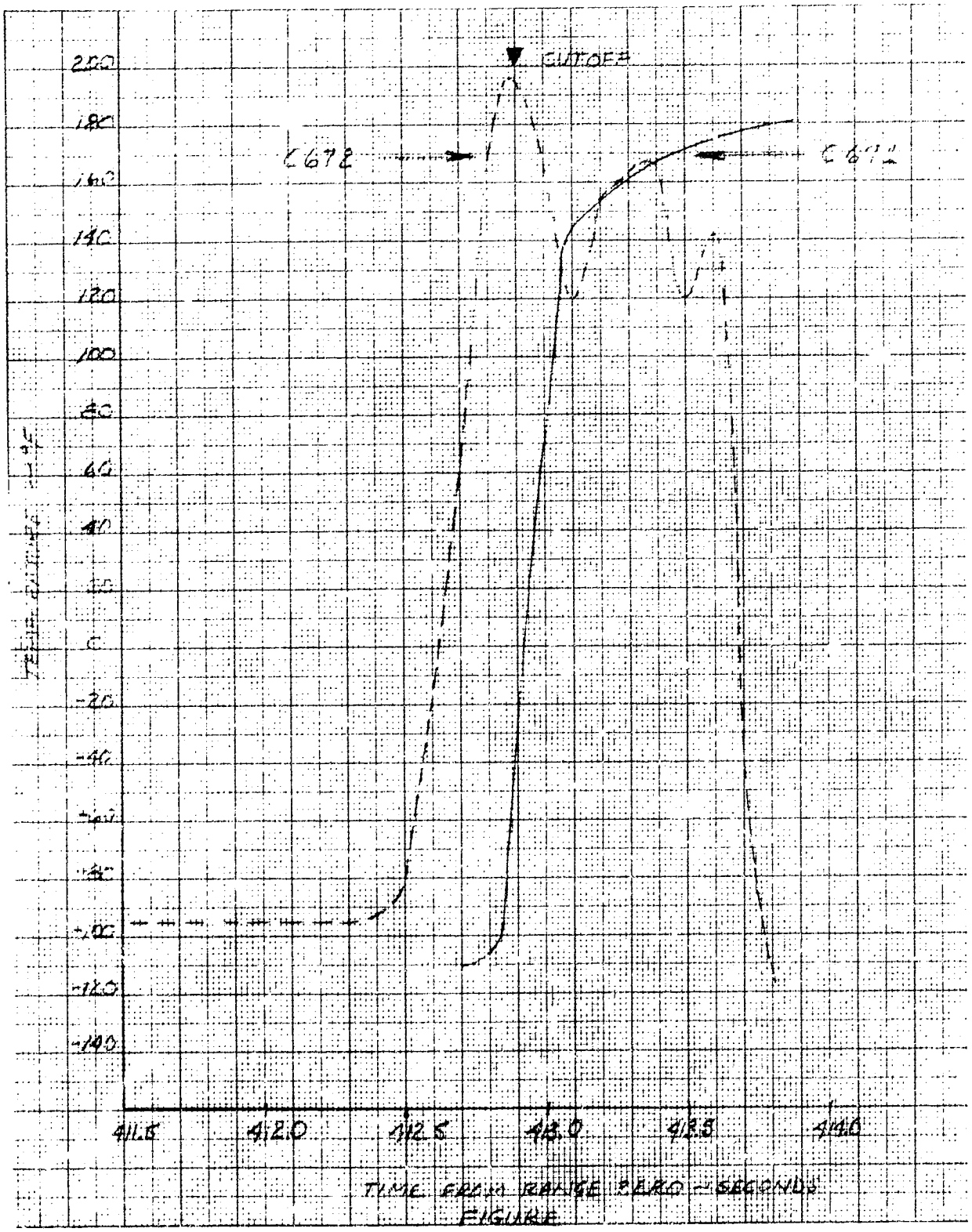

Figure 65. Engine Compartment Gas Temperatures

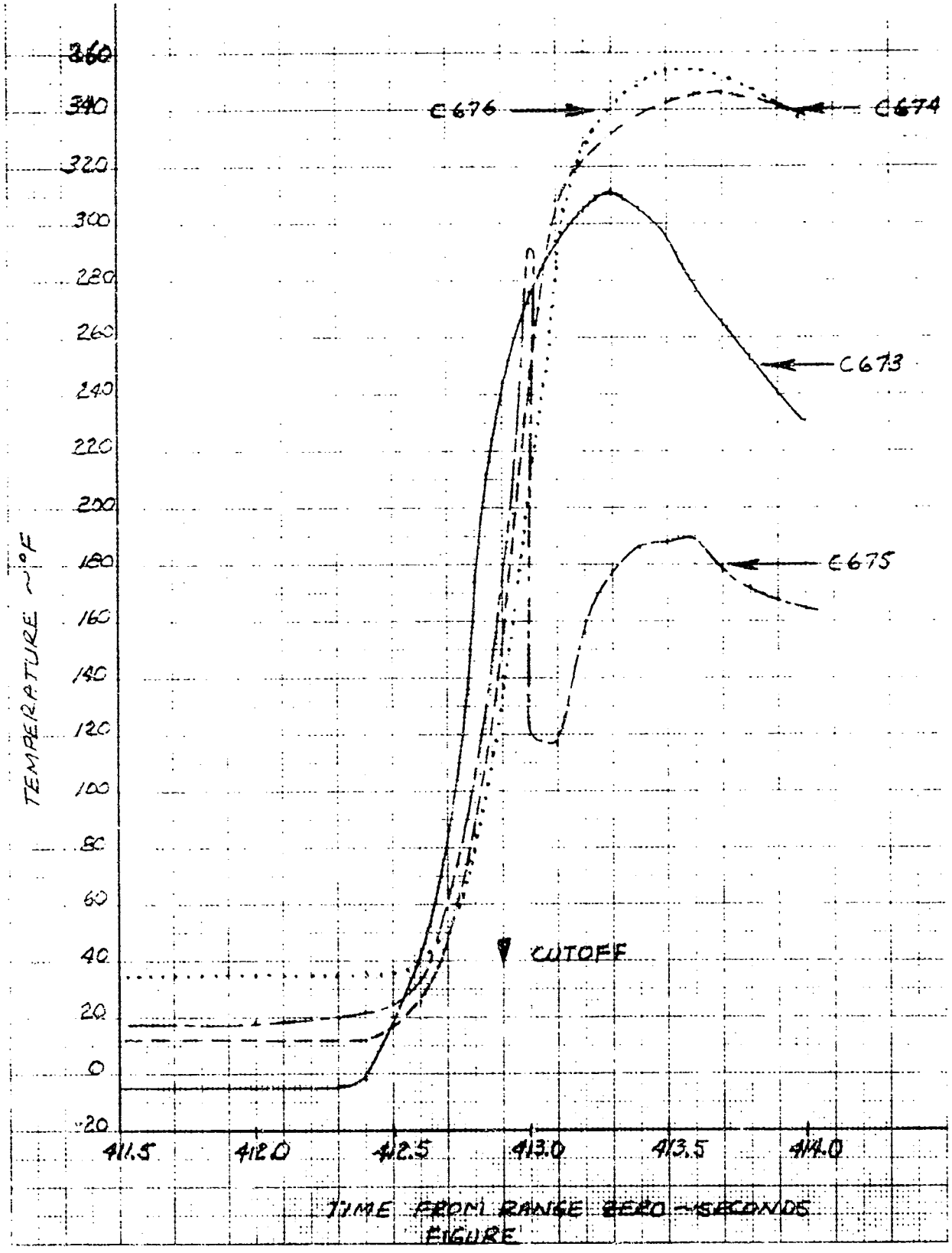

Figure 66. Heat Shield Curtain Gas Temperatures

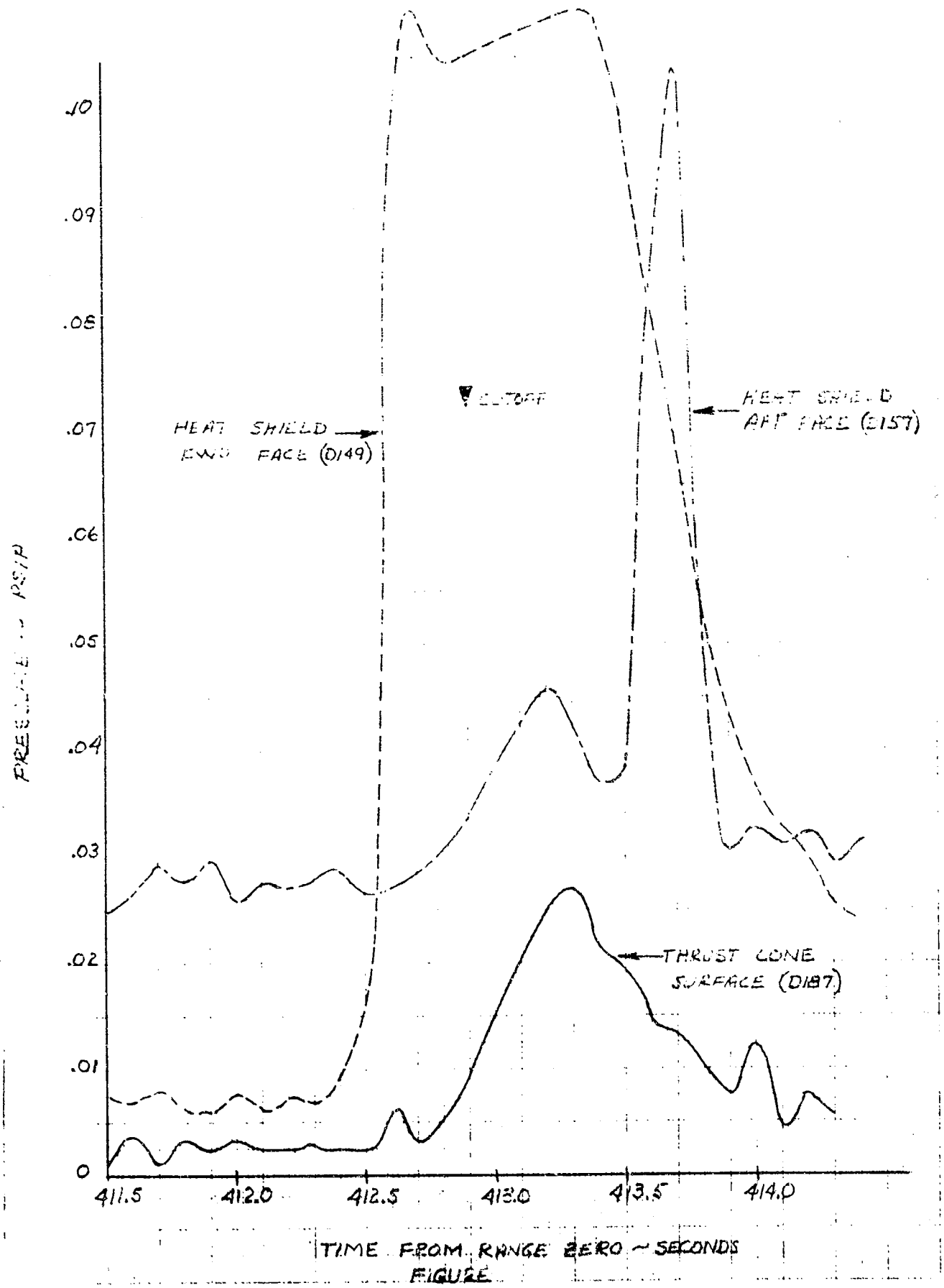

Figure 67. S-II Stage Compartment Pressures

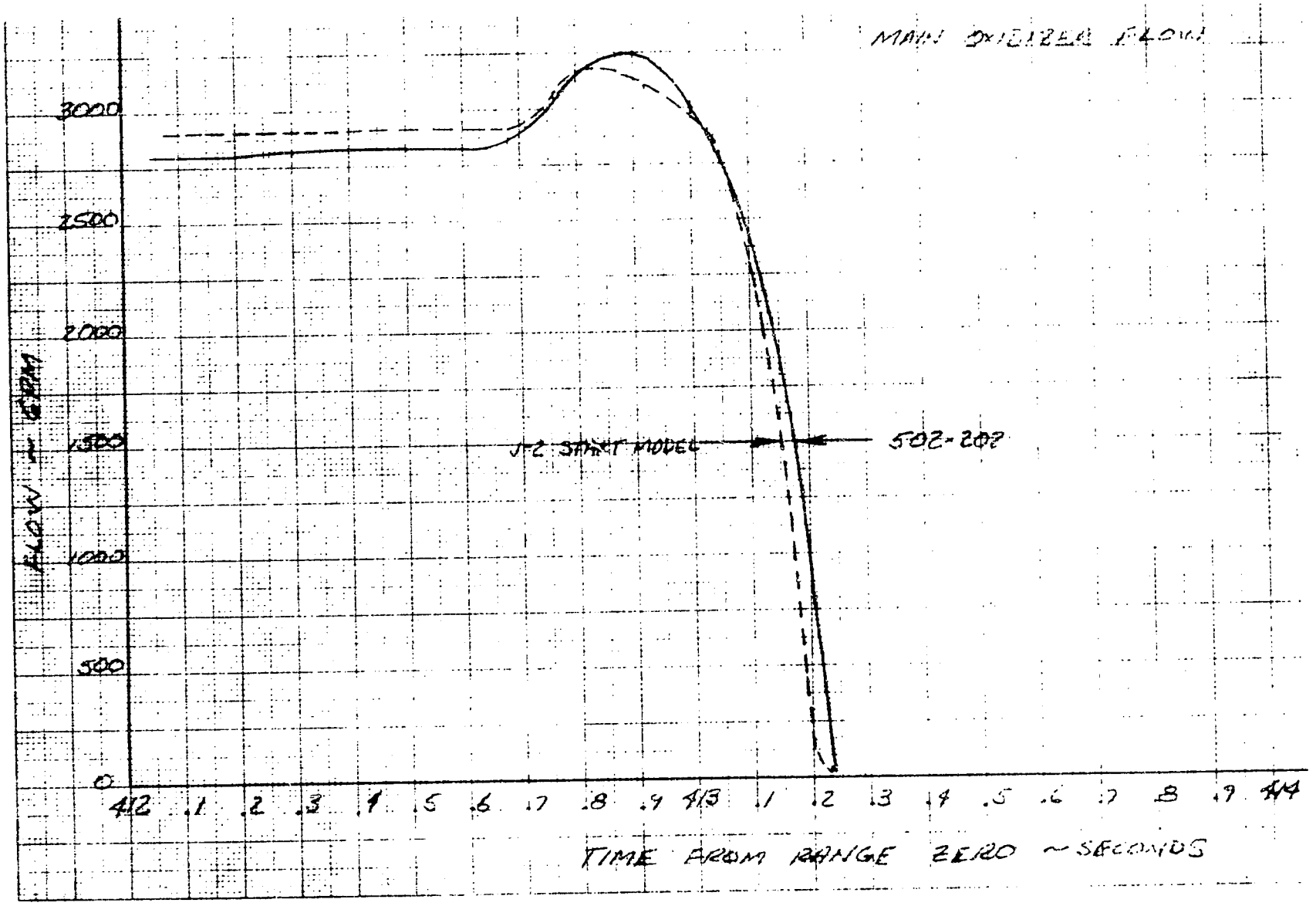

Figure 68. Main Oxidizer Flow

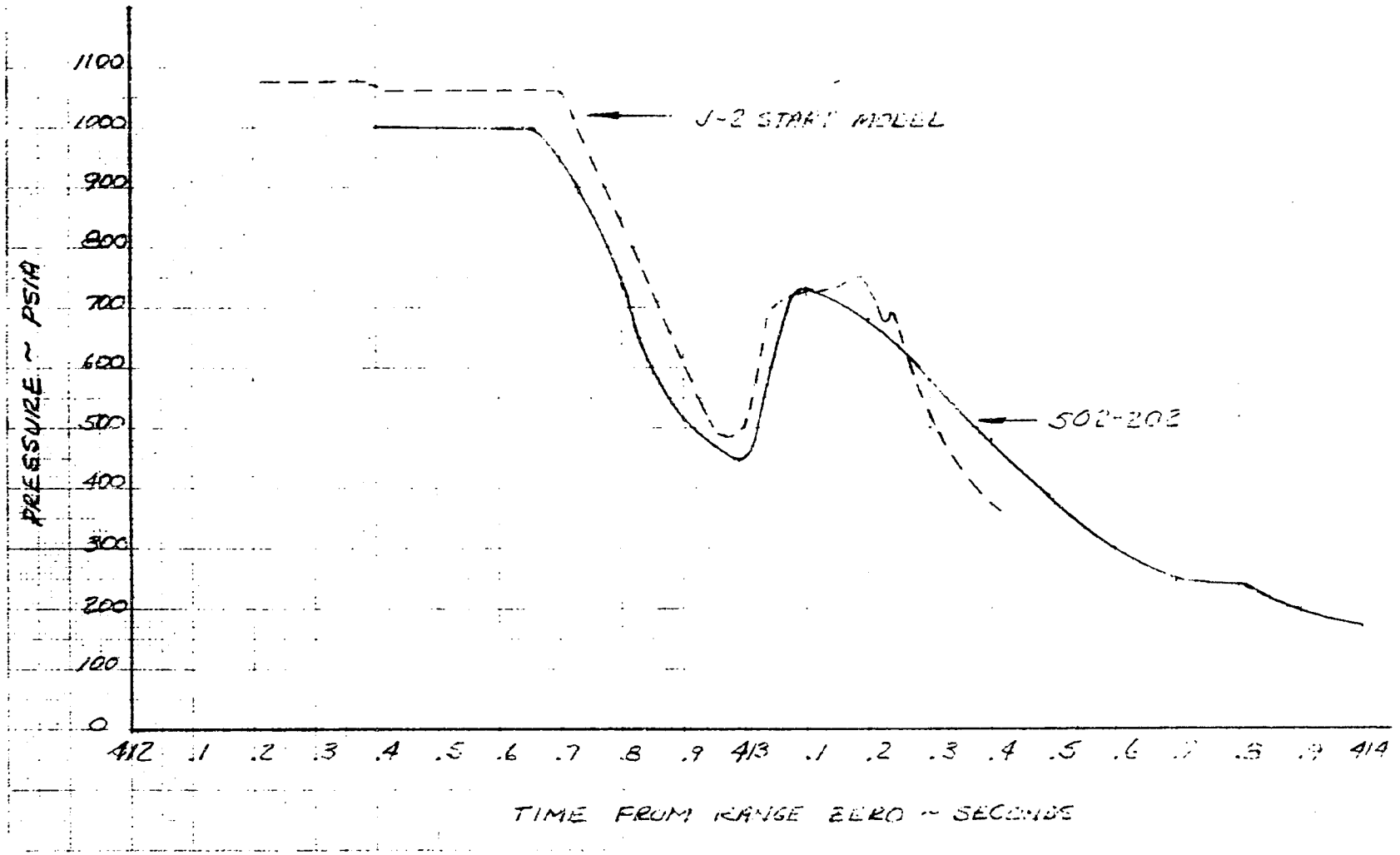

Figure 69. Oxidizer Pump Discharge Pressure

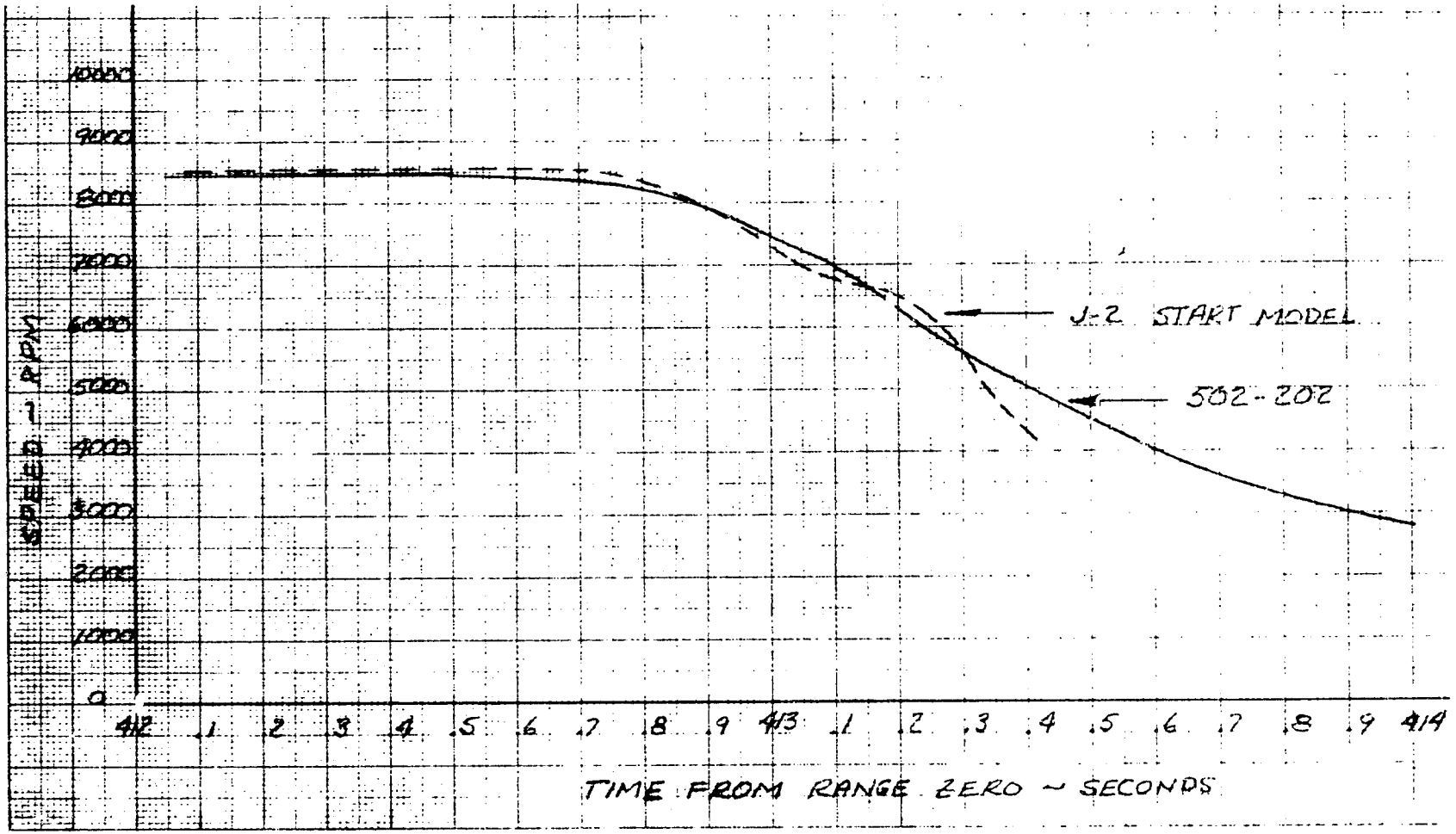

Figure 70. Oxidizer Pump Speed

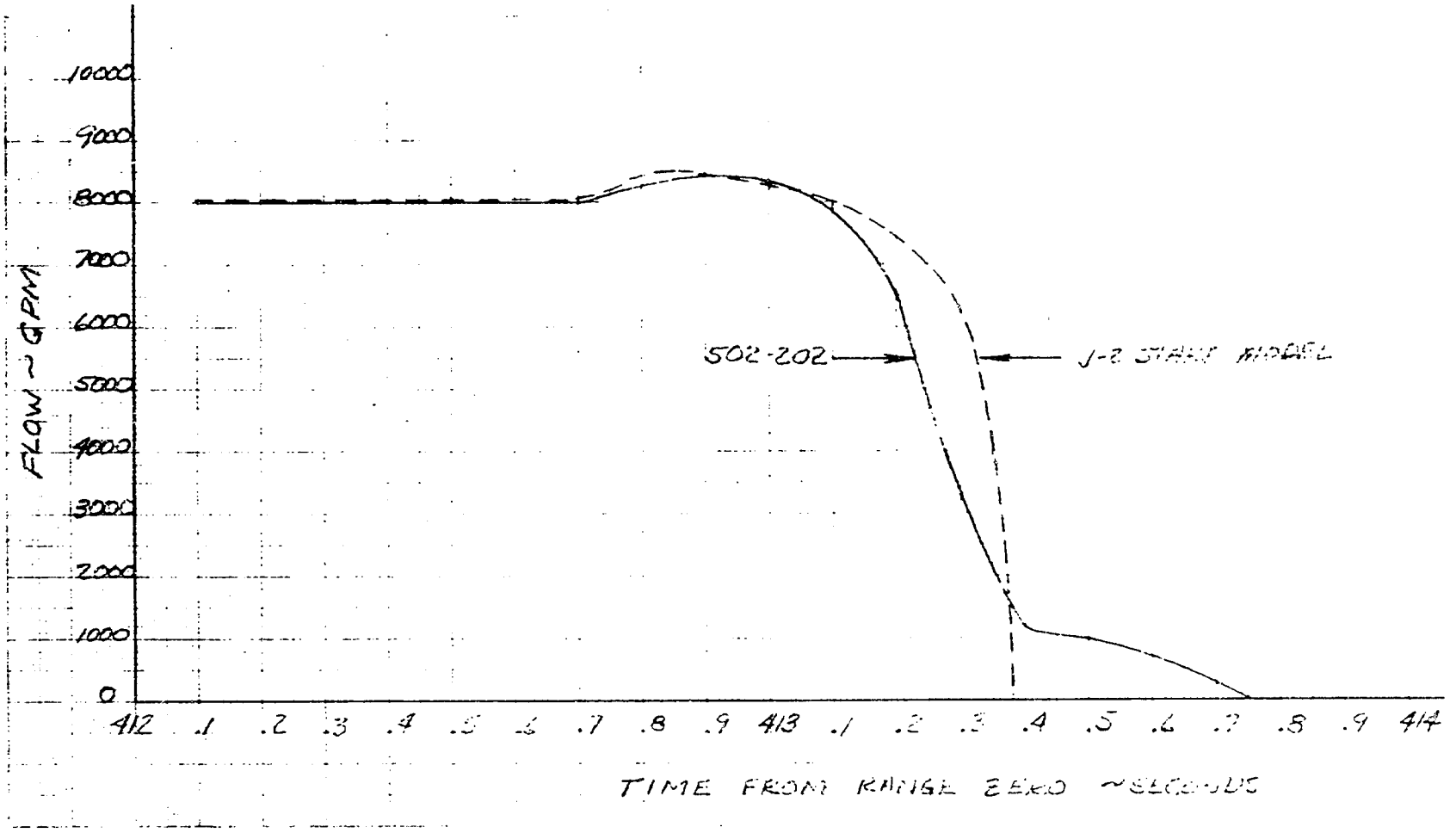

Figure 71. Main Fuel Flow

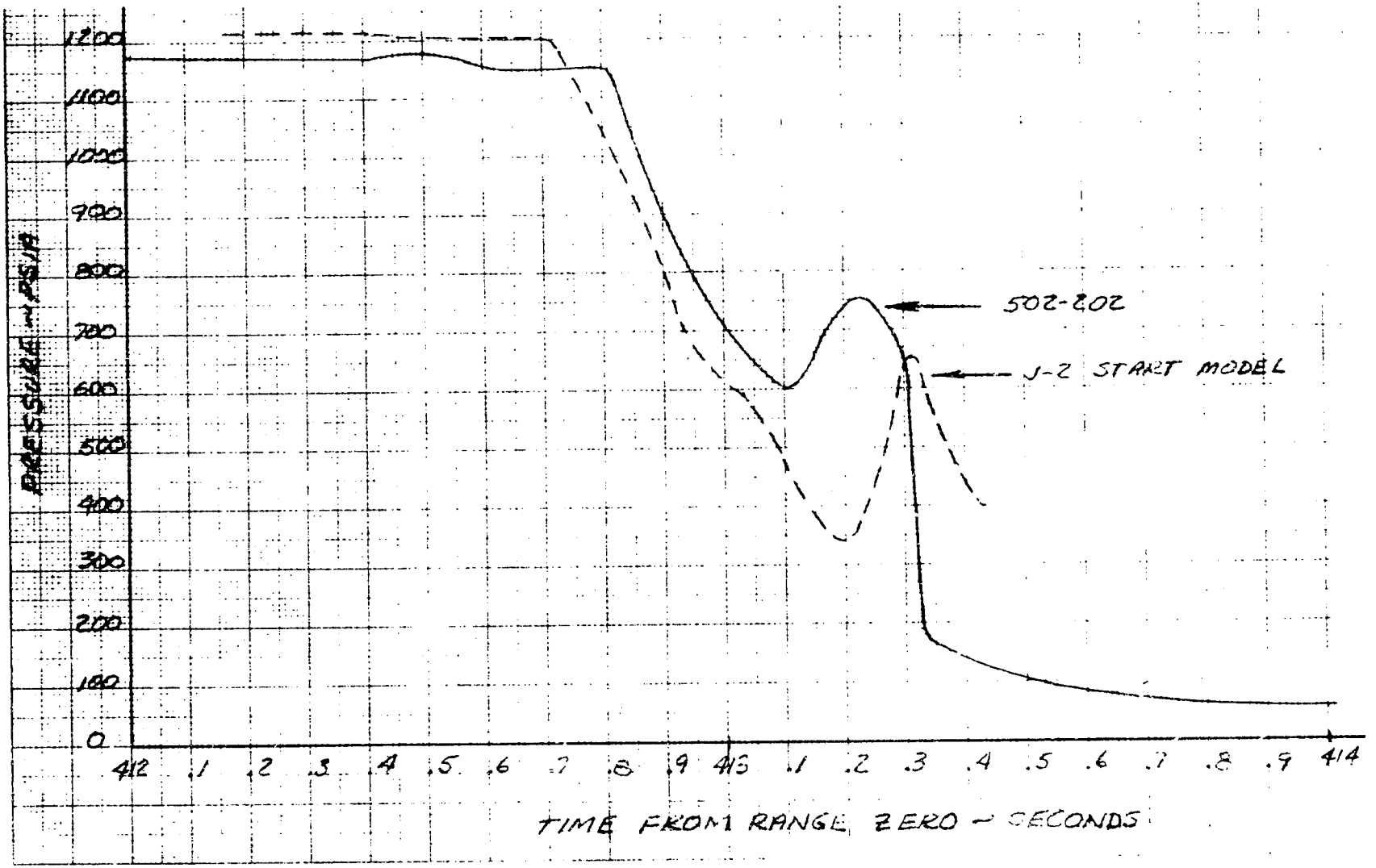

Figure 72. Fuel Pump Discharge Pressure

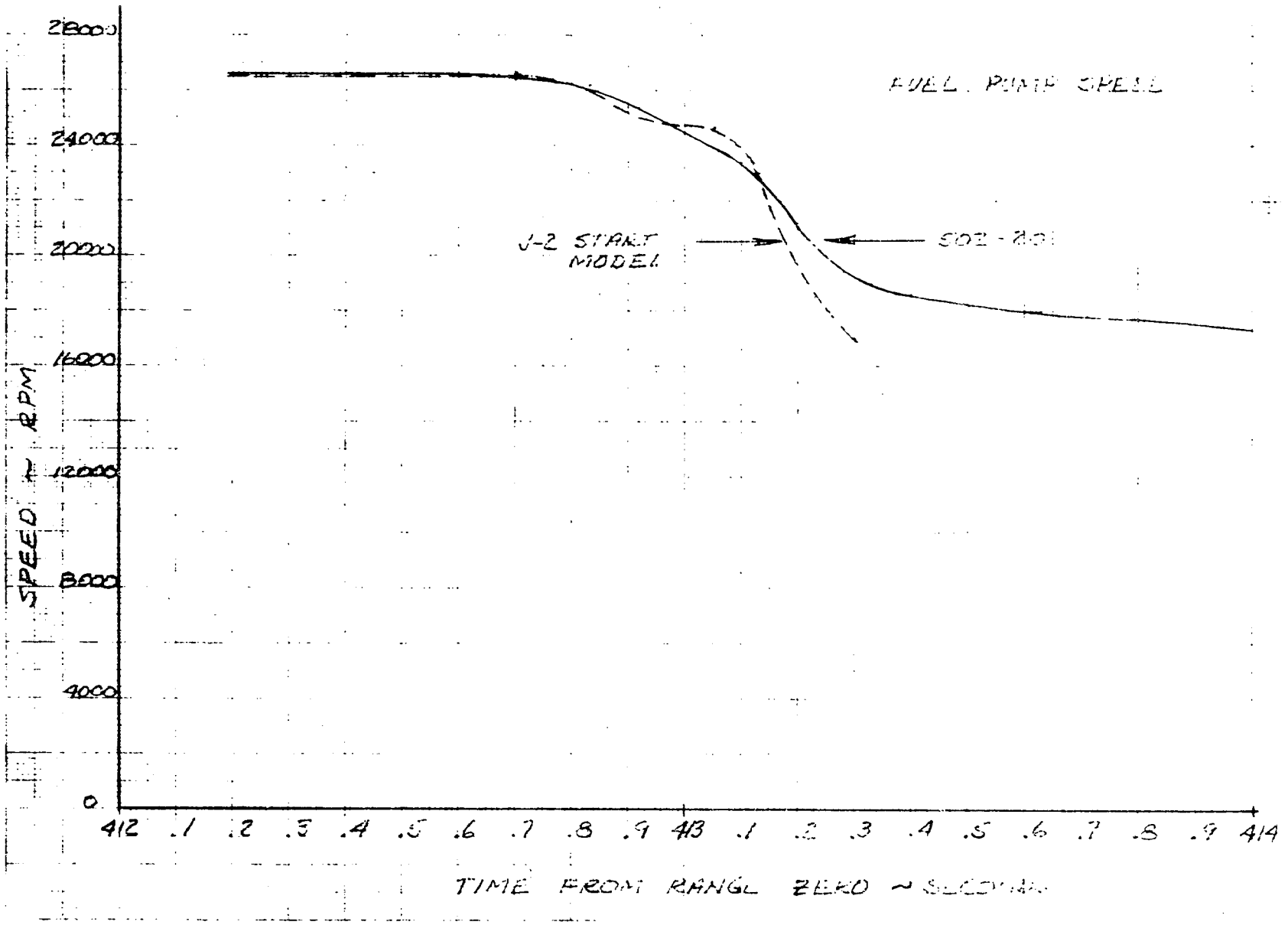

Figure 73. Fuel Pump Speed

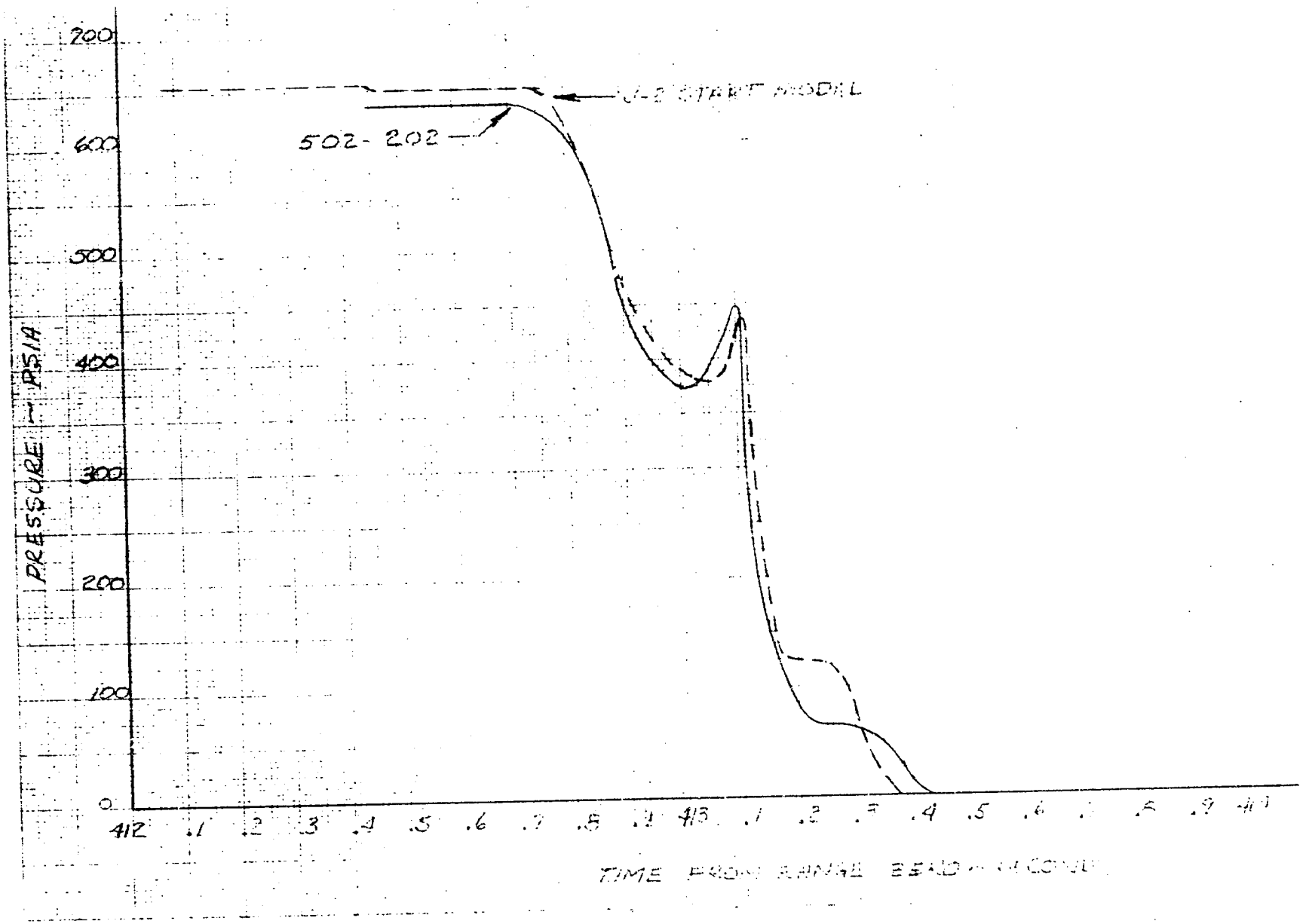

Figure 74. Gas Generator Chamber Pressure

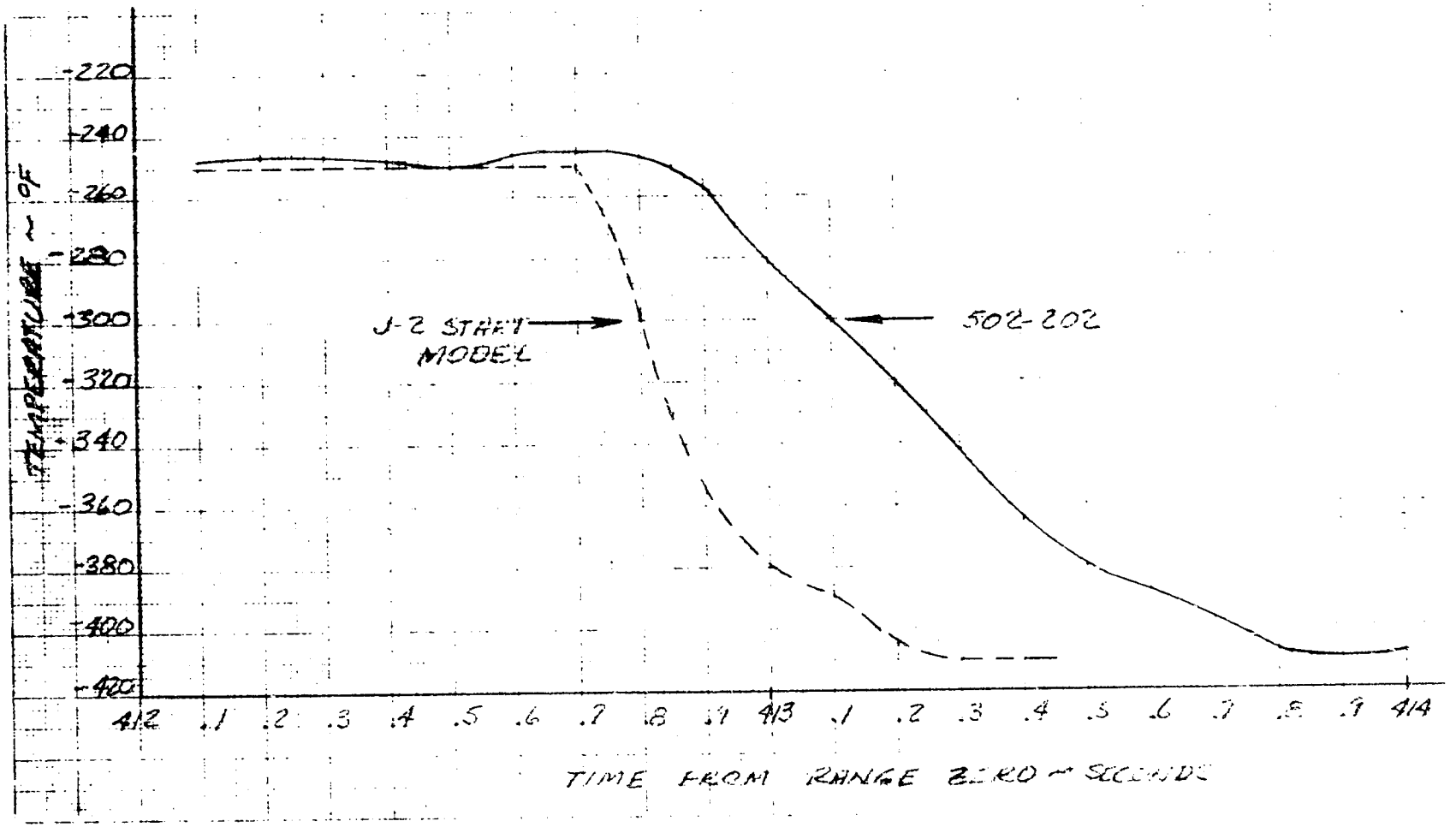

Figure 75. Main Fuel Injection Temperature

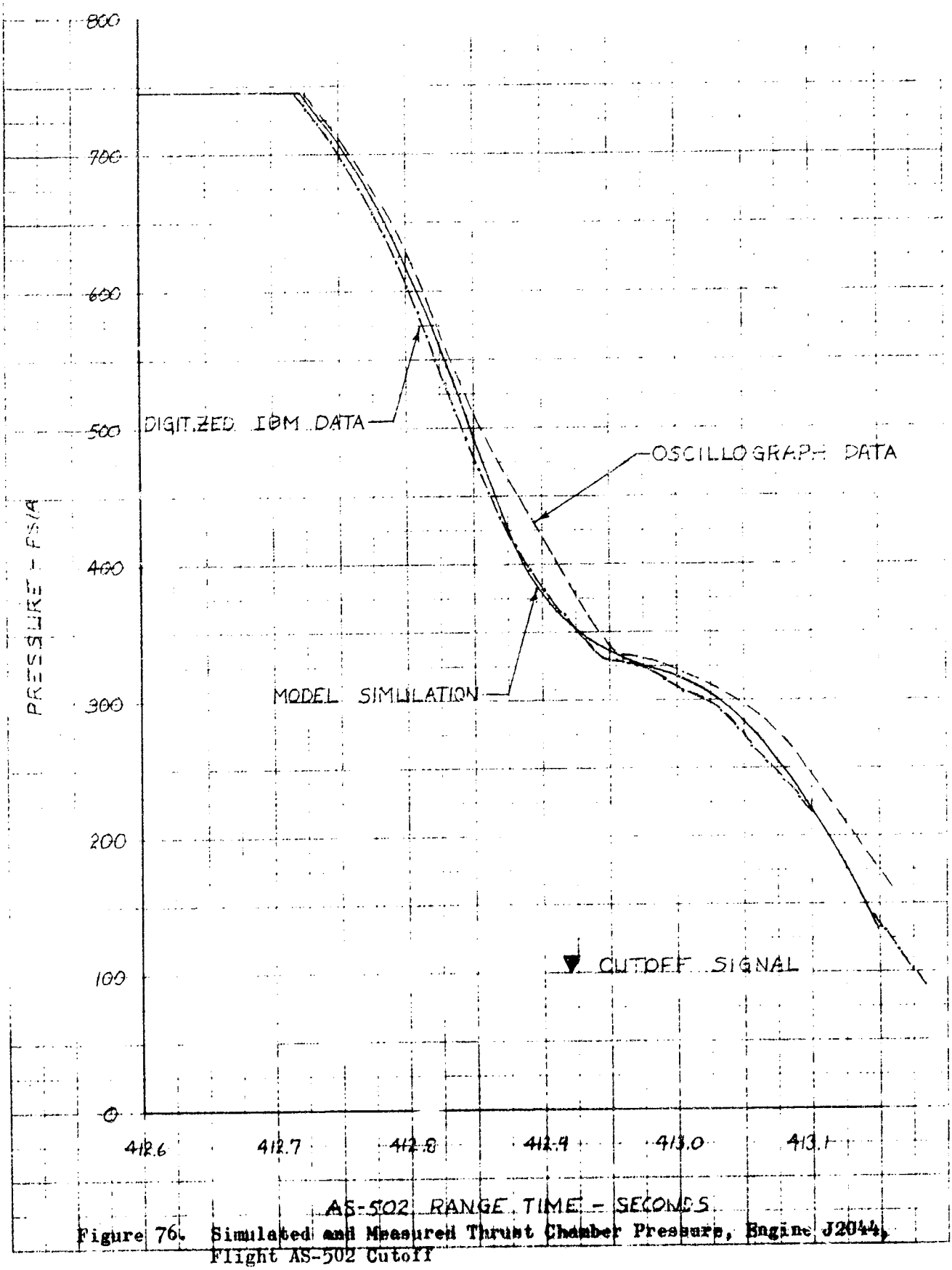

Figure 76. Simulated and Measured Thrust Chamber Pressure, Engine J2044, Flight AS-502 Cutoff

CUTOFF ANOMALIES

Anomalies discussed in this section occurred immediately preceding, during, or following the Engine 202 cutoff transient.

Engine 202 Bleed Valves Open Prematurely After Cutoff

Description of Event. Following cutoff of Engine 202, the oxidizer bleed valve left the closed position at cutoff plus 2.691 seconds and the fuel bleed valve left the closed position at cutoff plus 2.335 seconds.

Conclusion. There is no anomaly associated with the Engine 202 bleed valve operation, as compared with operation of bleed valves for the four remaining S-II engine positions.

Corroboration of Conclusion. Comparison of Engine 202 bleed valve times with operating times for the four remaining S-II engine positions is shown in Table 7.

Engine 202 Gas Generator Valve Reopens Following Cutoff

Description of Event. At 415.0 seconds range time, approximately 2 seconds following cutoff, the Engine 202 gas generator valve started open; by 416.0 seconds the gas generator valve had reached 13 percent open, and by 418.0 seconds the valve returned to 2 percent open and remained at that position.

Hypothesis. Due to very slow opening of the oxidizer turbine bypass valve, the oxidizer turbine bypass valve closing pressure gas was more slowly vented into the main oxidizer valve sequence outlet port. When the fast shutdown valve closed, the venting gas opened the gas generator valve.

Corroboration of Hypothesis. Oxidizer and fuel system pressures at the gas generator inlets were approximately 100 psia at 415.0 seconds; with this pressure at the inlets, approximately 75 psia pneumatic pressure is

TABLE 7

AS-502 S-II ENGINE BLEED VALVE TIMES AT CUTOFF

	Bleed Valve Times Engine Cutoff to Open, seconds	
Engine Position	Oxidizer	Fuel
201	2.383	2.700
202	2.691	2.335
203	7.668	3.226
204	3.167	3.134
205	3.467	2.727

required to open the gas generator valve to the point of contact between the valve actuator and the gas generator oxidizer poppet. Data on oxidizer turbine bypass valve closing cavity venting rates indicate that oxidizer turbine bypass valve pneumatic closing (cavity) pressure was 150 to 170 psia at 415.0 seconds. Therefore, if the fast shutdown valve had closed prior to 415.0 seconds and prevented further venting of gas generator valve opening pneumatic pressure, the system pressure would equalize and result in opening of the gas generator valve.

Oxidizer Turbine Bypass Valve Opens Slowly Following Cutoff

Description of Event. The oxidizer turbine bypass valve on Engine 202 started open at cutoff plus 6.885 seconds, and reached a maximum open position of approximately 95 percent at cutoff plus 10.460 seconds.

Hypothesis. The oxidizer turbine bypass valve opening control pneumatic line failed in such a manner as to prevent opening pressure from reaching the valve. The failure resulted in slow opening of the oxidizer turbine bypass valve by valve spring force only, thus venting closing pressure much more slowly than normal. The slow venting of the oxidizer turbine bypass valve closing side is associated with the anomalous partial opening of the gas generator valve after cutoff.

Corroboration of Hypothesis.

Pneumatic simulator tests were conducted with test setups simulating both a leaking oxidizer turbine bypass valve opening control line and a complete opening control line failure. The leaking opening control line was simulated by installation of a 3/8-inch solenoid at the oxidizer turbine bypass valve opening port; this solenoid was energized prior to cutoff. Complete failure of the oxidizer turbine bypass valve opening control line was simulated by disconnection of the line at the oxidizer turbine bypass valve. The following oxidizer turbine bypass valve opening delay times were obtained:

1. Simulated line leakage, 715 milliseconds
2. Simulated line failure, 4810 milliseconds

Oxidizer turbine bypass valve opening travel times were not recorded during the tests.

Engine 202 Start System Vents Following Cutoff

Description of Event. The Engine 202 start system (start tank) exhibited severe leakage/venting characteristics at 413.8 seconds range time. Figure 77 illustrates Engine 202 start tank pressure and temperature profiles from engine cutoff until termination of S-II telemetry transmission (approximately 590 seconds range time). The initial leakage/venting flowrate was approximately 0.2 lb/sec of gaseous hydrogen, decreasing to an approximately constant value of 0.017 lb/sec after 20 seconds.

Hypothesis. Leakage/venting of the Engine 202 start system resulted from rupture of the start tank liquid refill line downstream of the liquid refill check valve. Rupture of the liquid refill line occurred as a result of the engine compartment hot-gas fire, which occurred during cutoff of Engine 202. The decreasing leakage rate characteristic noted from flight data resulted from incomplete burnthrough or rupture of the liquid refill line (complete burnthrough was prevented by the immediate cooling action of the escaping gaseous hydrogen), followed by contraction of the liquid refill line as further cooling of the line by the expanding gas occurred. Figure 78 illustrates the location of the liquid refill line in relation to other engine components and depicts initial and final line rupture conditions.

Corroboration of Hypothesis. Analysis of flight data revealed that the start tank discharge valve had remained closed, and that the leakage/venting could not be attributed to this component. Review of start system component failure histories failed to reveal failure modes which would coincide with the observed failure.

Analysis indicates that start system leakage, based on the hypothesis stated above, was polytropic in nature, i.e., was initially close to an isentropic process, and later approached the isothermal case, as may be concluded from Fig. 77. Figure 79 is a plot of the calculated isentropic and isothermal processes for flow diameters versus time from engine cutoff.

The following calculations corroborate the polytropic process and flow area change mechanism:

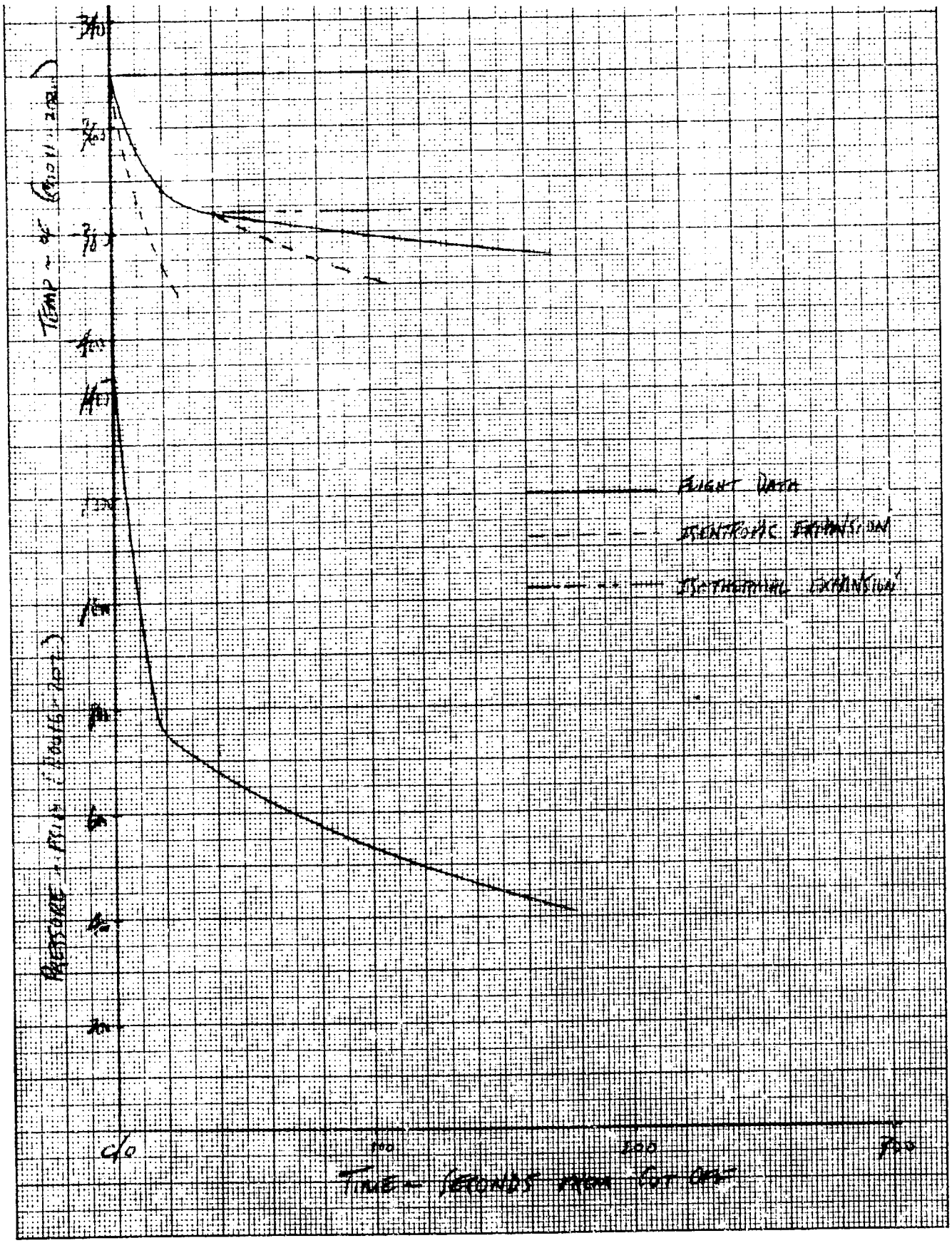

Figure 77. AS-502 Start Tank Blowdown Anomaly, Engine 202

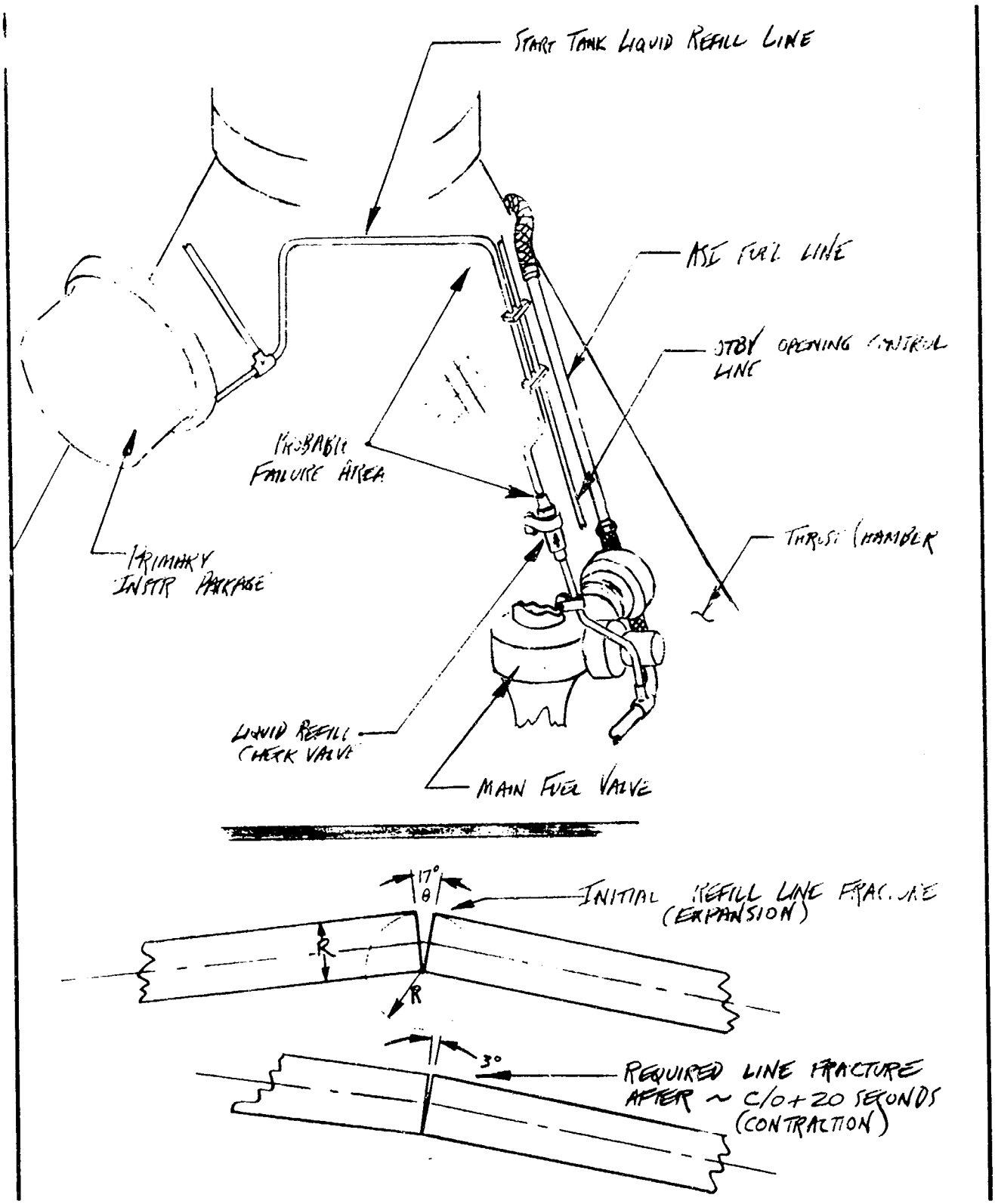

Figure 78. AS-502 Start Tank Blowdown Anomaly, Engine 202

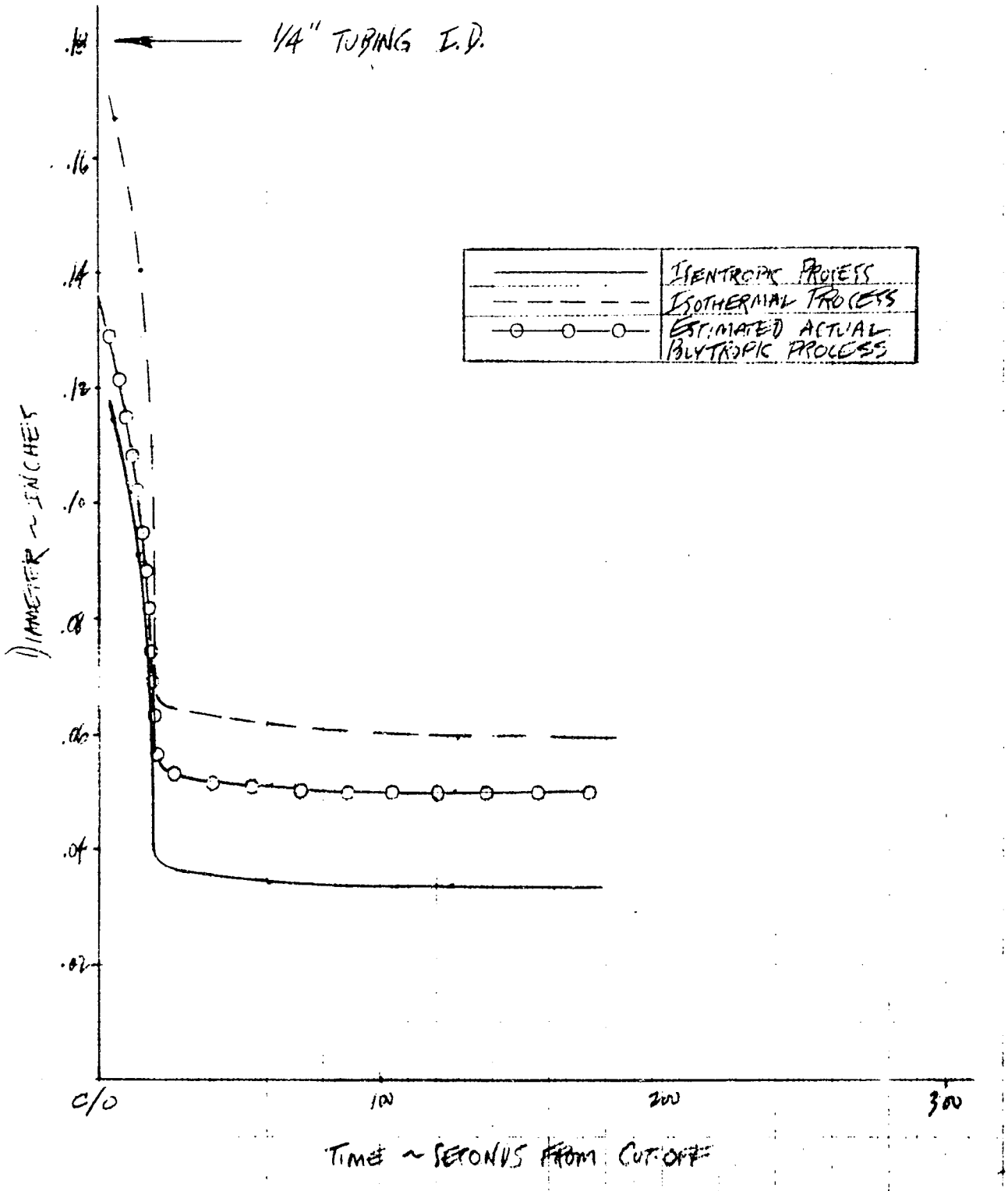

Figure 79. AS-502 Start Tank Blowdown Anomaly, No. 2 Engine

An isothermal start tank pressure decay can be approximated by the following expression:

$$P = P_o\, e^{-t/\beta} \tag{33}$$

where the time constant $\beta = \rho_o V/\dot{m}$ (34)

for choked flow

$$\dot{m} = \frac{CA_o P_o S}{\sqrt{RT_o}} \tag{35}$$

and

$$\rho_o = \frac{P_o}{RT_o} \tag{36}$$

Substituting Eq. 35 and 36 into Eq. 34 yields

$$\beta = \frac{V}{CA_o S\sqrt{RT_o}} = \frac{K_1}{\sqrt{T_o}} \tag{37}$$

Substituting Eq. 37 into 33 gives

$$P = \rho_o\, e^{-CA_o S\sqrt{RT_o}\; t/V} = P_o\, e^{-\sqrt{T_o}\; t/K_1} \tag{38}$$

For an isentropic expansion of the start tank

$$dQ = C_v dT + \frac{P}{J}\,\frac{dV}{W} = 0 \tag{39}$$

and from differentiating the equation of state

$$\frac{PdV + VdP}{WR} = dT \tag{40}$$

Substituting Eq. 40 into Eq. 39

$$C_V \left(\frac{PdV + VdP}{WR} \right) + \frac{P}{J} \frac{dV}{W} = 0$$

or

$$C_V (PdV + VdP) + R \frac{P}{J} dV = 0$$

Substituting $R = C_p - C_V$ in the above equation,

$$C_V (PdV + VdP) + (C_P - C_V) PdV = 0$$

Dividing by $C_V VP$

$$\frac{dP}{P} + \frac{C_P}{C_V} \frac{dV}{V} = 0$$

or

$$\frac{dP}{P} + k \frac{dV}{V} = 0$$

Rearranging the above equation

$$\dot{P} = -k \frac{dVP}{V}$$

and

$$dV = -dW \frac{RT_o}{P}$$

Substituting

$$\dot{P} = \dot{w} \frac{RT_o}{V} k \qquad (41)$$

For isentropic flow

$$\dot{w} = \frac{CAPS}{\sqrt{RT_o}}$$

Substituting into Eq. 41

$$\dot{P} = \frac{CAPS\ k\ RT_o}{\sqrt{RT_o}\ V} = \frac{CAS\ k\sqrt{RT_o}}{V}\ P$$

Integration by the LaPlace method yields

$$P = P_o\ e^{-\frac{\sqrt{RT_o}\ CAS\ k}{V}\ t} \tag{42}$$

$$P = P_o\ e^{-\sqrt{T_o}\ t/K_2} \tag{42a}$$

$$K_1 = \frac{V}{\sqrt{R}\ CA_oS} = \frac{4.2 \times 144}{\sqrt{767} \times \pi/4\ CSd_o^{\,2}}$$

$$K_1 = \frac{27.8}{CSd_o^{\,2}}$$

$$K_2 = \frac{27.8}{CkSd_o^{\,2}}$$

Checking the No. 2 engine start tank pressure and temperature decays at cutoff to cutoff plus 10 seconds for approximation of isentropic flow, the following equation suffices.

$$T = T_o \left(\frac{P}{P_o}\right)^{k-1/k} \tag{43}$$

for

$$P_o = 1430 \text{ psia}, \; P = 950, \; T_o = 110 \text{ R}; \; T = 96, \; k = 2.5,$$
$$T = 110 \; (950/1430)^{1.5/2.5} = 86 \text{ R}$$

86 R calculated vs 96 R flight data and is, therefore, a polytropic process as expected but approximating an isentropic one.

Similarly checking the flow process after the abrupt pressure decay change at cutoff plus 40 seconds to cutoff plus 80 seconds

$$P_o = 680 \text{ psia}, \; P = 575, \; T_o = 84 \text{ R}; \; T = 80, \; k = 3.5$$
$$T = 84 \; (575/680)^{2.5/3.5} = 84 \times 0.887 = 75 \text{ R}$$

75 R calculated vs 80 R flight data also indicates a polytropic process, but now more like an isothermal one. (Refer to Fig. 77.)

Since the start tank blowdown initially approaches an isentropic process and later an isothermal one, the required flow diameters will be calculated for both situations and compared. Equations 38 and 42 will be solved for Cd_o^2 using the start tank pressure and temperature transients over small time intervals.

First, the isentropic case:

$$P = P_o \, e^{-\frac{\sqrt{RT_o} \; CA_o S k}{V} t} \tag{42}$$

$$P = P_o \, e^{-\sqrt{T_o}/K_2 \cdot t} \tag{42a}$$

$$K_2 = \frac{V}{\sqrt{R} \; CA_o S \; k} \tag{44}$$

$$S = \left[kg_c \left(\frac{2}{k+1} \right)^{k+1/k-1} \right]^{1/2} \qquad (45)$$

Substituating into Eq. 44 for K_2

$$V = 4.2 \text{ ft}^3$$

$$R = 767 \text{ ft-lb/lb-R}$$

$$CA = \frac{\pi}{4} \ Cd_o^{\ 2}$$

$$S = \left[kg_c \left(\frac{2}{k+1} \right)^{k+1/k-1} \right]^{1/2}$$

$$\therefore K_2 = \frac{4.2 \times 144}{\sqrt{767} \times Cd_o^{\ 2} \cdot \pi/4 \times Sk} = \frac{27.8}{Cd_o^{\ 2} Sk} \qquad (46)$$

For particular values during start tank blowdown,

$$t_{c/o} = >t_{c/o+10 \text{ sec}} \quad T_o = 110 \text{ R}, \ T = 96 \text{ R}, \ P_o = 1430,$$

$$P = 950 \text{ psia}, \ \overline{k} = 2.5$$

Solving Eq.45 times k

$$k \left[kg_c \left(\frac{2}{k+1} \right)^{k+1/k-1} \right]^{1/2} = \left[2.4 \cdot 32.2 \left(\frac{2}{3.5} \right)^{3.5/1.5} \right]^{1/2}$$

$$= k \times \sqrt{21.6}$$

$$kS = 11.6$$

Substituting into Eq.46 for K_2

$$K_2 = \frac{27.8}{Cd_o^{\ 2}} 11.6 = \frac{2.4}{Cd_o^{\ 2}}$$

Substituting this value into Eq.42 and solving for Cd_o^2

$$\ell n \frac{P}{P_o} = \frac{\sqrt{T_o}}{k_2} \quad t = \frac{Cd_o^2 \sqrt{T_o}\, t}{2.4}$$

$$Cd_o^2 = \frac{2.4}{\sqrt{T_o}\, t} \quad \ell n \quad \frac{P}{P_o}$$

$$Cd_o^2 = \frac{2.4}{\sqrt{110}\ (10)} \quad \ell n \left(\frac{950}{1430}\right) = \frac{2.4 \times 0.408}{105} = 0.0093$$

$$Cd_o^2 = 0.0093$$

For flow conditions after the knee

$$t_{c/o+40 \text{ sec}} => t_{c/o+80 \text{ sec}} \quad T_o = 84 \text{ R}, \ T = 80, \ \bar{k} = 3.5,$$

$$P_o = 680 \text{ psia}, \ P = 575$$

$$S = \left[3.5 \times 32.2 \left(\frac{2}{4.5}\right)^{4.5/2.5}\right]^{1/2} = \sqrt{26.3} = 5.14$$

$$kS = 3.5 \times 5.14 = 18$$

$$kS = 18$$

into Eq. 46

$$K_2 = \frac{27.8}{Cd_o^2\ 18} = \frac{1.54}{Cd_o^2}$$

Substituting Eq. 42

$$Cd_o^2 = \frac{1.54}{\sqrt{T}\ t} \quad \ell n \frac{P}{P_o}$$

$$Cd_o^2 = \frac{1.54}{\sqrt{84}\ (40)}\ \ln\left(\frac{575}{680}\right) = 0.258/367 = 0.00069$$

$$Cd_o^2 = 0.00069$$

For third calculation,

$t_{c/o} = 100$ sec $=> t_{c/o} = 150$ sec

$P_o = 530$, $P = 450$, $T_o = 79$ R, $T = 76$ R, $k = 3.8$

$$S = \left[3.8 \times 32.2 \left(\frac{2}{4.8}\right)^{\frac{4.8}{2.8}}\right]^{1/2} = \sqrt{27.2} = 5.21$$

$kS = 3.8 \times 5.21$

$kS = 19.8$

$K_2 = 27.8/Cd_o^2$ $19.8 = 1.8/Cd_o^2$

$$Cd_o^2 = \frac{1.8}{\sqrt{T}\ t}\ \ln\frac{P}{P_o} = \frac{1.8}{\sqrt{0.79}\ \ (50)}\ \ln\left(\frac{450}{530}\right) = 6.6 \times 10^{-4}$$

$Cd_o^2 = 0.00066$

$t_{c/o} + 10$ sec $=>$ c/o + 20 sec, $T_o = 96$ R, $T = 89$ R, $P_o = 950$ psia,

$P = 750$, $k = 2.8$

$$S = \left[2.8 \times 32.2 \left(\frac{2}{3.8}\right)^{\frac{3.8}{1.8}}\right]^{1/2} = \sqrt{23} = 4.8$$

$kS = 13.4$

$K_2 = 27.8/Cd_o^2$ $13.4 = 2.08/Cd_o^2$

$$Cd_o^2 = \frac{2.08}{\sqrt{96}\ (10)}\ \ln\left(\frac{750}{950}\right) = 0.005$$

$Cd_o^2 = 0.005$

For high Re values, which is the case for gaseous hydrogen flow in small-diameter tubing, d_o/d_{line} ratio determines the value of "C."

For

$$(d_o/d_{line}) \leq 0.60, \quad C = 0.5;$$

$$(d_o/d_{line}) \doteq 0.7, \quad C = 0.7$$

Therefore, the effective flow diameters are as follows:

$t_{c/o}$ +	d_o	C	Cd_o^2
0 to 10	0.115	0.7	0.0093
10 to 20	0.091	0.6	0.005
40 to 80	0.034	0.6	0.00069
100 to 150	0.033	0.6	0.0006

Equation 38 represents the isothermal case

$$P = P_o e^{-\frac{CA_o S \sqrt{RT_o}}{V} t}$$

which differs from the isentropic expansion by a factor of k in the exponent only.

Solving for the equivalent flow diameters under constant temperature intervals

$$t_{c/o} = > c/o + 10 \text{ sec} \qquad \bar{T} = 100 \text{ R}$$

$$K_1 = 27.8/Cd_o^2 \; S = 27.8/Cd_o^2 \; 4.65$$

$$K_1 = 5.98/Cd_o^2 \; S$$

$$Cd_o^2 = \frac{5.98}{105} \ln (0.665) = 0.0224$$

$$Cd_o^2 = 0.0224$$

$t_{c/o}$ + 10 sec = > c/o + 20 sec $\quad \bar{T} = 92$ R

$K_1 = 27.8/Cd_o^2 \; 4.8 = 5.8/Cd_o^2$

$Cd_o^2 = \frac{5.8}{98} \ln (0.79) = 0.014$

$Cd_o^2 = 0.014$

$t_{c/o}$ + 40 sec = > c/o + 80 sec

$K_1 = 27.8/Cd_o^2 \; 5.14 = 5.41/Cd_o^2$

$Cd_o^2 = \frac{5.41}{9.18\ (40)} \ln (0.846) = 0.00242$

$Cd_o^2 = 0.00242$

$t_{c/o}$ + 150 sec = > c/o + 150 sec

$K_1 = 27.8/Cd_o^2 \; 5.21 = 5.33/Cd_o^2$

$Cd_o^2 = \frac{5.33}{\sqrt{79}\ (50)} \ln (0.85) = 0.00196$

$Cd_o^2 = 0.00196$

For

$C = 0.8$ at $d_o/d \geq 0.75$ and $C = 0.6$ at $d_o/d \leq 0.5$

$t_{c/o}$ +	d_o	C	Cd_o^2
0 to 10	0.167	0.8	0.0224
10 to 20	0.141	0.7	0.0140
40 to 80	0.062	0.6	0.00242
100 to 150	0.059	0.6	0.00196

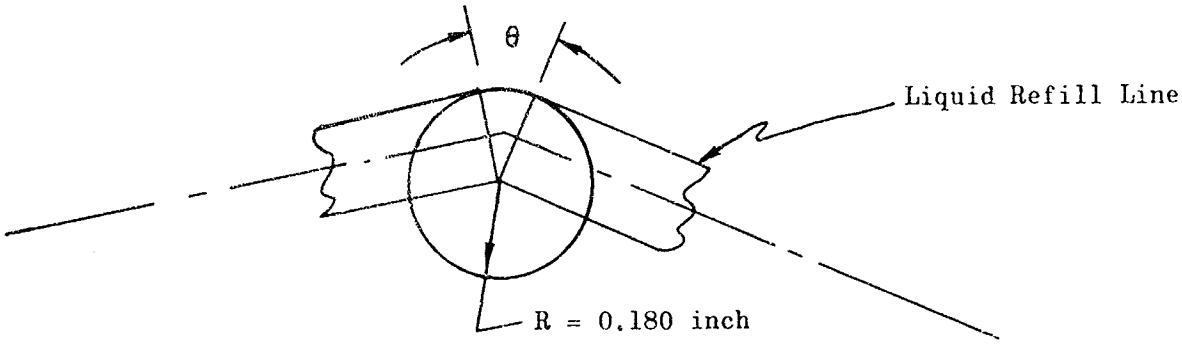

Calculation of the flow area formed by the line fracture:

$$\text{Surface area of sphere} = A = 4 \pi R^2$$

the included flow area being that portion of a sphere determined by θ

$$\therefore A_T = \frac{\theta}{2\pi} 4 \pi R^2 = 2 \theta R^2$$

$$A_T = 2 \theta R^2$$

where

θ = radians

Solving for the initial flow θ_i (c/o - c/o + 10 sec) by setting Eq. 46 equal to the calculated area,

$$A_c = A_T = 2 \theta (0.180)^2 = 0.0648 \theta \text{ in.}^2$$

$$A_c = \frac{\pi (0.13)^2}{4} = 0.0132 \text{ in.}^2$$

$$\theta = 0.0132/0.0648 = 0.204 \text{ radians}$$

or

$$\theta_i = 17 \text{ degrees}$$

Similarly, during the final phase of the blowdown,

$$\theta_f = \left(\frac{d_f}{d_i}\right)^2 \theta_i$$

$$\theta_f = \frac{0.0025}{0.0132} \times 17 = 3.2$$

$$\theta_f \approx 3 \text{ degrees}$$

Examination of the expansion/contraction mechanisms

$$\Delta \ell = 12\, \ell e\, \Delta T \qquad (47)$$

where

e = 13×10^{-6} in./in. F (stainless)

ℓ = refill line length

ΔT = temperature change

Hot-gas temperatures of 3000+ F would have been necessary to rupture the refill line. Assuming (-200 = > +80. F) temperature plus or minus 1 foot from the rupture would yield a $\Delta \ell$ by Eq. 47 of:

$$\Delta \ell = 12 \times 2 \times 1000 \text{ F} \times 13 \times 10^{-6} = 0.312 \text{ inch}$$

$$\Delta \ell \doteq 0.3 \text{ inch (assuming unrestrained tubing)}$$

This value results in sufficient expansion to produce the required θ,

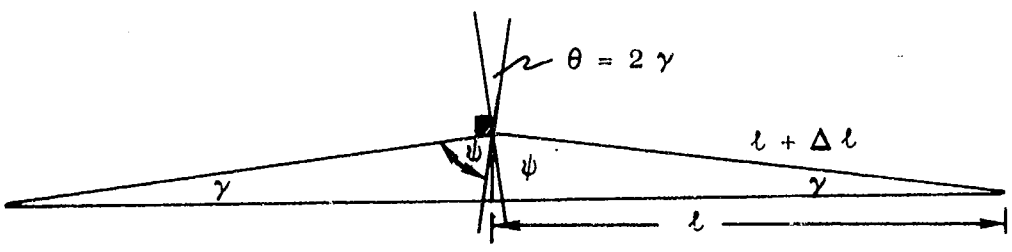

$$\cos^{-1} \gamma = \ell/\ell + \Delta \ell = \cos^{-1} 12/12.15$$

$$\gamma = 9 \text{ degrees or } 2\gamma = 18 \text{ degrees}$$

$$\theta = 18 \text{ degrees}$$

It is quite feasible that such a rupture area could result from severe heating of the tubing. The numbers were quite conservative in ℓ and ΔT, but neglect internal stresses.

Chilling of the line by the cold gaseous hydrogen results in the eventual contraction to the $\approx$ 3-degree θ condition.

Engine 202: Loss of Oxidizer System Integrity After Cutoff

Description of Event. Oxidizer system pressures and temperatures for Engine 202 decayed following engine cutoff, indicating loss of system integrity. If system integrity had been maintained, pressure would be locked up in the oxidizer feed system (e.g., 38 psia for engine 203) after cutoff, and would indicate saturation temperature corresponding to the pressure.

Conclusion. The oxidizer system was not maintained intact after engine 202 cutoff.

Corroboration of Conclusion. Data plots of engine 202 oxidizer pump inlet pressure (Fig. 80), PU valve outlet pressure (Fig. 81), and oxidizer pump discharge pressure (Fig. 82) indicate abnormal pressure decay following engine cutoff. Engine 203 exhibited no such decays in these parameters following cutoff.

The conclusion that the oxidizer system pressure decays resulted from loss of system integrity is further supported by decreasing oxidizer feed system temperatures (Fig. 83, 84, and 85). Engine 202 oxidizer inlet temperature, oxidizer pump discharge temperature, and gas generator oxidizer inlet temperature (gas generator bleed valve temperature) decreased to

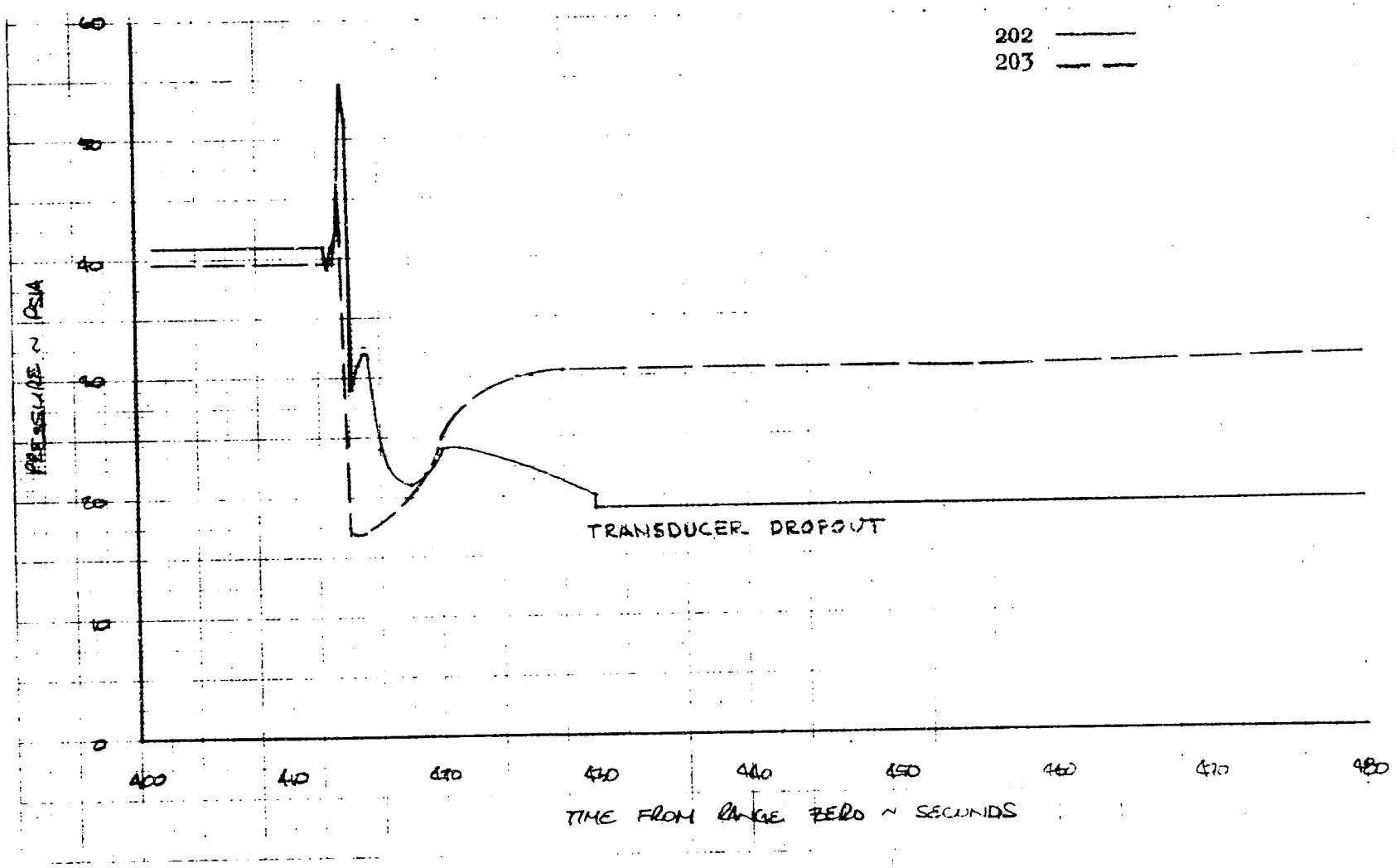

Figure 80. Oxidizer Pump Inlet Pressure

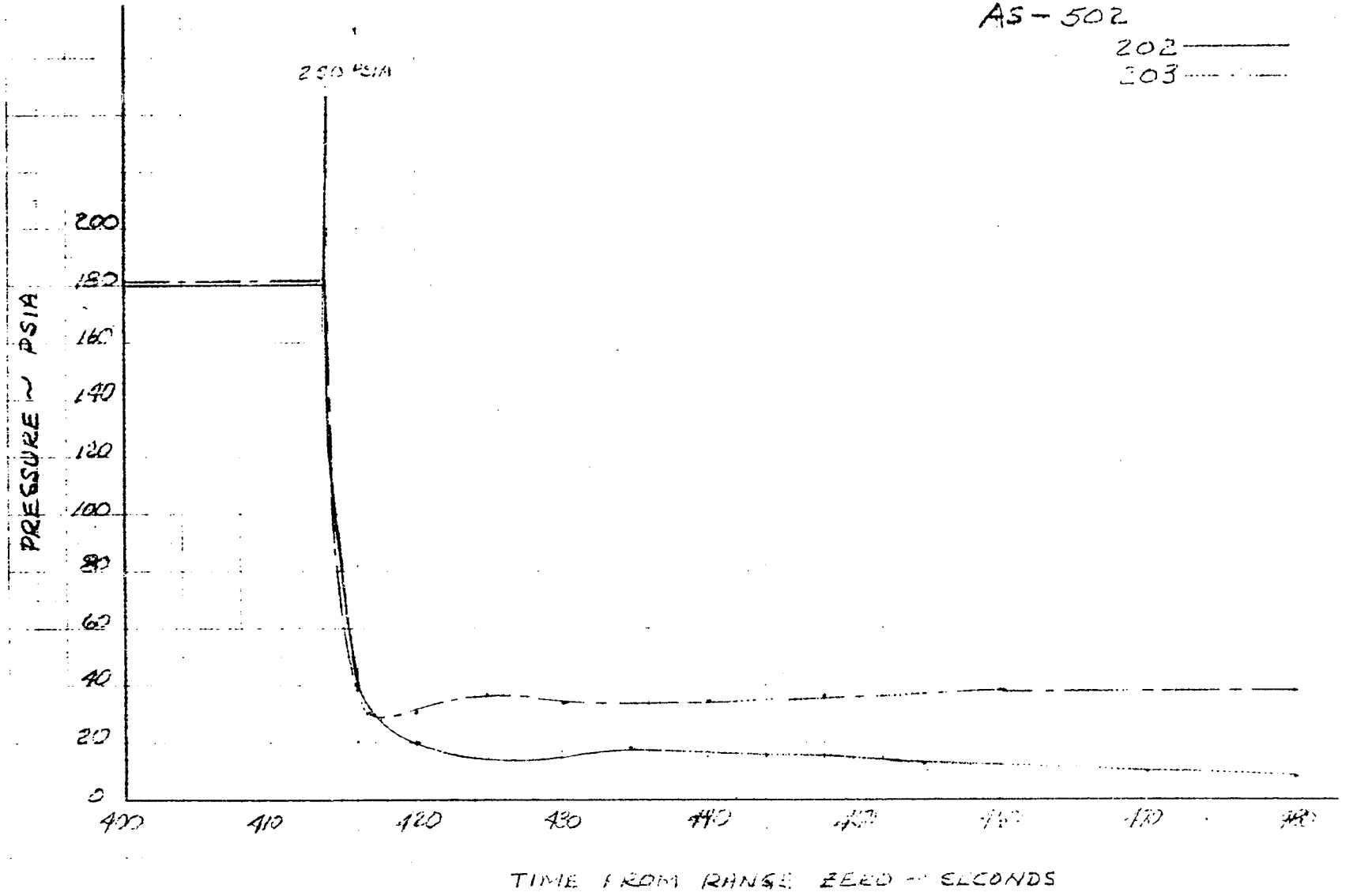

Figure 81. Propellant Valve Outlet Pressure(C 191)

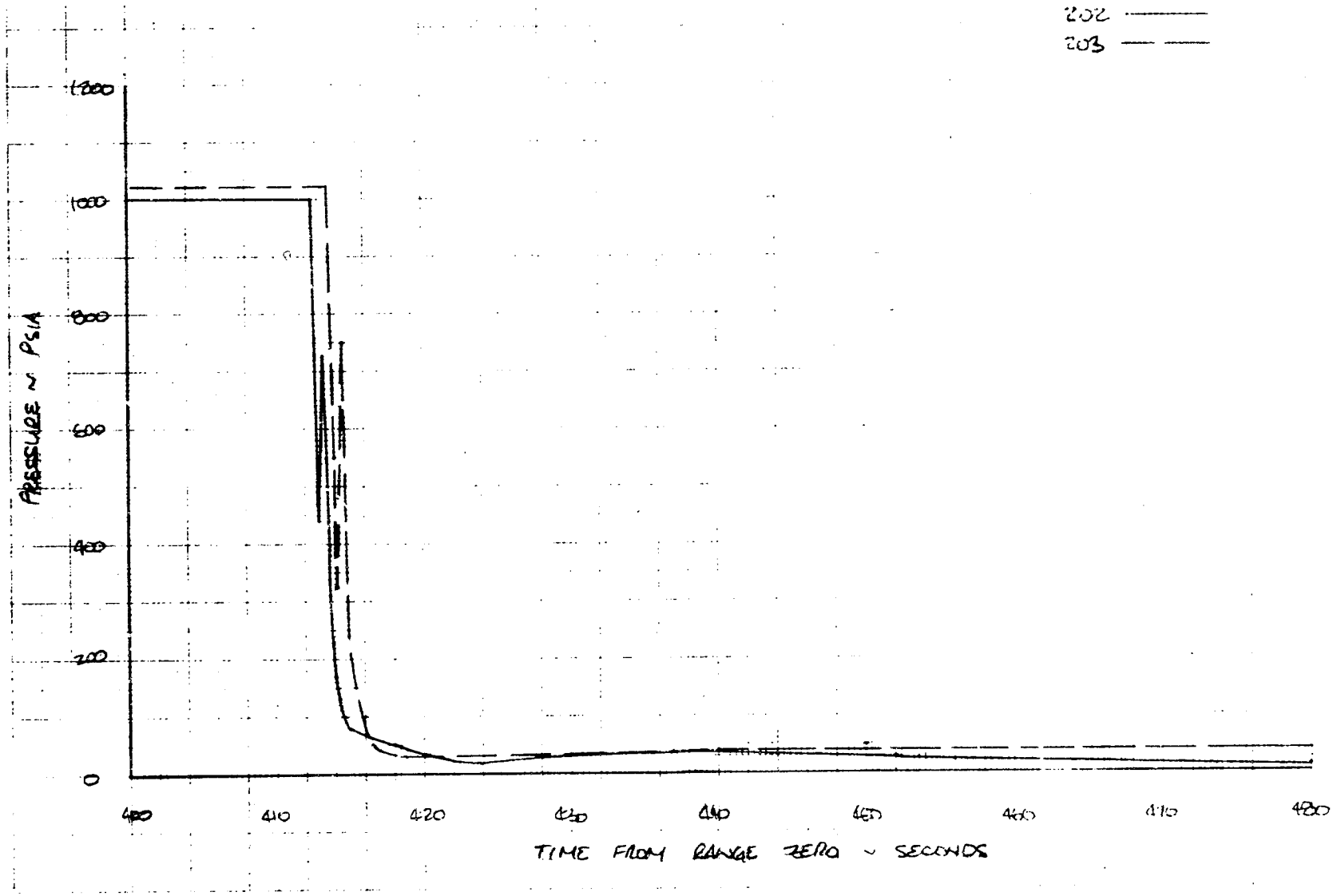

Figure 82. Oxidizer Pump Discharge Pressure

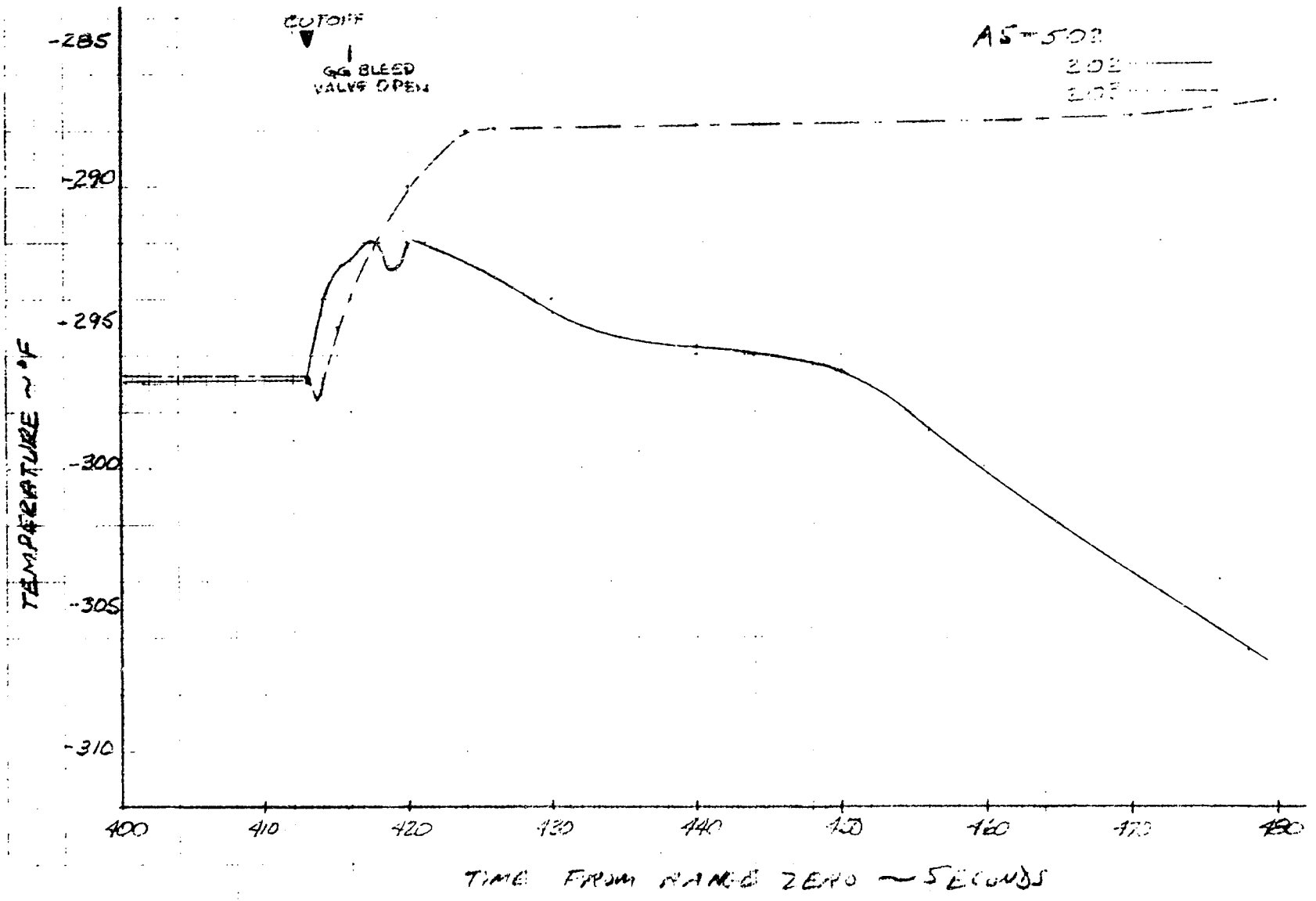

Figure 83. Oxidizer Engine Inlet Temperature (C 663)

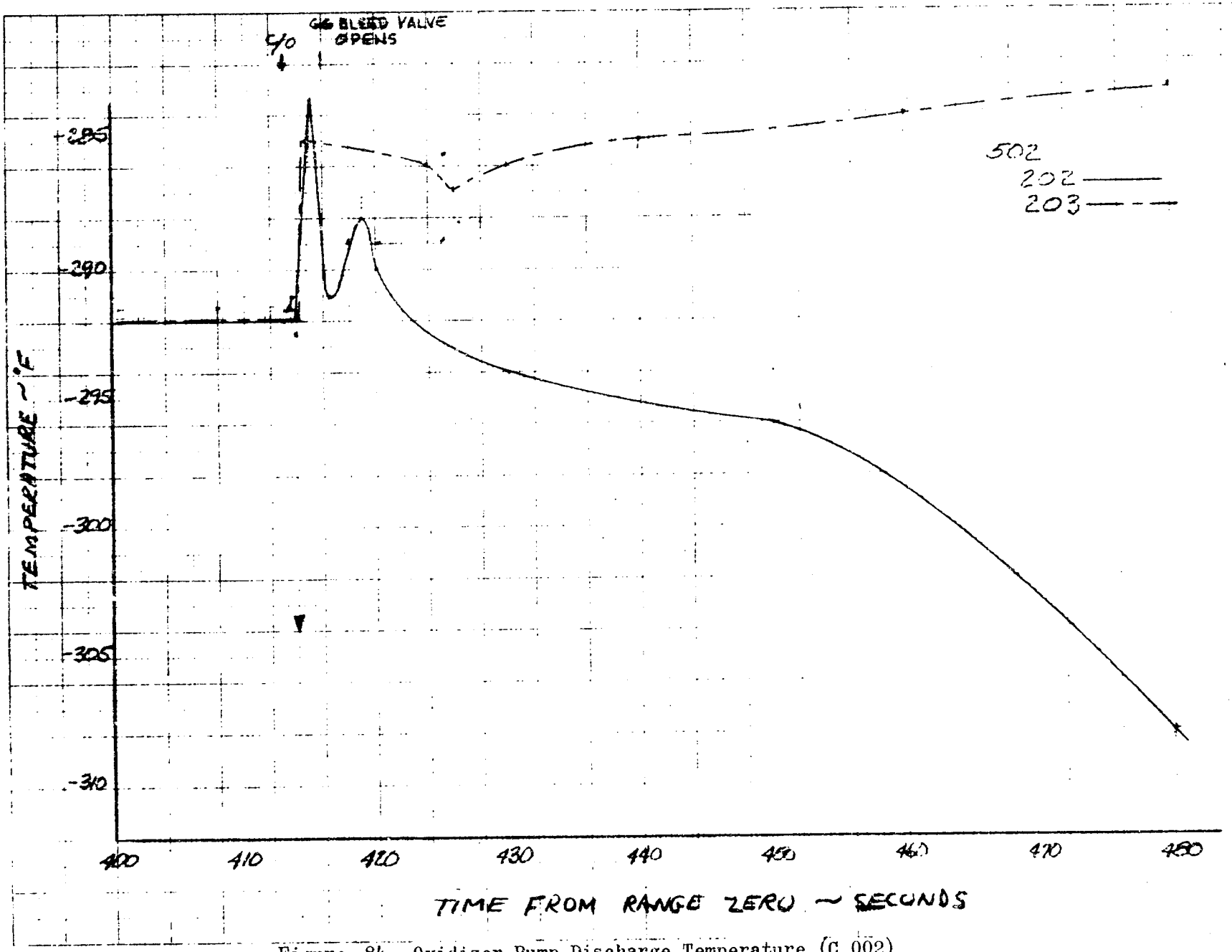

Figure 84. Oxidizer Pump Discharge Temperature (C 002)

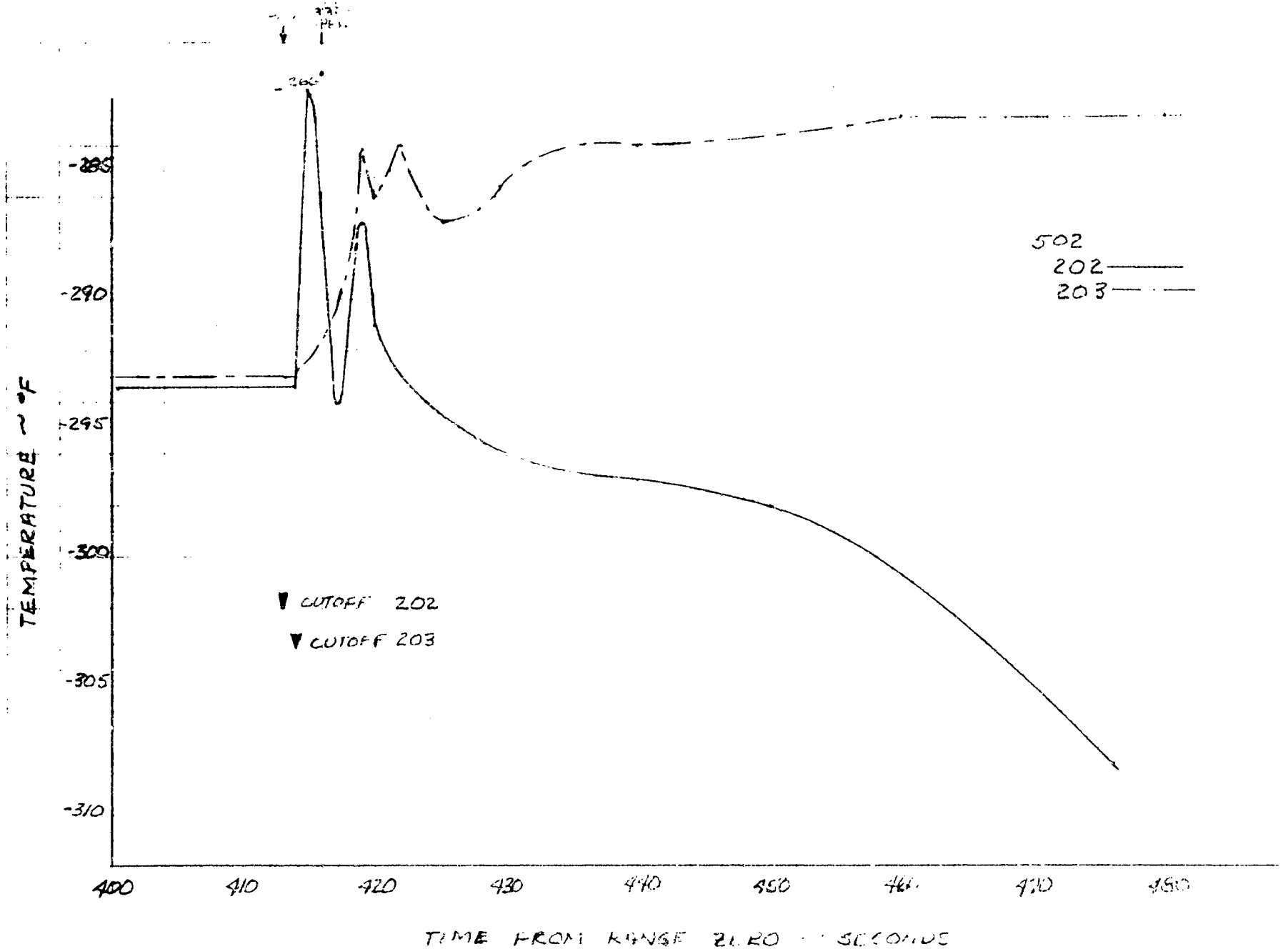

Figure 85. Gas Generator Oxidizer Inlet Temperature (C909)

approximately -308 F (transducer limit) by 65 seconds after cutoff; slope of the temperature curves at this point indicated that the temperature decrease would continue.

Because it is concluded that integrity of the Engine 202 fuel feed system was essentially maintained following cutoff, cooling of the oxidizer feed system could only be caused by vaporization of oxidizer within the system, i.e., decay of system pressure to below the oxidizer vapor pressure.

The location and size of the leak is inconclusive, based on available evidence; however, if the assumption is made that heat required for vaporization comes only from the liquid oxygen, an approximate minimum hole size may be calculated. Results of the calculations shown below indicate that a minimum hole area of 0.7 $in.^2$ would be required.

Calculation of Hole Area. The following calculations were made:

1. Average temperature decay = 0.25 F/sec
2. Heat input to liquid from vaporization:

$$Q = wcp\Delta T$$

$$\frac{dQ}{dt} = w(0.4)(0.25) = 0.1w \frac{Btu}{sec}$$

where

w = weight of liquid in system

3. Heat of vaporization of oxidizer = 92 Btu/lb
Rate of vaporization = $\frac{0.1w}{92} = 0.00109\ w \frac{lb}{sec}$

This rate of vaporization represents flow of vapor out of the system if the leak is above the liquid level or if the flow of liquid out of the system is being displaced by the vapor volume.

4. Assuming that the system is full (344 pounds liquid oxygen), then the flowrate of vapor is:

$$\dot{w} = 0.00109\ (344) = 0.375\ \text{lb sec}$$

5. Critical flow through a nozzle or well-rounded orifice is:

$$\dot{w} = a\sqrt{P_1\ pgk\left(\frac{2}{K-1}\right)^{\frac{k+1}{k-1}}}$$

At -292 F, saturation pressure is 20 psia

$$0.375\ \frac{\text{lb}}{\text{sec}} = \frac{A}{144}\sqrt{\left[(20)(144)\right]\left[0.35\right]\left[32.2\right]\left[1.45\right]\left[\frac{2}{1.45-1}\right]^{\frac{2.45}{0.45}}}$$

$$A = 0.43\ \text{in.}^2 \text{ at nozzle throat.}$$

6. If the discharge coefficient is assumed to be 0.65 for the hole, then

$$A = 0.66\ \text{in.}^2$$

The major significance of the 4.9 in.^{2} area number is that it is larger than the area calculated for vapor flow and indicates that the actual hole size is probably in excess of 0.7 in.^{2} area. The flow through the hole (leak path) is probably mixed phase (gas/liquid) rather than single phase (either gas or liquid).

Engine 202; Loss of Fuel System Integrity at Cutoff; Long Fuel Pump Speed Decay Following Cutoff

Description of Events. Some flight data suggest that following cutoff of Engine 202 at 412,925 seconds range time, engine fuel feed system integrity was lost, and fuel was dumped.

Engine 202 fuel pump speed decay following cutoff was unusually long, requiring 113 seconds to decay to zero rpm, as compared to approximately 45 seconds for a normal engine shutdown.

Conclusions. The fuel feed system was basically intact at cutoff, with only minor leakage occurring. The engine fuel inlet pressure instrumentation line (1/4-inch stage line) may have ruptured at cutoff, dumping fuel. The gas generator fuel valve reopened to allow a maximum of 0.13 lb/sec flow following engine shutdown. The fuel recirculation return relief valve was cracked open, venting the 80-psia return manifold pressure back into the fuel tank. No other leakages were found.

The long fuel pump speed decay following engine 202 cutoff was the result of the gas generator valve opening after cutoff, and of subsequent gas generator fuel valve opening and fuel flow, which supplied sufficient turbine power to extend the speed decay.

Corroboration of Conclusions. The two anomalies are related, and corroboration for both is presented concurrently in the following paragraphs.

The sequence of significant events related to the anomalies, referenced in range time, is as follows:

1. 412.925 seconds: engine 202 cutoff; pump speed decay begins
2. 414 seconds: engine 202 fuel pump inlet temperature pegs offscale (high); engine 202 fuel pump inlet pressure pegs offscale (low)
3. 414.2 seconds: engine 203 shutdown
4. 415 seconds: engine 202 gas generator valve partially reopens; gas generator pressure spike occurs
5. 415-460 seconds: gas generator fuel valve leakage occurs

6. 416 seconds: fuel bleed valves open (engines 202 and 203)
7. 426 seconds: engine 202 fuel pump inlet temperature pegs offscale (low)
8. 428 seconds: engine 203 fuel pump rotation stops
9. 520 seconds: engine 203 fuel pump rotation stops
10. 576 seconds: stage command shutdown

Figures 86 through 96 present fuel feed system pressures and temperatures, gas generator pressures and temperatures, fuel pump speed, and main fuel flow for engines 202, 203, and 204. The same parameters for engines 201 and 205 are similar to engine 204, and are not included.

Following shutdown of engines 202 and 203, their fuel bleed valves opened, engine 201, 204, and 205 fuel bleed valves remained closed, and the stage fuel recirculation return manifold shutoff valve remained closed. Fuel feed systems for engines 202 and 203 were manifolded to the stage recirculation return manifold through the bleed valves and lines. In the time period from 415 seconds to 570 seconds, fuel pump interstage pressures, balance piston cavity pressures, and pump discharge pressures were 75 to 80 psia; at approximately 580 seconds, all of these pressures dropped to 60 psia. Fuel pump inlet pressure for engine 203 pegged offscale high at 55+ psia, and the same parameter for engine 202 pegged offscale low at 20 psia. Fuel pump discharge temperatures, gas generator fuel inlet temperatures, and engine 203 fuel pump inlet temperatures indicated -410 F throughout this time period; fuel saturation temperature at 80 psia is -409.8 F.

Data indicate that fuel feed systems on engines 202 and 203 were intact following shutdown. The systems were connected through the recirculation return manifold because the engine fuel bleed valves opened at engine shutdown. The common system pressure of 80 psia was maintained by the

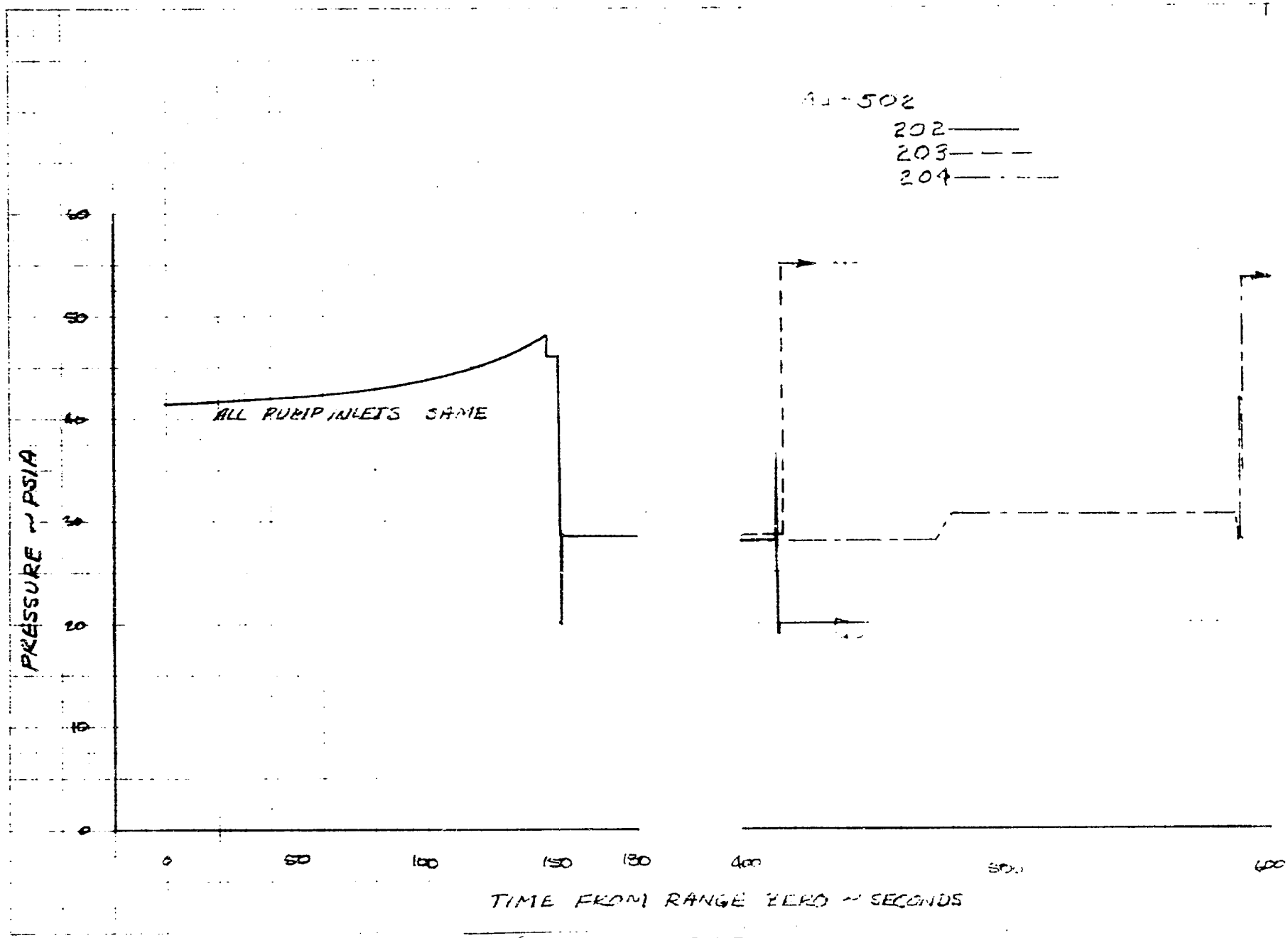

Figure 86. Fuel Pump Inlet Pressure

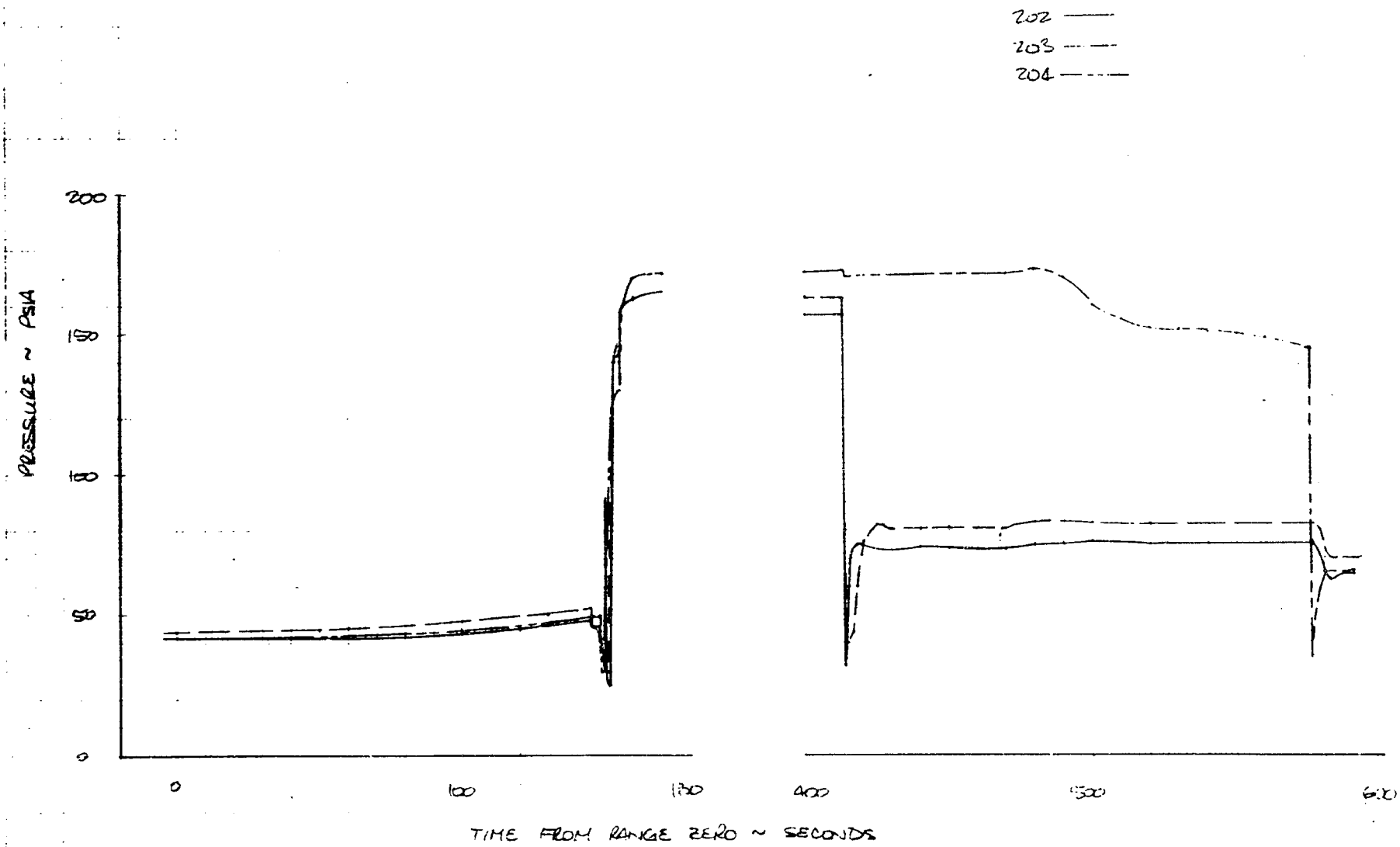

Figure 87. Fuel Pump Interstage Pressure (D0256)

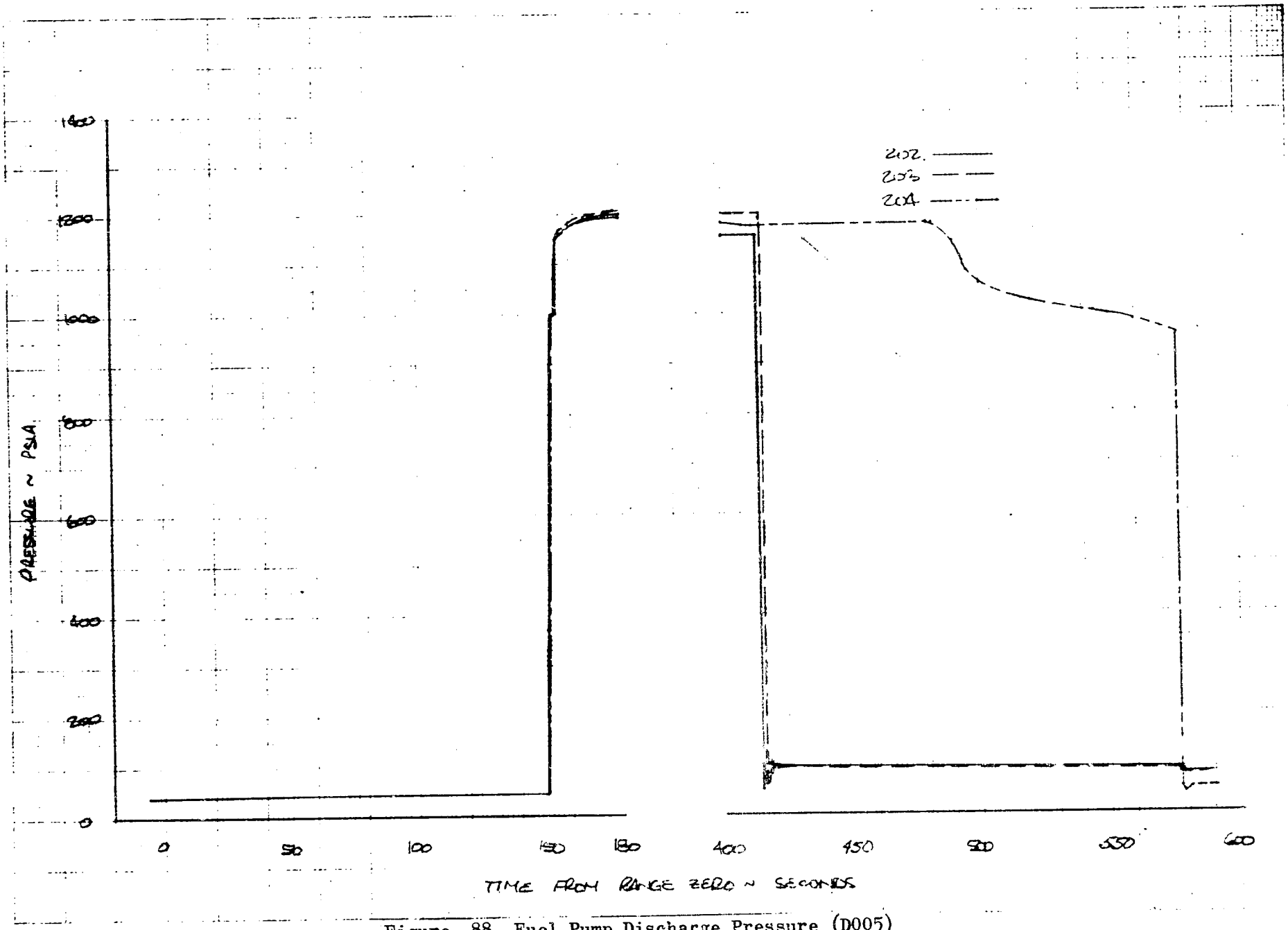

Figure 88. Fuel Pump Discharge Pressure (D005)

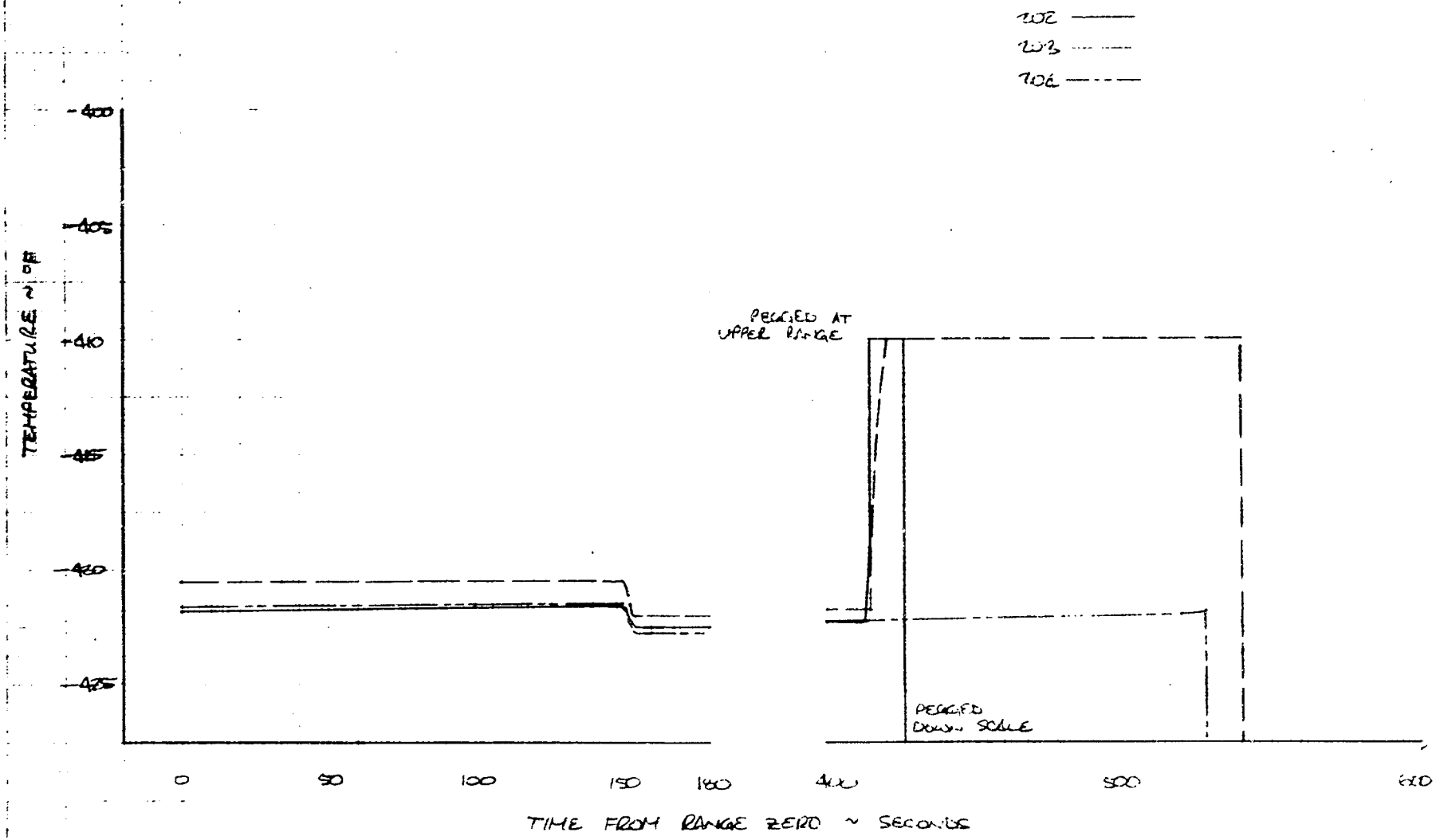

Figure 89. Fuel Pump Inlet Temperature (C0664)

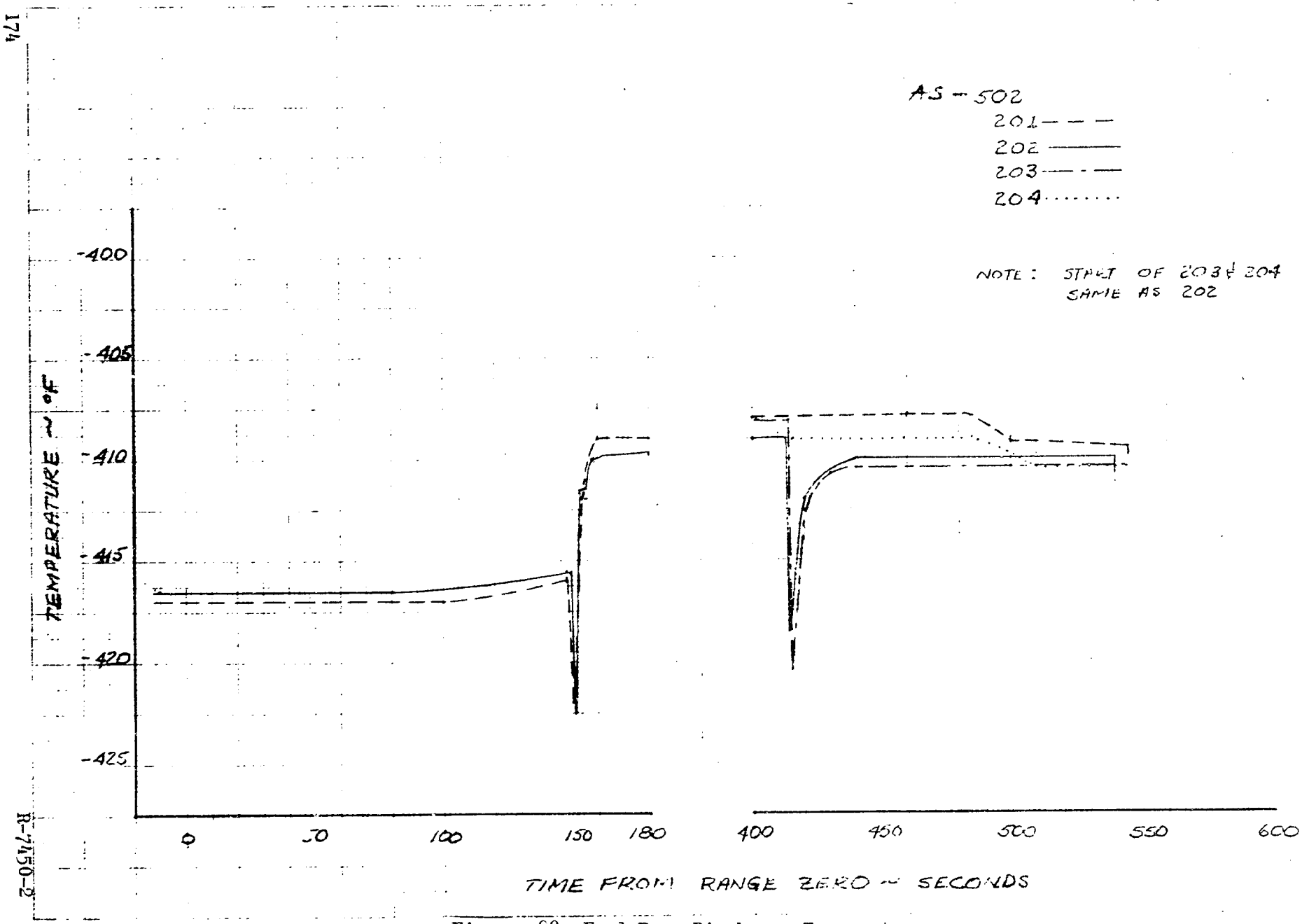

Figure 90. Fuel Pump Discharge Temperature

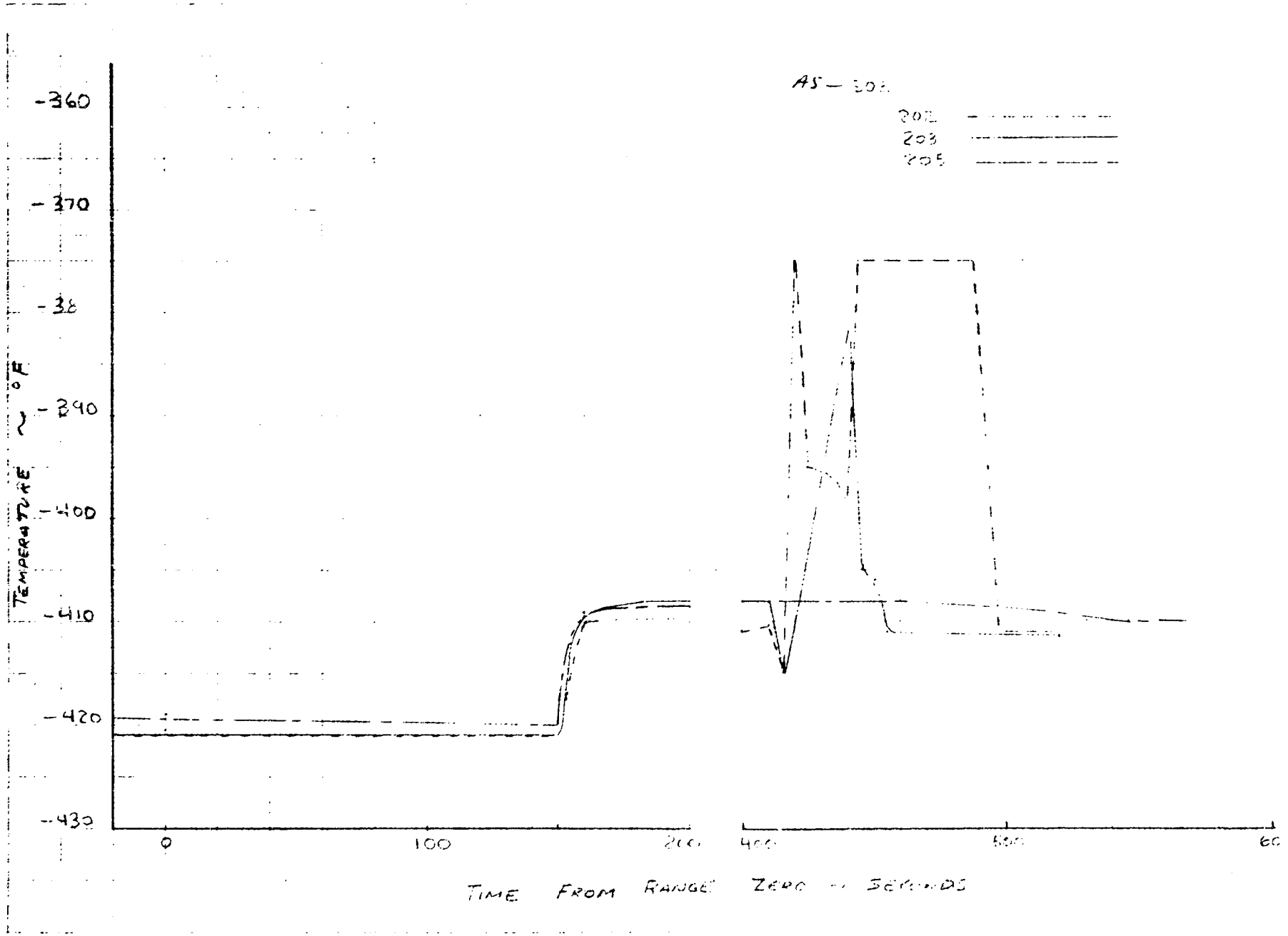

Figure 91. Gas Generator Fuel Inlet Temperature (C0008)

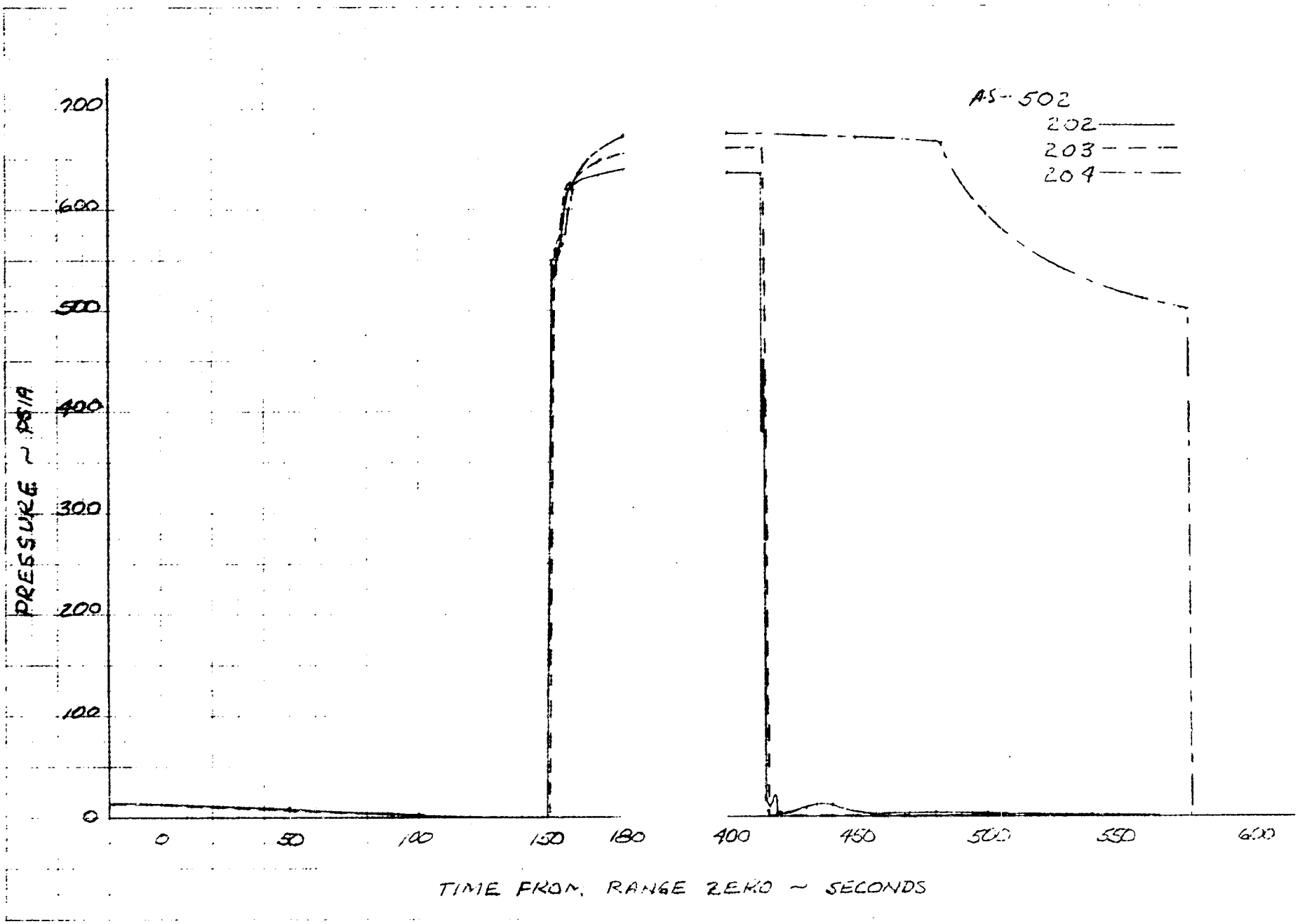

Figure 92. Gas Generator Chamber Pressure

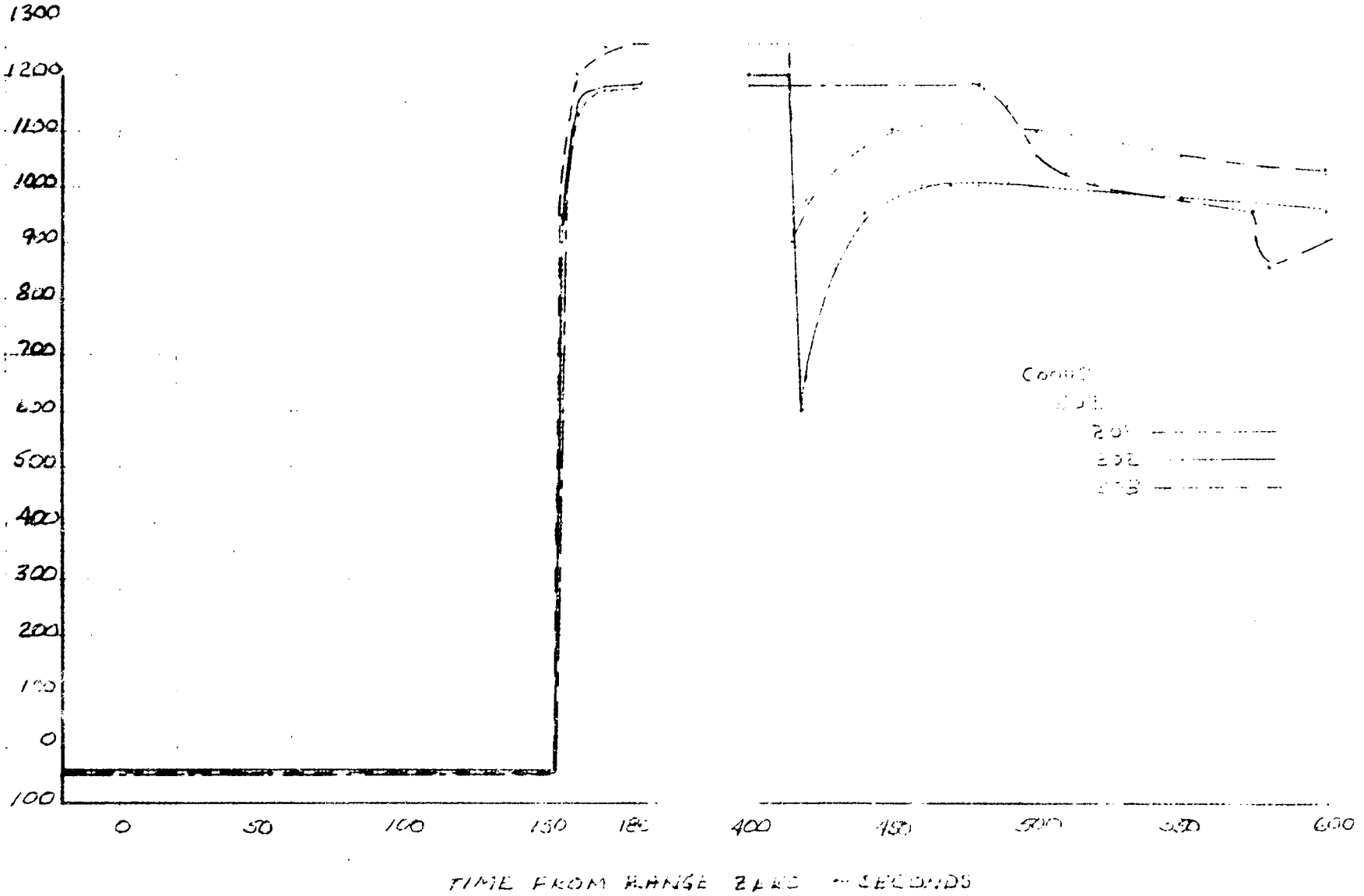

Figure 93. Fuel Turbine Inlet Temperature

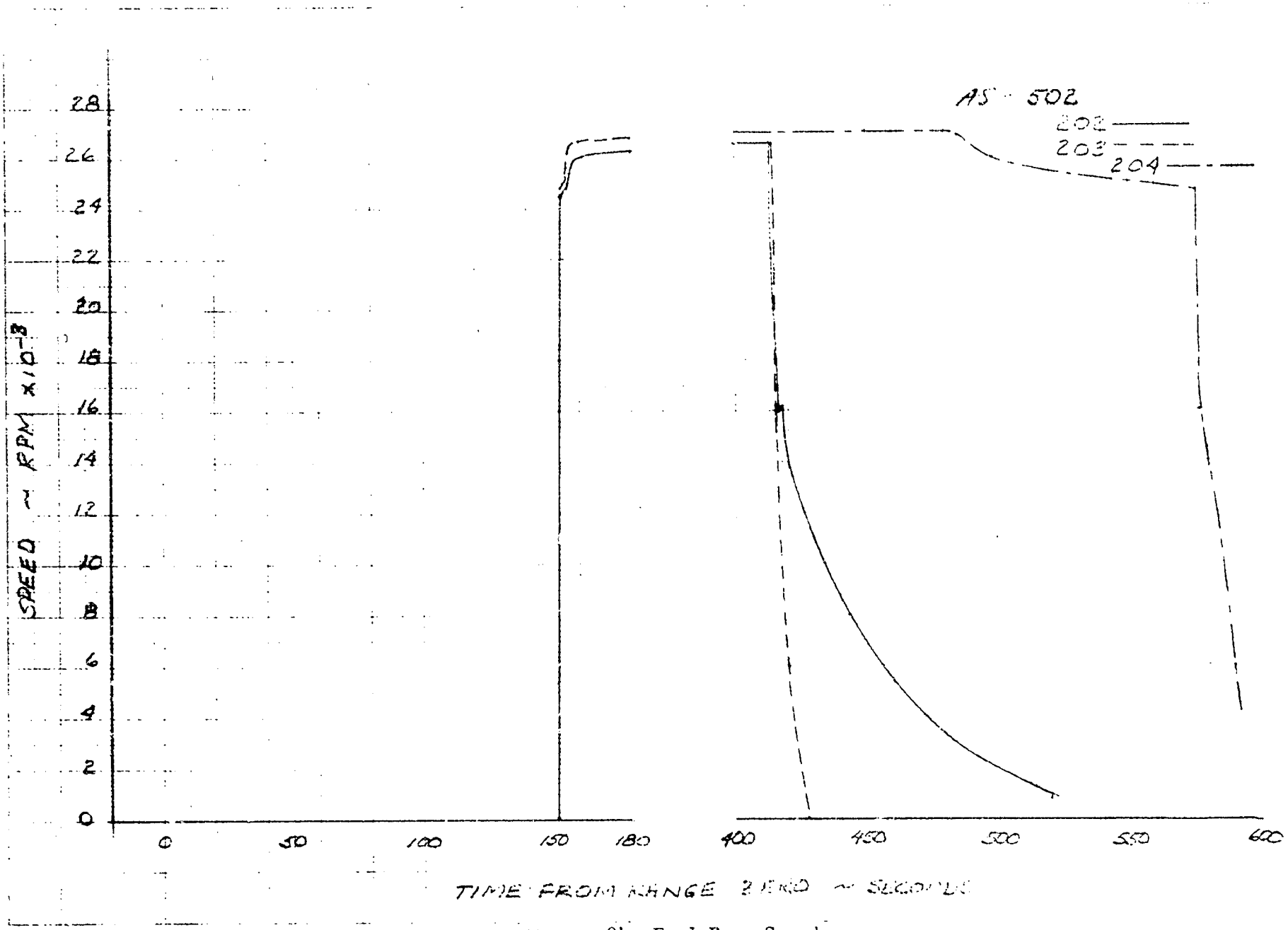

Figure 94. Fuel Pump Speed

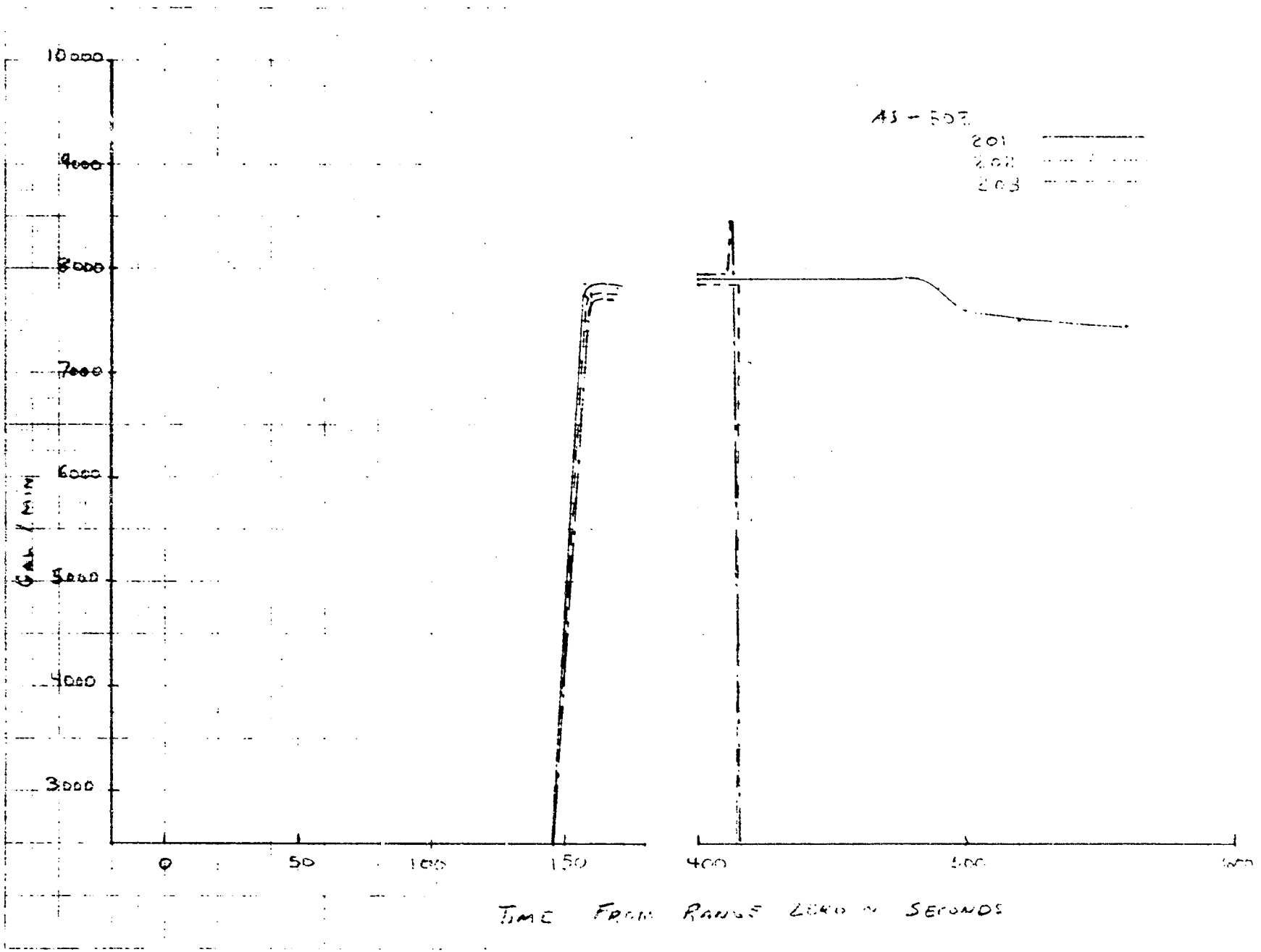

Figure 95. Main Fuel Flow (F0001)

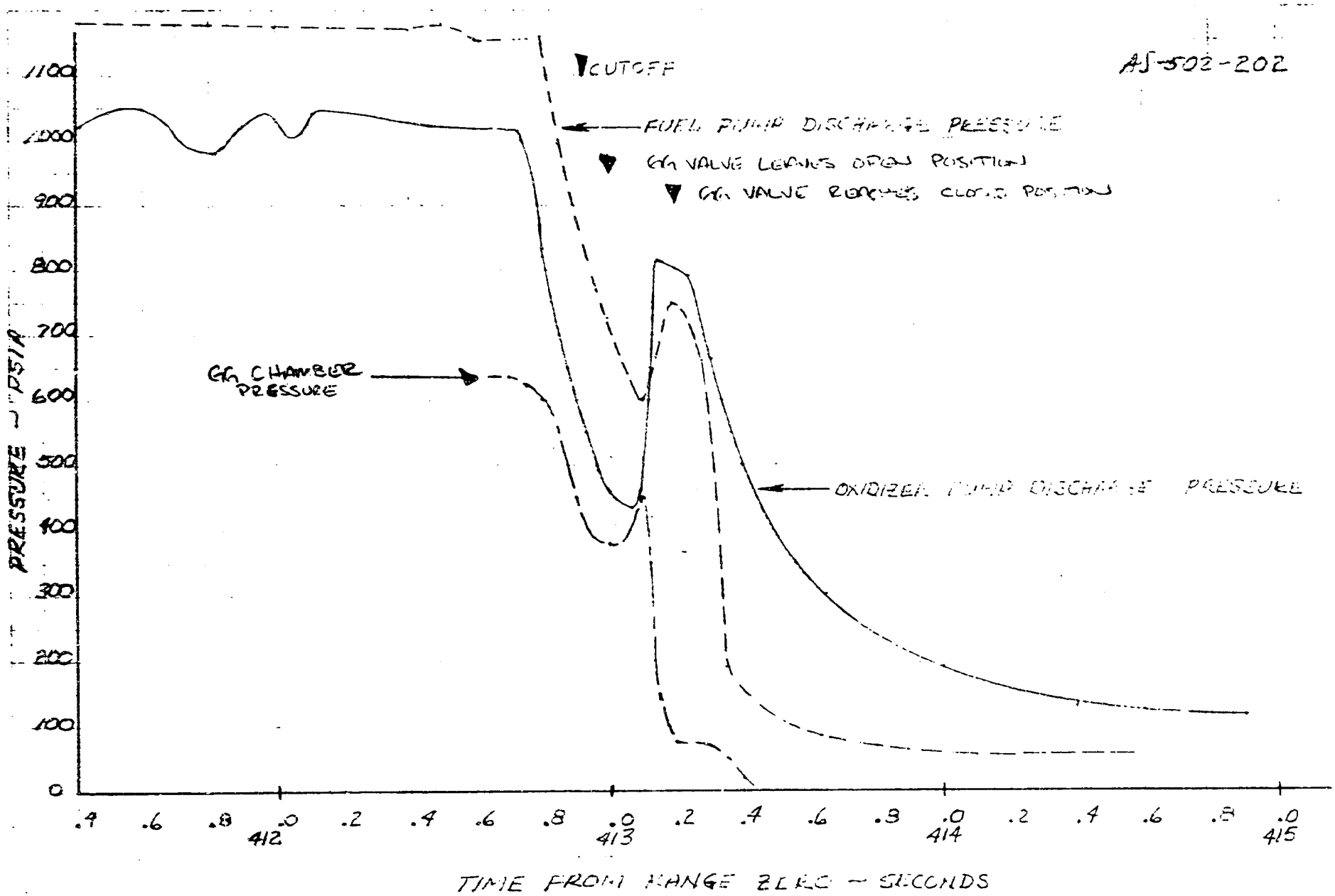

Figure 96. Engine 202 Pump Discharge Pressures and Gas Generator Chamber Pressure vs Time

relief valve in the stage fuel recirculation return shufoff valve; this relief valve has a cracking pressure of $45\ ^{+10}_{-5}$ psia, with a fuel tank pressure of 32 psia; the 80-psia pressure would indicate that the relief valve was at least partially open. Engine 202 extended turbopump rotation after cutoff provided the energy source necessary to maintain the 80-psia fuel system pressure (converting turbopump kinetic energy to heat in the fuel, forming a gas volume sufficient to maintain the pressure).

Engine 202 fuel pump inlet pressure pegged offscale low immediately at engine cutoff and fuel pump inlet temperature pegged high to -410 F at cutoff (412.977 seconds), and then offscale low at 426 seconds; loss of engine inlet pressure suggests either that the instrumentation lines ruptured at cutoff or that other instrumentation mechanical failure occurred. The upward temperature spike at cutoff is normal and occurred on all engines. The downward temperature spike at 426 seconds is unexplained. Because the fuel feed system was intact following cutoff and contained some liquid at this time, the -427 F temperature is considered erroneous and probably resulted from instrumentation failure.

At 415 seconds, the gas generator valve partially opened, and then closed again. Gas generator chamber pressure (Fig. 92) spiked to approximately 20 psia, decays to 5 psia, then rose back to 12 psia for approximately 30 seconds. The latter rise appears to be the result of a leaking gas generator fuel valve. The leaking fuel, picking up heat from the gas generator combustor, entered the turbine at approximately 1000 F and provided sufficient torque to maintain fuel pump rotation for the extended period observed. Table 8 presents gas generator and fuel turbine parameter data versus time; it is assumed that fuel within the turbopump was in a gaseous state and that the pump power load resulted from windage; turbine torques stated are sufficient to result in the extended pump speed decay.

TABLE 8

S-II ENGINE 202 GAS GENERATOR AND FUEL TURBINE PARAMETERS VS TIME

Range Time (Sec.)	GG Pc (psia)	Fuel Turbine Inlet Temp (°F)	Fuel Pump Speed (RPM)	Fuel Turbine Torque (in-lbs)
410	670	1200	26,600	--
415	20	630	19,000	672
420	4	670	14,200	135
425	6	780	12,500	200
430	9	850	11,000	302
435	12	900	9,700	410
440	11	940	8,700	370
445	7	960	7,700	235
450	5	980	6,800	170
455	3	990	6,100	105
460	1	1000	5,400	35
465	0	1000	4,800	0

Engine 202: Gas Generator Chamber Pressure Spike During Cutoff Transient

Description of Event. At 413.10 seconds, gas generator chamber pressure (engine 202) spiked to 450 psia from 380 psia.

Conclusions. The engine 202 gas generator chamber pressure spike following engine cutoff was a result of oxidizer and fuel pump pressure increases and closure of the gas generator valve oxidizer poppet.

Corroboration of Conclusions. At approximately 413.05 seconds, oxidizer pump discharge pressure began a rapid increase from 440 psia. This rapid increase resulted directly from closure of the main oxidizer valve. Fuel pump discharge pressure continued to decay until 413.10 seconds and then began to increase because of closure of the main fuel valve. At approximately 413.10 seconds, the gas generator valve oxidizer poppet closed, stopping oxidizer flow to the gas generator. The gas generator spike is caused by rapid buildup of oxidizer system pressure in association with the fuel system pressure decay.

Engine 202 Oxidizer Turbine Outlet Pressure Increase: 412.5 to 412.9 Seconds Range Time

Description of Event. Engine 202 oxidizer turbine outlet pressure increased approximately 3 psi between 412.5 and 412.9 seconds.

Conclusion. Erroneous data.

Corroboration of Conclusion. Figures 97 through 103 illustrate the following conclusions:

1. Upstream pressures, i.e., gas generator chamber pressure and oxidizer turbine inlet pressure, did not increase.

2. Upstream temperatures, i.e., fuel and oxidizer turbine inlet temperatures, did not increase.

3. Oxidizer turbine outlet temperature did not change.

4. Oxidizer turbine bypass valve position did not change.

Engine 202 Instrumentation Package Temperatures Rise at Engine Cutoff: 413 Seconds Range Time

Description of Event. Engine 202 primary and auxiliary instrumentation package temperatures changed at cutoff from a slow continuous decrease trend to an abrupt rapid rise, and then leveled off during the remaining 140 seconds preceding cutoff of S-II engines 201, 204, and 205 (Fig. 104).

Hypothesis. The temperature rise indicated by the engine 202 instrumentation packages is attributed to a fire in the area of engine 202 (associated with cutoff), followed by stabilization at a new environmental condition with engines 201, 204, and 205 firing.

Corroboration of Hypothesis. The abrupt temperature rise indicates a very high Q in the areas of the instrumentation packages such as might be caused by an engine area fire at cutoff. This condition is corroborated by numerous temperature measurements in the engine compartment.

The new temperature level sought by both instrumentation packages represents a more moderate level of heat emission such as would exist with only engines 201, 204, and 205 in operation.

Engine 202: Decreased Helium Usage at Cutoff

Description of Event. Review of initial data indicated that engine 202 helium usage was low at cutoff.

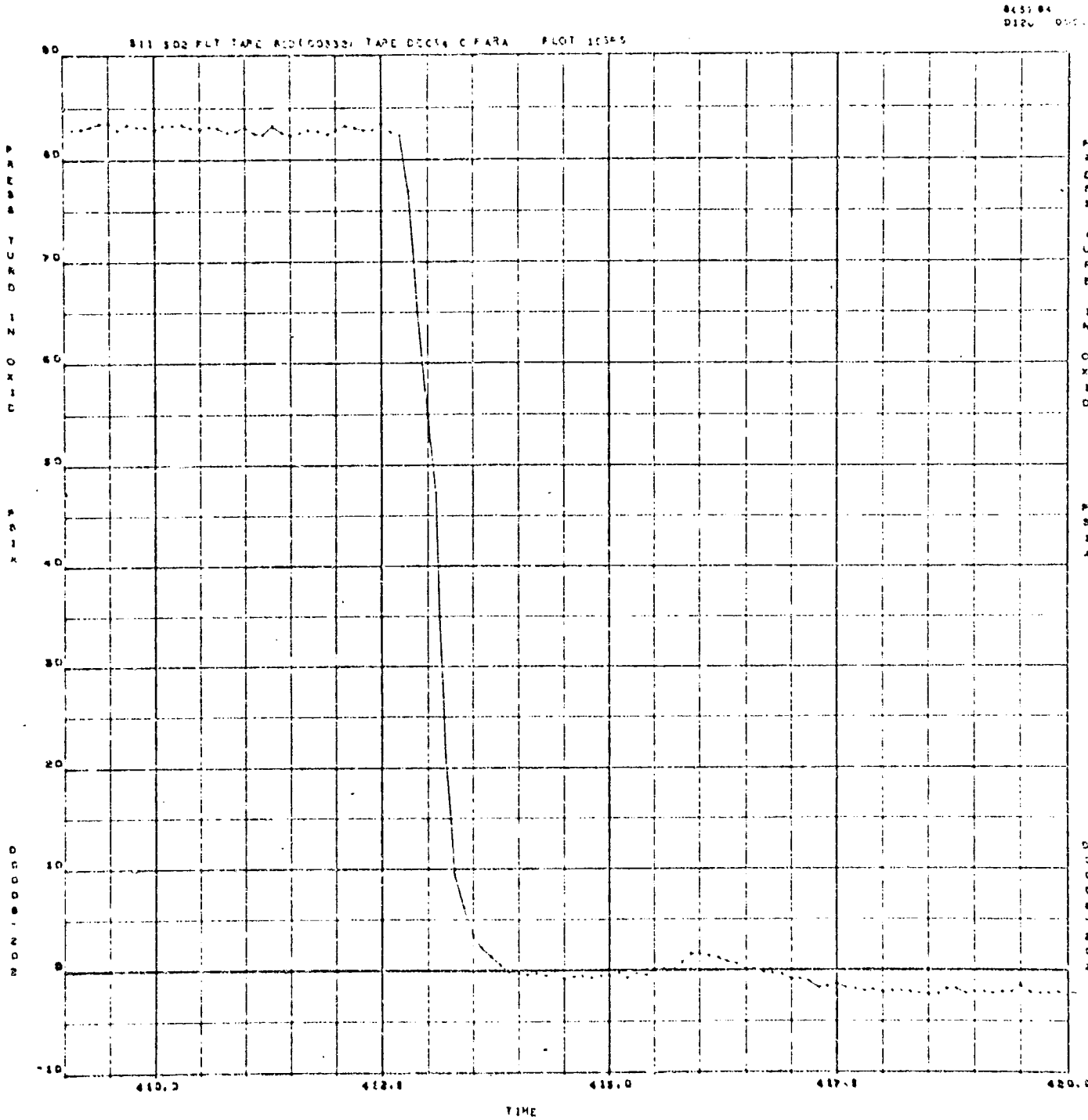

Figure 97. Oxidizer Turbine Inlet Pressure

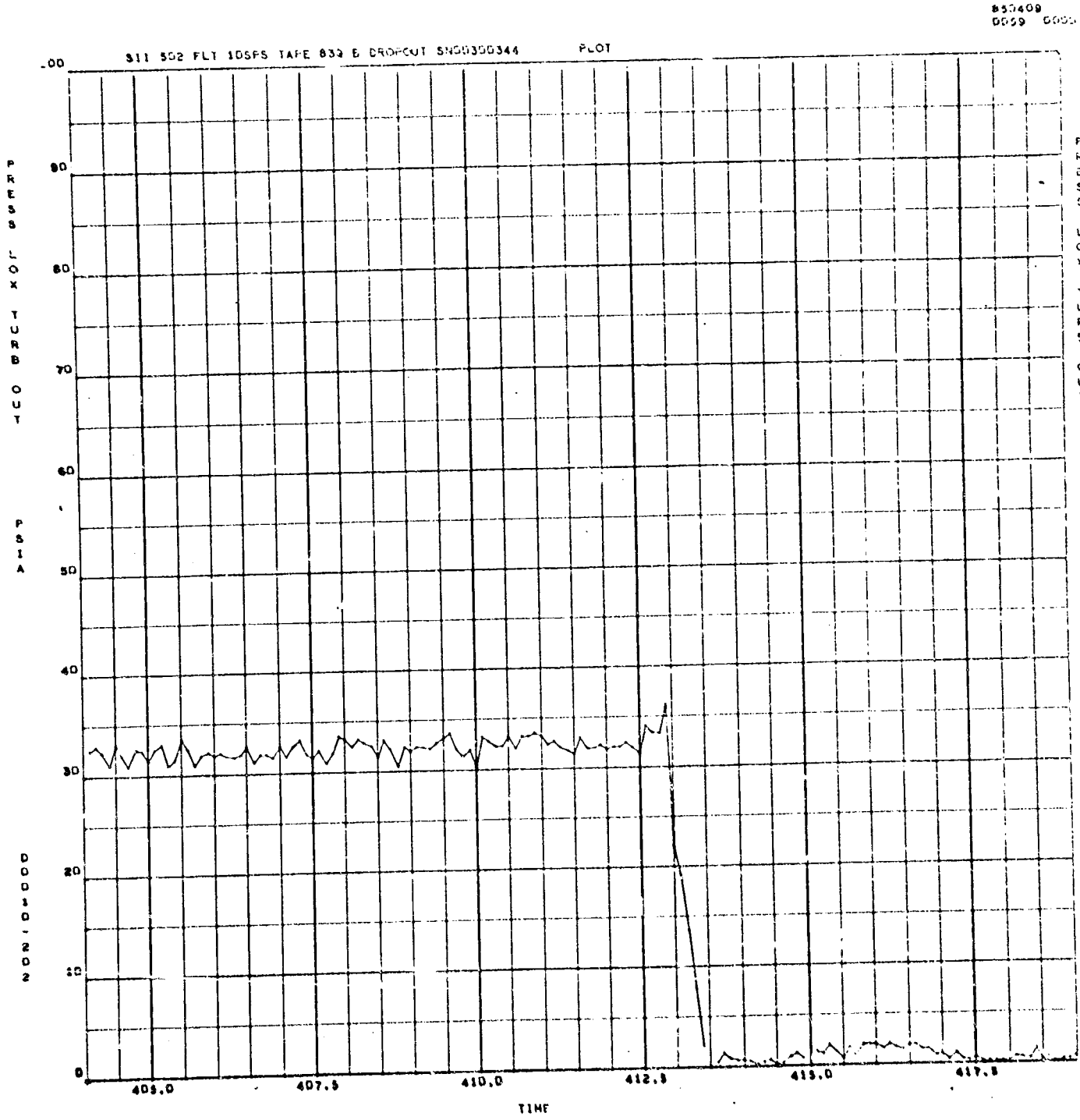

Figure 98. Oxidizer Turbine Outlet Pressure

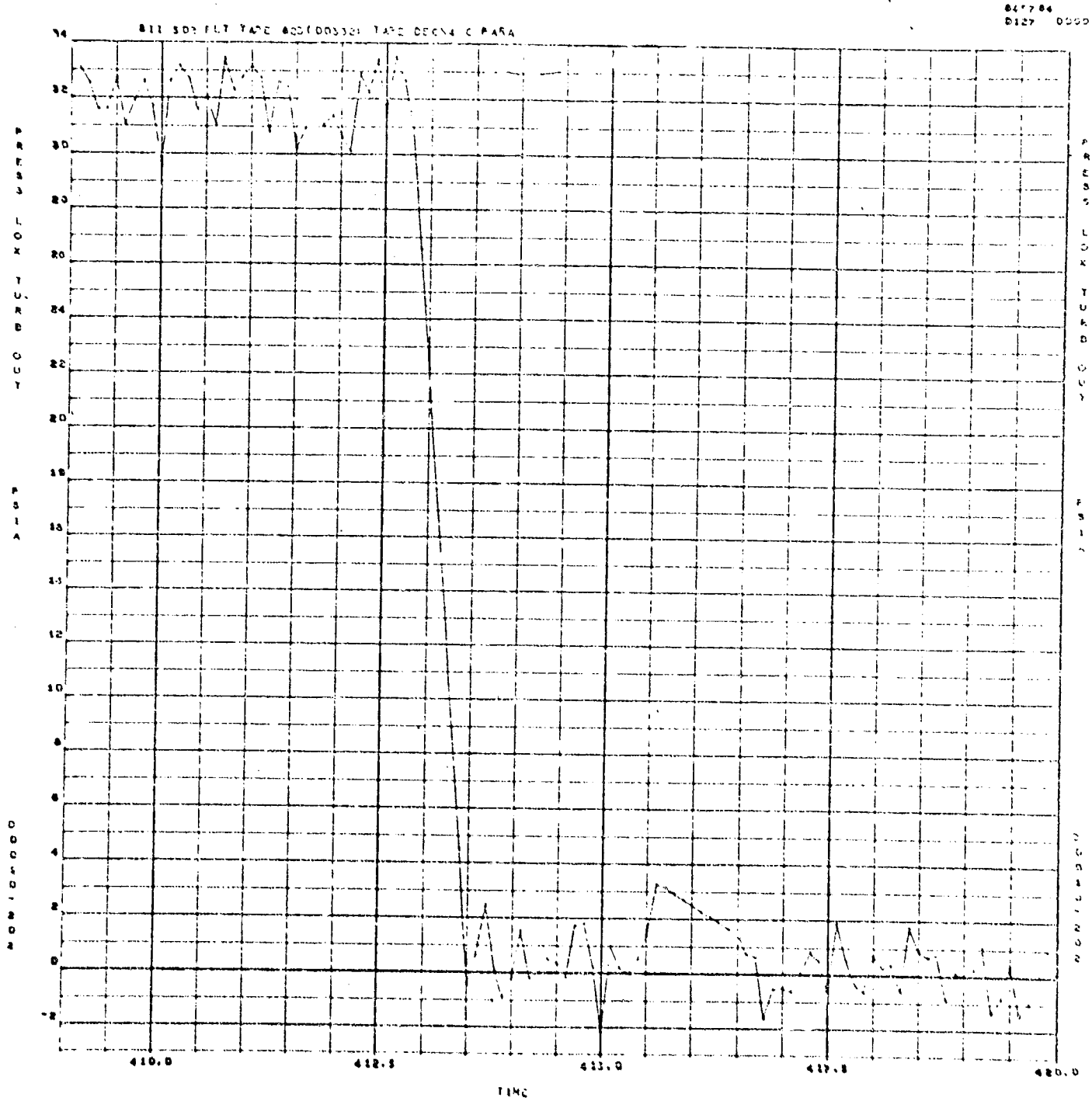

Figure 99. Oxidizer Turbine Outlet Pressure

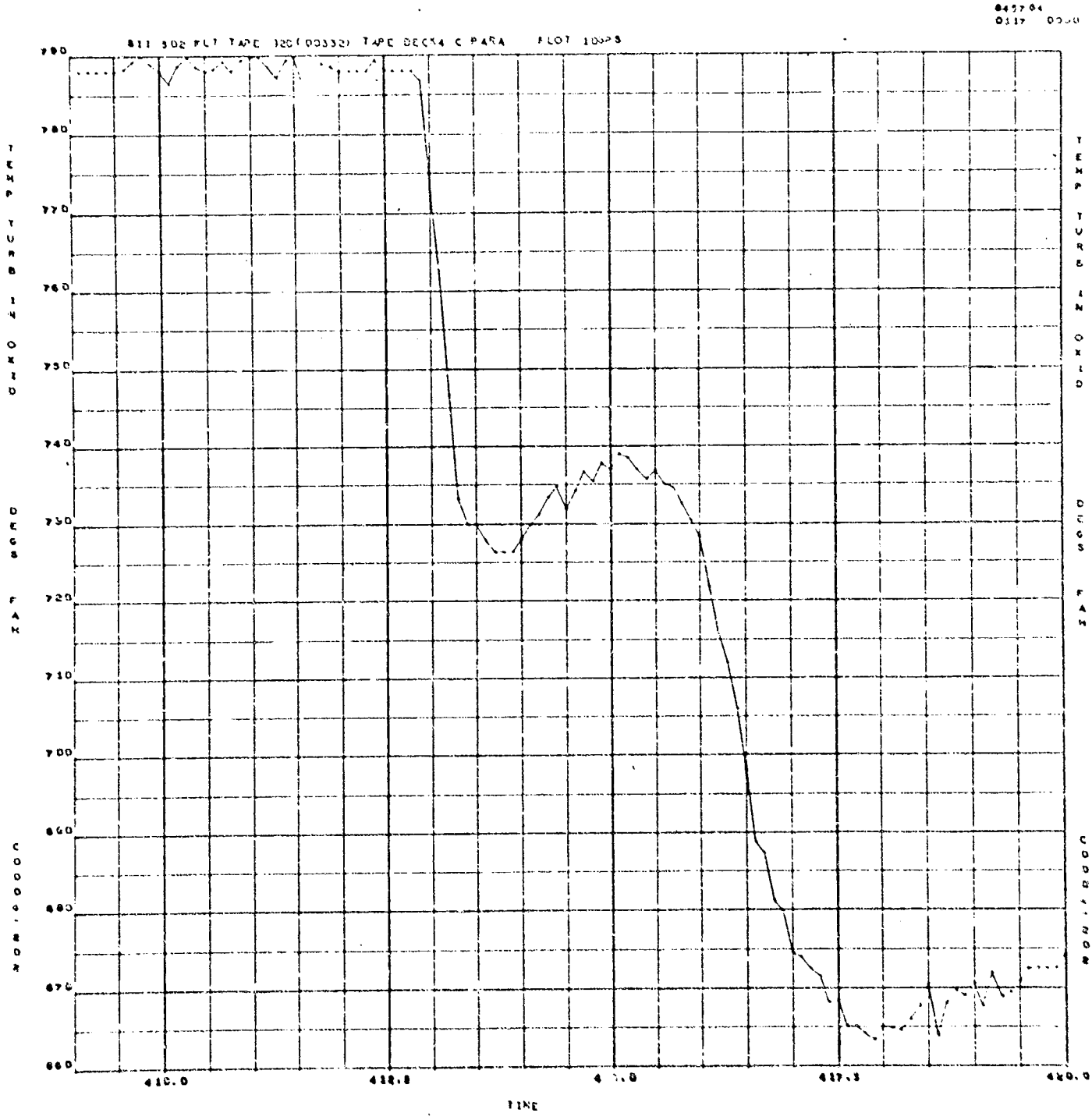

Figure 100. Oxidizer Turbine Inlet Temperature

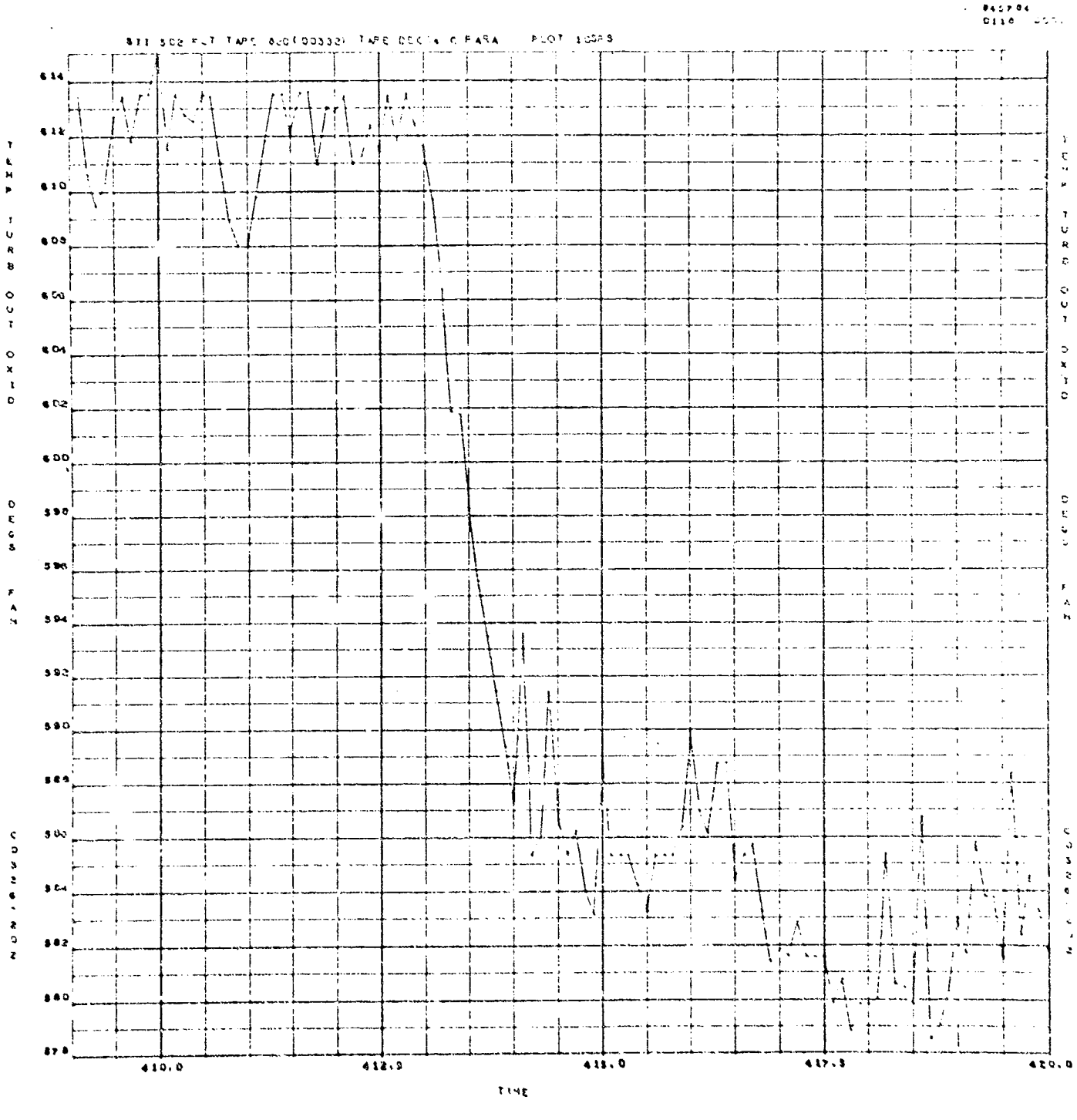

Figure 101. Oxidizer Turbine Outlet Temperature

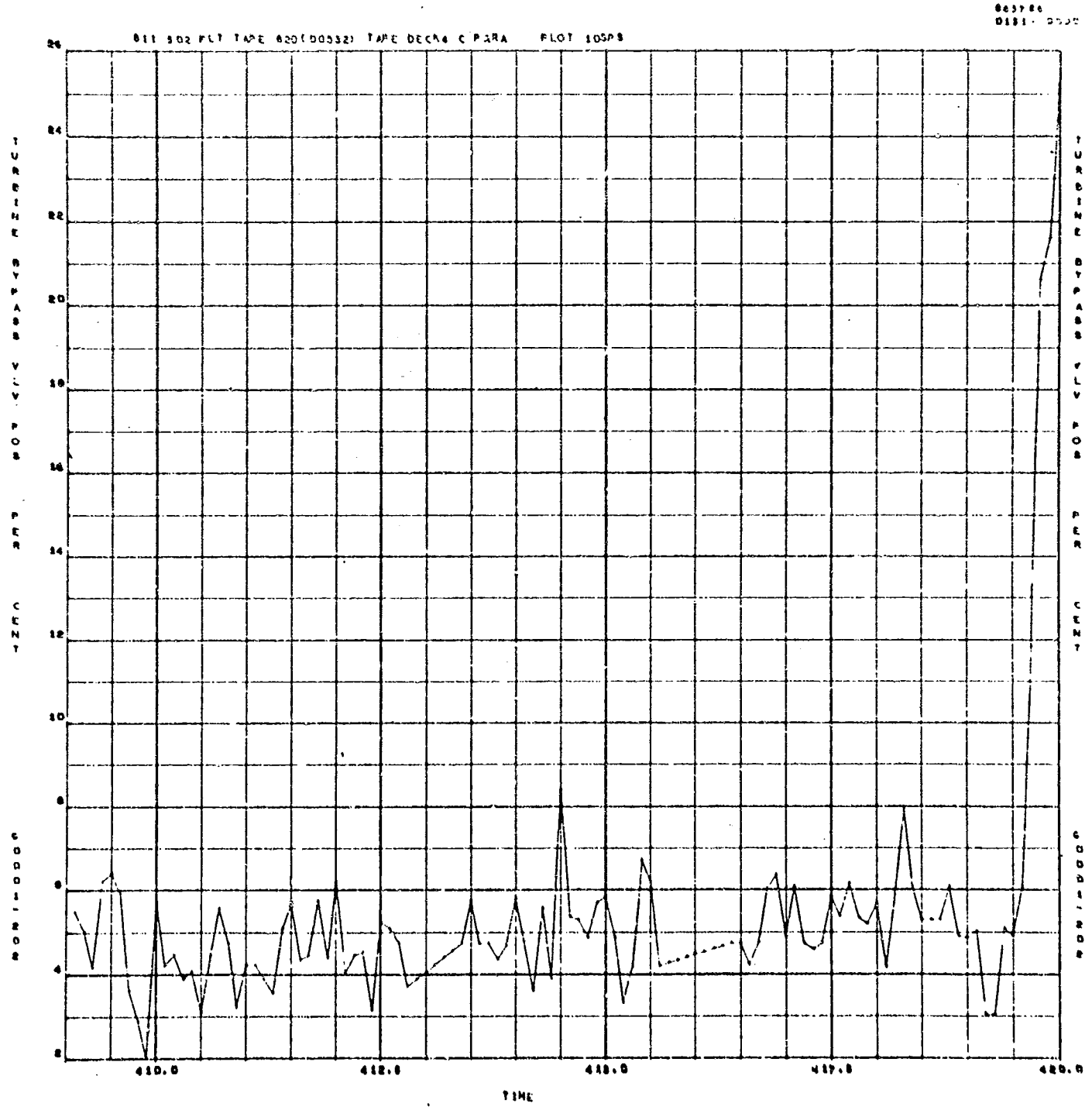

Figure 102. Turbine Bypass Valve Position

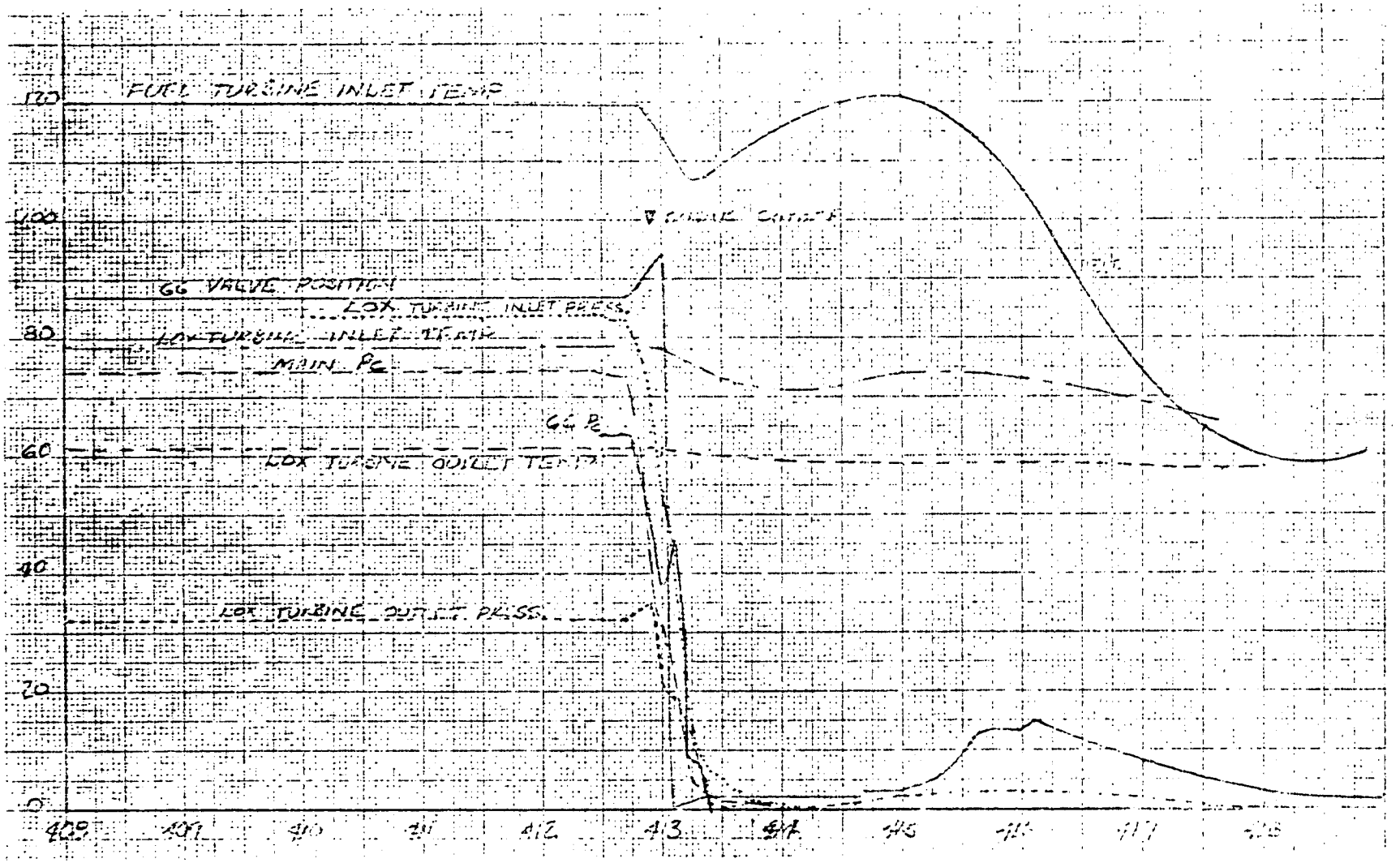

Figure 103. Engine 202 Instrumentation Parameter at Cutoff

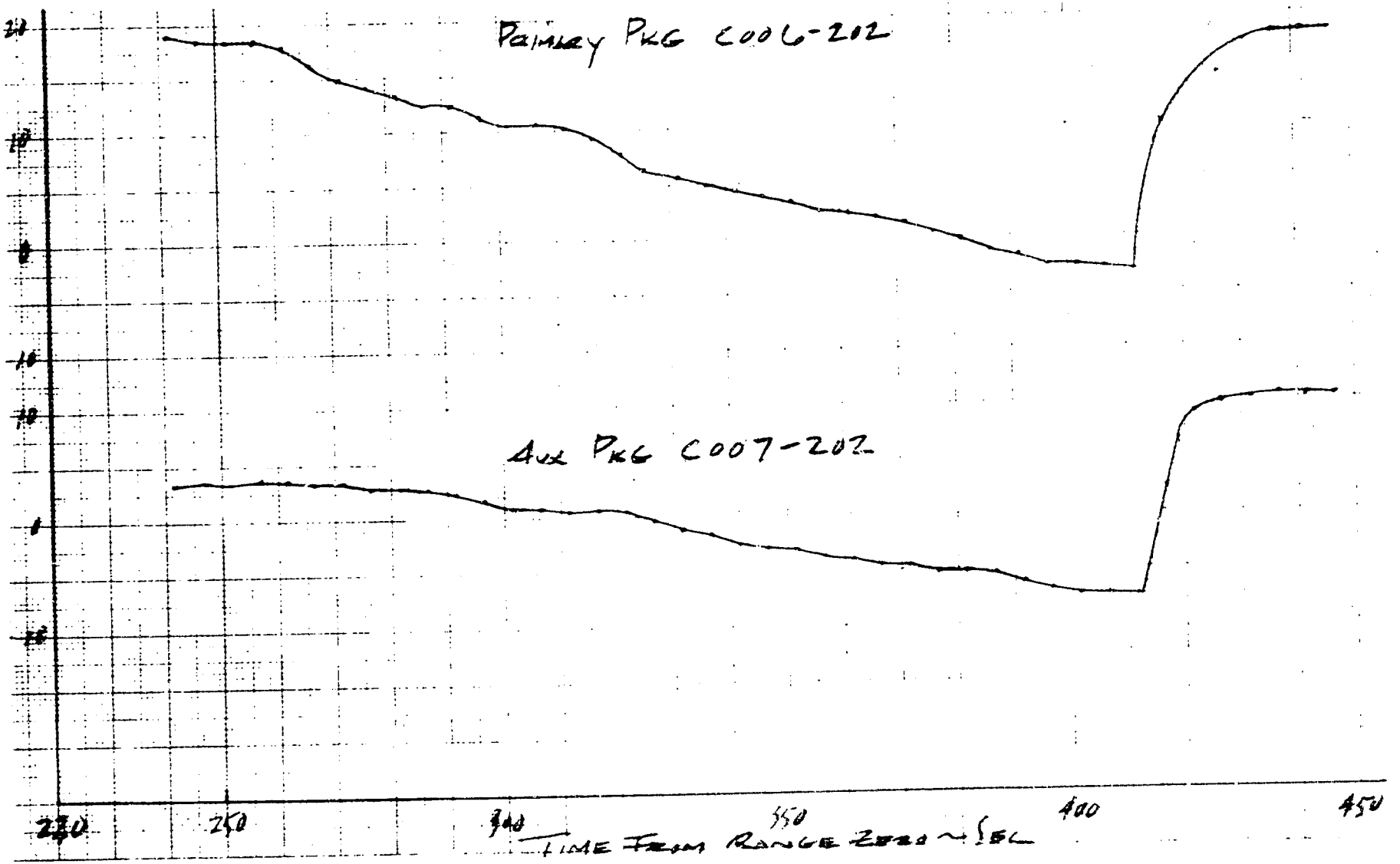

Figure 104. Instrumentation Packages Temperatures

Conclusions. There was no anomaly associated with cutoff helium usage for engine 202.

Corroboration of Conclusion. A cutoff helium usage equation that predicts the normal pressure loss has been developed. This equation is based on isothermal flow and has been modified by an empirically verified coefficient. This equation utilizes helium tank pressure and temperature just prior to cutoff.

$$\Delta P = P - \left[P^{1/\alpha} - \left(\frac{T}{P^{\frac{\alpha-1}{\alpha}}} \right) K \right]^{\alpha}$$

where

ΔP = normal expected pressure loss

P = helium tank pressure prior to cutoff

T = helium tank temperature prior to cutoff

α = ratio of specific heat (1.67 for helium)

K = empirical coefficient = 0.36

Using the above equation, the predicted helium usage for engine 202 was 54 psi; actual measured helium usage was 60 psi, thus corroborating the conclusion that engine 202 helium usage was normal and that there is no anomaly associated with decreased helium usage.

Engine 202: Loss of Oxidizer Pressurization System Integrity Following Cutoff

Description of Event. Engine 202 heat exchanger outlet temperature decreased to approximately -260 F for approximately 3 seconds following engine cutoff, and then gradually increased to approximately -60 F at S-II stage cutoff. Figures 105 through 124 describe AS-502 S-II engine heat exchanger and stage oxidizer pressurization system operation.

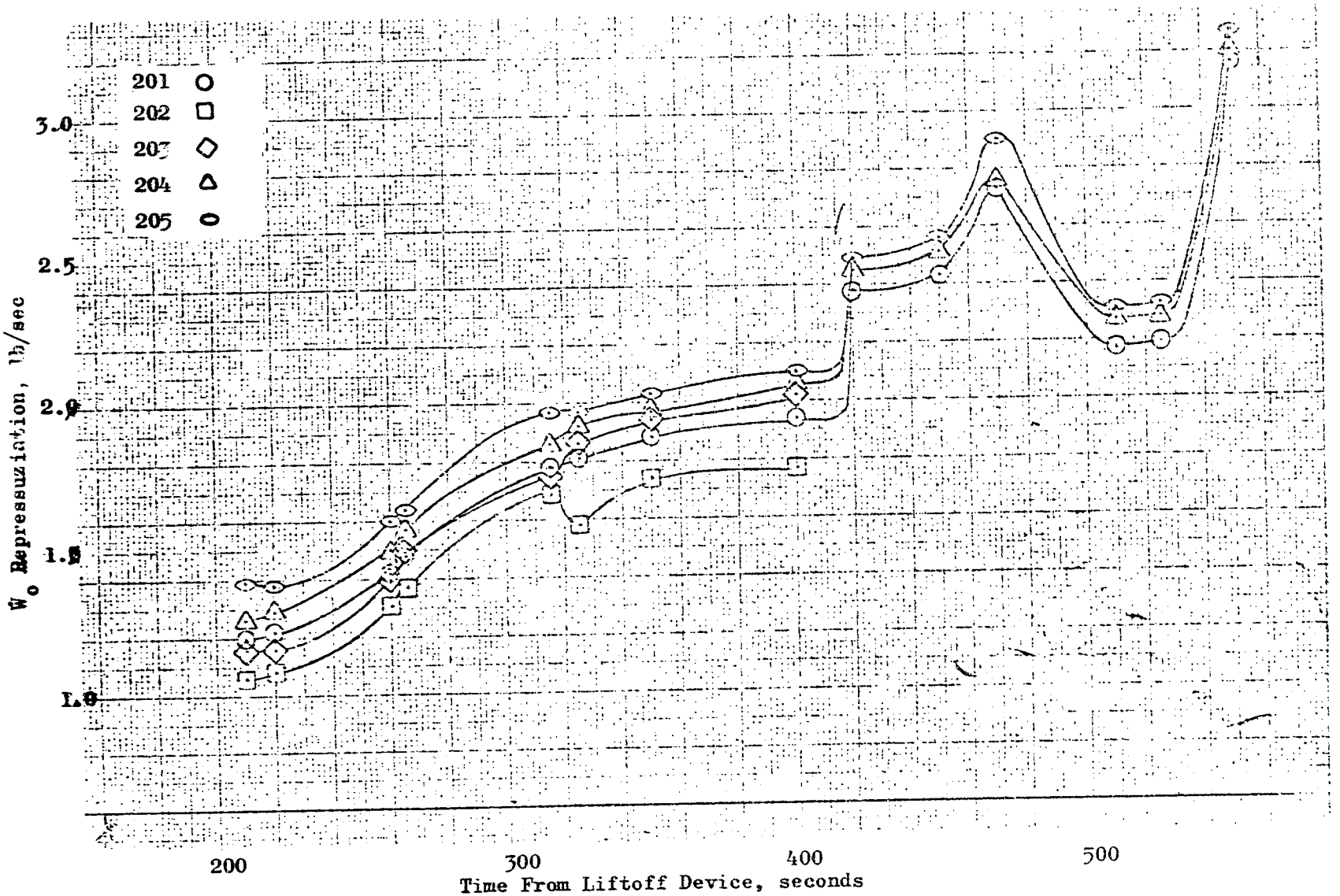

Figure 105. S-II Stage Oxidizer Pressurization

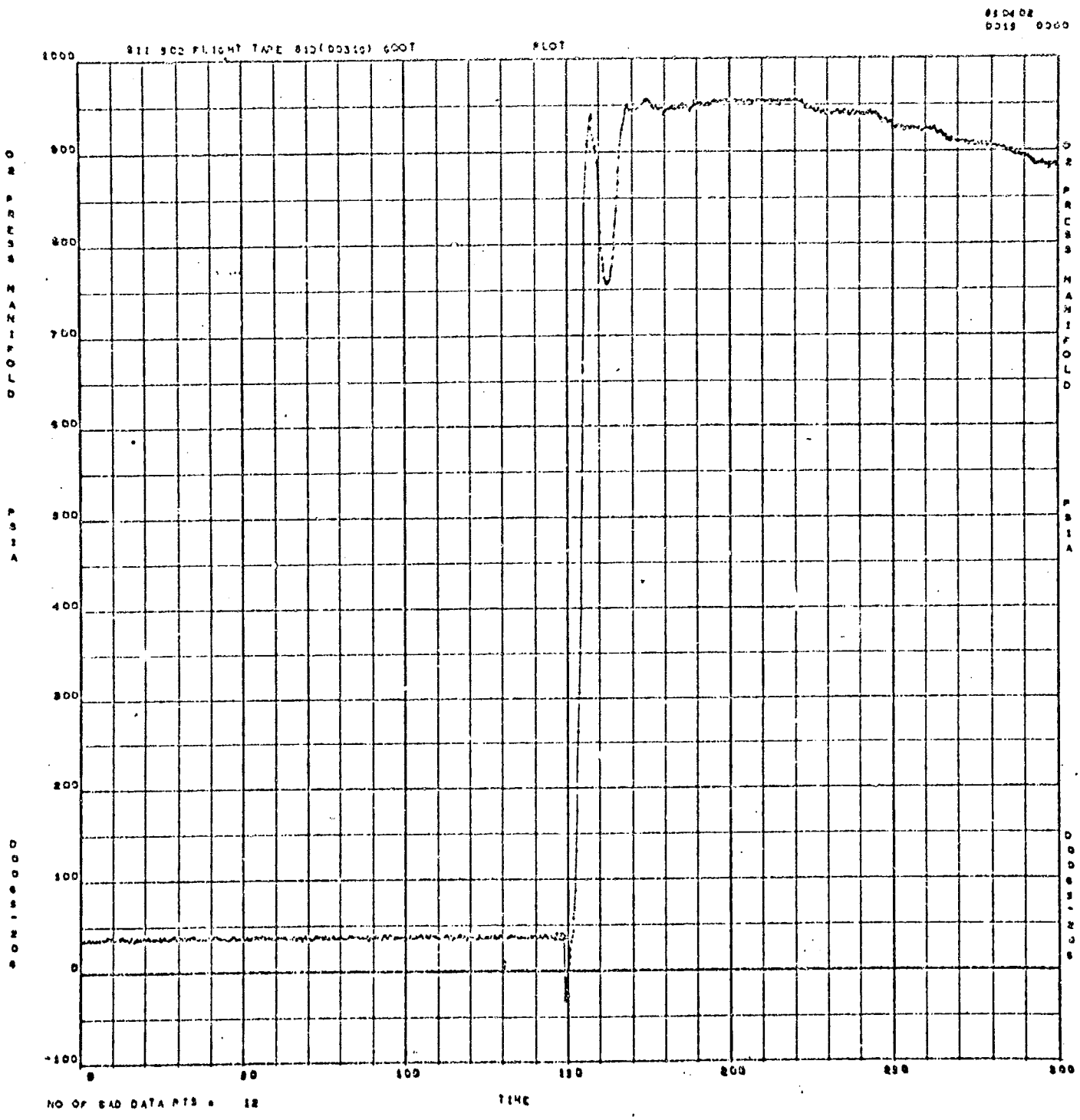

Figure 106. Oxidizer Manifold Pressure

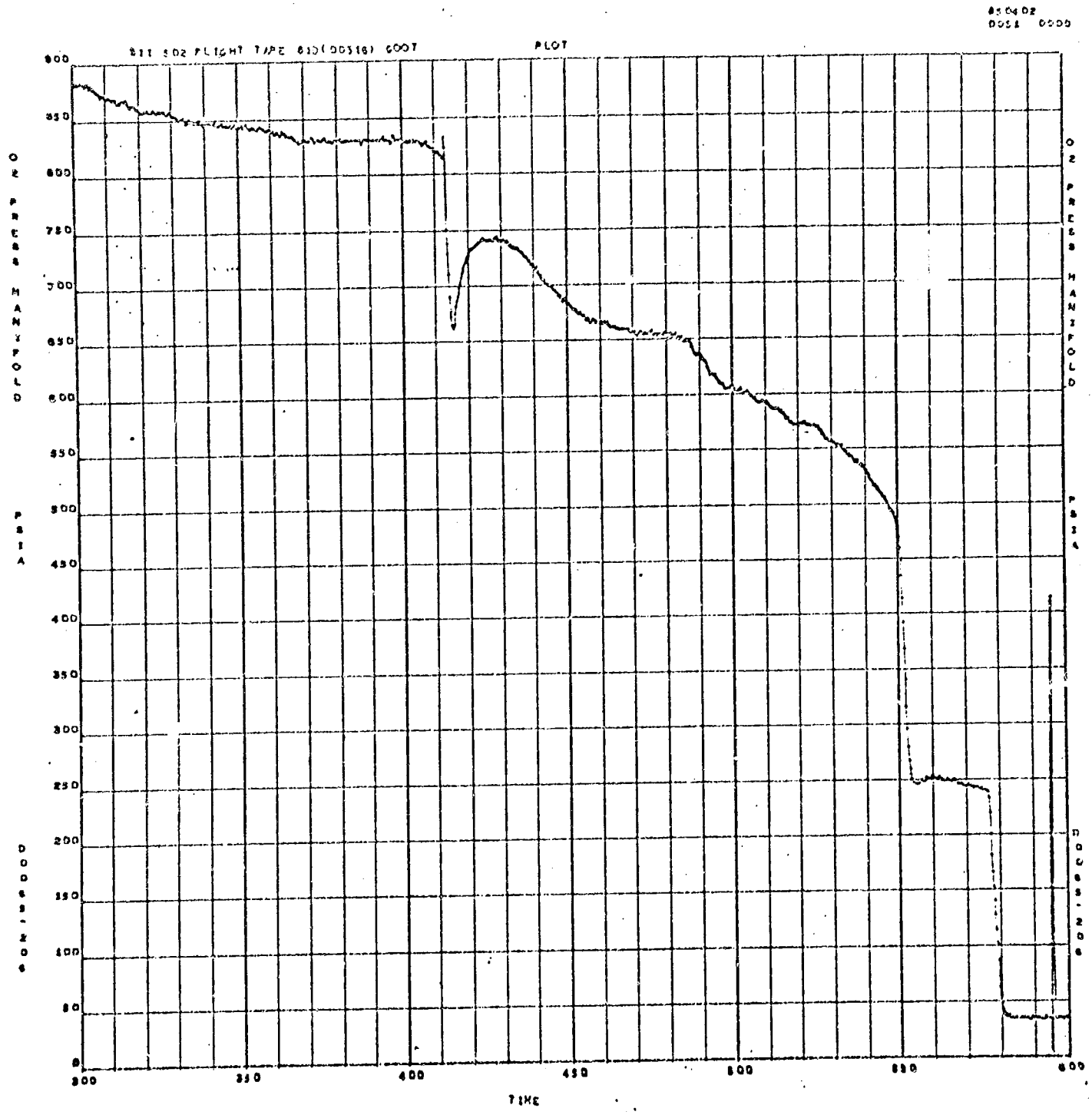

Figure 107. Oxidizer Manifold Pressure

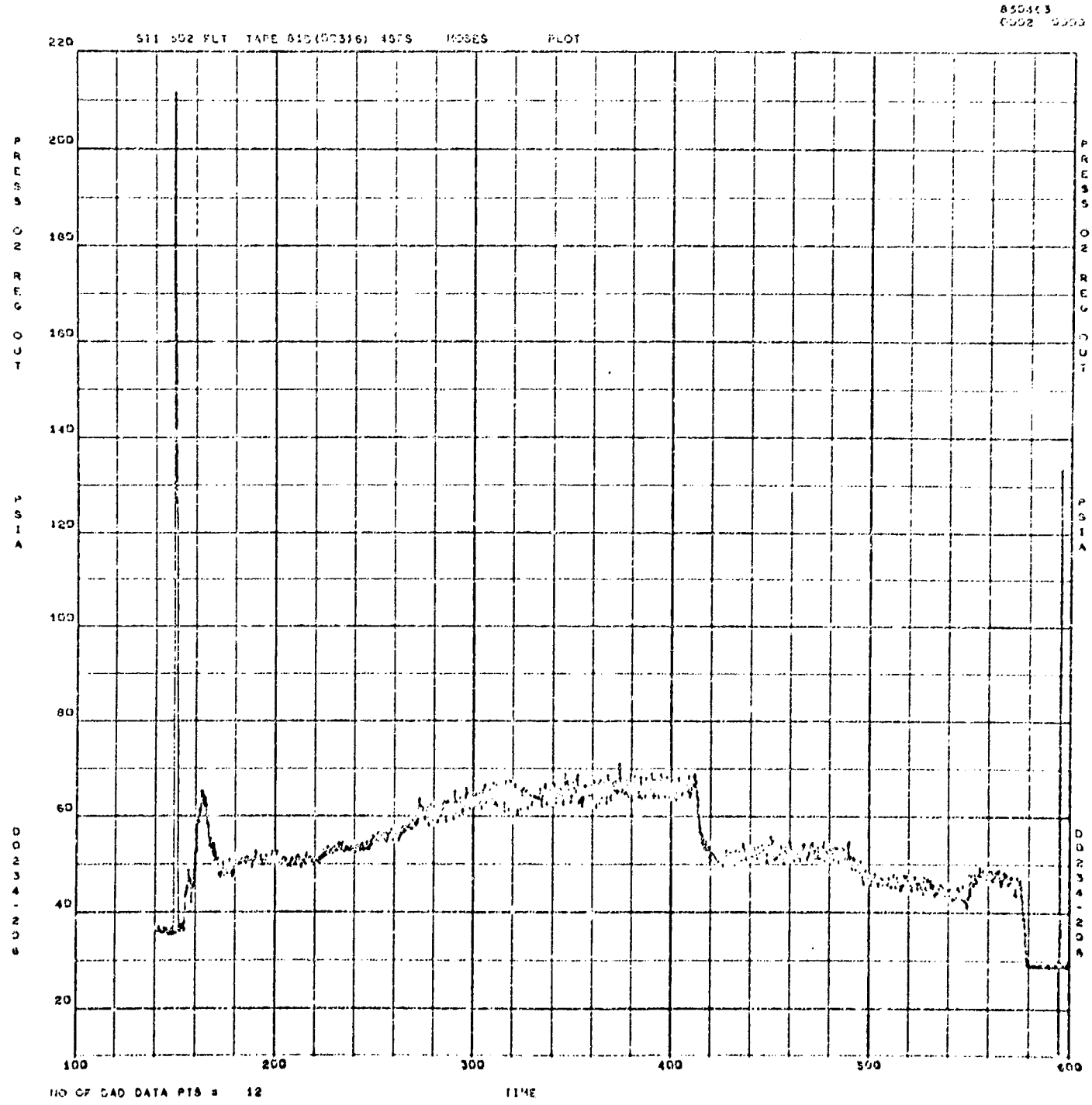

Figure 108. Oxidizer Regulator Outlet Pressure

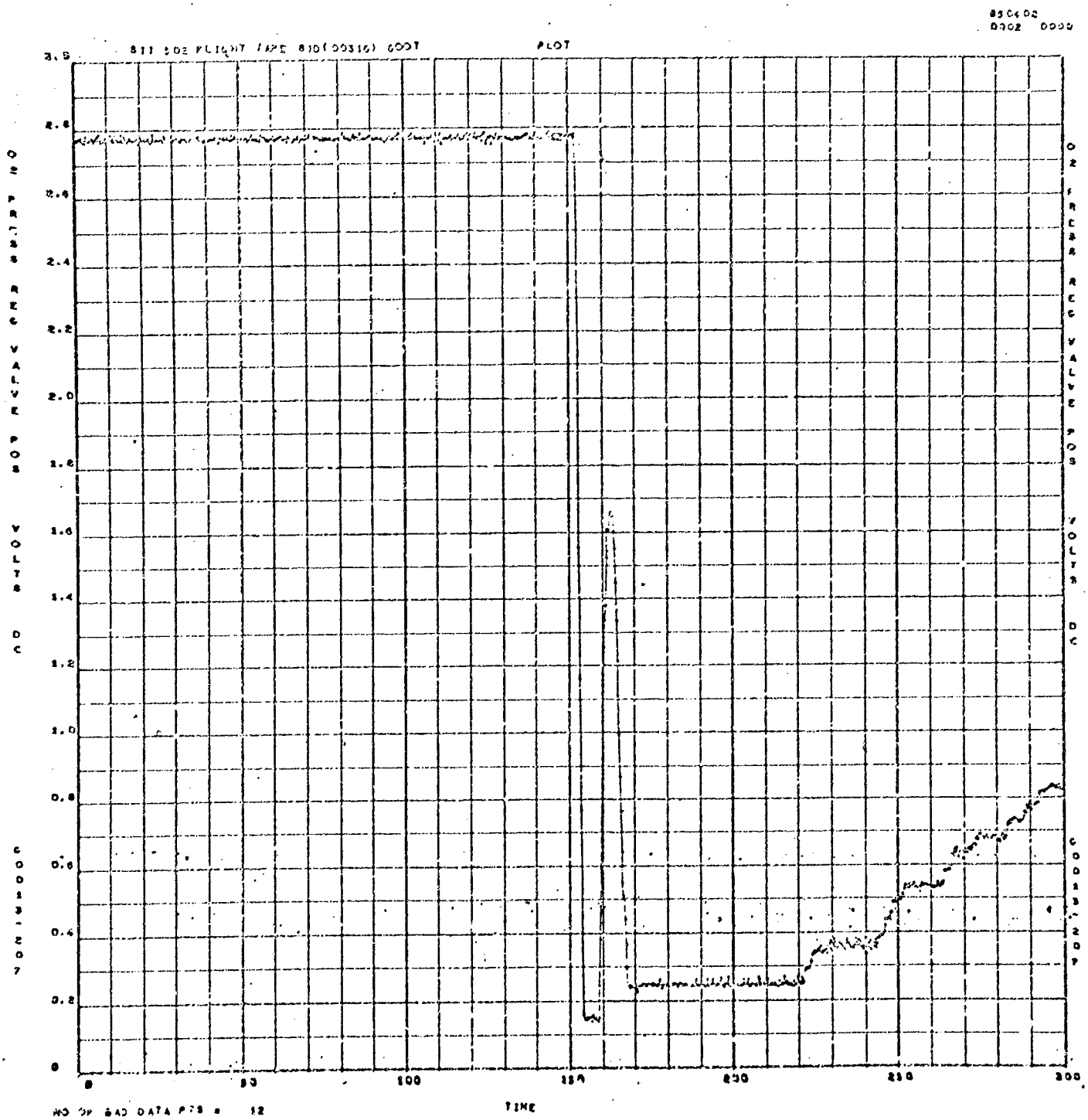

Figure 109. Oxidizer Regulator Pressure Valve Position

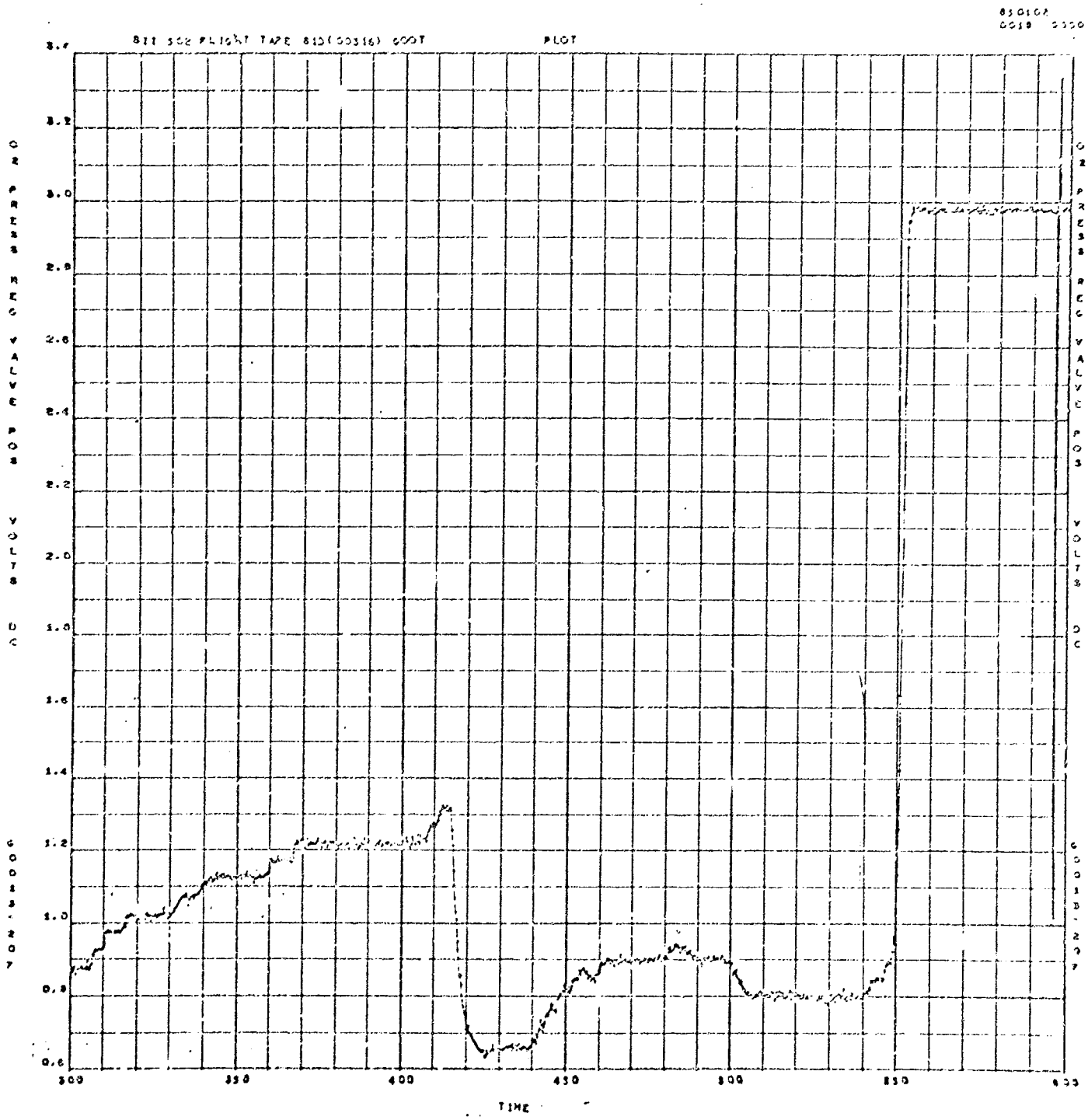

Figure 110. Oxidizer Regulator Pressure Valve Position

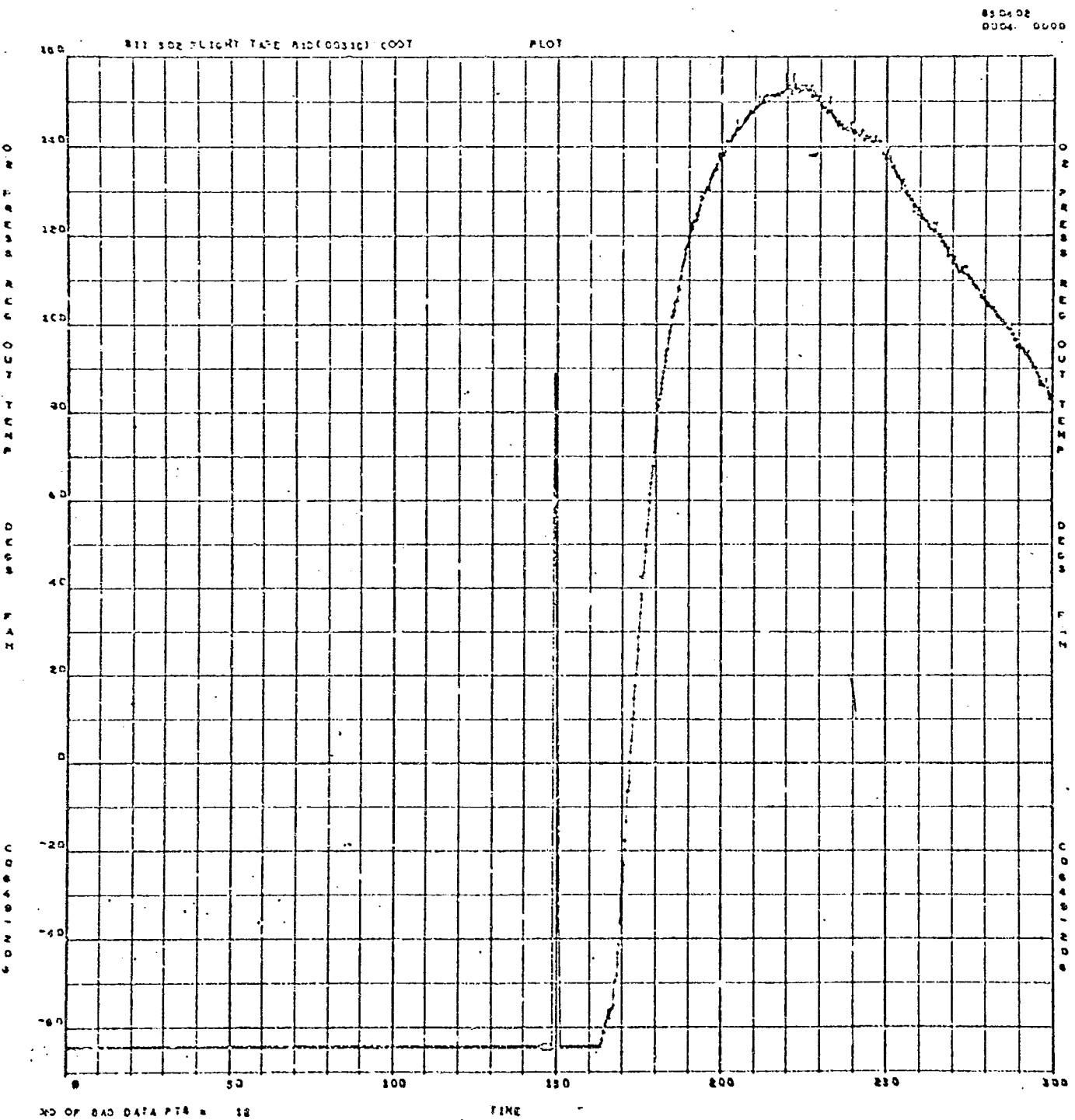

Figure 111. Oxidizer Regulator Pressure Outlet Temperature

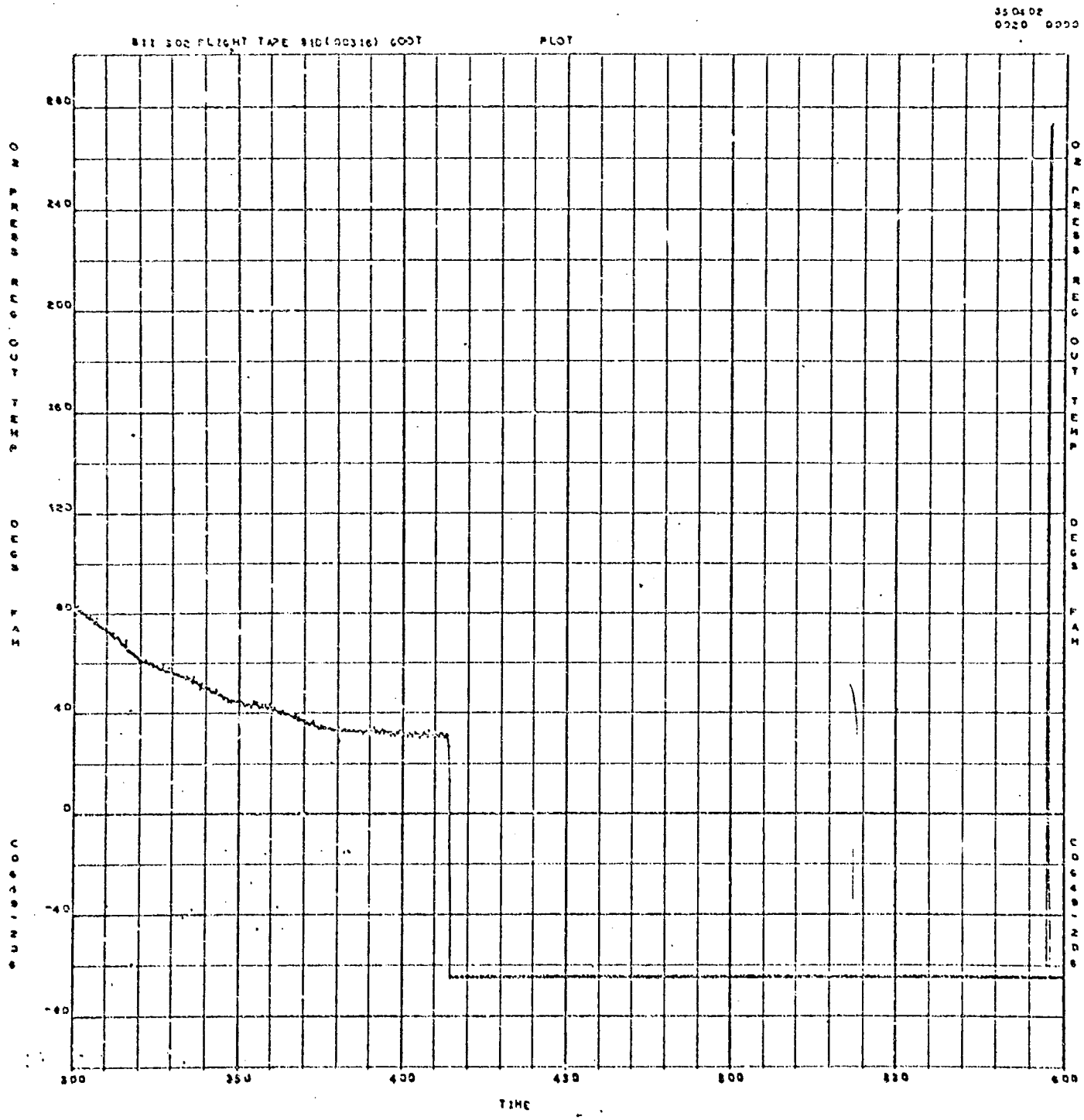

Figure 112. Oxidizer Regulator Pressure Outlet Temperature

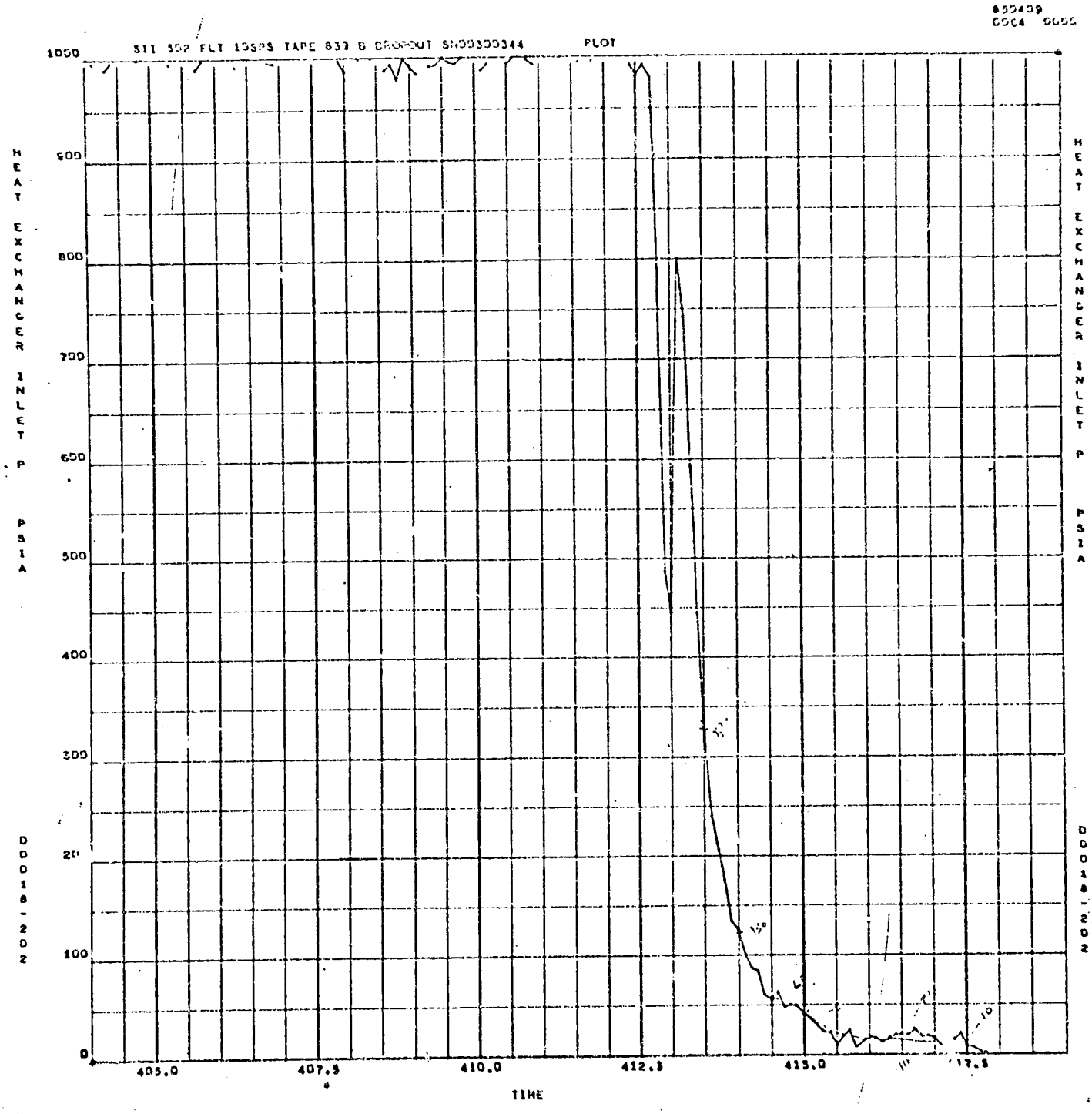

Figure 113. Heat Exchanger Inlet Pressure

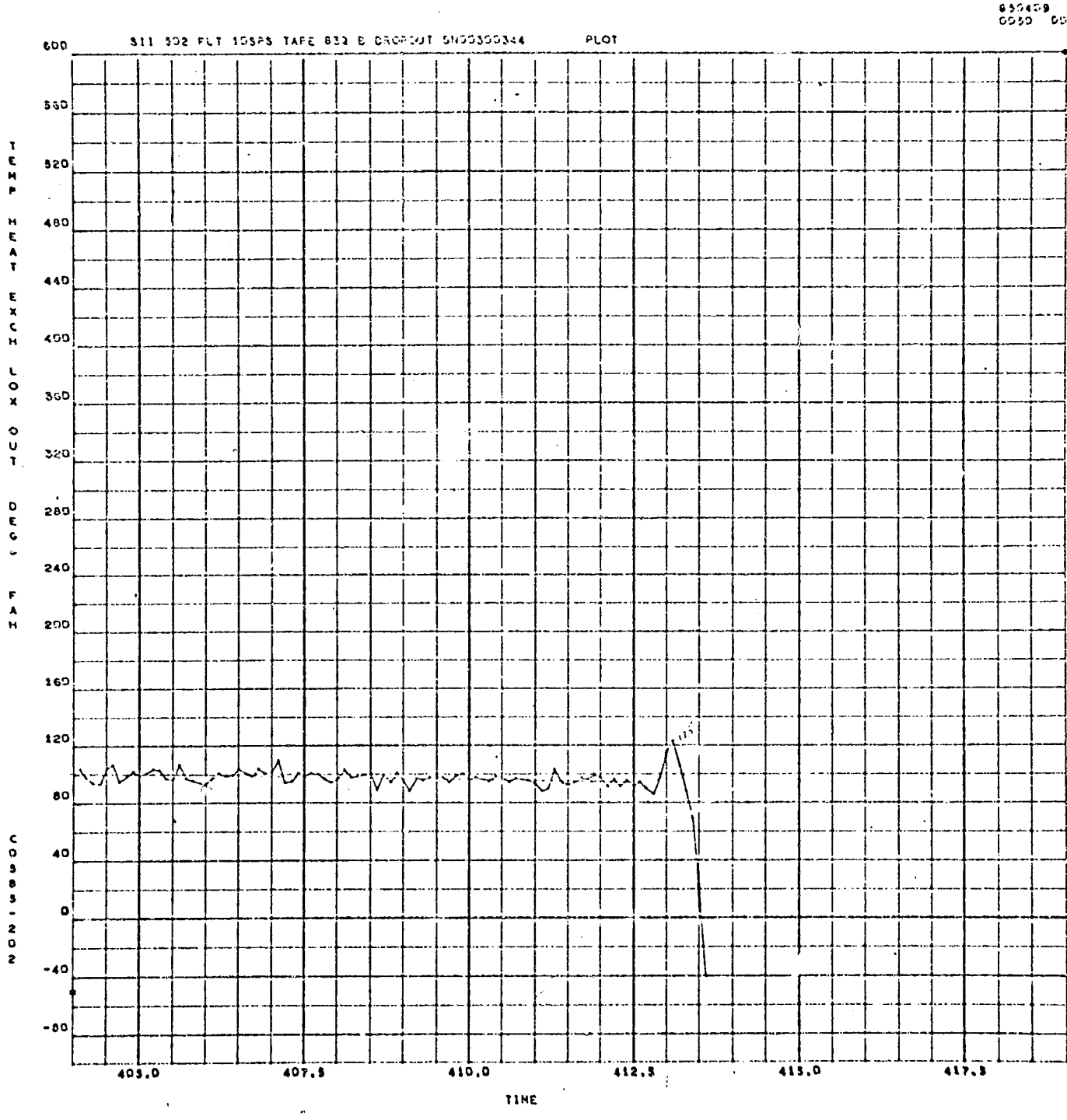

Figure 114. Heat Exchanger Oxidizer Outlet Temperature

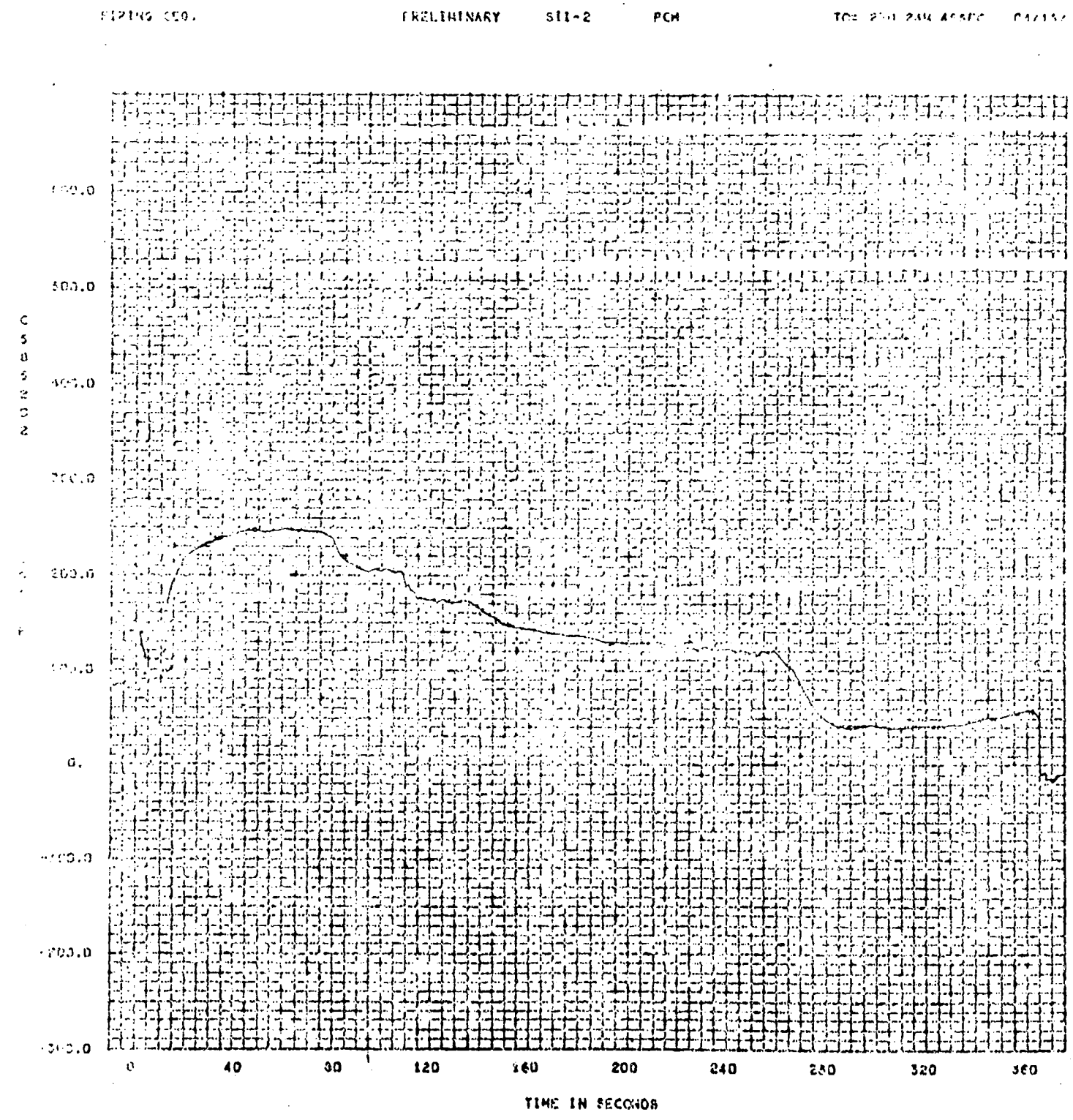

Figure 115. Stage Acceptance Helium Outlet Temperature

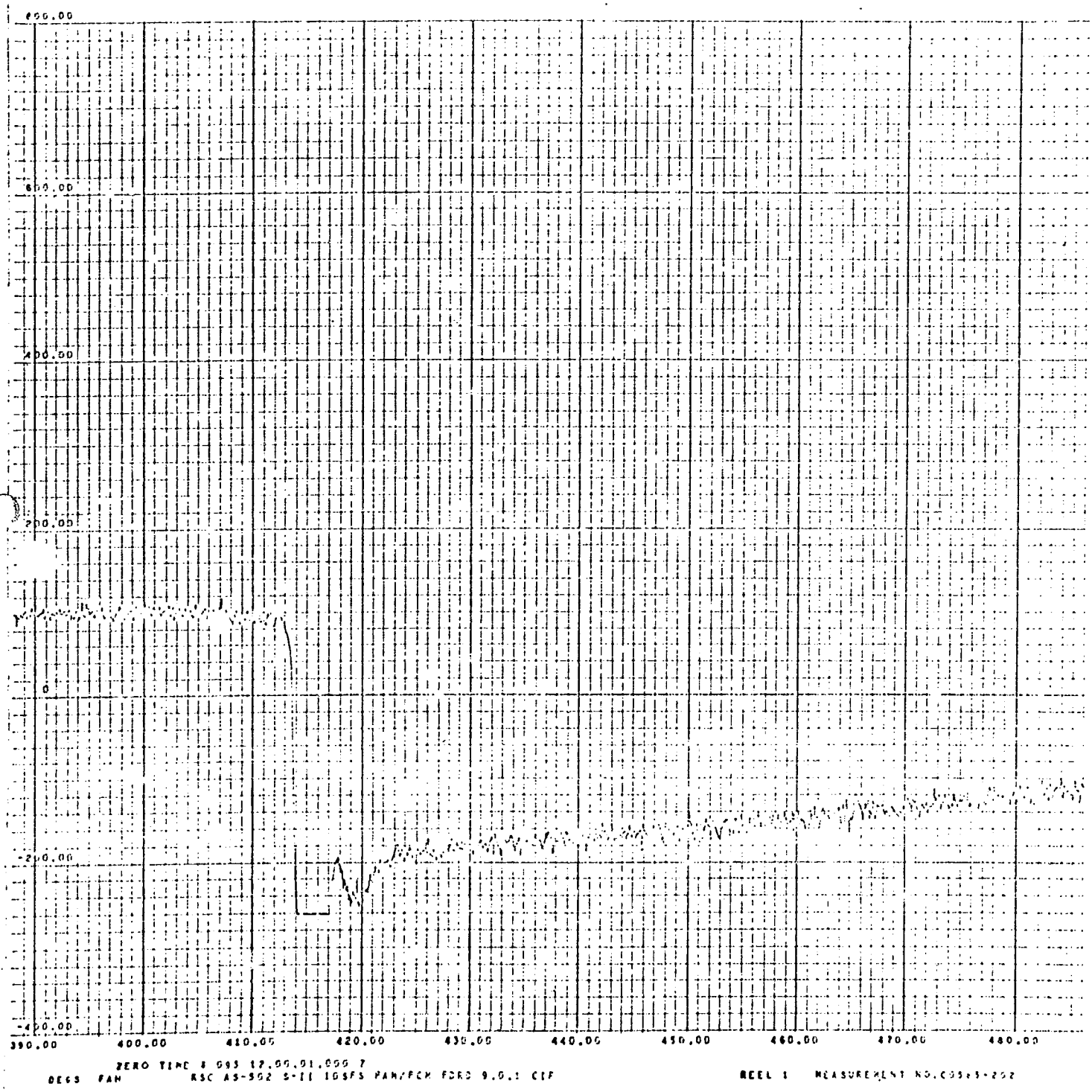

Figure 116. Engine 202 Heat Exchanger Outlet Temperature

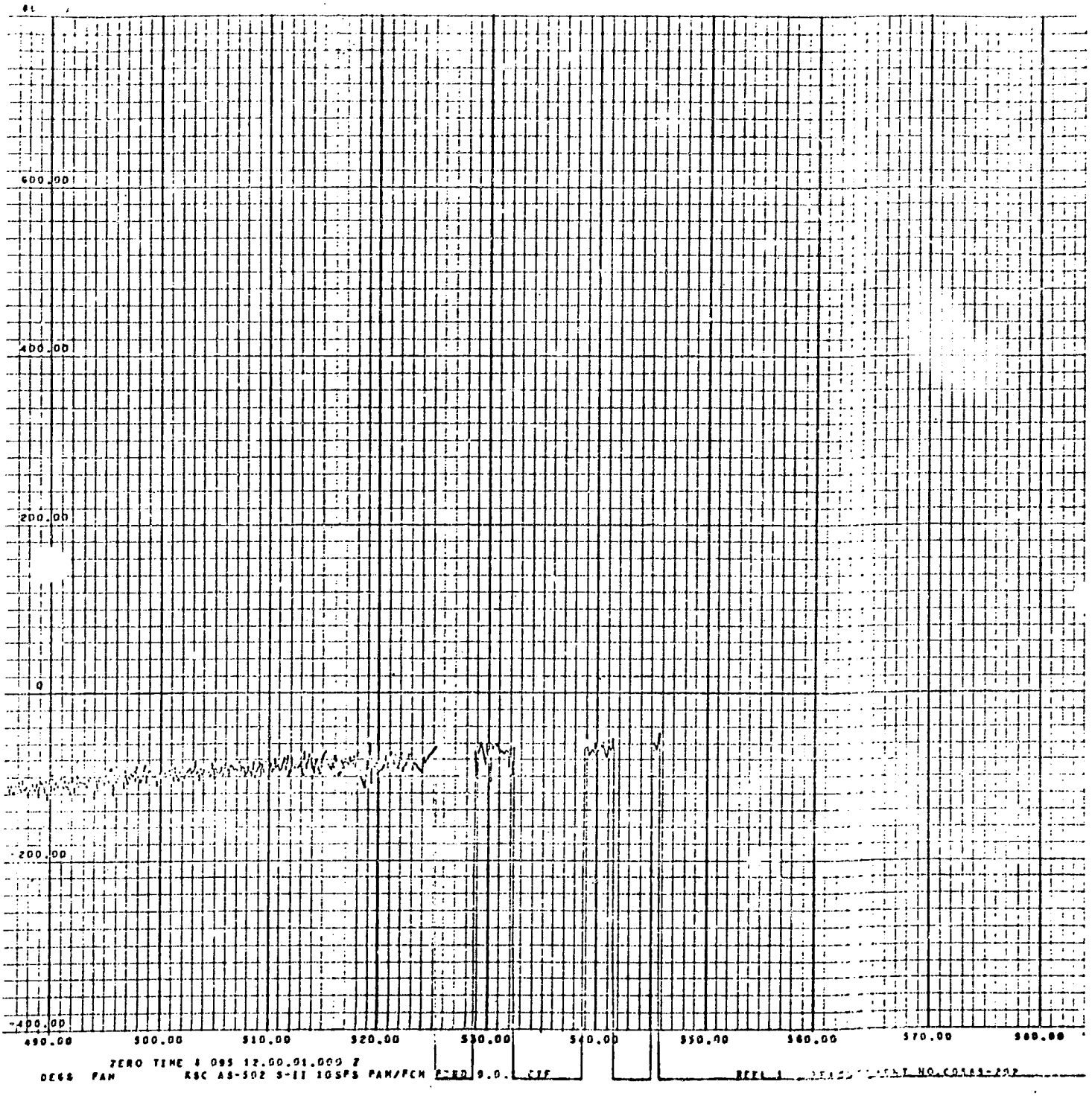

Figure 117. Engine 202 Heat Exchanger Outlet Temperature

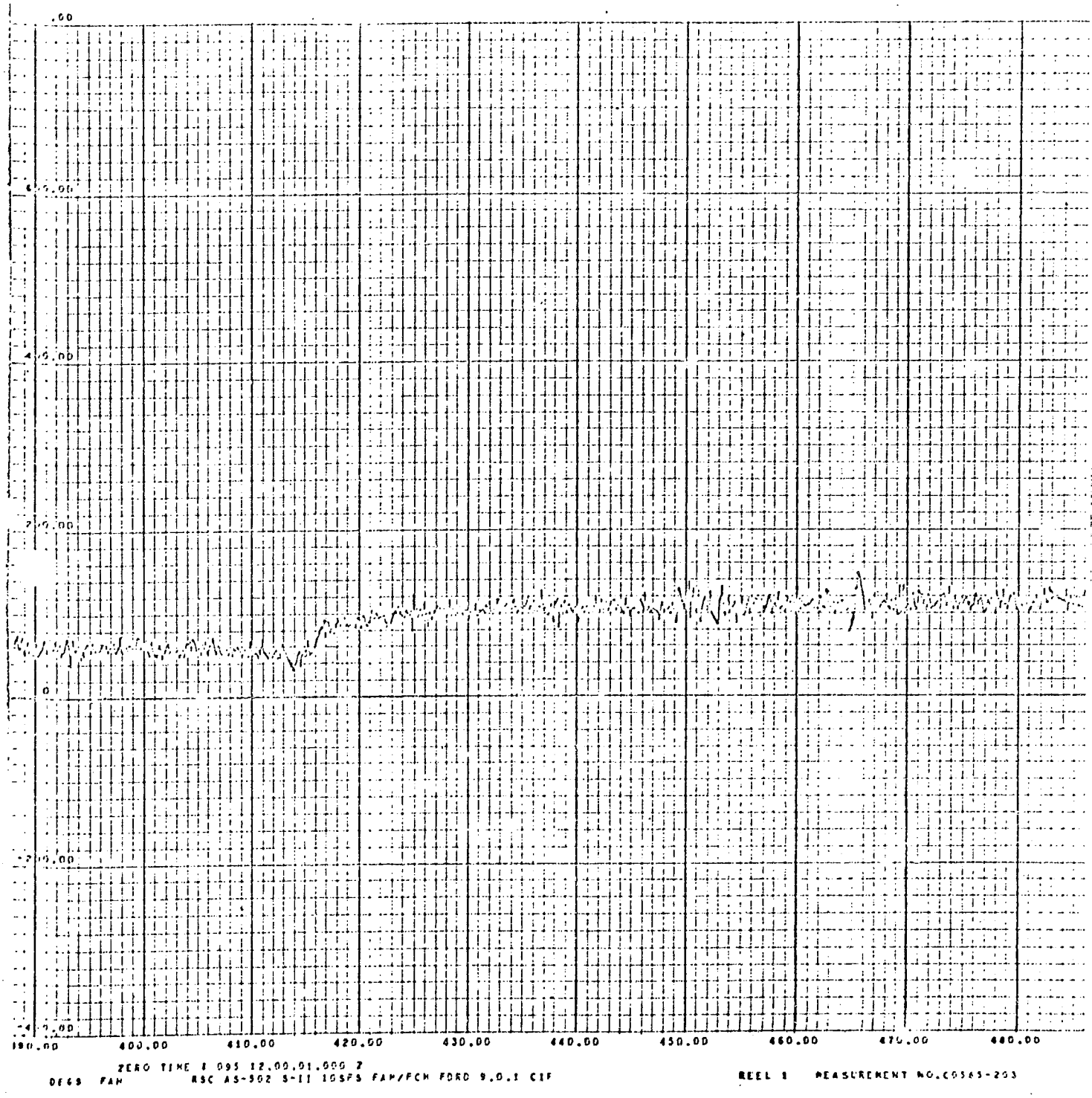

Figure 118. Engine 203 Heat Exchanger Outlet Temperature

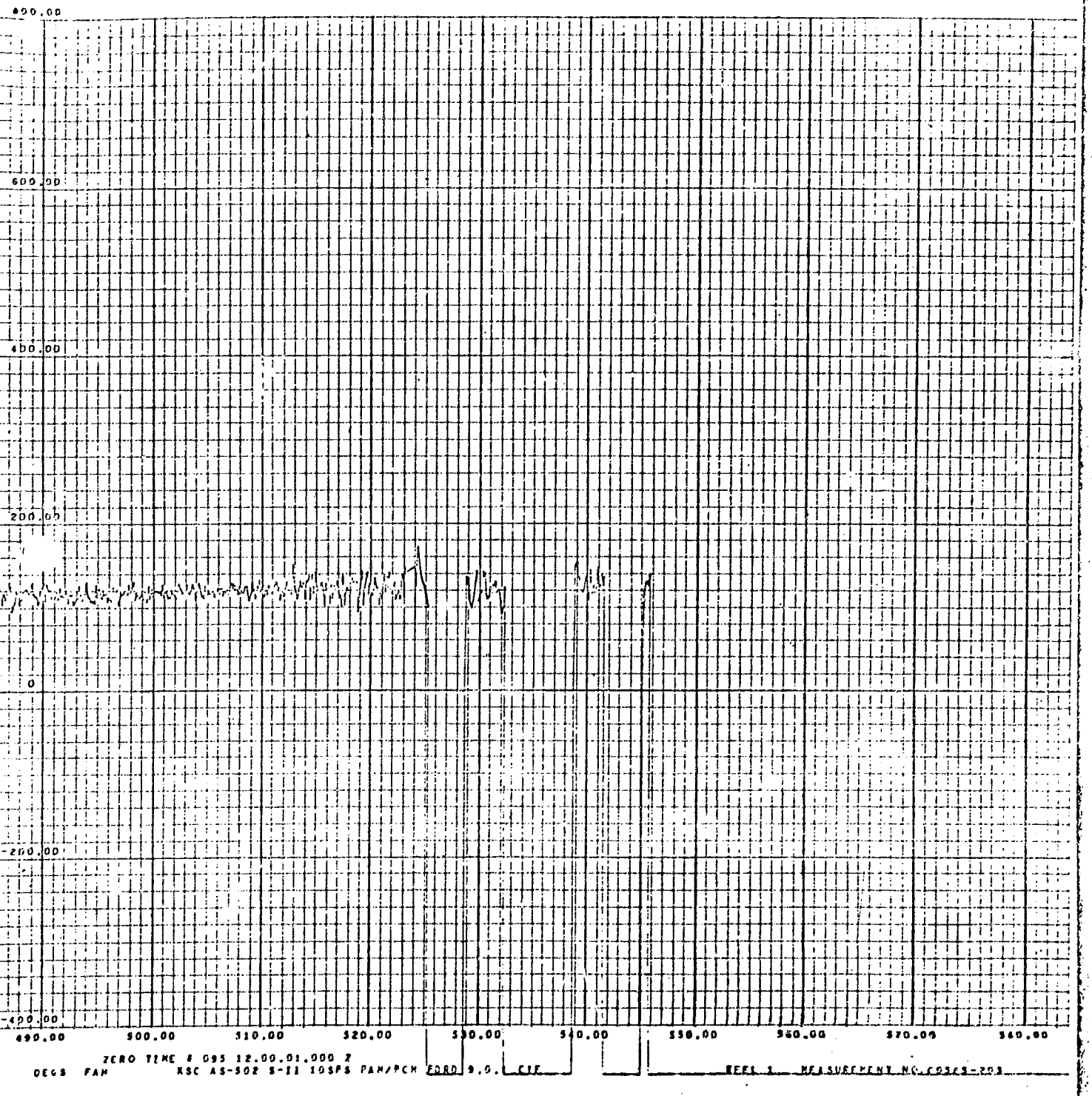

Figure 119. Engine 203 Heat Exchanger Outlet Temperature

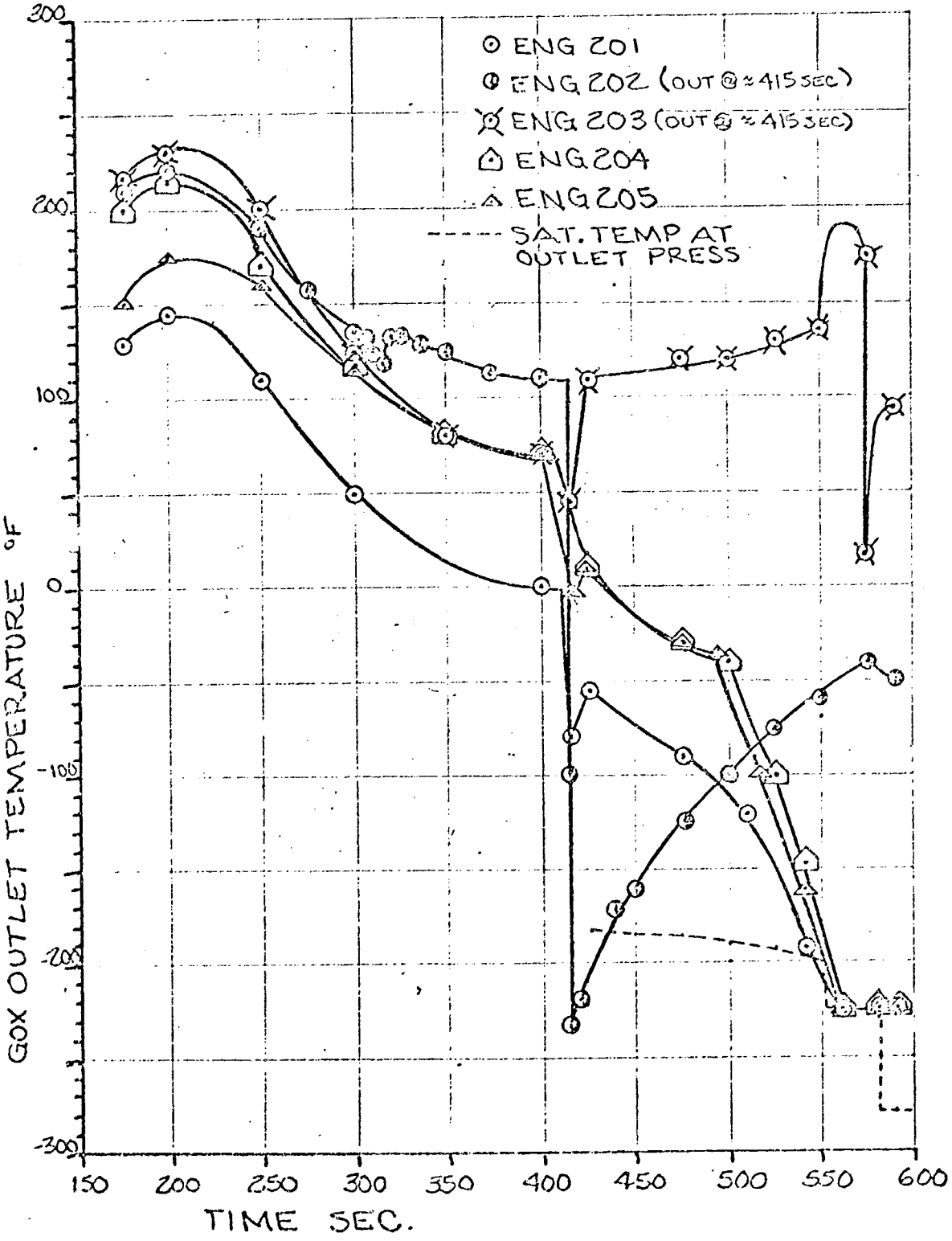

Figure 12C. Flight AS-502 S-II Heat Exchange Data

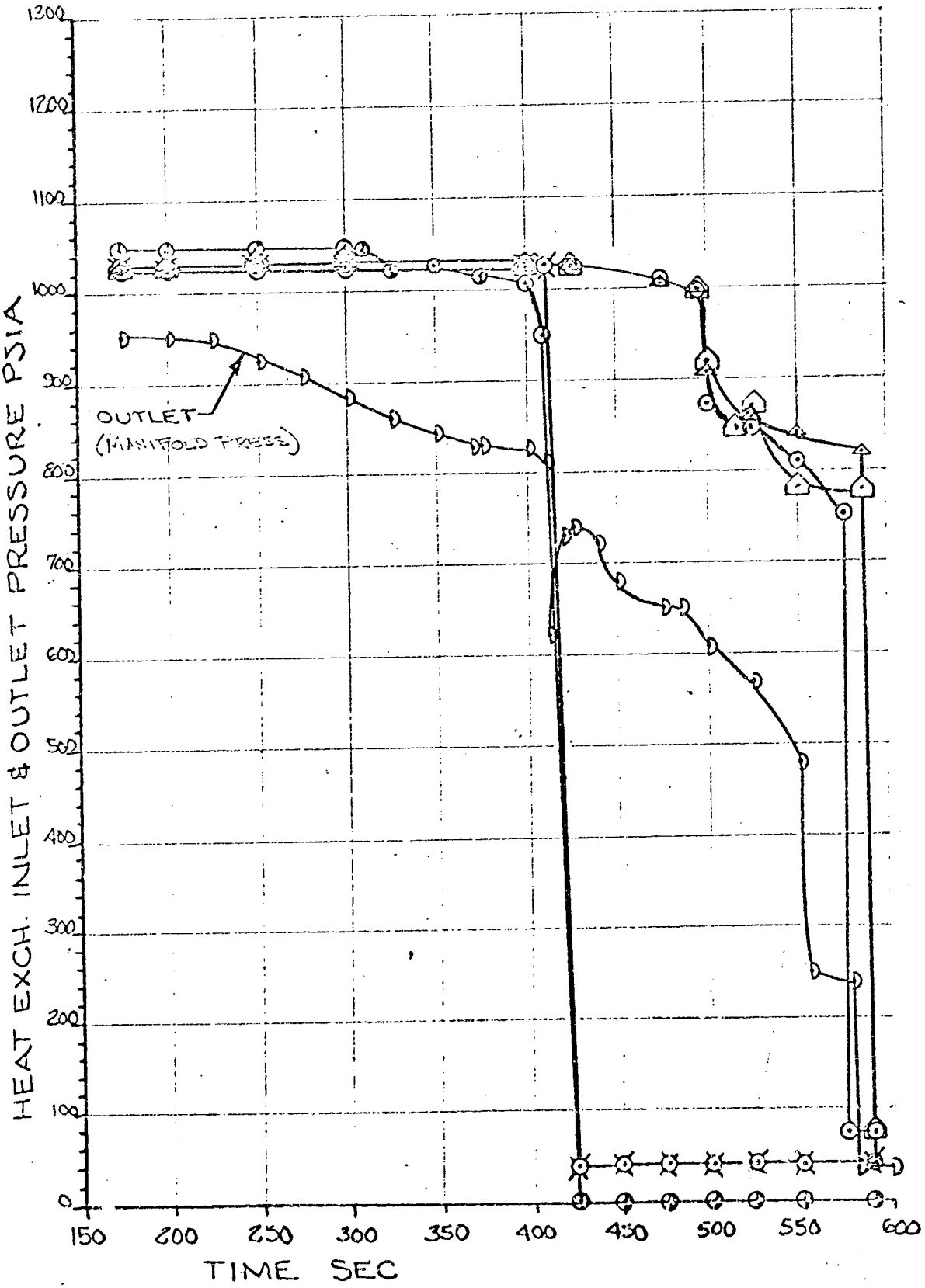

Figure 121. Flight AS-502 S-II Heat Exchange Data

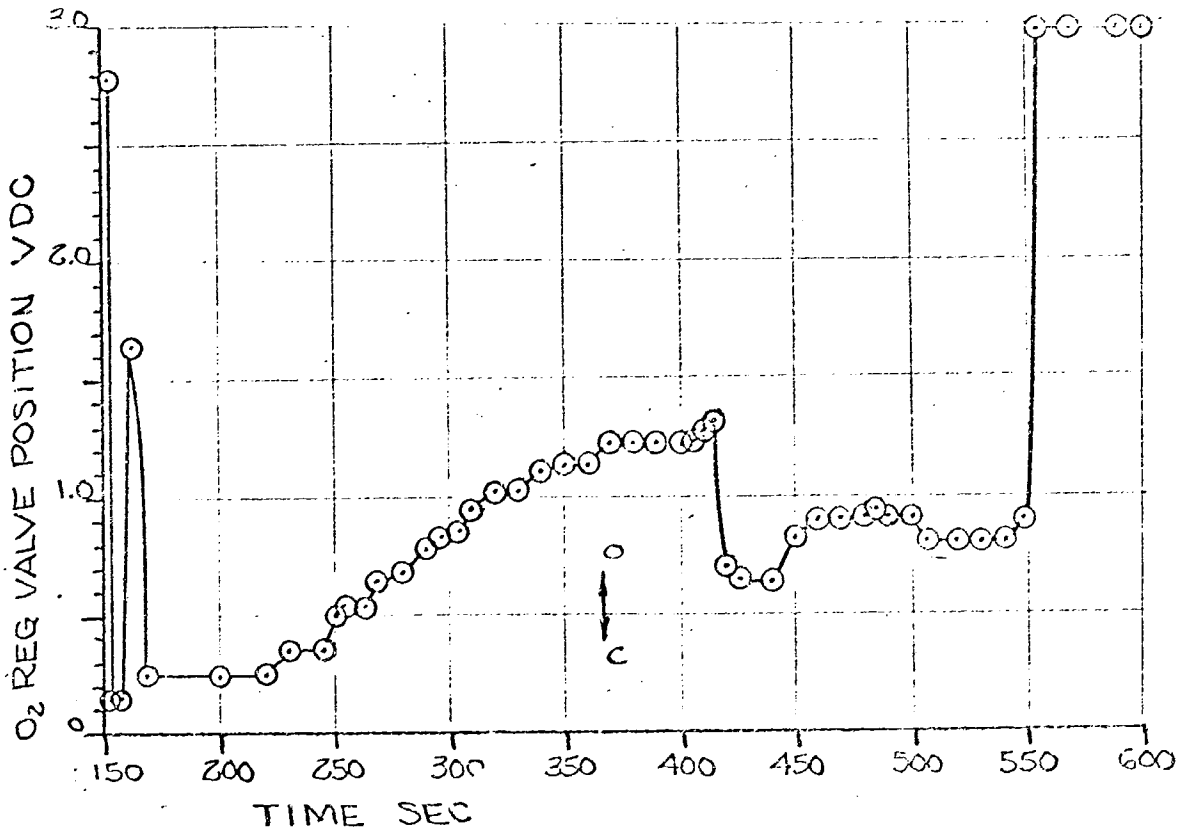

Figure 122. Flight AS-502 S-II Heat Exchange Data

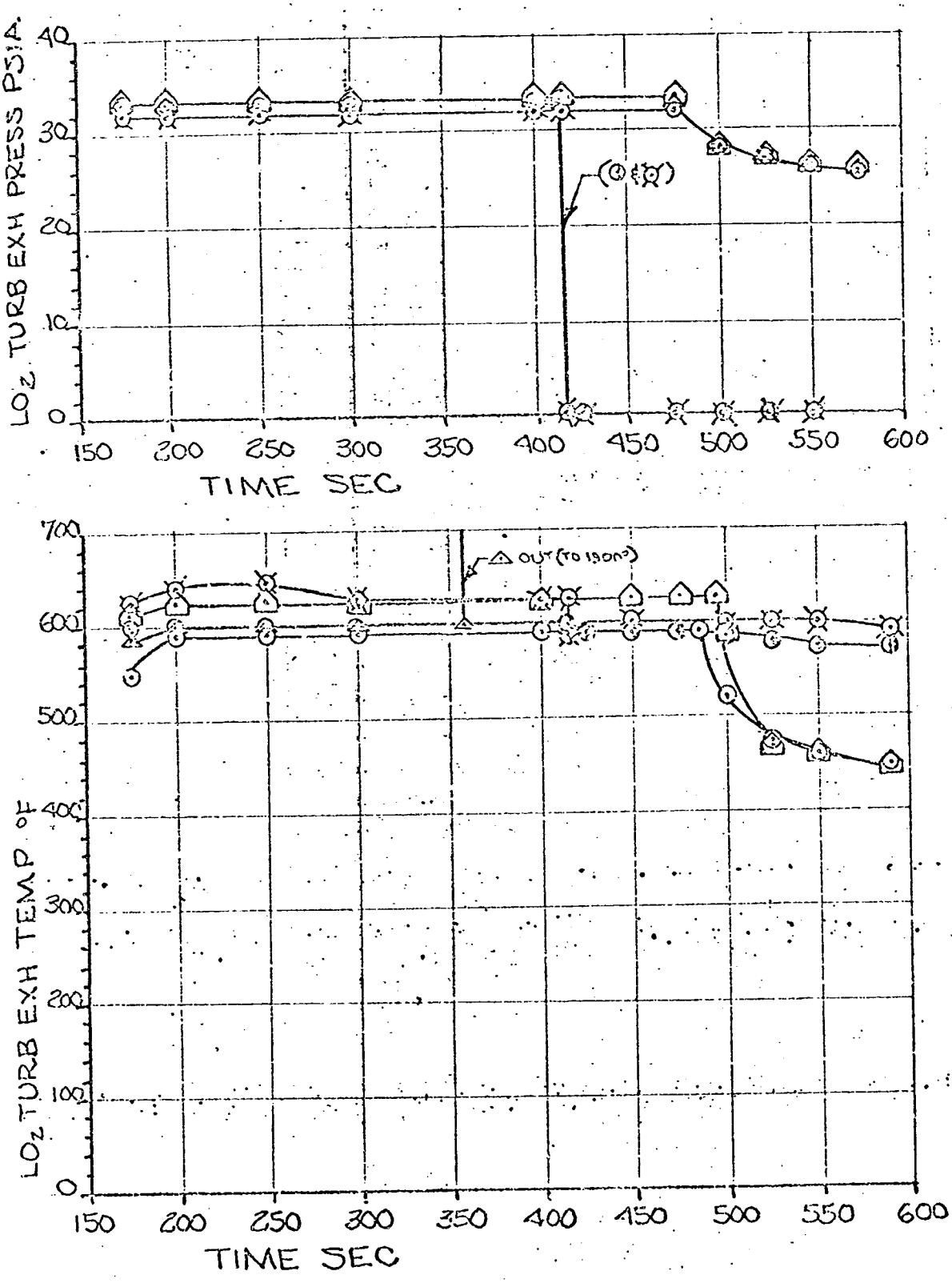

Figure 123. Flight AS-502 S-II Heat Exchange Data

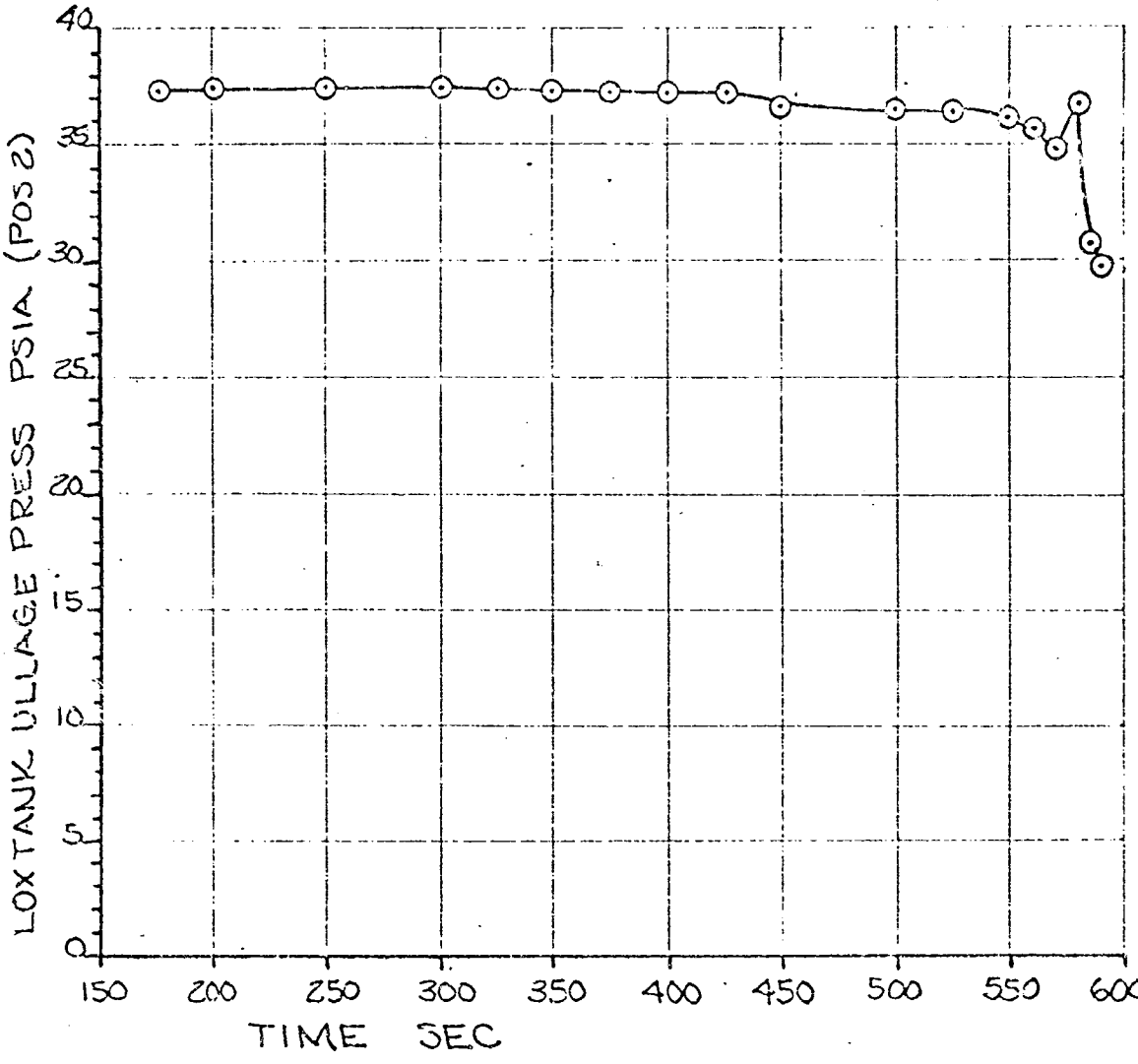

Figure 124. AS-502 S-II Flight Heat Exchanger Data

Hypothesis. Integrity of the engine 202 oxidizer pressurization system was lost during cutoff of the engine; the point in the system at which the integrity loss occurred was between the engine heat exchanger outlet temperature transducer and the stage check valve (stage side of the customer connect panel).

The decrease in heat exchanger outlet temperature to -260 F following cutoff indicates that heat exchanger oxidizer flow continued after the heat source (turbine exhaust) to the exchanger had been removed; the oxidizer flow continued until the heat exchanger antiflood check valve closed (approximately 7 to 17 seconds after engine cutoff when heat exchanger ΔP reached 20 psi). Flow should have stopped almost immediately on cutoff, i.e., when heat exchanger inlet pressure was equal to or less than the stage O_2 manifold pressure. Because loss of heat exchanger outlet line integrity upstream of the heat exchanger outlet temperature transducer would not result in the observed temperature drop (i.e., no oxidizer flow), and loss of line integrity downstream of the stage check valve would result in permanent loss of stage O_2 manifold pressure, it is hypothesized that the integrity loss occurred between the two points.

Corroboration of Hypothesis. Engine 202 heat exchanger outlet temperature decreased to an unusually low temperature at cutoff, indicating continuing oxidizer flow (as compared to the engine 203 cutoff).

The loss of stage O_2 manifold pressure at cutoff of engines 202 and 203 was temporary. The fact that stage O_2 manifold pressure did not recover to the level observed prior to cutoff of engines 202 and 203 is attributed to increased heat exchanger oxidizer flow (decreased heat exchanger outlet temperature) of the three engines remaining in operation.

Main Battery Current and Main D-C Bus Voltage Spikes:
412.8 Seconds Range Time

Description of Event. At range time 412.8 seconds, main battery current (stage) spiked up from a level of 55 amperes to 86 amperes. Main d-c bus voltage (stage) spiked down from a level of 29.3 to 28.7 volts.

Hypothesis. The current/voltage spikes observed in the flight data indicate a momentary short circuit, probably resulting from a fire or insulation breakdown. No evidence can be found to indicate abnormal operation of any electrical equipment operating on the main battery at this time.

Corroboration of Hypothesis. Drawing of excessive amperage from the battery at the 412.8-second time is supported by the associated drop in main d-c bus voltage (Fig.125 and 126), and is typical of short circuit or insulation breakdown conditions. The possibility of an engine compartment fire as the cause of a momentary short circuit at approximately the same range time as the current/voltage spike anomalies is supported by environmental data.

Engine 202 Propellant Utilization Valve Opens and Closes Following Cutoff: 418 Seconds Range Time

Description of Event. At approximately 418 seconds range time, the engine 202 propellant utilization valve opened 6 degrees and then reclosed. Analysis of flight data revealed that all S-II engine PU valves had exhibited the same anomaly. There were no engine performance changes, engine compartment environmental changes, or supporting system anomalies at this time that would contribute to, or result from, the anomalous PU valve operation. Figure 127 illustrates typical PU valve position traces for S-II engine during AS-501 and AS-502 flights. Burn time for engines 201, 204, and 205 was longer during the AS-502 flight than during AS-501; therefore, the PU valves remained closed for a longer duration.

Conclusions. The sudden change in vehicle velocity/attitude which occurred at cutoff of S-II engines 202 and 203 resulted in sloshing of propellants within the S-II tanks. Propellant tank liquid level sensors signalled the PU computer to open the engine PU valves and, when the sloshing damped out or ceased, signalled the PU computer to reclose the valves.

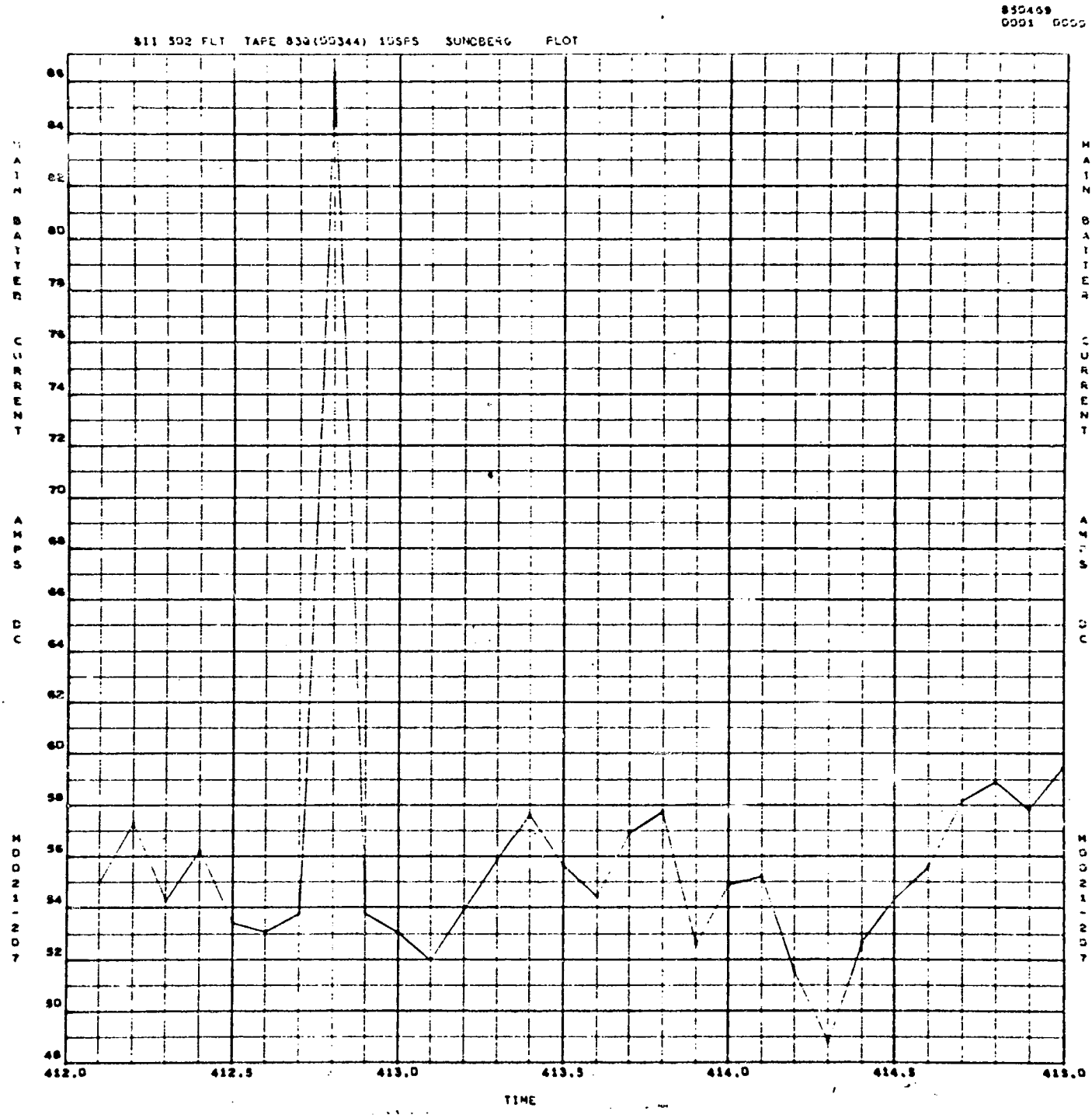

Figure 125. Main D-C Battery Current

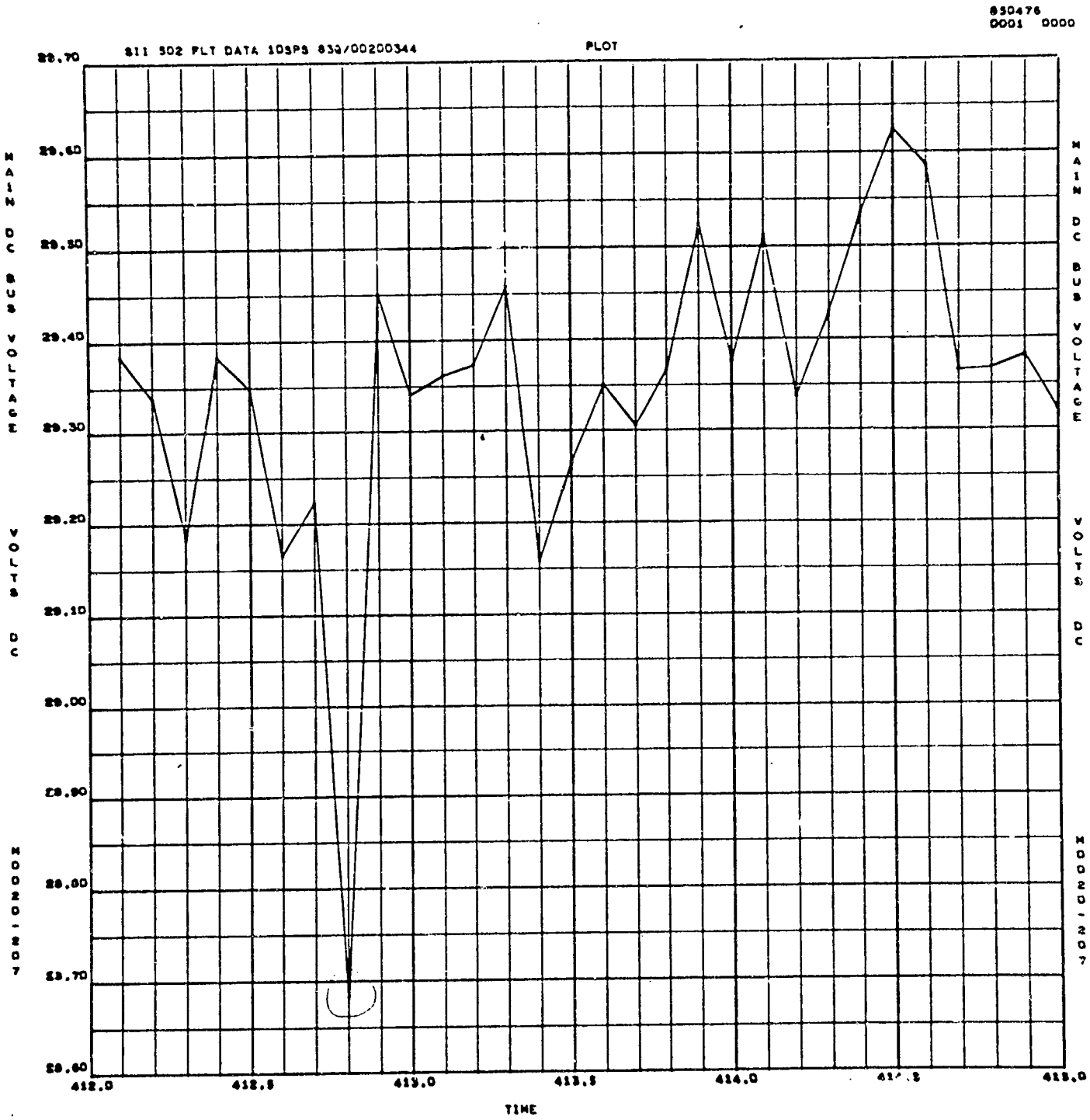

Figure 126. Main D-C Bus Voltage

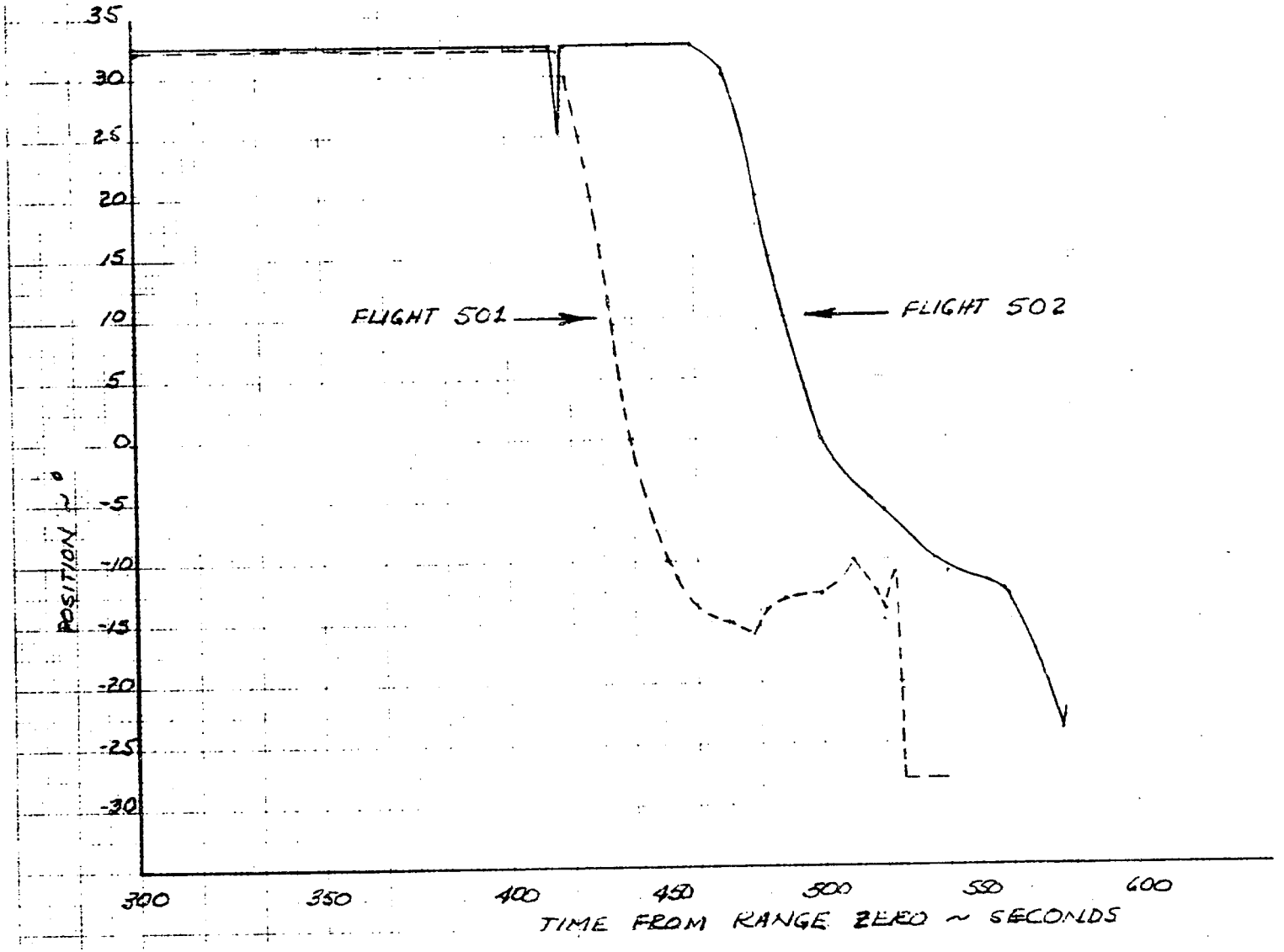

Figure 127. S-II Propellant Utilization Valve Position
(Typical of the Five Engines)

Corroboration of Conclusions. The PU computer error signal corroborates excursion of PU valves at 418 seconds. Figure 128 illustrates engine 202 PU valve error signal (net error signal) at 418 seconds. No performance shift was observed for the three S-II engines remaining in operation at this time because the PU valve has a 14-degree overlap in the closed position.

Engine 202: Loss of Hydraulic Fluid From the Engine Actuation System Following Cutoff

Description of Event. Approximately 5.5 seconds following cutoff of engine 202, data indicated loss of hydraulic fluid from the engine actuation system as follows:

1. Sudden loss of hydraulic reservoir pressure, i.e., 170 psi/sec as compared to 5 psi/sec normal pressure decay following engine cutoff (Fig. 129).
2. Sudden decrease in reservoir volume (percent of capacity) from 10 to 0 percent in 0.5 second, as opposed to a normal increase to 75 percent approximately 60 seconds after cutoff as a result of reservoir filling from the accumulator (Fig. 130).

Conclusions. Loss of engine 202 engine actuation system hydraulic fluid occurred following engine cutoff; the hydraulic fluid loss resulted from leakage at the low-pressure side of one or both actuators. The cause of the leakage is indeterminate.

Corroboration of Conclusions. The engine 202 accumulator pressure decay rate following engine cutoff was approximately 30 percent slower than anticipated. This reduction in decay rate indicates that fluid was not leaking at the high-pressure line between the accumulator and actuators, but rather at the low-pressure side; the decay rate further indicates that

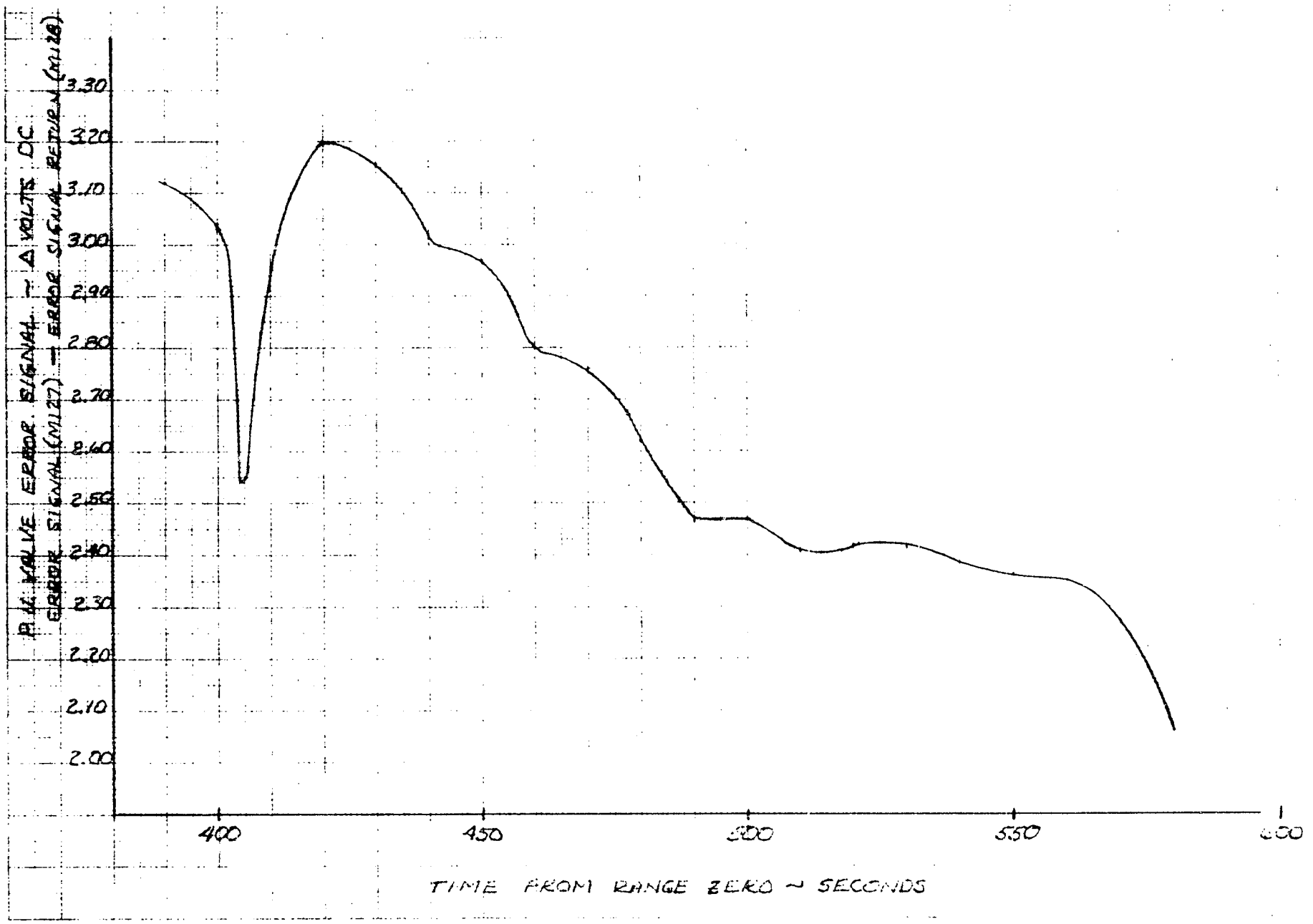

Figure 128. Propellant Utilization Valve Error Signal, Engine 202

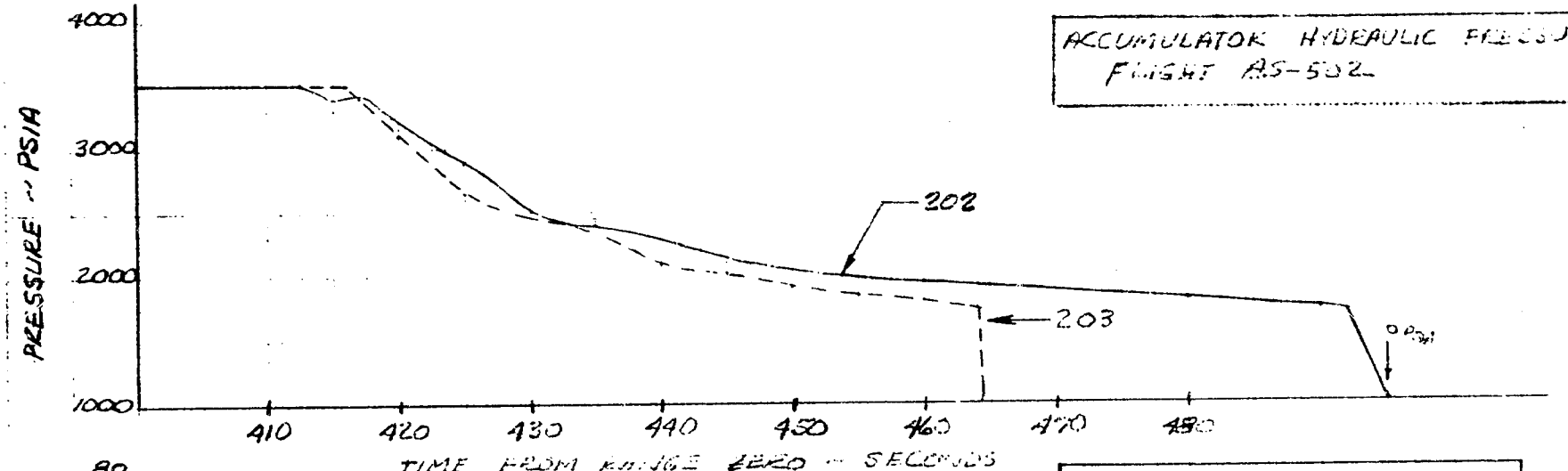

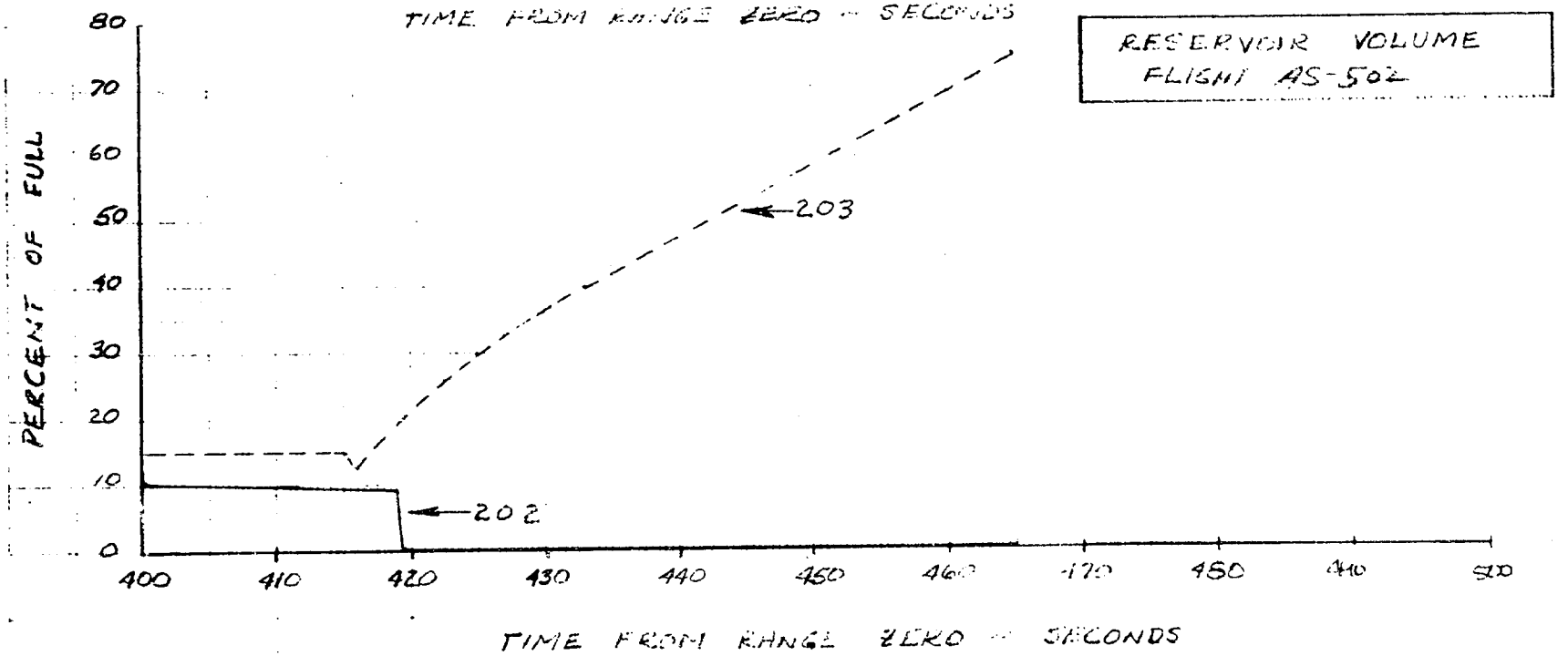

Figure 129. Accumulator Hydraulic Pressure and Reservoir Volume, Engines 202 and 203

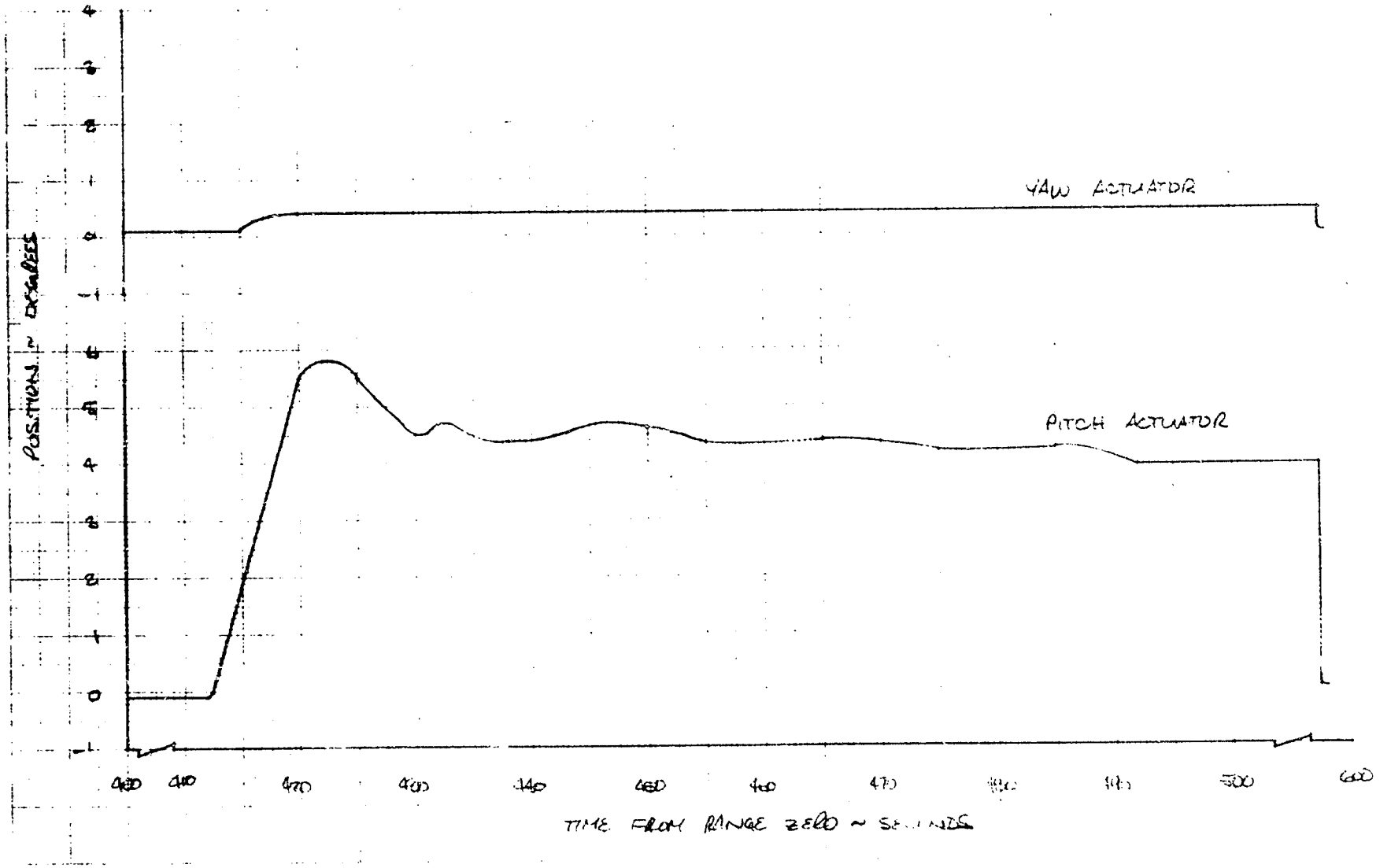

Figure 130. Actuator Position, Engine 202

viscosity of the hydraulic fluid had been increased by chilling of the hydraulic system, beginning at approximately 260 seconds range time. The accumulator bleeds down to the hydraulic fluid reservoir through the actuator servovalves at a very low rate (approximately 0.2 gpm), and any change in fluid viscosity will inversely affect the bleed rate.

The severity of hydraulic system chilling is indicated by hydraulic lockup of the engine 202 yaw actuator at approximately 3200-psia accumulator pressure (415 seconds range time). The lockup function is performed by a differential pressure valve, connected across the actuator cylinder volumes, which is actuated whenever the Δ P across the actuator falls between 1300 and 1700 psi. The lockup condition was achieved with 3400 psia at the high-pressure side, thus indicating that the low-pressure side had experienced higher than normal pressure because of increased fluid viscosity.

The engine 202 yaw actuator had indicated chilling conditions at 282 seconds range time, as evidenced by erratic behavior of the Δ P transducer, a hypothesis that has since been verified by laboratory testing of the transducer at the Space Division of North American Rockwell Corporation, Seal Beach, California.

Yaw actuator lockup was indicated by lack of change in actuator position despite application of a signal commanding position change. Pitch actuator lockup occurred at 490 seconds range time; accumulator pressure was 1700 psia, indicating a normal lockup sequence (Fig. 129 and 130).

ENGINE 203 CUTOFF: RANGE TIME 414.2 SECOND

Description of Event

Operation of engine 203 (S-II cluster position No. 3, engine S/N J2058) was prematurely terminated at 414.277 seconds range time, following cutoff of engine 202.

Engine Anomalies. No anomalies were noted in operation of engine 203 which would result in cutoff.

Supporting System Anomalies. Analysis of flight data related to cutoff of engines 202 and 203 indicates that events occurred in the following abnormal sequence:

1. Engine 202 cutoff
2. Engine 203 oxidizer prevalve started closed
3. Engine 202 fuel prevalve started closed
4. Engine 203 oxidizer prevalve reached closed position
5. Engine 202 fuel prevalve reached closed position
6. Engine 203 cutoff, initiated by dropout of mainstage OK pressure switches upon decay of oxidizer injection pressure
7. Engine 202 oxidizer prevalve started closed
8. Engine 203 fuel prevalve started closed
9. Engine 202 oxidizer prevalve reached closed position
10. Engine 203 fuel prevalve reached closed position

Conclusions

Control exercised over closing of the engine 203 oxidizer prevalve following engine 203 cutoff should have been applied to the engine 202 oxidizer prevalve; control exercised over closing of the engine 202 oxidizer prevalve following engine 203 cutoff should have been applied to the engine 203 oxidizer prevalve; therefore, engine 203 cutoff resulted from an oxidizer prevalve closing signal originating in the engine 202 prevalve control circuit, i.e., crossed prevalve control commands.

ENGINES 201, 204, AND 205: PERFORMANCE SHIFT FOLLOWING CUTOFF OF ENGINES 202 AND 203

Description of Event

At approximately 415 seconds range time, the majority of instrumentation parameters for the three S-II engines (201, 204, and 205) remaining in operation at that time shifted.

Hypothesis

Electrical problem; it is believed that cutoff of engines 202 and 203 reduced the main battery load, causing a change in telemetry ground currents and shifting the telemetry system power level.

Corroboration of Hypothesis

Data indicated that shifts occurred simultaneously for engines 201, 204, and 205. It is unlikely that simultaneous shifting of performance would occur in three engines at the same time.

The performance shifts occurred in such independent parameters as helium regulator out pressures, helium tank pressures and temperatures, and start tank pressures and temperatures. Instrumentation parameters indicating shifts, and the magnitude of the shifts for engines 201, 204, and 205, are listed in Table 9.

TABLE 9

S-II ENGINES 201, 204, AND 205 APPARENT
PERFORMANCE SHIFTS AT 415 SECONDS

Instrumentation Parameter	S-II Engine		
	201	204	205
Oxidizer Pump Inlet Temperature, F	-0.13	-0.07	-0.13
Oxidizer Pump Discharge Temperature, F	-0.07	-0.18	-0.14
Fuel Pump Inlet Temperature, F	-0.03	-0.09	-0.05
Fuel Pump Discharge Temperature, F	-0.06	-0.06	-0.08
Main Fuel Injection Temperature, F	-4.5	-0.3	+3.3
Start Tank Gas Temperature, F	-0.1	-1.2	-0.7
Helium Tank Gas Temperature, F	-0.9	-0.1	-1.5
Thrust Chamber Jacket Temperature, F	-3.0	-2.4	-8.1
Oxidizer Pump Bearing Temperature, F	+0.1	-0.2	-0.1
Electrical Control Assembly Temperature, F	-1.1	-1.0	-1.6
Auxiliary Instrumentation Package Temperature, F	+1.7	+1.0	+3.8
Primary Instrumentation Package Temperature, F	-0.6	+0.3	-1.0
Oxidizer Pump Inlet Pressure, psi	-2.75	-3.70	-3.25
Oxidizer Pump Discharge Pressure, psi	-4.3	-13.2	-10.2
Fuel Pump Inlet Pressure, psi	+0.19	-0.49	
Fuel Pump Discharge Pressure, psi	-7.4	-6.4	-10.3
Main Oxidizer Injection Pressure, psi	+1.1	-11.6	-9.8
Main Fuel Injection Pressure, psi	+2.3	-5.7	-4.3
Thrust Chamber Pressure, psi	-1.5	-5.7	-2.8
Gas Generator Chamber Pressure, psi	+0.8	+2.7	-3.8
Start Tank Pressure, psi	-0.2	-6.3	-2.1
Helium Tank Pressure, psi	-11.4	-19.8	-21.4
Engine Regulator Outlet Pressure, psi	-1.6	-4.3	-4.9
Fuel Turbine Inlet Temperature, F	+3.2		
Oxidizer Turbine Inlet Temperature, F	-4.3	-7.0	-8.8
Main Oxidizer Flow, gpm	-11.0	-5.8	-7.0
Main Fuel Flow, gpm	-0.1	-3.4	-7.5
Oxidizer Pump Speed, rpm	-15.1	+2.7	-3.1
Fuel Pump Speed, rpm	-31.9	-19.5	-34.7

ANOMALIES NOT RELATED TO OR NOT CONTRIBUTING TO FLIGHT FAILURE

Engine 202 anomalies discussed in this section are either unrelated to the AS-502 S-II flight failure or are of a minor nature not contributory to the failure.

ENGINE 202 PERFORMANCE SHIFT: RANGE TIME 215 SECONDS

Description of Event

At 215 seconds range time, engine 202 experienced a performance shift characterized by a thrust increase of approximately 900 pounds followed by a decrease to the preshift value. There were no discernible engine compartment or supporting equipment anomalies at this time.

Conclusions

Through review and analysis of data, it is concluded that:

1. There were two performance shifts, i.e., one at approximately 218 seconds and one at approximately 226 seconds, as reflected in main chamber pressure.
2. Performance (P_c) returned to its preshift value following each shift.
3. The shifts resulted from minor gas generator oxidizer bootstrap line ΔP shifts.
4. No correlation has been established between these performance shifts and subsequent anomalies.

Corroboration of Conclusions

Possible causes of the performance shifts investigated and results of analysis are as follows:

1. Pump inlet pressure change: none occurred
2. Pump inlet density shift: none occurred
3. Hydraulic pump horsepower change: none occurred; no gimbaling at this time
4. ASI fuel line failure
5. ASI oxidizer line failure
6. Fuel pressurization line failure
7. Gas generator oxidizer bootstrap line ΔP shift

} Unlikely; performance returned to original value. Many values would shift in wrong direction.

Table 10 presents shifts in selected engine parameters between 215 and 219 seconds range time in comparison to parametric shifts normally associated with gas generator oxidizer bootstrap ΔP shift. It may be seen that the flight shifts are in the direction of the bootstrap line ΔP shift, but of lower magnitude, indicating a minor ΔP shift condition as the causative factor.

ENGINE 202 GAS GENERATOR OXIDIZER INJECTION PRESSURE DECAY: RANGE TIME 350 SECONDS

Description of Event

Starting at 350 seconds range time, gas generator oxidizer injection pressure began to decay from 760 psia. All other engine parameters continued at the 350-second levels. By 412.6 seconds range time, gas generator oxidizer injection pressure had decayed to 390 psia. At 412.7 seconds, gas generator oxidizer injection pressure spiked to 590 psia, and then decayed

TABLE 10

S-II, ENGINE J2044 CHAMBER PRESSURE SHIFT AT 215 SECONDS

	Value at 215 Seconds	Shift at 225 Seconds	Oxidizer Bootstrap Line ΔP Shift	Shift 215 to 219 Seconds
Temperatures				
Fuel Pump Discharge	-409 F	0	0	0
Oxidizer Pump Discharge	-291.2 F	0	0	0
Fuel Turbine Inlet	1190 F	+1	+29	+3
Oxidizer Turbine Inlet	785 F	+2	+22	+2
Gas Generator Fuel Valve Inlet	-408.6 F	0	0	0
Gas Generator Oxidizer Valve Inlet	-292.8 F	0	0	0
Main Fuel Injection	200 R	0	0	0
Oxidizer Turbine Outlet	610 F	+2	0	+1
Thrust Chamber Jacket	-328 F	0	0	0
Heat Exchanger Outlet	220 F	0	0	0
Engine Inlet Oxidizer	-296 F	0	0	
Engine Inlet Fuel	-422.4 F	0	0	
Pressures				
Main Fuel Injection	850	+3	+10	+5
Gas Generator Fuel Injection	730	+4	+11	+5
Fuel Pump Balance Piston Cavity	500	0	+	
Fuel Pump Discharge	1224	+6	+16	+7
Main Oxidizer Injection	943	+4	+12	+5
Gas Generator Oxidizer Injection	765	+3	+12	+3
Oxidizer Turbine Inlet	840	+0.2	+	+0.1
Oxidizer Pump Bearing Coolant			+	
Oxidizer Turbine Outlet	33	0	0	0
Oxidizer Pump Discharge	1071	-1	+14	+
Thrust Chamber	759	+1	+9	+
Gas Generator Chamber	635	+0	+9	
Heat Exchanger Inlet			+	+
Engine Inlet Oxidizer	424	0	0	0
Engine Inlet Fuel	28.5	0	0	0
PU Valve Inlet			+	+
PU Valve Outlet	185	0		
Oxidizer Pump Primary Seal	17		+0.6	0
Fuel Tank Ullage			0	0
Fuel Ullage			0	0
Fuel Pump Interstage	167	0	+	+
Flowmeters				
Main Fuel Flow, gpm	8368	-2	+	0
Main Oxidizer Flow, gpm	2878	+3	+	0

during the cutoff transient (Fig. 131). During the period in question, engine compartment and engine component temperatures indicated cooling in the area of Engine 202.

Hypotheses

Decay of gas generator oxidizer injection pressure resulted from plugging of the gas generator oxidizer injection pressure line, probably with solid oxygen, between the gas generator oxidizer injection manifold port and the tee to the gas generator oxidizer injection pressure transducer. Continued pressure decay resulted from leakage past the gas generator oxidizer purge check valve or from continued cryogenic chilling of the gas generator oxidizer injection pressure line.

Corroboration of Hypotheses

Engine compartment, and engine and stage component environmental data indicate cryogenic chilling in the area of Engine 202. This chilling could result in freezing of oxygen in the instrumentation line when the line was chilled to -340 F. The gas generator valve position potentiometer indicates valve closure of 4 percent; this apparent motion is probably due to cryogenic chilling of the gas generator valve body, with the same cryogenic chilling source impinging on the gas generator oxidizer injection pressure line. The pressure recovery noted is probably due to heating in the engine area at cutoff, melting the plug sufficiently to allow the recovery. Just prior to start of gas generator oxidizer injection pressure decrease, the pressure was 760 psi. Therefore, assuming no decay in manifold pressure at cutoff, the ΔP from P_1 to P_2 is 370 psi.

$$\Delta_{head} = \frac{(370 \text{ psi})(144 \text{ in.}^2/\text{ft}^2)}{(70 \text{ lb/ft}^3)} = 70 \text{ ft}$$

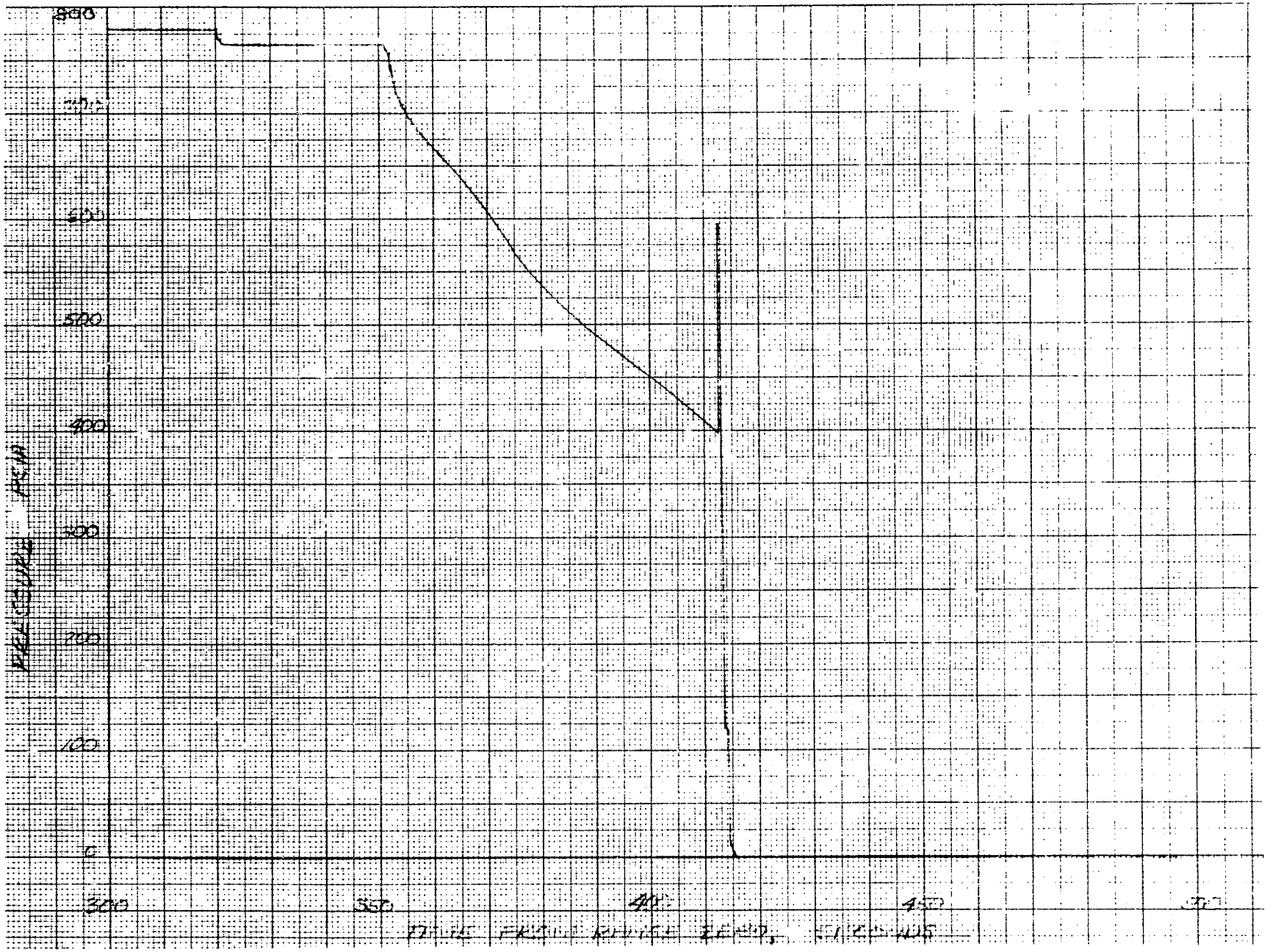

Figure 131. Engine 202 Gas Generator Oxidizer Injection Velocity

By breaking the line into four segments, each with a resistance, the Δ_{head} is $\Delta_{head} = h_1 + h_2 + h_3 + h_4$, where $h = \frac{K^2}{2g}$

$$h = \frac{Kv^2}{2g}$$

Entrance effect $K_1 = 0.50$; 1/16-inch tube $K_2 = f\ (L/D)$

Assuming Re = 105 f = 0.017

$K_2 = 0.136$

Exit effect from 1/16-inch tube

$K_3 = 0.80$

1/4-inch tube $K_4 = 0.017 \left(\frac{10}{0.188}\right) \left(\frac{0.0625}{0.188}\right)^2 = 0.100$

$$\therefore 760 \text{ ft} = \frac{(0.50 + 0.136 + 0.80 + 0.100)v^2}{64.4}$$

$$v^2 = 32 \times 10^4 \text{ ft}^2/\text{sec}^2$$

$$v = 168 \text{ ft/sec}$$

$$\dot{w} = \rho Av$$

$$\dot{w} = (70 \text{ lb/ft}^3)(2.12 \times 10^{-5} \text{ ft}^2)(168 \text{ ft/sec})$$

$$\dot{w} = 0.250 \text{ lb/sec}$$

For a 0.026 lb/sec leak below the gas generator oxidizer orifice, fuel turbine inlet temperature decreases 9.1 F and P_c decreases 2.9 psi.

$$\therefore \Delta_{T_{GG}} = \frac{0.250\ (-9.1)}{0.026} = -87.1 \text{ F}$$

$$\Delta_{P_c} = \frac{0.250\ (-2.9)}{0.026} = -27.8 \text{ psi}$$

Since the above performance shifts were not realized, the indicated ΔP was not due to flow.

Possible cause of the indicated pressure loss is plugging of the instrumentation line, accompanied by slight leakage of the check valve, thus allowing the indicated decay.

APPENDIX A

FLIGHT SUPPORT TESTING

Testing in support of analysis and investigation into AS-502 S-II flight problem areas was conducted on both engine system and component levels at various Rocketdyne facilities and at the NASA-MSFC pressure-fed thrust chamber test stand.

ENGINE SYSTEM TESTING

A combined S-II/S-IVB flight support test program was conducted at the Rocketdyne Santa Susana Field Laboratory, test stand VTS-2, utilizing J-2 R&D engines J004-5 and J-16-4. Three of the tests conducted were related to analysis of the S-II, Engine 202 anomalies, and are described in the following paragraphs.

Test 313-035 (Engine J004-5)

The primary objective of this test was to simulate partial failure of the ASI fuel line, followed by complete failure of the line; i.e., two-stage failure mode. (Figure A-1 is a schematic presentation of the test setup.)

An initial ASI fuel line leakage rate of 0.5 lb/sec was simulated; no significant change in engine performance was noted. Complete failure of the ASI fuel line was simulated by opening an overboard vent at the thrust chamber manifold and closing the ASI fuel valve. At the same time, the simulated leakage rate at the downstream vent between the ASI fuel line downstream flex section and the ASI injector was increased. This resulted in failure of the tee fitting at the downstream vent due to combustion of residual fuel in the ASI fuel line; overboard flow of ASI combustion products occurred at the failed tee, but no damage resulted from the fire because of the relatively cool temperature of the combustion products (estimated at 300 to 500 F). No significant injector loss was noted. Slight erosion of the ASI nozzle was noted; however, erosion penetration of the injector fuel manifold did not occur.

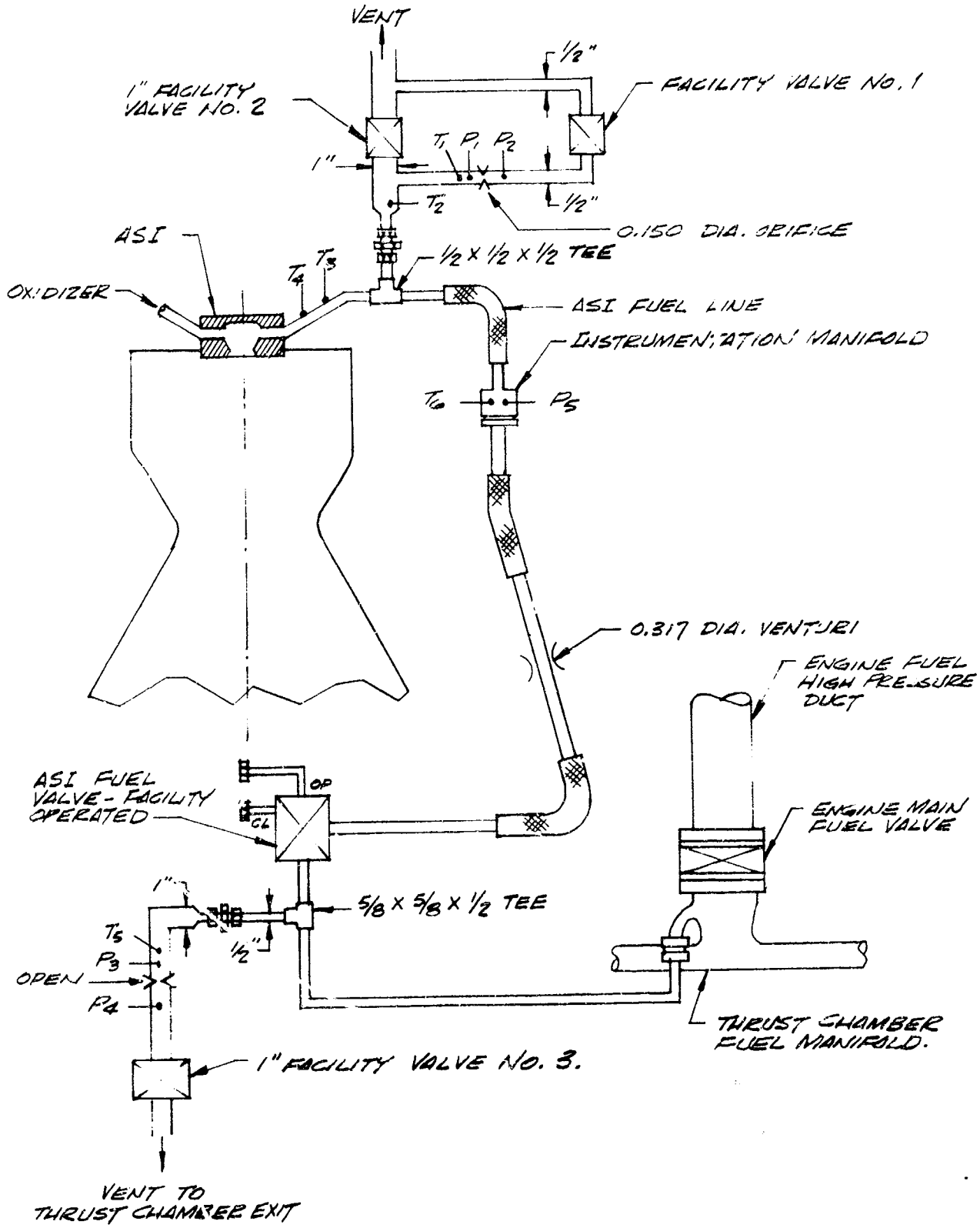

Figure A-1. Engine Configuration ASI Fuel Line Evaluation (Test 313-035)

Test 313-036 (Engine J004-5)

The primary objective of this test was to simulate an initial partial failure of the ASI fuel line, progressing to complete failure of the line. Figure A-2 presents a graphic illustration of the test setup. Leakage was simulated in the ASI fuel line between the first (upstream) and second flex sections; the leakage rate was increased in such a manner as to obtain a rapid ASI mixture increase. Engine operation continued with an oscillatory flow condition in the ASI fuel line, until the overboard leakage rate was again increased; at this time reverse flow from the ASI through the ASI fuel line was obtained. Posttest hardware inspection revealed that erosion of the ASI cavity and burnthrough into the thrust chamber injector fuel manifold had occurred.

Test 313-041 (Engine J016-4)

The primary objective of this test was to obtain slowly increasing ASI mixture ratio during engine operation, followed by simulated failure of the ASI fuel line. During the test, ASI mixture ratio was slowly increased from 1.8 to 20. ASI erosion commenced at a mixture ratio of 2.5 and continued until after the simulated line failure. Severe ASI nozzle erosion occurred, with burnthrough into the main injector fuel manifold and into two oxidizer elements. Figure A-3 illustrates the test setup.

MSFC THRUST CHAMBER COMPONENT TESTING

ASI/thrust chamber component testing was conducted at MSFC, test position 502, a high-pressure, LOX/LH_2 component test stand. Primary objectives of this testing included determination of the extent of injector damage incurred when operating with abnormal (high) ASI mixture ratio, and determination of the effect of a damaged injector on engine performance.

A series of four tests was conducted (217-1 through 217-4). Two of the tests, 217-2 and 217-4, simulated tests applicable to S-II, intended to

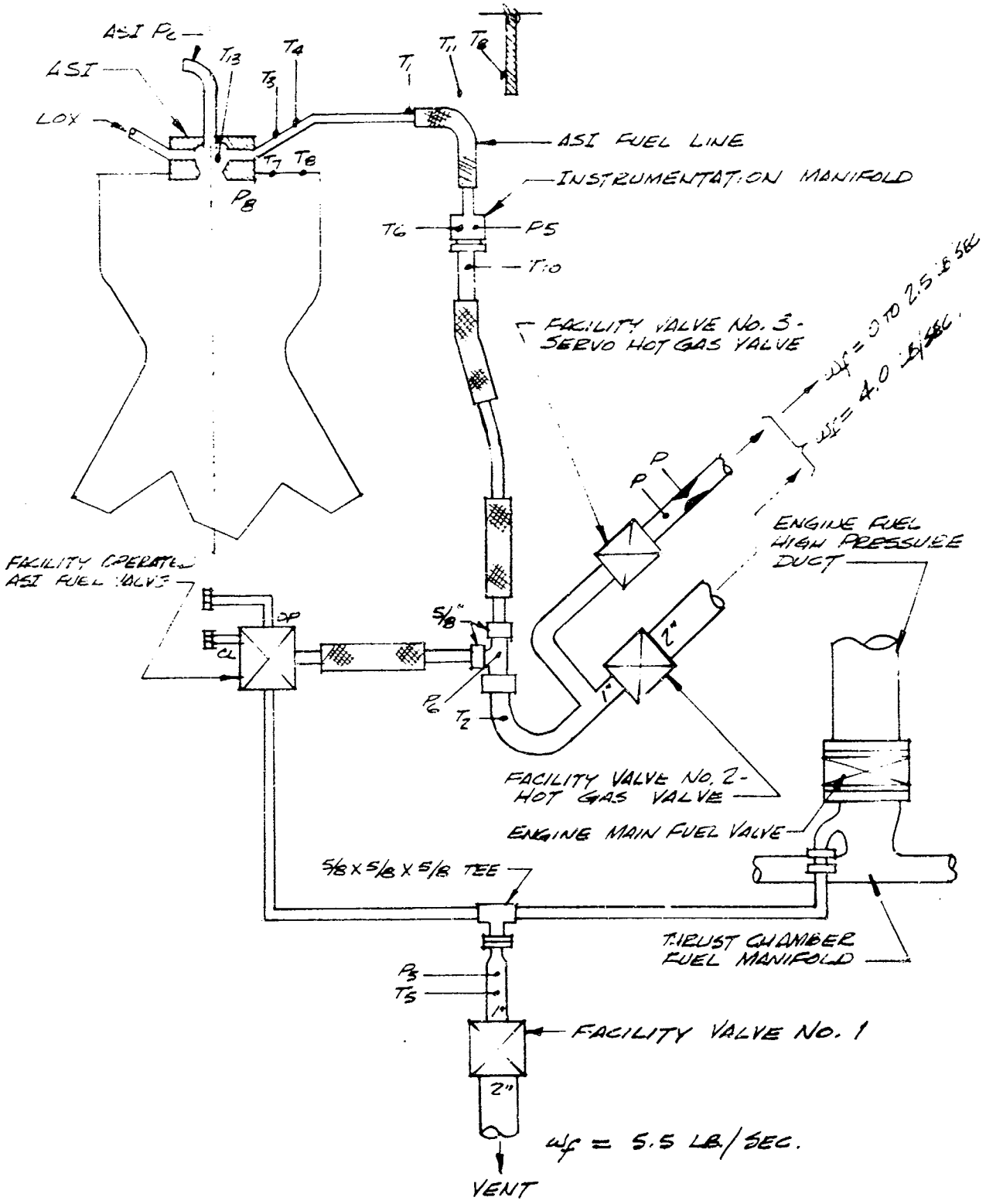

Figure A-2. Engine Configuration, ASI Fuel Line Evaluation (Test 313-036)

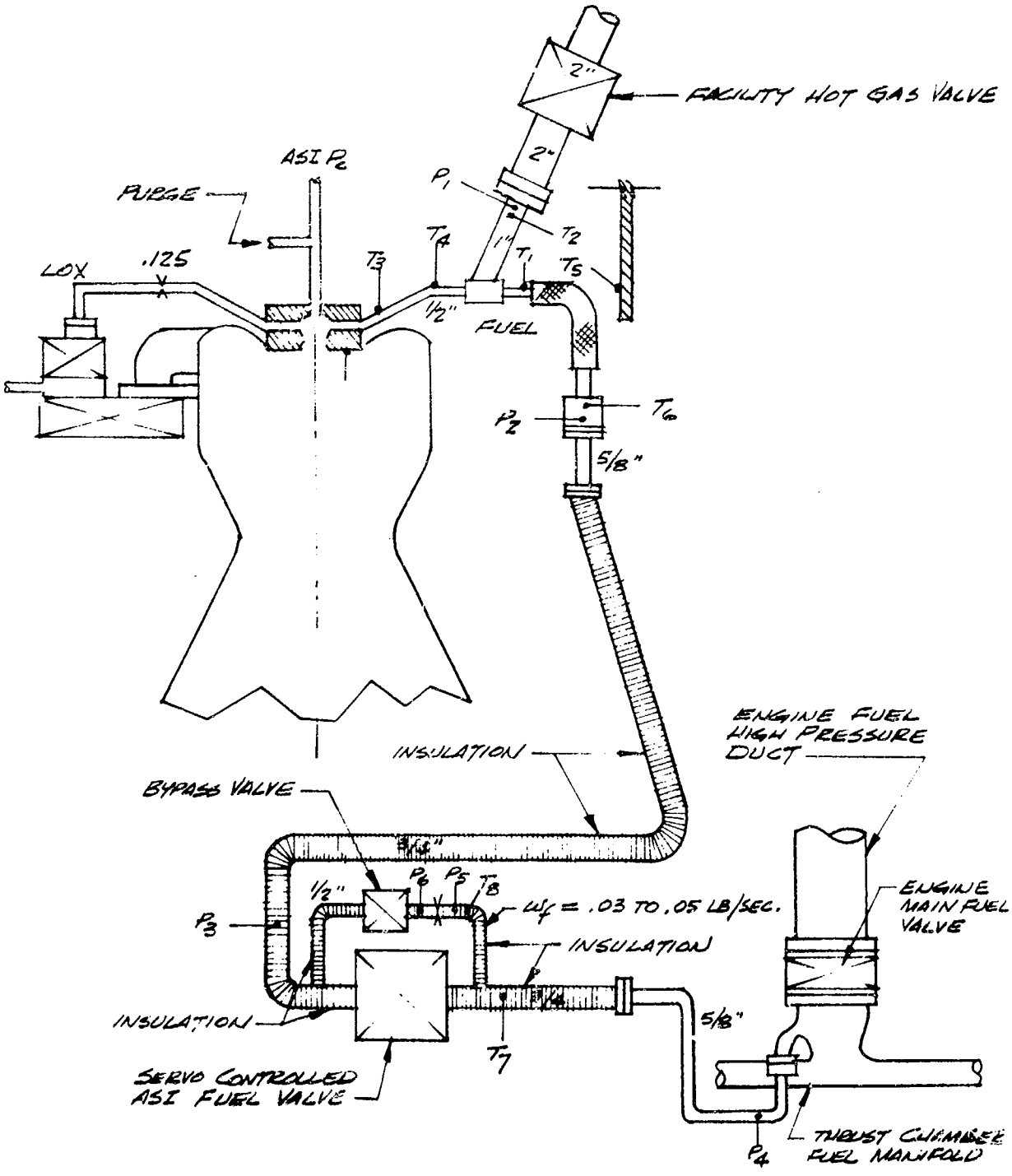

Figure A-3. Engine Configuration, ASI Fuel Line Evaluation (Test 313-041)

approximate an ASI fuel line rupture and resultant ASI mixture ratio of 10:1 (o/f). The test setup utilized is illustrated in Fig. A-4.

The ASI was utilized as the ignition source for the thrust chamber and employed a sparks-on, 50-millisecond oxidizer lead start. The thrust chamber was started using a full-flow fuel lead preceded by igniter oxidizer to facilitate main propellant ignition. Both the ASI and the thrust chamber used a fuel-rich cutoff. ASI-only operation was restricted to less than 1.2 seconds by means of sequencing and safety cutoff circuits. The highest recorded ASI mixture ratio during start transient was 1.42 (o/f). ASI fuel line leakage was simulated by closing the No. 1 ASI fuel valve (Fig. A-4) approximately 1 second after attaining stable mainstage operation.

Results attained during tests 217-2 and 217-4 are as follows. Main injector damage was incurred during test 217-2. Severe continuous main injector burning and erosion began at approximately 212 seconds mainstage and appeared to quench after approximately 7.1 seconds; short, sporadic bursts of intense burning continued to occur from the initial quenching point until cutoff.

The ASI nozzle erosion did not penetrate any oxidizer passages, but subsequent vacuum checks disclosed a longitudinal crack that extended into the oxidizer post of element No. 3, row 1.

Significant main injector, main chamber, and ASI seal damage was incurred during test 217-4. A total of 15 oxidizer passages (including two oxidizer "doghouses") were violated by erosion. Very intense continuous main injector burning and erosion began immediately after the No. 1 ASI fuel valve (Fig. A-4) was ramped closed; the burning continued until approximately 3 seconds prior to cutoff at which time the burning appeared to diminish slightly. Two thrust chamber tubes in the lower nozzle were ruptured during test 217-4; analysis of test data and instrumentation motion pictures and appearance of the ruptured tubes indicate that the damage was caused by ejected injector material striking the nozzle interior

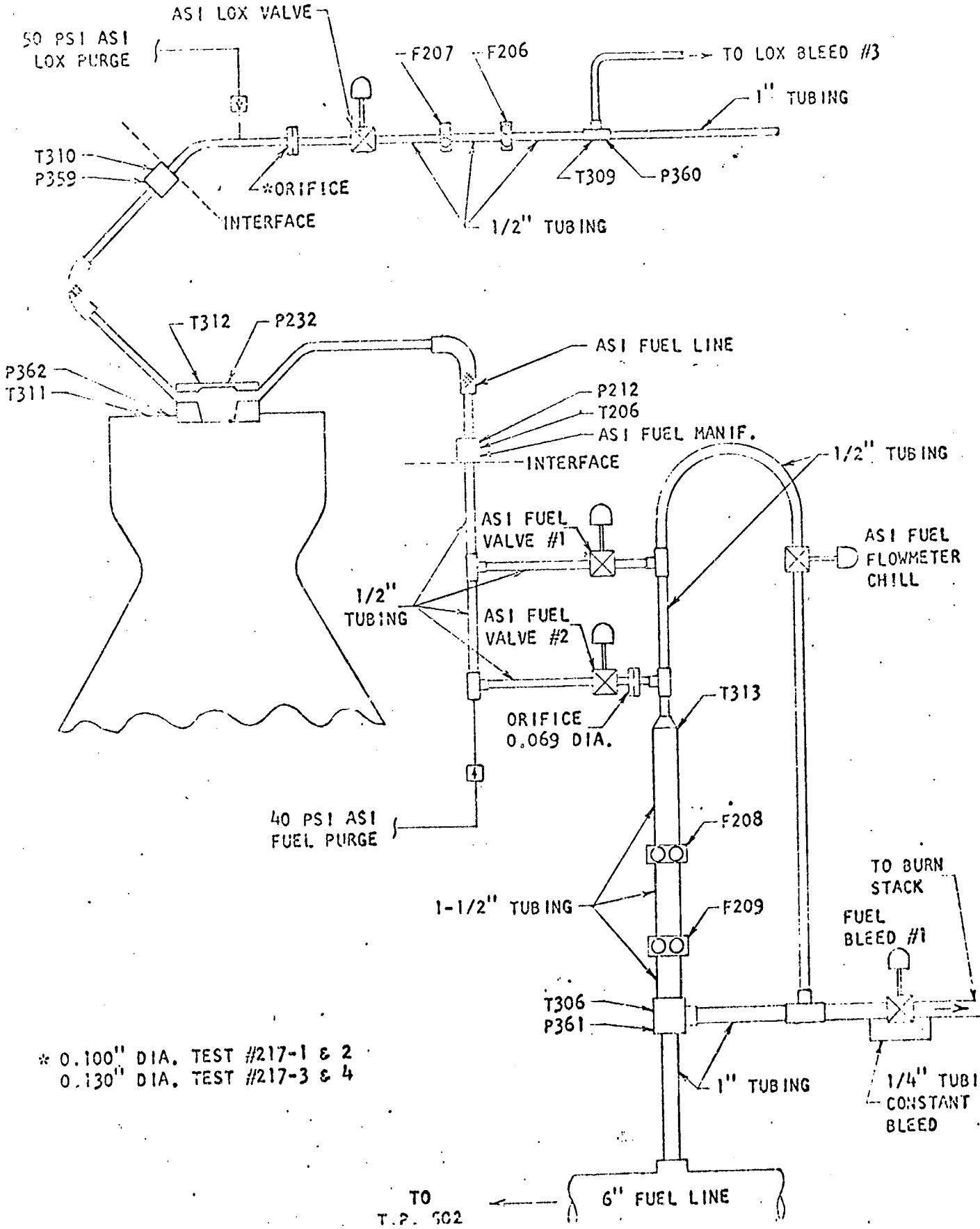

Figure A-4. ASI Feed System Schematic

wall. These ruptures resulted in (1) 8 to 9 lb/sec of main fuel being dumped into the lower nozzle, and (2) application of significant side loads to the thrust chamber.

A c* efficiency "tail-off" of 1 percent was observed during the latter 7 seconds of test 217-2 and the latter 12 seconds of test 217-4. The following suggest that this effect primarily resulted from pressurant (nitrogen) dilution of the main oxidizer.

1. The magnitude of c* efficiency loss was the same for both tests, whereas the extent of main injector damage was markedly different.
2. The observed "tail-off" occurred concurrently with a rise in main oxidizer temperature; the rate of "tail-off" increased with the rate of temperature rise.
3. Oxidizer tank ullage was less than 50 percent during the "tail-off" periods.
4. The oxidizer tank pressure (approximately 1300 psig) was well above the critical pressure of oxygen, permitting facile diffusion of nitrogen into the oxygen.

Pertinent test results and data are presented in Table A-1 and in Fig. A-5 through A-9.

CONCLUSIONS

The following conclusions were developed, based upon results of Rocketdyne tests 313-035, 313-036, and 313-041, and data acquired during MSFC thrust chamber component tests 217-2 and 217-4:

1. Erosion of the main injector can occur over a relatively long duration without generation of instability and without catastrophic failure.

FOLDOUT FRAME 1

TABLE A-1

MSFC THRUST CHAMBER TEST R

Test No.	Date, 1968	Event	Thrust Chamber			ASI		
			Chamber Pressure, psia	Mixture Ratio	Fuel Injection Temperature, R	Chamber Pressure, psia	Mixture Ratio	Inj Temp
217-1	2 May	---	---	---	---	---	---	
217-2	3 May	Prior to valve ramp	766	6.15	226	860	.68	
		Following valve ramp	766	6.18	224	798	5.87	
		Cutoff	760	6.25	226	807	6.18	
217-3	7 May		---	---	---	---	---	
217-4	7 May	Prior to v valve ramp	762	5.70	NG	906	.98	
		Following valve ramp	762	5.70	---	829	9.15	
		Following tube rupture	750	5.62*	---	806	9.15	
		Cutoff	740	5.63*	---	793	9.70	

FOLDOUT FRAME 2

1

TEST RESULTS

Fuel Injection Temperature, R	Mainstage Duration, seconds	Remarks	Hardware Condition
---	2.0	High Pc limit cutoff; check-out test	No change in hardware condition
115	23.4	Fuel depletion cutoff; simulation test	No damage to thrust chamber. ASI fuel side spark plug severely eroded. Main injector ASI nozzle eroded through to main fuel compartment 360 degrees. Erosion began 1 inch downstream seal seat and extends outboard to within 0.09 inch of row No. 1 oxidizer passages. Vacuum check disclosed a longitudinal crack into element No. 3, row No. 1 oxidizer post. Damaged spart plug and main injector were replaced.
113	---		
108	---	---	
---	1.0	Observer cutoff for fuel fire	No change in hardware condition
NG	23.7	Fuel depletion cutoff; simulation test	Thrust chamber tube No. 362 has a full tube width gate split from 5.75 to 7.25 inches upstream thrust chamber exit. Tube No. 363 has a full tube width split from 5.25 to 6.25 inches upstream thrust chamber exit. ASI fuel-side spark plug severely eroded. ASI lower lip severely eroded. ASI nozzle severely eroded over entire length and outboard to row No. 2. All elements in row No. 1 eroded away. Elements No. 4 and 5, row No. 2 eroded away. Element No. 2, row No. 2 oxidizer post penetrated at tip. Oxidizer doghouses No. 3 and 8 violated by erosion. Face plate eroded away outboard to row No. 2.
---	---	---	
---	---	---	
---	---	---	

FOLDOUT FRAME 1
M/R
AST PROBE THERMOCOUPLE
TIC MIX
AST M/R
TIC dif
MAIN LOX INJECTOR PR
E_O
R_f
ASI PROBE TEMP (°F)
TIC dif

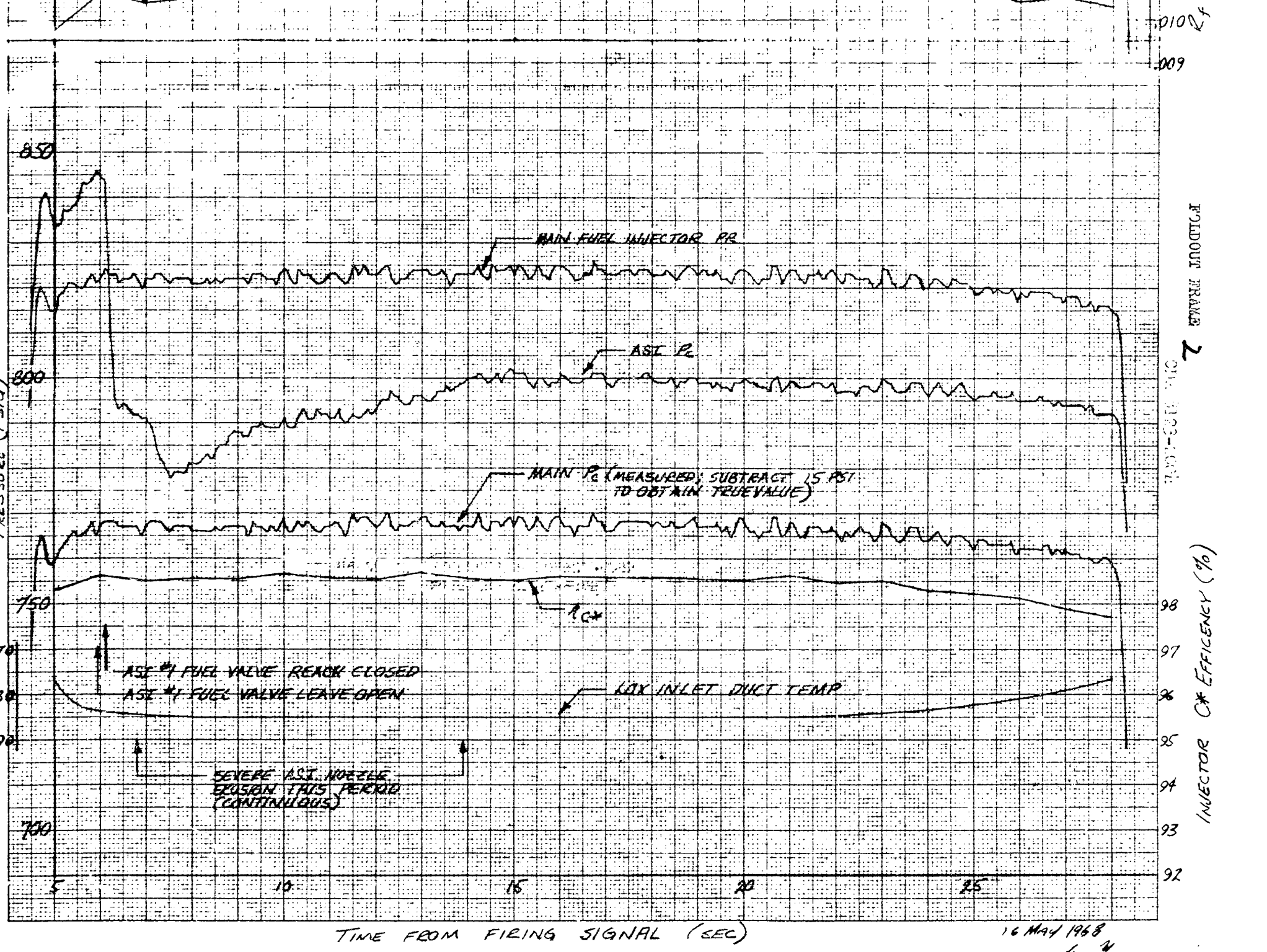

16 MAY 1968

R-7450-2

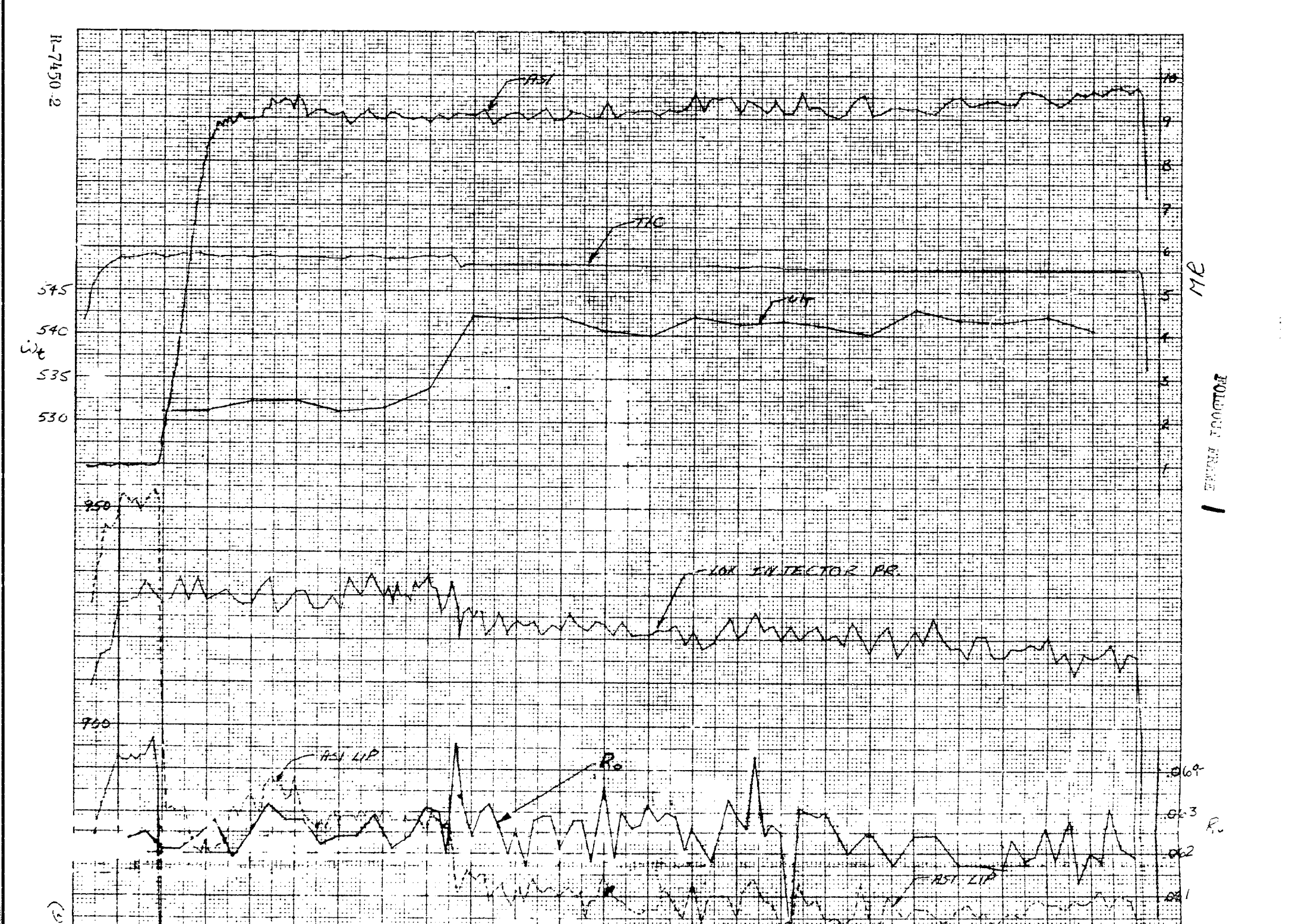
R-7450-2
RST
TAC
545
540
535
530
950
LOX INJECTOR PR.
750
RST LIP
R_o
RST LIP
MP
1

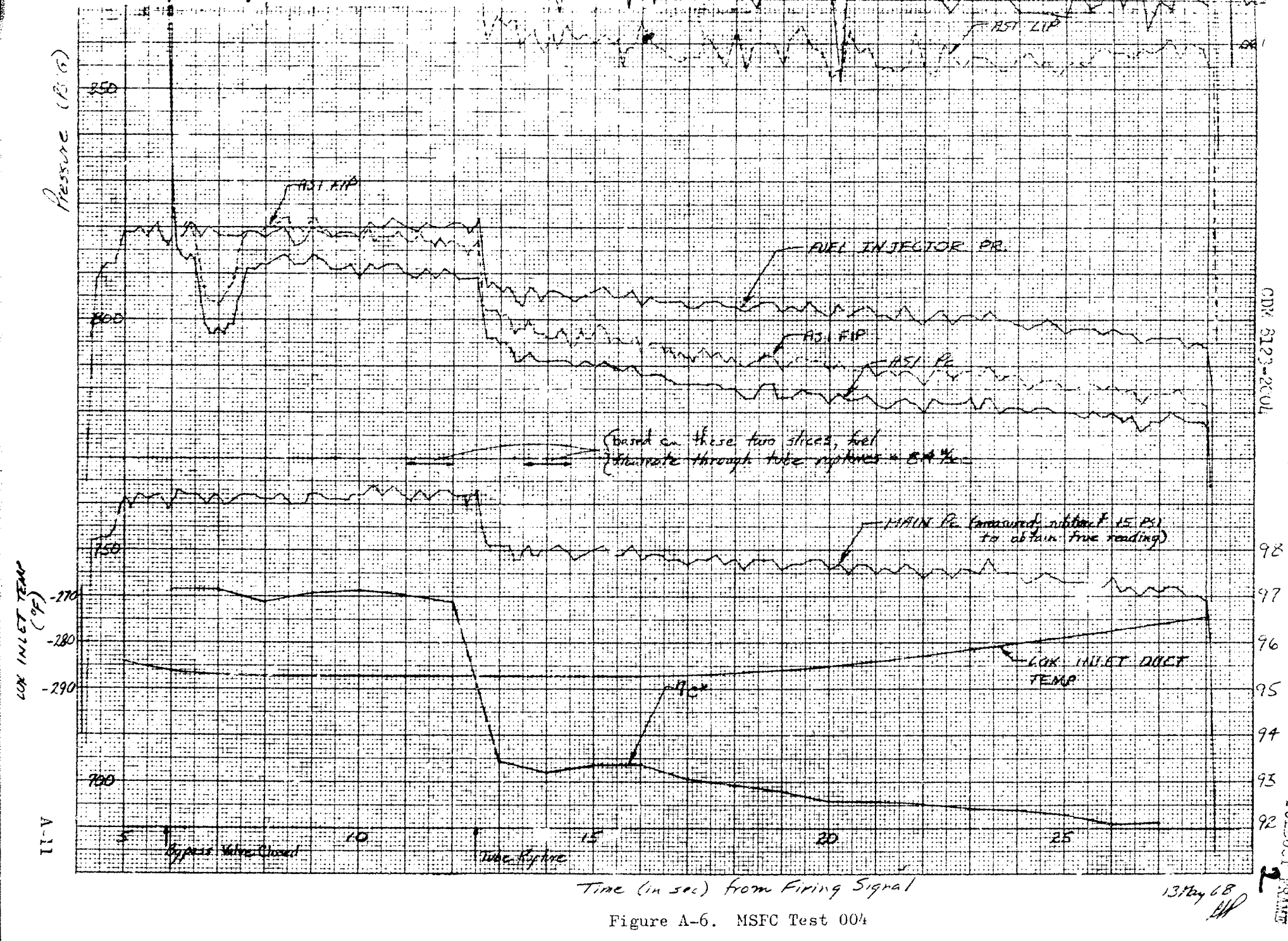

Figure A-6. MSFC Test 004

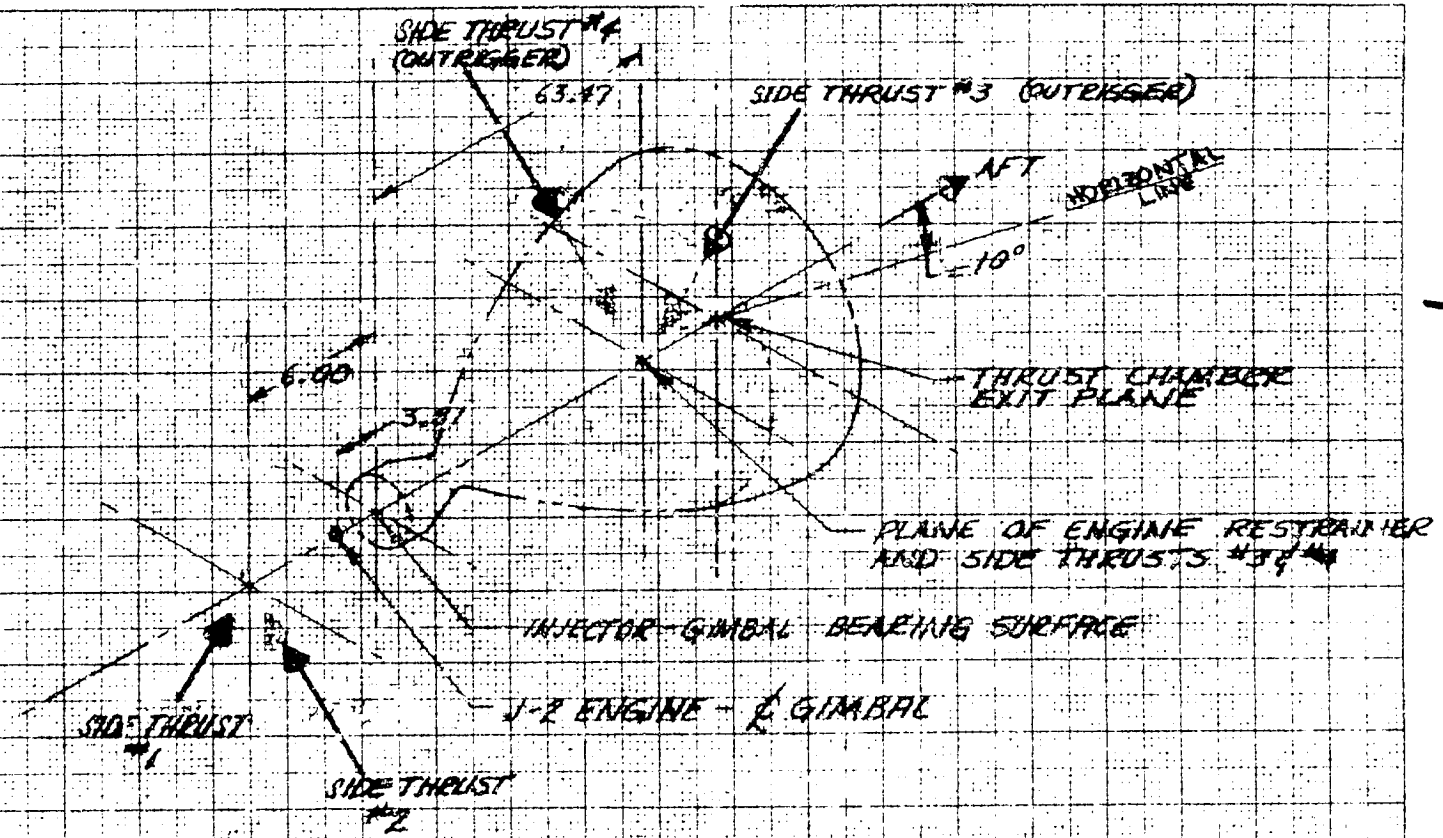
SIDE THRUST #4
(OUTRIGGER)
63.47
SIDE THRUST #3 (OUTRIGGER)
AFT
HORIZONTAL LINE
10°
6.60
3.81
THRUST CHAMBER EXIT PLANE
PLANE OF ENGINE RESTRAINER AND SIDE THRUSTS #3 & #4
INJECTOR-GIMBAL BEARING SURFACE
J-2 ENGINE - ℄ GIMBAL
SIDE THRUST #1
SIDE THRUST #2

+4.0

+3.0

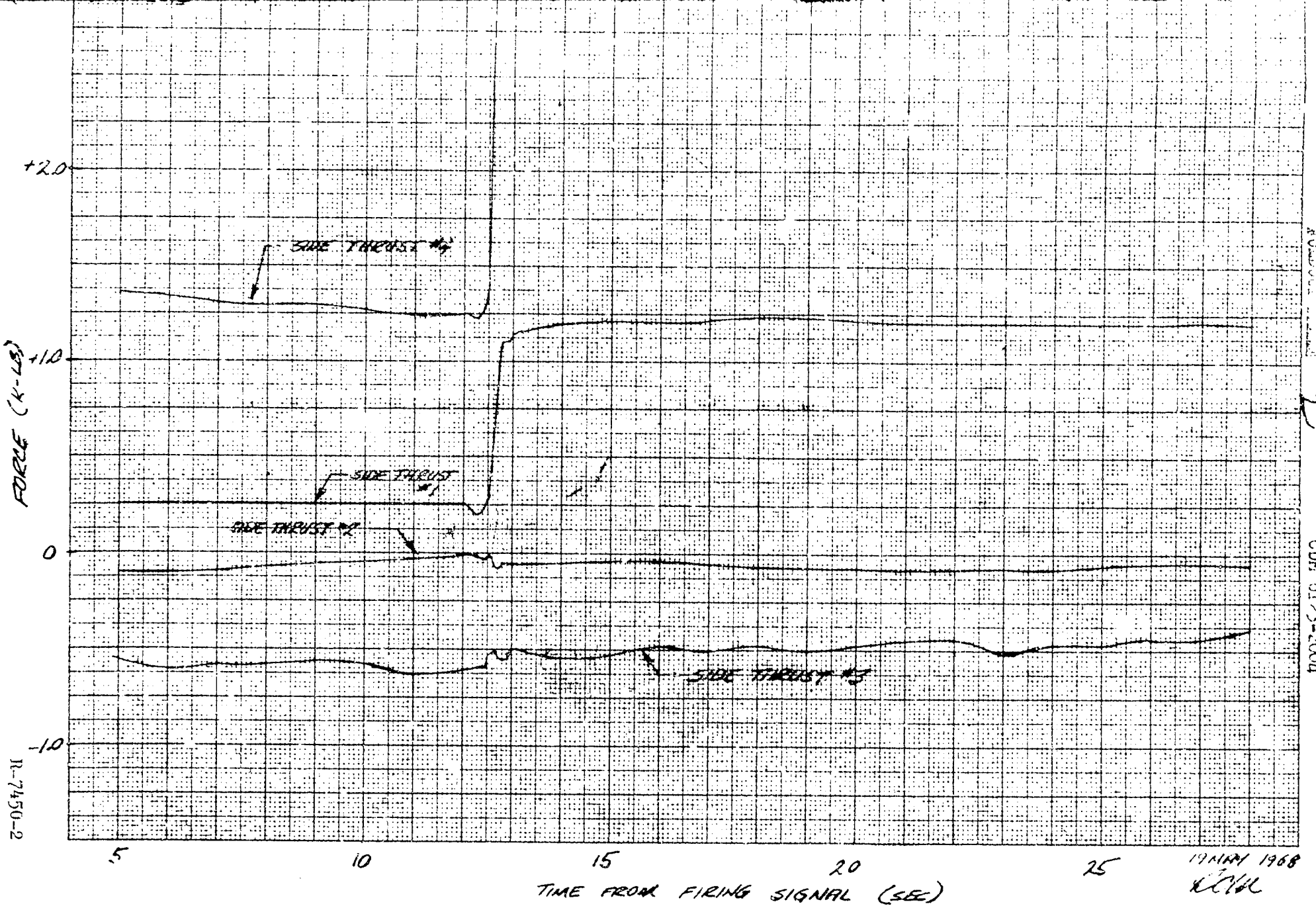

Figure A-7. MSFC Test 217-4

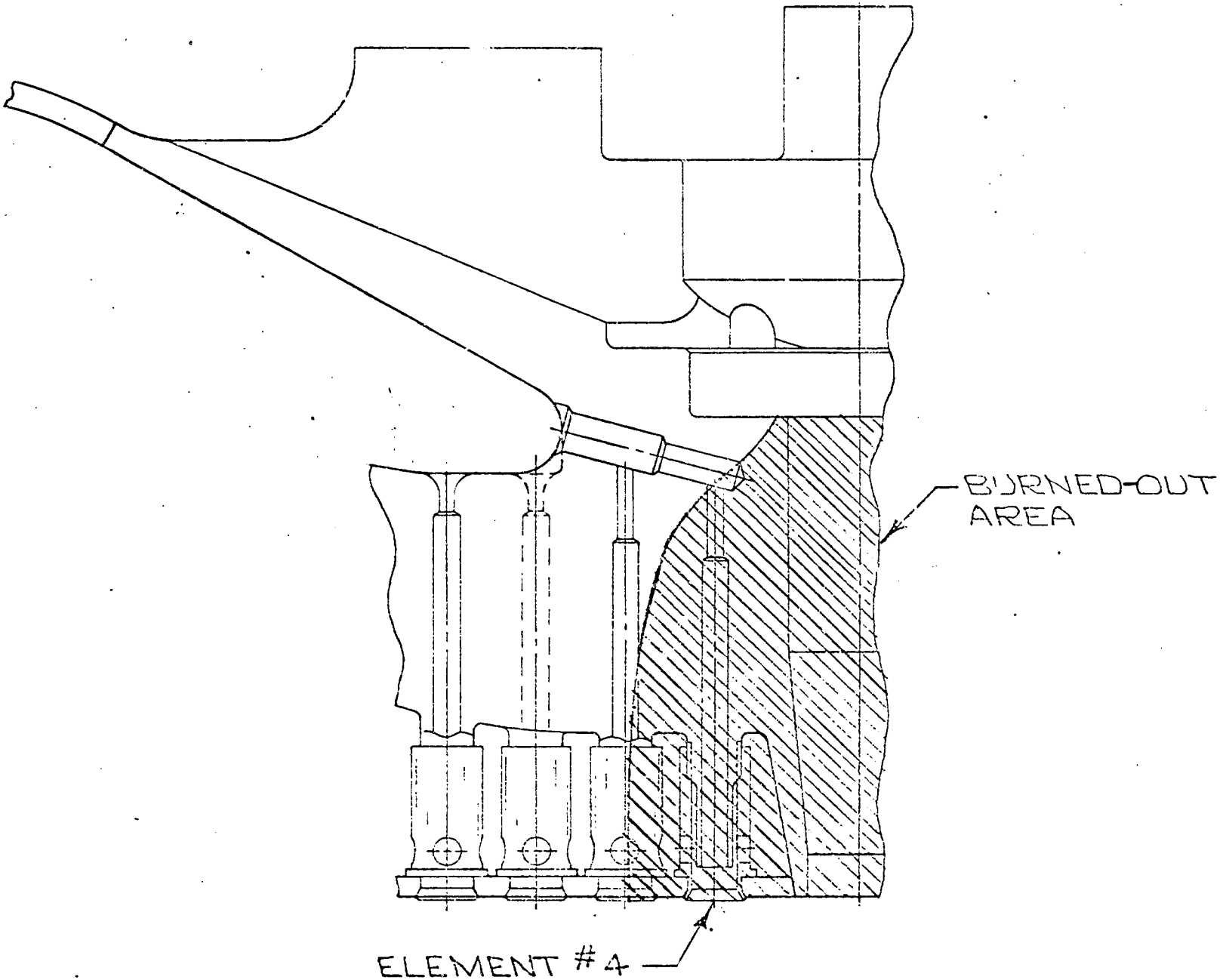

Figure A-8. Posttest Injector Condition, MSFC ASI Fuel Line Failure Simulation (Area of Greatest Damage)

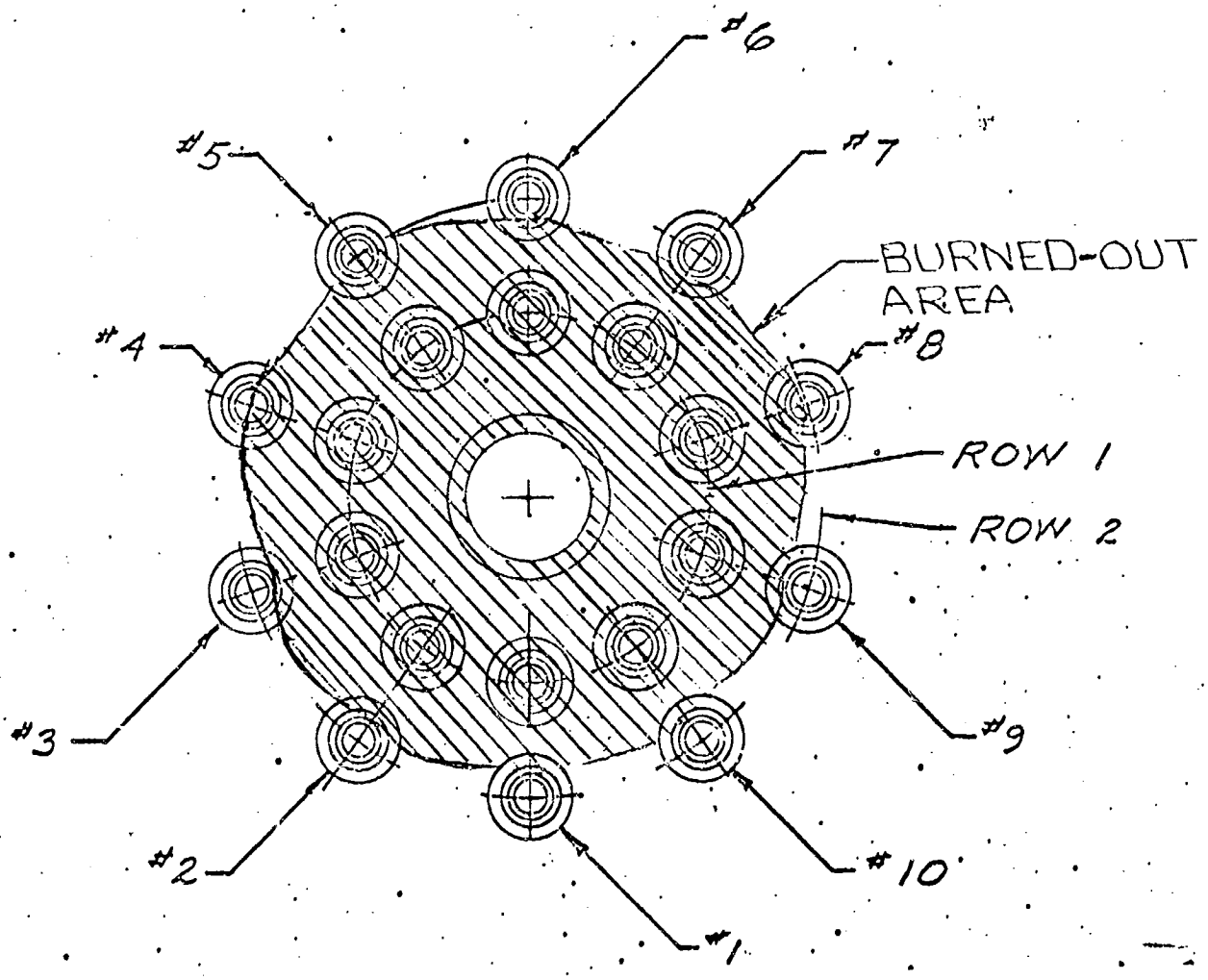

Figure Posttest Injector Condition, MSFC ASI Fuel Line Failure Simulation (View of Face)

2. Thrust chamber P_c and c* efficiency were unaffected by erosion and penetration of the main injector fuel manifold, oxidizer manifold, and oxidizer elements in the vicinity of the ASI nozzle.

3. The c* efficiency is reduced by opening to atmosphere any portion of the ASI injector or main injector.

4. Erosion of the ASI nozzle can occur with an ASI oxidizer/fuel mixture ratio as low as 2.5.

5. Damage to the thrust chamber nozzle resulted from ejected injector fragments.

6. Side forces, i.e., moment loading at the gimbal bearing, can result from failure of thrust chamber tubes with attendant fuel leakage flow to the interior of the thrust chamber nozzle.

APPENDIX B

ALTERNATE HYPOTHESES

Specific hypotheses considered during analysis and investigation of major AS-502 S-II flight problem areas are listed herein, along with brief statements of substantiating information and/or data not in agreement with the hypotheses. Hypotheses listed are referenced to range time.

RANGE TIME 220 TO 318 SECONDS

Gradual engine performance decay, engine compartment and engine component temperatures decrease.

Hypothesis 1

Progressive fuel leak emanating from fuel tank pressurization system (thrust chamber injector manifold)

Substantiating Information.

1. Apparent performance decay at 260 seconds
2. Engine components began to chill at 220 seconds.
3. General direction of chilling source matches the location of the fuel tank pressurization boss.
4. Amount of leakage required to cause the apparent performance decay (2.5 lb/sec) is within the flow capability of the fuel tank pressurization system.
5. This system could then have ruptured at the 319-second time, as noted in the material for that anomaly.

Data Not In Agreement With Hypothesis.

1. Difficult to relate this failure mode to cutoff failure, as noted in the 319-second anomaly

2. No previous line failures

3. Site test data not in agreement with observed flight data

Hypothesis 2

Progressive fuel leak emanating from the ASI fuel line (thrust chamber inlet manifold)

Substantiating Information.

1. Leak at the thrust chamber inlet manifold fitting or in the lower flex section could cause the observed chilling of engine components beginning at 220 seconds range time.

2. Engine vibration could cause leakage to increase with time (fatigue) to the point where engine compartment temperatures decrease, and finally to complete rupture of the line (319-second performance shift).

3. Amount of leakage required to cause the apparent performance decay (2.5 lb/sec) is within the flow capability of the ASI fuel delivery system.

4. This failure mode can be related to the cutoff failure, as noted in the 319-second anomaly.

Data Not In Agreement With Hypothesis.

1. Leak does not contribute side forces to create observed actuator loads after the 319-second performance shift.

Hypothesis 3

Progressive fuel leak at thrust chamber heat shield (external)

Substantiating Data.

1. Failure of one or more tube-to-nozzle tension band braze joints due to heat shield loading and/or engine vibration could cause a fuel leak on the inboard side of Engine 202.
2. Fuel leak from this area could cause engine components to chill down, as it matches the general coolant region defined by the temperature measurements.
3. A tube-to-band braze joint failure due to vibration can propagate from tube to adjacent tube, thus giving rise to progressive performance loss.
4. Amount of leakage attributed to this type of failure could support the noted performance loss.

Data Not In Agreement With Hypothesis.

1. Abrupt performance loss at 319 seconds would have to be caused by sudden failure of a number of tube-to-band braze joints; 10 to 12 tube failures are required to have a performance shift.
2. Difficult to relate this failure mode to cutoff failure
3. Insufficient flowrate to create observed actuator loads

Hypothesis 4

Progressive fuel leak at exit of thrust chamber (external)

Substantiating Data.

1. Tube leaks could cause chilling of hydraulic system and engine components.

Data Not In Agreement With Hypothesis.

1. To be a progressive leak, it would have to be a tube-to-braze joint failure, such as Hypothesis 3, probably at the exit manifold or aft hat band location. No known abnormal loading is imposed in that area during flight in addition to the normal vibration load from engine operation.
2. This failure mode does not adapt readily to the abrupt performance decay at 319 seconds nor to the cutoff failure.

Hypothesis 5

Fuel leak at thrust chamber exit (internal)

Substantiating Data.

1. Fuel leak will cause a performance loss.

Data Not In Agreement With Hypothesis.

1. Internal tube leak is not progressive and will not yield gradual performance degradation.
2. Internal leak is confined to exhaust plume, therefore will not result in chilling of engine area as noted in temperature data.

RANGE TIME 319 SECONDS

Engine 2044 rapid performance shift.

Hypothesis 1

Fuel leak at thrust chamber injector manifold (pressurization hose)

Substantiating Information.

1. Leak would be at least 7 lb/sec, which is close to the required flowrate at this manifold, and directionally matches the analog model.
2. Leak at this manifold could cause chilling of the hydraulic lines and gimbal actuators and flight instrumentation packages.

Data Not In Agreement With Hypothesis.

1. Leak at this manifold does not result in cutoff failure unless the elbow and hose could physically twist around so as to strike the area (C03a or the ignition detector probe) and rupture the dome or cause a fire. Force generated by flow from the hose is not sufficient to tear it loose in this manner. Also, knocking off C03a would not give enough flow area to match the cutoff failure.
2. Available flowrate will not create observed actuator loads.

Hypothesis 2

Fuel leak at thrust chamber inlet manifold (ASI fuel line)

Substantiating Data.

1. Result of leak at this manifold directionally matches analog model.
2. This leak could cause erosion of the ASI and ASI fuel line at the dome, which could eventually erode dome and cause it to rupture under pressure.
3. Cold fuel from this leak could spray on the flight instrumentation packages and hydraulic components causing them to chill down.

4. Flow from this leak could match the 10 lb/sec required to produce the shift if the ASI fuel line boss on the thrust chamber fuel inlet elbow failed (produces 7 lb/sec).

Data Not In Agreement With Hypothesis.

1. The fuel pump speed and actuator load changes that were noted do not fit the model.
2. Available flowrate will not create observed actuator loads.

Hypothesis 3

Fuel leak at exit of thrust chamber (external)

Substantiating Data.

1. Leak could cause chilling of hydraulic system and instrumentation packages.

Data Not In Agreement With Hypothesis.

1. Leak would have to be on inboard side of thrust chamber to create the observed actuator loads; however, this is highly unlikely because the heat shield protects this part of the bell from falling objects.
2. Fuel pump speed and thrust chamber jacket temperature go in wrong direction to match model.

Hypothesis 4

Fuel leak at thrust chamber heat shield (external)

Substantiating Data.

1. Leak at this location would give actuator loads in the right direction.
2. Leak could cause chilling of hydraulic system and instrumentation packages.

Data Not In Agreement With Hypothesis.

1. If heat shield shifted and moved into engine, it would have to break numerous large-diameter struts to do so, and would also hit engines 1, 3, and 5 because of the symmetry of the shield.
2. The large turbine exhaust manifold inlet elbow is the first thing that the shield would hit if it moved over into the engine. This would cause only a hot-gas leak.
3. Fuel pump speed and thrust chamber jacket temperature change in wrong direction to match model.
4. Temperature measurements in this area do not indicate a leak.

Hypothesis 5

Fuel leak at exit of thrust chamber (internal)

Substantiating Data.

1. Test results indicate that injector pieces may strike the thrust chamber nozzle creating internal fuel leaks.
2. Fuel leak of 7 lb/sec at exit manifold would cause observed actuator loads.
3. Fuel leak at 7 lb/sec would cause observed 319 seconds performance shift.

Data Not In Agreement With Hypothesis.

1. Fuel pump speed and thrust chamber jacket temperature go in wrong direction to match model.
2. Patch on tube 123 could blow out, but resultant force would be on wrong side of thrust chamber to produce observed actuator loads.

The following hypotheses were investigated as possible causes for the performance shift and rejected for the reasons indicated:

1. Oxidizer system leak--analysis indicates that 22 lb sec oxidizer leak is required to give the observed engine performance decay. Engine data do not indicate any oxidizer leak.
2. Valve failure--review of data showed no engine or vehicle valve position changes during the performance shift.

RANGE TIME 319 SECONDS

Engine 202 pitch and yaw actuator Δ P shift.

Hypothesis 1

Inboard external fuel leak of 17 lb/sec at thrust chamber exit

Substantiating Information.

1. Would give required load

Data Not In Agreement With Hypothesis.

1. Performance data indicate only 7 to 10 lb/sec fuel leak.
2. Would not cause cooling found above heat shield

3. Does not agree with calorimeter data

4. Would require object to drop from under heat shield; none available

5. Does not match thrust chamber ΔP

Hypothesis 2

Inboard external fuel leak of 21 lb/sec at heat shield attach point

Substantiating Information.

1. Would give required load

2. Heat shield curtain could damage thrust chamber.

3. An object from the interstage could strike the chamber.

4. Would give a cryogenic leak into the boattail

Data Not In Agreement With Hypothesis.

1. Pull tests on flame curtain did not damage thrust chamber tubes.

2. Flame curtain temperatures do not chill.

3. Flow rate does not match 7 to 10 lb/sec required for performance shift.

4. Does not match thrust chamber ΔP

Hypothesis 3

Inboard external leak from fuel tank pressurization hose of 15 lb/sec with hose expanded to flame shield

Substantiating Information.

1. Would give required load

Data Not In Agreement With Hypothesis.

1. Flowrate not in agreement with 7 to 10 lb/sec required for performance shift.
2. Flame curtain temperatures do not chill.
3. R&D test data do not match performance shift.
4. Stage H_2 pressurization system data shows line to be intact.

Hypothesis 4

ASI fuel line failure

Substantiating Information.

1. Data match observed performance shift.
2. Would chill boattail

Data Not In Agreement With Hypothesis.

1. Would not give load of required direction or magnitude.

Hypothesis 5

Outboard internal thrust chamber fuel leak of 11 lb/sec at exit

Substantiating Information.

1. Would give required loads

Data Not In Agreement With Hypothesis.

1. Thrust chamber ΔP data do not support 11 lb/sec leak.
2. Would not cause external chilling

Hypothesis 6

Inboard exhaust system leak of greater than 7 lb/sec

Substantiating Information.

1. Would give required load.

Data Not In Agreement With Hypothesis.

1. Temperatures in boattail do not indicate hot-gas leakage.
2. System analyzed to be intact at cutoff.
3. Does not match performance shift
4. Requires a 72 $in.^2$ hole in exhaust system

Hypothesis 7

Inboard oxidizer leakage of 180 lb/sec

Substantiating Information.

1. Would give required load
2. Would chill boattail

Data Not In Agreement With Hypothesis.

1. Performance loss was 7 to 10 lb/sec of fuel.
2. Leakage rate too high; engine data do not indicate any oxidizer leak.

Hypothesis 8

Fuel inlet duct inner bellows pressurized

Data Not In Agreement With Hypothesis.

1. Load in wrong direction
2. AS-502 still had relief valves on annulus.

Hypothesis 9

Stage oxidizer duct support failed and loaded oxidizer side of engine.

Data Not In Agreement With Hypothesis.

1. Duct would be supported by stage thrust structure.
2. Insufficient load

Hypothesis 10

Hole through thrust chamber to hot gas to cause leak of 3.1 lb/sec just above exit plane.

Substantiating Information.

1. Would give required load

Data Not In Agreement With Hypothesis.

1. Aft heat shield temperature does not rise.
2. Would require impact of object under heat shield
3. Not indicated in performance data

Hypothesis 11

Heat exchanger leak of 7 lb/sec; turbine exhaust gas and main thrust chamber exhaust gas

Substantiating Information.

1. Would give required load

Data Not In Agreement With Hypothesis.

1. Would heat boattail instead of cooling it
2. R&D data comparison does not support failure.
3. Flight data do not confirm failure mode.

Hypothesis 12

Failure of gimbal bearing fabroid liner by effects of S-IC boost.

Data Not In Agreement With Hypothesis.

1. Effects of S-IC boost not sufficient to overload and flake fabroid.

Hypothesis 13

Oxidizer or fuel pump support failure

Data Not In Agreement With Hypothesis.

1. Insufficient load

Hypothesis 14

Unbalance of 1.5-psi compartment pressure across entire engine above heat shield

Data Not In Agreement With Hypothesis.

1. Compartment interstage pressures do not indicate over 0.05 psia.

Hypothesis 15

Inboard external leak at fuel tank pressurization manifold of 66 lb/sec

Substantiating Information.

1. Would give required load
2. Would chill boattail

Data Not In Agreement With Hypothesis.

1. Only 7 to 10 lb/sec flow loss indicated
2. Only 80 lb/sec flow through main chamber
3. R&D test data do not match performance shift observed.

Hypothesis 16

Outboard internal thrust chamber fuel leak of 23 lb/sec near turbine exhaust manifold

Substantiating Information.

1. Would give required loads

Data Not In Agreement With Hypothesis.

1. Not supported by thrust chamber ΔP data and transient data
2. Would not cause external effects and temperatures

Hypothesis 17

Gimbal bearing failure

Substantiating Information.

1. Would give required load

Data Not in Agreement With Hypothesis.

1. Cannot explain mechanical failure to account for displacement of gimbal bearing by this amount

Hypothesis 18

Heat shield supports failed and allowed shield to rest on chamber.

Substantiating Information.

1. Loading in required direction

Data Not In Agreement With Hypothesis.

1. Would require heat shield to move against gravity
2. Would not explain performance shift

Hypothesis 19

Large external indentation in thrust chamber of 10 to 20 $in.^2$ projected area

Substantiating Information.

1. Would explain loads

2. Impact from external object possible

3. External object could damage ASI fuel line.

Data Not In Agreement With Hypothesis.

1. Would require 7 to 10 lb/sec fuel leakage to explain performance shift

2. Would not explain boattail chilling prior to 319 seconds

3. Would require considerable impact to dent chamber (greater than 2000 ft-lb)

RANGE TIME 412.3 SECONDS

Engine 2044 rapid performance decay and subsequent engine cutoff.

Hypothesis 1

Burn through oxidizer dome (internally)

1. Partial failure of the ASI fuel line at 220 seconds results in high ASI mixture ratio and erosion of the ASI nozzle.

2. Erosion of the injector continues until 412.3 seconds, at which time breakthrough to the oxidizer dome occurs and oxidizer flow begins to increase.

3. Chamber pressure begins to drop and fuel flow increases; performance decays until cutoff is initiated.

Hypothesis 2

Burn through oxidizer dome (externally)

1. Partial fialure of the ASI fuel line at 220 seconds results in high ASI mixture ratio and erosion of ASI nozzle and injector.

2. Complete separation of the ASI fuel line at 319 seconds allows hot ASI gases to back flow through the ASI fuel line and impinge externally on the oxidizer dome.

3. Erosion of oxidizer dome continues until 412.3 seconds, at which time breakthrough to the oxidizer dome occurs and oxidizer flow begins to increase.

4. Chamber pressure begins to drop and fuel flow increases; performance decays until cutoff is initiated.

Substantiating Information.

1. Oxidizer flow increase indicating failure downstream of flowmeter.

2. Pressure in oxidizer system is maintained for approximately 60 seconds following cutoff, indicating failure is downstream of MOV.

3. Rapid decay of main oxidizer injection pressure compared to oxidizer pump discharge pressure indicates failure downstream of MOV.

The following malfunctions were investigated as possible causes for the rapid performance decay and rejected for the reasons indicated:

Fuel Feed Systems

1. Inlet Duct Failure

   a. Fuel injection temperature did not rise.

   b. Fuel turbine inlet did not rise.

   c. Oxidizer turbine inlet did not rise.

   d. Fuel flow should not increase.

2. Turbopump Failure

   a. Fuel injection temperature did not rise.

   b. Fuel turbine inlet did not rise.

c. Oxidizer turbine inlet temperature did not rise.

d. Fuel flow should not increase.

3. High-Pressure Duct Failure

a. Fuel injection temperature did not rise.

b. Fuel turbine inlet temperature did not rise.

c. Oxidizer turbine inlet temperature did not rise.

d. Increasing fuel eliminates failure upstream of flowmeter.

4. Gas Generator Bootstrap Line Failure

a. Fuel and oxidizer flows should increase.

b. Fuel turbine inlet and oxidizer turbine inlet temperatures did not rise.

5. Gas Generator Bypass Valve Failure

a. Position micro indicates proper operation.

b. Fuel turbine inlet and oxidizer turbine inlet temperatures did not rise.

6. Main Fuel Valve Failure

a. Position trace indicates proper operation.

b. Fuel injection temperature did not rise.

c. Fuel flow should not increase.

7. Thrust Chamber

a. Fuel injection temperature did not rise.

b. Fuel turbine inlet and oxidizer turbine inlet temperatures did not rise.

<u>Oxidizer Feed System</u>

1. Inlet Duct Failure

a. Oxidizer flow would not increase.

b. Oxidizer pump speed would increase.

c. System integrity is maintained after cutoff.

2. Turbopump Failure

a. Oxidizer flow would not increase.

b. Fuel flow would not increase.

c. Bearing coolant temperature indicated no problem.

3. High-Pressure Duct Failure

a. Failure upstream of flowmeter would not result in increase in oxidizer flow.

b. Failure any place in duct would not result in system integrity being maintained after cutoff.

4. Gas Generator Bypass Valve Failure

a. Position micro indicates proper operation.

b. Failure any place in duct would not result in system integrity being maintained after cutoff.

5. Main Oxidizer Valve Failure

a. Position trace indicates proper operation.

b. Oxidizer flow should not increase.

Gas Generator and Exhaust System

1. Gas Generator Valve Failure and Combustion System--Burnout, Crossover Duct Failure, Oxidizer Turbine Bypass Valve Opens

a. Failures indicated in this system would result in power being removed from turbines with no increase in oxidizer or fuel flows.

b. Gas generator valve and oxidizer turbine bypass valve position traces and micros indicate proper operation.

ASI System

1. ASI Oxidizer and Fuel Lines

a. Loss of either line would not result in cutoff, unless failure of fuel line earlier in test resulted in erosion of ASI through to oxidizer dome.

Start System

1. Spin Line Failure

   a. Failure would result in power being removed from turbines with no turbine increase in fuel or oxidizer flows.

APPENDIX C

ENGINE 202 (J-2 ENGINE J2044) HISTORY AND CONFIGURATION

S-II stage anomalies that occurred during flight of the AS-502 vehicle appear to be centered around Engine 202 (J-2 S/N J2044); accordingly, analysis of the anomalies included a review of the history of this engine from completion of buildup through vehicle launch. This complete chronological history, including all significant engine events occurring prior to launch, is itemized in Table C-1.

ENGINE ACCEPTANCE

J-2 engine S/N J2044 was subjected to a hot-fire acceptance test series at the Rocketdyne Santa Susana Field Laboratory during this period 13 through 15 October 1965. The engine accumulated 676.1 seconds of mainstage operation during the series, which consisted of four tests. The engine was accepted by the Government on 15 November 1965, following completion of postfiring electrical and mechanical checkouts. Acceptance testing of engine J2044 appears to have been normal in all respects.

STAGE ACCEPTANCE

Engine J2044 was subjected to two hot-fire operations during acceptance of the AS-502 S-II stage at the Mississippi Test Facility, with respective durations of 365.1 seconds and 367.8 seconds. The stage was shipped to KSC on 20 May 1967, engine J2044 having accumulated 1409.0 seconds in six starts, well within allowable limits.

CONCLUSIONS

Analysis of the chronological history of engine J2044 (Table C-1) does not reveal any relevance to the S-II stage anomalies that occurred during flight of the AS-502 vehicle.

TABLE C-I. ENGINE 2044 CHRONOLOGICAL HISTORY

DATE Mo/Day/Yr	LOCATION	ECP'S EFIRS - UCRS	EFFORT	STAGE/ENGINE TEST SEC.	DISPOSITION	REMARKS
10-13-65	R/D		Acceptance Firing	Eng 73.6		All objectives achieved.
10-14-65	R/D	OFR 19314F (UCR)	Acceptance Firing	Eng 22.9		Test terminated. GGOT transducer replaced.
10-14-65	R/D		Acceptance Firing	Eng 503.1		All objectives achieved.
10-15-65	R/D		Acceptance Firing	Eng 76.5		All objectives achieved.
10-20-65	R/D		Fuel T/P intermediate seal replaced		Excessive leakage	
10-22-65	R/D		Changed start tank			Installed newer tank. Old S/N 0003, New S/N 4067986
10-30-65	R/D	OFR 23404F (UCR)	Changed oxidizer turbine bypass valve & OTBV pos. indicator.		Failed pneu. sys. leak check	OTBV old S/N 4062176, new S/N 4075882 Pos. indicator Old S/N 4E172, New S/N 4F112
11-15-65	R/D		Final Gov. acceptance DD250	Total 676.1		Config. 3x5 11x13 20x23x25 28x30x32x34 38x40 51x52 61x 64x68 70x72x78 80x82x84x86 88x97x99x101x106 108x116 118x 122 125x130 132x134x137 144x 149x152 153x155x158x161x173x 179
11-29-65	S/B	UCR 001343	During electrical connector hookup, bent pin occurred. Pin straightened.		Satisfac-tory	No damage occurred to connector
11-30-65	S/B	UCR 001347	During ECP 419 Mod. (3) wires to plug P-54 insulation not to spec.		Harness replaced.	
11-30-65	S/B	ECP MD J2-419 168	Armored harness assy mod Modification			Kit 18-503171-10 Mod. Instr. R5436-419, 9-25-65.
11-17-65	S/B	J2-432 176	Replacement Pressurization tube, spark igniters			Kit 18-651207 Mod. Instr. R5436-432, 9-29-65.

TABLE C-1 (Continued)

TE (Day/Yr)	LOCATION	ECP'S EFIRS - UCRS	EFFORT	STAGE/ENGINE TEST SEC.	DISPOSITION	REMARKS
2-22-65	S/B	J2-394 148	Modified hydrogen tank press. hose assembly			Kit 18-106868 Mod. Instr. R 5436-394 Old S/N 042, new S/N 017
2-27-65	S/B	UCR 005475	Accomplishing ECP J2-432 spark cables (G-1 & G-2) cut to determine if pressurized. Tubes repaired.			Portion of tubes removed were returned to Engineering Canoga for analysis.
2-27-65	S/B	UCR 005476	Accomplishing ECP J2-432 spark cables cut (G-1 & G-2) to determine if pressurized. Tubes repaired.			Portion of tubes removed were returned to Engineering for analysis.
3-31-66	S/B	None	Inspected lox turbopump turb. wheels & stator assy.		Acceptable	S/N 6634949 special inspection Rev. "N" R-3825-3
4-1-66	S/B	UCR R001650	STDV Seal damage		Seal Replaced	P/N 404656-57
4-2-66	S/B	J2-455 188	Modified GG opening control system orifice.			Orifice size 0.044 mod. instr. R5436-455-1, 1-13-66.
4-2-66	S/B	J2-465 190	Modified tube assy T/C purge			Old S/N 070, New S/N 0X13 Mod Instr. R5436-465, 11-24-65
4-4-66	S/B	J2-369 151 R4	Replacement of Fuel Inj. Temp. Transducer			Old S/N 7837, New S/N 12500 Old S/N 7841, New S/N 12732 Mod. Instr. R5436-369, 11-18-65.
4-18-66	S/B	ECP MD J2-510 218	Replacement M/S pressure switch			Kit 18-557908 Mod. Instr. R5436-510, 4-1-66

TABLE C-1 (Continued)

DATE (Mo/Day/Yr)	LOCATION	ECP's MFIR's-UCR's	EFFORT	STAGE/ENGINE TEST SEC.	DISPOSITION	REMARKS
4-20-66	S/B	UCR R001648	Start tank chase I Weldment discrepancy - tank removed and replaced			Discrepancy found during weldment radiographic inspection
4-21-66	S/B	UCR R001649	During start tank installation HAFLEX seal between STDV and flange was scratched		Seal replaced	P/N 404656-45
4-25-66	S/B	J2-399 202 R4	Modify start and control sys.			Kit #1[illegible] Mod. Instr. R5436-[illegible], 3-17-66
4-29-66	S/B	UCR R001657	1" crack in turbine manifold returned Canoga and repaired Reinstalled & checked out		Satisfactory	Discrepancy noted during leak check of Lox pump
5-3-66	S/B	J2-434 180	Relocation of No. 2 H/S press. switch			Kit No. 1[illegible]-047-10 Mod. Instr. R5436-434-1, 1-20-66
5-17-66	S/B	UCR R001671	During Lox T/P inspection the H/Ex inlet seal had a scratch		Seal replaced	P/N 404651-[illegible]
5-19-66	S/B	J2-507 226	Deletion OTBV Instrumentation tube			P/N 703536 Kit No. 1[illegible]-706464 Mod. Instr. R543[illegible]-507, 4-22-66
5-25-66	S/B	J2-459 205 R2	Replacement of ECA			Old P/N 407397, New S/N 4079039, Kit #1[illegible]557922, Mod. Instr. R543[illegible]-459, 2-2-66
5-25-66	S/B	J2-431 177	Heat exchanger orifice change			Orifice size 1.4 Kit No. 1[illegible]-41037[illegible], Mod. Instr. R5436-431, 1-31-66
5-26-66	S/B	UCR R001672	Upon removing the test plate from OTBV, seal had a scratch		Seal replaced	P/N 404677
5-26-66	S/B	R3325-10	Inspected start tank assy.		Weld Seam Satisfactory	Inspected in accordance with R3325-10 instruction

R-7450-2

TABLE C-1 (Continued)

DATE (Mo/Day/Yr)	LOCATION	ECP's EFIR's-UCR's	EFFORT	STAGE/ENGINE TEST SEC.	DISPOSITION	REMARKS
6-12-66	S/B	UCR R001690	Gimbal assy bolt pattern out of tolerance - Gimbal assy removed and replaced			Discrepancy found during engine installation into the stage
6-20-66	S/B	UCR R001692	Electrical harness clamping block-loose between stage clamps		Replaced with new item	P/N 502865
7-16-66	S/B	J2-529 230	Replacement of ASI Oxidizer tube assembly			Kit #10-406907 Mod. Instr. R 5436-529, 6-[illegible]-66
7-27-66	S/B	EFIR J2-3A	Inspected for redundant lines T/P Purge manifold assembly		Satisfactory	
8-22-66	S/B	EFIR J2-7	Inspection of first stage turbine wheel		Satisfactory	T/P Assy S/N 4076763
9-16-66	S/B	EFIR J2-1	Insp. oxid. primary seal drain line support bracket		Satisfactory	P/N 408730
10-5-66	S/B	ECP MD J2-540 240	Remove insulation from T/C purge line			Kit No. 10-406995 Mod. Instr. R5436-540, 9-23-66
10-12-66	S/B	J2-525 234	Replacement of STDV Drain			Kit No. 10-558273 Mod. Instr. R5436-525, 9-22-66
10-25-66	S/B	UCR R001848	T/C closure damaged		Item replaced	P/N RA20941-11
10-31-66	S/B	J2-545 235	Removal of Instr. Bosses from T/C Exh. Gas Manifold			Kit No. 10-410629 Mod. Instr. R5436-545
11-1-66	S/B	J2-544 236	Incorp. double weld shot peened flange to tube joint		Leak check at MTF	Kit No. 10-558266 Mod. Instr. R5436-544, 9-[illegible]-66
11-4-66	S/B	J2-549 247	Addition of accelerometer mount on Lox dome			Kit No. A-10-704605 Mod. Instr. R5436-549, 10-[illegible]-66
11-17-66	S/B	J2-437 246	Deletion ASI P_c stage static Instr. Line		Leak check at MTF	Kit No. A-10-704468 Mod. R5436-437-1, 11-15-66

TABLE C-1 (Continued)

DATE (Mo/Day/Yr)	LOCATION	NCR's EFIR's-UCR's	EFFORT	STAGE/ENGINE TEST SEC.	DISPOSITION	REMARKS
11-29-66	S/B	EFIR J2-17A	Inspect fuel pump stabilizer pin		Satisfactory	
11-30-66	S/B	UCR 001857	Upon performing ECP J2-419 wire insulation not in spec. plug P-51		Harness replaced	P/N 502079-11
12-13-66	S/B	EFIR J2-14	Inspection of STDV four-way control valve		Leak check at MTF	Part S/N 8263397
1-8-67	S/B	UCR 001889	Quill shaft had surface rust		Shaft brushed - use as is	P/N 458168
7-15 Jan. 1967	S/B	UCR R001890	Lox turbopump replaced with Lox pump with thick turbine wheels		Leak check at MTF	Old pump S/N 6634949 reworked pump S/N 4067110 installed. Total test time when installed 1938 seconds

TABLE C-1 (Continued)

DATE (Mo/Day/Yr)	LOCATION	ECP's EFIRs - UCRs	EFFORT	STAGE/ENGINE TEST SEC.	DISPOSITION	REMARKS
1-27-67	S/B		Stage shipped to MTF			Eng. Config. MD 3X5 11X13 20X 23X25 28X30X32X34 38X40 51X53 61X64X68 70X72X76 80X82X84X86 88X89X99X101X106 108X116 118X 122 123X130 132X134X137 144X 148 149X151 155X156X158X161X 168X173X176X177X190X190X202X 205X218X226X230X234X236X240X 246 247
2-14-67	MTF	UCR 004020	Seal damage, improper handling		Replaced	
2-16-67	MTF	UCR 004021	Oxid. Turbine inlet press. line adapter seal leak		Replaced	
2-16-67	MTF	UCR 004022	Oxid. Turbine outlet Press. line adapter seal leakage		Replaced	
2-16-67	MTF	UCR 004023	Unused instr. port hot gas seal leakage		Replaced	
2-19-67	MTF	EFIR J2-18A	Inspection of STDV opening control line adapter assy 557438		Satisfactory	
2-19-67	MTF	EFIR J2-16A	Inspection OTBV for proper nozzle install.		Satisfactory	
2-24-67	MTF	UCR 004025	Dent in hot gas manifold			Dent exceeded R 3825-3 manual requirement accepted as is by Engineering, Canoga Park.
2-27-67	MTF	UCR 004028	Seal leakage		Replaced	Found during leak check of GOX system

TABLE C-1 (Continued)

DATE (Mo/Day/Yr)	LOCATION	ECP's EFIRs - UCRs	EFFORT	STAGE/ENGINE TEST SEC.	DISPOSITION	REMARKS
2-27-67	MTF	ECP MD J2-582 259	Replacement ignition detector probe			Kit No 18-558262
2-27-67	MTF	J2-575 256	Replace augmented spark ign. line			Kit No 18-406365
2-27-67	MTF	J2-437 246 R1	Deletion of ASI P_c stage static instr. line.			Nit No 18-704468
3-1-67	MTF	EFIR J2-5A	Inspection ASI lox line & OTBV & MFV control lines		Satisfactory	
3-8-67	MTF	UCR 004050	GG Fuel purge flow 1200 scims - Required 2400 scims			P/N 557755 check valve replaced.
3-10-67	MTF	UCR 004056	H/E inlet lox press. line adapter leak		Seal replaced.	
3-11-67	MTF	UCR 004052	GG control valve sequence problem			Control valve replaced.
3-14-67	MTF	UCR 004053 UCR 004054	Excessive lube on threads oxidizer poppet assembly			
3-15-67	MTF	UCR 004059	GG poppet delay 152 MS			Orifice 0.047 removed and replaced with orifice 0.044.
3-16-67	MTF	EFIR J2-21A	Inspection of start tank girth weld		Satisfactory	
3-20-67	MTF	ECP MD J2-544 236	Leak check only			Modification accomplished at Seal Beach

TABLE C-1 (Continued)

DATE o/Day/Yr	LOCATION	ECP's EFIRs - UCRs	EFFORT	STAGE/ENGINE TEST SEC.	DISPOSITION	REMARKS
-20-66	MTF	EFIR J2-14B	Leak check only.			Modification accomplished at Seal Beach.
-23-67	MTF	UCR 004063	GG Control line weld leak			Sleeve rewelded - leak check complete.
-23-67	MTF	UCR 004057	Penetration of Braze joint inadequate per EFIR J2-23			Line modified per ECP J2-437-2.
-23-67	MTF	ECP MD 437-2 246	Rework of ASI P_c line			ASI S/N 4077607
-23-67	MTF	EFIR J2-23	Inspection of ASI P_c line braze joint		Rejected	Incorporated ECP J2-437-2 corrected problem.
-25-67	MTF	UCR 004C30	Oxid. turbine inlet press. line adapter seal leak.		Seal replaced	
-25-67	MTF	UCR 004070	ASI cable against VSC No 1 improper support clamp positioning.			ASI cable support clamps repositioned by rotating 20°.
-31-67	MTF		Acceptance static test		0 - sec.	Test terminated at L-7 minutes of auto phase due to stage problem.
6-67	MTF		Acceptance static test		365.1 sec	Observer cutoff
7-67	MTF	EFIR J2-5B	Inspection of ASI lox line & OTBV & MFV control line		Satisfactory	
7-67	MTF	UCR 007504	Start tank cover buckled & indented.			Repaired per R 3825-3 manual.

TABLE C-1 (Continued)

DATE Mo/Day/Yr	LOCATION	ECP's EFIRs - UCRs	EFFORT	STAGE/ENGINE TEST SEC.	DISPOSITION	REMARKS
4-6-67	MTF	ECP MD J2-511 219	Install filter assembly pneu. accumulator primary flt. instr. package.			Kit No 18-557431
4-8-67	MTF	UCR 004082	Distortion duct assy upper section bellows convolution.			Duct replaced.
4-15-67	MTF	ECP MD J2-575 278 R3	Replace augmented spark igniter line			Kit No 18-406365-20
4-15-67	MTF		Acceptance static test		367.8	Lox depletion cutoff
4-15-67	MTF	UCR 007517	Scorched area at hot gas cross-over Instr. port seal			Instr. port seal replaced as precautionary measure.
4-20-67	MTF	ECP MD J2-370 150	Removal stage static test instrumentation			Kit No. 18-704442, except NN1 NN2 TF-1.
4-24-67	MTF	ECP MD J2-513 221	Replacement of poppet for retiming MOV assembly.			Kit No. 18-558259
4-24-67	MTF	EFIR J2-5B	Inspection of ASI lox line & OTBV & MFV control line		Satisfactory	
4-24-67	MTF	EFIR J2-25	Inspection of T/C fuel jacket purge check valve		Satisfactory	
4-24-67	MTF	ECP MD J2-408 227 R-1	Deletion ofaltitude oxid. turbine bppass orifice			Kit No 18-303928
4-24-67	MTF	EFIR J2-10	Leak test start tank vent & relief valve.		Satisfactory	

TABLE C-1 (Continued)

DATE (Mo/Day/Yr)	LOCATION	ECP's EFIRs - UCRs	REPORT	STAGE/ENGINE TEST SEC.	DISPOSITION	REMARKS
4-27-67	MTF	LCP MD J2-551 277 R1	Removal of Braze joint in ASI P_c line			Accomplished by Rocketdyne personnel, Kit No 8 (18-704734-10)
5-1-67	MTF	UCR 007527	Resistance shift occurred in transducer			Replace transducer.
5-3-67	MTF	ECP MD J2-434 180	Relocation of No 2 M/S press. switch.			Kit No. 18-550047-10
5-8-67	MTF	ECP MD	Component insulation provide for			Kit No. 18-146055 No 8 hat band accomplish at KSC
5-20-67	MTF	MTF	Ship stage to KSC			Eng. Confi. 3X5 11X13 20X23X 25 28X30X32X34 36X40 51X53 61X64X68 70X72X76 80X82X84X86 88X97X99X101X106 108X116 118X122 123X130 132X134X137 144X148 153X155X158X161X168X 173X176 177X179 180X188X190X 202X205X218 219X221X224X226X 227X230X234 236X240X246 247X25 X259X277 278
6-5-67	KSC	UCR R003912	P-2 connector white deposits on threads, pin bent, case scored & metal chips			Cleaned, resurfaced case end straightened pin - retained for use.
6-6-67	KSC	UCR R007876	ECA J2 & J3 receptacles contaminated white deposit			Cleaned and retained for use.
6-7-67	KSC	UCR R007839	Quill shaft corrosion		Replaced	
6-9-67	KSC	UCR R007899	MOV corrosion idler shaft end flange			Cleaned and retained for use P/N 409969

R-7504

C-11

TABLE C-1 (Continued)

DATE (Mo/Day/Yr)	LOCATION	ECP's EFIRs - UCRs	EFFORT	STAGE/ENGINE TEST SEC	DISPOSITION	REMARKS
6-24-67	KSC	UCR R007841	ASI valve-corrosion & pitting on scaling surface of outlet flange		Replaced.	P/N 308880
7-20-67	KSC	UCR 010638	ECA (2) helicoil inserts deformed		Replaced.	P/N 502670-11 inserts replaced & assy retained for use
8-8-67	KSC	UCR 010641	Fuel turbine seal leakage greater than allowable by manual.			Judged acceptable by Engr. & retained for use.
9-21-67	KSC	UCR 010813	Start tank vent line-System over-pressurized		Replaced	P/N NA5-260059
9-21-67	KSC	UCR 010806	Valve-System overpressurized		Replaced	1. No provisions for reweld-Added to FCRR 2. Start tank name plate missing-plate replaced. 3. No QA acceptance for weld on control line.
10-3-67	KSC	EFIR J2-28	Replacement of ASI ignition detector bracket bolt.			
10-18-67	KSC	ECP J2-552 MD 251	Insulation of oxid; T/P volute inlet & high pressure duct		Complete	Kit No 18-146001
11-16-67	KSC	J2-587 291	Reidentification of M/S pressure switch		Complete	Kit No 18-558111
11-16-67	KSC	J2-607 289 298	Replacement of vent port check valve		Complete	Kit No 18-558264
11-16-67	KSC	J2-551 R-1 277	Reidentification of ASI assembly		Complete	Kit No 18-704734

TABLE C-1 (Continued)

DATE (Mo/Day/Yr)	LOCATION	ECP's EFIRs - UCRs	EFFORT	STAGE/ENGINE TEST SEC.	DISPOSITION	REMARKS
1-8-68	KSC	UCR 010616 010617	Oxid. T/P turbine seal Purge checkvalve flow below requirement		Replaced	Flow measured at 2350 scims judged acceptable by Engineering and retained fo use.
1-9-68	KSC	J2-620 301 R-1	Primary seal drain line oxid. T/P turbine seal		Complete	1. Weld leak at stub out - weld repass made. 2. Weld leak at sleeve - weld repass made.
1-10-68	KSC	UCR 010629	T/P purge manifold assy. Check valve far below allowable			Judged acceptable and retai for use. P/N 103838
1-17-68	KSC	EFIR J2-26	Insp. MOV bearing for contamination		Satisfactory	
1-17-68	KSC	EFIR J2-24B	Inspect of ECA for possible contamination		Satisfactory	
1-17-68	KSC	ECP MD J2-581 257 R2	Install of interim insulation of LOX system also OTBV and fast shut down valve.		Complete	Kit No 18-146020
1-17-68	KSC	J2-538 244 R-1	Install. of air filler valves on ASI and GG igniter cable assembly.		Complete	Kit No 18-558258
1-24-68	KSC	trans. 010647	Strut-clevis area damaged.		Replaced	P/N 502466
1-24-68	KSC	trans. 010648	Pin shank scored		Replaced	P/N 502295

TABLE C-1 (Continued)

DATE (Mo/Day/Yr)	LOCATION	ECP's EFIRs - UCRs		STAGE/ENGINE TEST SEC.	DISPOSITION	
2-6-68	KSC	ECP MD J2-470 319 R-1	Replaced purge control valve		Complete	1. Pressure was not decreased to 225-250 psig during leak check as required per DAR 2-3"d"-Performed per stage doc. HE tank press. 1500 psi
2-15-68	KSC	ECP MD J2-606 324 R-1	Incorporation of improved timers in ECA		Complete	1. Female receptical (J2) ding .005 & .008 - Reworked per R-3825-3 manual. 2. Female connector (J3) ding .020 outer sealing surface reworked per R-3825-3 manual. 3. ECA G-4 igniter cable pressurized 27.8 psig, communication check showed 22.2. Repair cable per R-3825-3 manual & repressurized to 28 psig. 4. ECA G-1 igniter cable pressurized 27.8 psig. Communications check 24 psig Recheck satisfactorily.
2-16-68	KSC	EFIR J2-31	Inspection of MOV sequence valve for lip seal leakage.		Satisfactory	
2-16-68	KSC	ECP MD J2-483 224	Install. of insulation to T/C hat bands, support ring, MFV, and ECA.		Complete	
3-1-68	KSC	EFIR J2-32	Inspection of adapter 702528 and adapter assy 703350 for correct material.		Satisfactory	

TABLE C-1 (Concluded)

DATE (Mo/Day/Yr)	LOCATION	ECP'S EFIRS - UCR'S	EFFORT	STAGE/ENG. TEST SEC.	DISPOSITION	REMARKS
4-2-68	KSC	ECP MD J2-370 150 R2	Removal of static stage instr. NN1, NN2, TF1		Complete	Kit No. 18-704442.
4-2-68	KSC	ECP MD J2-594 269 R3	Installation of redundant start & He Tank Instrumentation		Complete	Kit No. 18-704728.
4-4-68	KSC		LAUNCH	TOTAL ENGINE TEST SECONDS: 1409.0 sec.		Engine Configuration: 3x5 11x13 20x23x25 28x30x32x34 38x40 51x55 61x64x[illegible] 70x72 x76 80x82x84x86 88x97x99x101 x106x108x116 118x122 123x130 132x134x137 144x146 150x155x 165x158x161x168x173x176 177x 179 180x182x190x202x205x208 219x221x224x226x227x230x234 236x240x244x246 247x251x256 257x259x269x277 278x289x291 x298x301x219x324.
	NOTE:	Information pertaining to engine J2044 outlined on these charts was taken from available documentation and reflects significant information pertaining to effort which could effect successful engine operation.				

UNCLASSIFIED

Security Classification

DOCUMENT CONTROL DATA - R & D

(Security classification of title, body of abstract and indexing annotation must be entered when the overall report is classified)

1 ORIGINATING ACTIVITY (Corporate author) Rocketdyne, a Division of North American Rockwell Corporation, 6633 Canoga Avenue, Canoga Park, California 91304	2a. REPORT SECURITY CLASSIFICATION UNCLASSIFIED 2b. GROUP

3 REPORT TITLE

J-2 ENGINE AS-502 (APOLLO 6) FLIGHT REPORT S-II and S-IVB STAGES
S-II STAGE FAILURE ANALYSIS

4 DESCRIPTIVE NOTES (Type of report and inclusive dates)

Flight Report

5 AUTHOR(S) (First name, middle initial, last name)

Rocketdyne Engineering

6 REPORT DATE	7a. TOTAL NO. OF PAGES	7b. NO. OF REFS
21 June 1968	298	0

8a. CONTRACT OR GRANT NO.	9a. ORIGINATOR'S REPORT NUMBER(S)
NAS8-19 b. PROJECT NO. c. d.	R-7450-2 (Volume 2) 9b. OTHER REPORT NO(S) (Any other numbers that may be assigned this report)

10 DISTRIBUTION STATEMENT

11 SUPPLEMENTARY NOTES	12. SPONSORING MILITARY ACTIVITY
	NASA-MSFC Huntsville, Alabama

13 ABSTRACT

This is Volume 2 of a five-volume report on the operation of the J-2 engines during the flight of Apollo/Saturn AS-502. This volume presents the analysis of the premature shutdown of J-2 engines J2044 and J2058.

The volumes of this report are:

Volume 1: Flight Performance Analysis
Volume 2: S-II Stage Failure Analysis
Volume 3: S-IVB Stage Failure Analysis
Volume 4: Flight Failure Verification Testing
Volume 5: Post-Flight Design Modifications

DD FORM 1 NOV 65 1473

UNCLASSIFIED

Security Classification